

# VU Research Portal

## Climate change impact assessment using MOSAICC in Morocco

Balaghi, Riad; El Hairech, Tarik; Alaouri, Meriem; Motaouakil, Soundouce; Benabdelouahab, Tarik; Mounir, Fouad; Lahlou, Mouanis; Arrach, Redouane; Abderrafik, Mustapha; Colmant, Renaud; Evangelisti, Mauro; Poortinga, Ate; Kuik, O.J.; Delobel, Francois

2016

### **document version**

Publisher's PDF, also known as Version of record

### **document license**

Unspecified

[Link to publication in VU Research Portal](#)

### **citation for published version (APA)**

Balaghi, R., El Hairech, T., Alaouri, M., Motaouakil, S., Benabdelouahab, T., Mounir, F., Lahlou, M., Arrach, R., Abderrafik, M., Colmant, R., Evangelisti, M., Poortinga, A., Kuik, O. J., & Delobel, F. (2016). *Climate change impact assessment using MOSAICC in Morocco*. INRA-Morocco.

### **General rights**

Copyright and moral rights for the publications made accessible in the public portal are retained by the authors and/or other copyright owners and it is a condition of accessing publications that users recognise and abide by the legal requirements associated with these rights.

- Users may download and print one copy of any publication from the public portal for the purpose of private study or research.
- You may not further distribute the material or use it for any profit-making activity or commercial gain
- You may freely distribute the URL identifying the publication in the public portal ?

### **Take down policy**

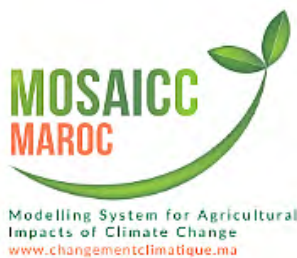
If you believe that this document breaches copyright please contact us providing details, and we will remove access to the work immediately and investigate your claim.

### **E-mail address:**

[vuresearchportal.ub@vu.nl](mailto:vuresearchportal.ub@vu.nl)



# Climate change impact assessment using MOSAICC in Morocco



The Modelling System for Agricultural Impacts of Climate Change



**Authors :** Riad BALAGHI, Tarik EL HAIRECH, Meriem ALAOURI, Soundouce MOTAOUAKIL, Tarik BENABDELOUAHAB, Fouad MOUNIR, Mouanis LAHLOU, Redouane ARRACH, Mustapha ABDERRAFIK, Renaud COLMANT, Mauro EVANGELISTI, Ate POORTINGA, Onno KUIK, François DELOBEL.

**With contributions of:** René GOMMES, Michele BERNARDI, Oscar ROJAS, Migena CUMANI, Jose Manuel GUTIERREZ, Dirk RAES, Patricia MEJIAS MORENO, Arjen VRIELINK, Frederic REYNES, Philip WARD, Philippe GROSJEAN, Daniel SAN MARTIN, Patricia MEJIAS, Simone TARGETTI, Hideki KANAMARU, Laila TRIKI, Mohamed BADRAOUI.

This report technical report is a joint publication of the National institute for Agronomic Research of Morocco (INRA-Morocco) and the Food and Agriculture Organization of the United Nations (FAO). Use, reproduction and dissemination of this material is encouraged. Except where otherwise indicated, material may be copied, downloaded and printed for private study, research and teaching purposes, or for use in non-commercial products or services, provided that appropriate acknowledgement of INRA-Morocco and FAO as the source and copyright holder is given and that INRA-Morocco and FAO's endorsement of users' views, products or services is not implied in any way. This publication could be downloaded [www.changementclimatique.ma](http://www.changementclimatique.ma) website.

Legal Deposit : 2016MO3882

ISBN : 978-9954-0-6702-4

INRA-Morocco, 2016

Contact: [riad.balaghi@gmail.com](mailto:riad.balaghi@gmail.com)

Institut National de la Recherche Agronomique

Avenue Ennasr Rabat, Maroc

BP 415 RP Rabat, Maroc

[www.inra.org.ma](http://www.inra.org.ma)

Tel : +212 537 77 09 55

Fax : +212 537 77 00 49

# Content

I.INTRODUCTION.....	1
II.THE MOSAICC PLATFORM.....	6
1.Description of the server.....	6
2.Installation of the server computer in DMN.....	7
2.1.Rack.....	7
2.2.Power supply.....	8
2.2.1.Air conditioner.....	8
2.2.2.Networking.....	9
3.Installing the MOSAIC software.....	10
3.1.Installation prerequisites.....	10
3.1.1.NTP Client.....	10
3.1.2. HTTP Server and WEB.....	10
3.1.3.Serveur FTP.....	10
3.1.4.Database server.....	11
3.1.5.Software and base libraries.....	11
3.1.6.General software and libraries.....	11
3.2.Installation.....	12
3.2.1.Download of tools and models.....	12
3.2.2.Preparation of the database.....	13
3.2.3.Preparation of system files.....	14
3.2.4.Installation of Drupal.....	15
3.3.Administration of the MOSAICC system.....	15
3.3.1.Users, roles and profiles.....	15
3.3.2.Experiences.....	17
3.3.3.Management of disk space.....	18
3.3.4.Security and backup.....	19
III.THE CLIMATIC COMPONENT.....	20
1.Interpolation of reference climatic data.....	20
1.1.Climate data used.....	20
1.2.Loading climate series in MOSAICC.....	22



1.3. Interpolation of current climate data.....	22
1.3.1. Inputs.....	22
1.3.2. The main components of the topography and distance from the sea.....	24
1.3.3. Preliminary analysis and interpolation.....	26
1.3.4. Interpolation of PET.....	33
2. Downscaling climate projections.....	34
2.1. Validation.....	36
2.2. Loading future time series from SD portal to the MOSAICC system.....	36
IV. AGRONOMIC COMPONENT.....	40
1. Calibration of AquaCrop for rainfed areas.....	41
1.1. Calibration of AquaCrop for rainfed wheat.....	41
1.2. Calibration of AquaCrop for rainfed barley.....	42
1.3. Prediction of wheat and barley yields in rainfed areas.....	43
1.3.1. Prediction of wheat yields.....	43
1.3.2. Prediction of barley yields.....	45
2. Calibration of AquaCrop for irrigated areas.....	46
V. ECONOMIC COMPONENT.....	48
1. The DCGE Model.....	49
2. Input data.....	51
2.1. Sets and benchmark data of variables.....	51
2.2. Parameter values for coefficients.....	53
2.3. Growth rates of exogenous variables.....	54
2.4. Climate change shocks.....	55
2.5. Output data.....	59
VI. HYDROLOGICAL COMPONENT.....	60
1. Introduction.....	60
2. Methodology.....	61
2.1. Study area.....	61
2.2. Moulouya.....	62
2.3. Tensift.....	63
2.4. Sebou.....	64
2.5. Loukkos.....	65



2.6. Bouregreg and Chaouia.....	66
2.7. Oum Er Rbia.....	66
2.8. Souss-Massa-Draâ.....	67
2.9. Climate models.....	68
2.10. Hydrological model.....	68
3. Results and discussion.....	70
3.1. Spatial distribution of water resources.....	70
3.2. Hydrological model calibration.....	70
VII. FORESTRY COMPONENT.....	74
1. Introduction.....	74
2. Method.....	76
2.1. Presentation of the study area.....	76
2.1.1. Climate.....	77
2.1.2. Topography.....	78
2.1.3. Pedology.....	79
2.1.4. Forest vegetation.....	79
2.1.5. Anthropic activities.....	79
2.1.6. Forest management.....	80
2.1.7. Climate data.....	80
2.1.8. Initial communities.....	81
2.1.9. Species parameters.....	82
2.2. Experimental design.....	84
2.2.1. Calibration.....	85
2.2.2. Ecoregions.....	86
2.2.3. Forestry interventions.....	87
VIII. THE MOSAICC WEB-GIS PORTAL.....	88
1. Introduction.....	88
2. Technology overview.....	90
3. The CC Impact tool.....	90
3.1. The single mode of the CC Impact tool.....	95
3.2. The comparison mode of the CC Impact tool.....	99
4. The Simulator tool.....	102
4.1. Functionalities.....	104



4.1.1. Chart display function.....	105
4.1.2. Evolution of agro-meteorological variables function.....	107
4.2. Architecture of the system.....	108
4.2.1. Conceptual diagram of the data.....	108
4.2.2. Database tables.....	108
4.2.3. Software architecture.....	112
IX. CLIMATE CHANGE TRENDS IN MOROCCO.....	114
1. Precipitations.....	114
2. Maximum temperature.....	116
3. Minimum temperature.....	117
X. CLIMATE CHANGE IMPACTS ON AGRICULTURE, WATER AND FORESTS	
.....	120
1. Impacts on wheat and barley yields.....	120
1.1. Impacts on wheat yields.....	121
1.2. Impacts on barley yields.....	122
2. Impacts on water.....	124
3. Impacts on forests.....	130
3.1. Impacts without disturbance.....	130
3.1.1. Impacts on species distribution.....	131
3.1.2. Impacts on total biomass.....	131
3.2. Impacts with forestry interventions.....	134
3.3. Comparison of results with and without forestry interventions. .	135
3.3.1. Distribution.....	135
3.3.2. Average biomass.....	136
3.3.3. Quercus suber.....	137
3.3.4. Cork production.....	138
4. Impacts on agricultural economy.....	139
XI. TRAINING AND DISSEMINATION MATERIAL.....	144
XII. CONCLUSION AND RECOMMENDATIONS.....	146
XIII. REFERENCES.....	149
XIV. ANNEXES.....	155
1. Annex 1.....	155
2. Annex 2.....	157





3. Annex 3.....	159
4. Annex 4.....	161
5. Annex 5 : Distributed hydrological model STREAM.....	163
6. Annex 6: Data analysis method.....	165
7. Annex 7 : Yield indices.....	167
8. Annex 8 : A technical description of the model.....	172
9. Annex 9 : Installation and configuration of CC Impact tool.....	187
9.1. User requirements.....	187
9.2. Technology overview.....	187
9.3. Server installation.....	190
9.4. CMS installation.....	191
9.5. CMS configuration.....	199
9.6. CMS customization.....	213
9.7. Result Overview Module.....	216
10. Annex 10 : Architecture of the Simulation Tool.....	224
10.1. Architecture.....	224
10.1.1. Description of the tools.....	224
10.1.2. Linux server.....	224
10.1.3. Web Apache.....	224
10.1.4. PostgreSQL / PostGIS.....	224
10.1.5. MapServer.....	225
10.1.6. OpenLayers.....	225
10.1.7. Languages.....	226
10.2. Installation and configuration of the map server.....	227
10.2.1. Installation and configuration of PostgreSQL.....	227
10.2.2. Installation and configuration of PostGIS.....	228
10.2.3. Installation of phpPgAdmin.....	228
10.2.4. Installation of MapServer.....	229
10.2.5. Edition of MapFile.....	229
10.3. Setting up the database with PostgreSQL / PostGIS.....	229
10.4. Development of the map interface.....	229
10.5. API OpenLayers API, Ext and GeoExt.....	230
10.6. Using basemaps.....	230





10.6.1. Google Maps.....	230
10.6.2. Open Street Maps.....	231



## List of figures

Figure 1: Components of the MOSAICC system.....	2
Figure 2: User interface of the MOSAICC system.....	3
Figure 3: Dissemination Web portal of the MOSAICC system.....	4
Figure 4: Rack where MOSAICC is hosted, located at the Climatological Applications Centre of DMN.....	8
Figure 5 : Power redundancy board.....	8
Figure 6: Air-conditioning cabins.....	9
Figure 7 : Cabin network connections: unifying LAN and WAN VPN Firewalls. 9	
Figure 8 : Global view of the MOSAIC web page with different modules and functions.....	15
Figure 9 : Distribution of users of MOSAICC by role.....	16
Figure 10 : Distribution of users of MOSAICC by profile.....	17
Figure 11 : Distribution of experiments per module.....	18
Figure 12 : Inventory of experiences by function.....	18
Figure 13 : Location of the synoptic weather stations used.....	21
Figure 14 : Digital terrain model and shapefile of the study area.....	23
Figure 15 : Cumulated contribution of the 40 Principal Components (%) to the total variance.....	24
Figure 16 : Contribution (%) of each Principal Component to the total variance.....	25
Figure 17 : Standard deviation in (m) of each Principal Component.....	25
Figure 18 : Distribution of PCA by synoptic station of DMN.....	33
Figure 19 : Representative Concentration Pathways (RCP) scenarios (IPCC, 2015).....	35
Figure 20 : AquaCrop flowchart indicating the main components of the soil-plant-atmosphere continuum.....	41
Figure 21 : Simulated (AquaCrop) and observed official wheat grain yields (tons/ha), from 1981 to 2010 cropping seasons in Beni Mellal province.....	42
Figure 22 : Simulated (AquaCrop) and observed official barley grain yields (tons/ha), from 1981 to 2010 cropping seasons in Fes, Safi and Meknes provinces.....	43
Figure 23 : Predicted wheat yields (tons/ha) for the period 2010-2009, for the average of the models CanESM2, MIROC-ESM and MPI-ESM-LR, and according to scenario RCP4.5.....	44
Figure 24 : Predicted wheat yields (tons/ha) for the period 2010-2009, for the average of the models CanESM2, MIROC-ESM and MPI-ESM-LR, and according to scenario RCP8.5.....	44

Figure 25 : Predicted barley yields (tons/ha) for the period 2010-2009, for the average of the models CanESM2, MIROC-ESM and MPI-ESM-LR, and according to scenario RCP4.5.....	45
Figure 26 : Predicted barley yields (tons/ha) for the period 2010-2009, for the average of the models CanESM2, MIROC-ESM and MPI-ESM-LR, and according to scenario RCP8.5.....	46
Figure 27 : Location of experimental sites in the irrigated plain of Tadla.....	46
Figure 28 : Simulated and observed durum wheat grain yields in irrigated area of Tadla plain.....	47
Figure 29: Simplified production and demand structure of the economic model with one commodity produced by two activities.....	50
Figure 30: Projected GDP growth rates in socioeconomic pathways SSP3 and SSP5. (Source: based on © SSP Database (Version 1.0) <a href="https://secure.iiasa.ac.at/web-apps/ene/SSPDB">https://secure.iiasa.ac.at/web-apps/ene/SSPDB</a> ).....	55
Figure 31: Models and data flows.....	55
Figure 32: Technical shift parameter $\theta$ in the activity production function..	56
Figure 33: Projected yield changes for barley in the favorable and unfavorable regions in the RCP4.5 climate change scenario as elaborated by the CanESM2 climate model .....	58
Figure 34 : The Moulouya, Tensift and Sebou basin are highlighted on a land-use (left) and digital elevation map (right). The locations of the outlets used for model calibration are indicated with a dot and a number. The names corresponding to the numbers are shown right from the figures.....	62
Figure 35 : The size of the upstream basin corresponding to each outlet used for the Moulouya, Tensift and Sebou watersheds.....	62
Figure 36 : The monthly averaged water yield (P-PET) as calculated from the Era-interim data. This data was also used for model calibration.....	70
Figure 37 : The monthly distributions in measured (blue) and modeled discharge volumes (box-plots) for the Moulouya basin. Each plot represents a different outlet. The STREAM parameters R2 and VE for each outlet are displayed in the graphs.....	71
Figure 38 : The monthly distributions in measured (blue) and modeled discharge volumes for the Sebou basin. Each plot represents a different outlet. The STREAM parameters, R2 and VE for each outlet are displayed in the graphs.....	72
Figure 39 : The monthly distributions in measured (blue) and modeled discharge volumes for the Tensift basin. Each plot represents a different outlet. The STREAM parameters, R2 and VE for each outlet are displayed in the graphs.....	72
Figure 40 : The monthly distributions in measured (blue) and modeled discharge volumes (box-plots) for the Loukkos basin. The plot represents the “Pont torreta” outlet. The STREAM parameters R2 and VE for the outlet are displayed in the graphs.....	73
Figure 41 : Location of the Maâmora forest (Bagaram, 2014).....	77

Figure 42: Ombrothermic diagrams of Bagnouls and Gausсен for the three stations in Maâmora, 1980–2013.....	78
Figure 43: Maximum temperatures in the Maâmora forest for three models and two scenarios, 2001–2099 (Blue solid line: model CanESM2 and scenario RCP4.5; blue dotted line: model CanESM2 and scenario RCP8.5 ; green solid line: model MIROC-ESM and scenario RCP4.5 ; green dotted line: model MIROC-ESM and scenario RCP8.5 ; red solid line: MPI-ESMLR model and scenario RCP 4.5 ; red dotted line: MPI-ESM-LR model and scenario RCP8.5.....	81
Figure 44: Initial communities map of the Maâmora forest.....	82
Figure 45: Calibration of <i>Quercus suber</i> in the Maâmora forest.....	86
Figure 46: Eco-regions map of the Maâmora forest.....	87
Figure 47: The MOSAICC Web-GIS portal <a href="http://www.changementclimatique.ma">www.changementclimatique.ma</a> ..	89
Figure 48: The CC Impact tool.....	91
Figure 49: The variable selector of the CC Impact tool.....	92
Figure 50: The forestry component of the CC Impact tool.....	94
Figure 51: The economy component of the CC Impact tool.....	95
Figure 52: The CC Impact tool, in single variable mode.....	96
Figure 53: The Hydrology component of CC Impact tool, displaying maps the water availability (left), and charts and tables of discharge (right).....	97
Figure 54: Location of the four studied basins.....	98
Figure 55: Water discharge in the Moulouya basin.....	99
Figure 56: The comparison mode of the CC Impact tool.....	100
Figure 57: Tables displayed by the comparison mode of the CC Impact tool. ....	101
Figure 58: Monthly data comparison displayed by the comparison mode of the CC Impact tool.....	102
Figure 59: The MOSAICC WEB-GIS portal, showing cumulated rainfall by 2040, at grid level (4.5x4.5 km).....	103
Figure 60: Evolution of the climatic variables by 2090, according to RCP8.5, MPI-ESM-LR model in the district of Ain Nzagh (province of Settат).....	104
Figure 61 : Functionalities of the Simulator tool.....	105
Figure 62 : Regional average maximum temperatures between June and August, estimated in the decades 2060 and 2070, according to scenario RCP8.5 and using the MIROC-ESM model displayed with OpenStreetMap basemap..	107
Figure 63 : Deviation from the reference period (1980-2010) of cumulative rainfall between October and April, estimated in decade 2070 , according to RCP8.5 scenario and using the average climatic model.....	107
Figure 64: Tabular and graphic evolution of the agro-meteorological variables for Meknes-Tafilalet region, between the months of October and April, estimated in decade 2070, according to RCP8.5 scenario and using average climatic model.....	108
Figure 65: Data flow chart.....	111

Figure 66: General architecture of the Simulator tool.....	113
Figure 67: Rainfall change (%), compared to reference period (1971-2000), at province administrative level, according to RCP4.5 and RCP8.5 scenarios and for average climate model.....	115
Figure 68: Maximum temperature change (°C), compared to reference period (1971-2000), at province administrative level, according to RCP4.5 and RCP8.5 scenarios and for average climate model.....	117
Figure 69: Minimum temperature change (°C), compared to reference period (1971-2000), at province administrative level, according to RCP4.5 and RCP8.5 scenarios and for average climate model.....	119
Figure 70: Wheat yield (t/ha) projections, according to RCP4.5 and RCP8.5 scenarios and for average climate model.....	121
Figure 71: Wheat yield change (%) projections, according to RCP4.5 and RCP8.5 scenarios and for average climate model.....	122
Figure 72: Barley yield (t/ha) projections, according to RCP4.5 et RCP8.5 scenarios and for average climate model.....	123
Figure 73: Barley yield change (%) projections, according to RCP4.5 and RCP8.5 scenarios and for average climate model.....	124
Figure 74 : The water balance for the MIROC-ESM (top), CanESM2 (middle) and MPI-ESM-LR (bottom) for the RCP4.5 (top of each GCM) and the RCP8.5 (bottom of each GCM) scenarios for the periods 2010-2040, 2040-2070 and 2070-2100. The data were compared to the historical data of each GCM. Positive values indicate an increase in water availability compared to the 1971 - 2000 period, negative values a decrease.....	125
Figure 75 : Scenarios for Mohamed V, the most downstream point in the Moulouya basin.....	126
Figure 76 : Scenarios for Belksiri, the most downstream point in the Sebou basin.....	127
Figure 77 : Scenarios for Talmest, the most downstream point in the Tensift basin.....	127
Figure 78 : Scenarios for Pont torreta station, the most downstream point in the Loukkos basin.....	128
Figure 79 : Scenarios for Rass fathia station in the Bouregreg basin.....	128
Figure 80 : Scenarios for Ait ouchen station in the Oum Er rbia basin.....	129
Figure 81 : Scenarios for Agouilal station in the Souss-Massa-Draa basin..	130
Figure 82: Comparison of species distribution in the forest of Maâmora without disturbance, 2010/2090 (Model CanESM2).....	131
Figure 83: Total biomass (in tons of dry matter per hectare) for each species in the Maâmora forest without disturbance, 2010–2090 (model CanESM2). Black curve: reference scenario; Green curve: RCP4.5 scenario; Red curve: RCP8.5 scenario.....	132
Figure 84: Comparison of species distribution in the Maâmora forest in 2090 with forestry interventions (Model CanESM2).....	134

Figure 85: Comparison of the number of sites where each species is present with (red curve) and without (blue curve) forestry interventions, as compared with the number of sites where each species occurs in 2010 (CanESM2 model and RCP4.5 scenario).....	135
Figure 86: Comparison of the evolution over time of average total biomass of each species with (red curve) and without (blue curve) forestry interventions in the Maâmora forest (tonnes of dry matter per hectare) (CanESM2 model and RCP4.5 scenario).....	137
Figure 87: Total standing and living biomass in gigagrammes of dry matter for <i>Quercus suber</i> with (red dashed curve) and without (black curve) forestry interventions for the entire Maâmora forest.....	138
Figure 88: Ratio of the number of cohorts within the age range to produce cork, with (red curve) and without (blue curve) harvest in the Maâmora forest, 2010–2090 (CanESM2 model and RCP 4.5 scenario).....	139
Figure 89 : Change in median monthly discharge and streamflow variability for all basins in the Moulouya (a), Sebou (b) and Tensift (c) basin for the periods 2010-2040 (left) 2040-2070 (middle) and 2070-2100 (right) for MIROC-ESM model and RCP8.5 scenario.....	156
Figure 90 : Change in median monthly discharge and streamflow variability for all basins in the Loukkos , Bouregreg, Souss Massa Draa and Oum Er rbia basins for the periods 2010-2040 (left) 2040-2070 (middle) and 2070-2100 (right) for MIROC-ESM model and RCP8.5 scenario.....	158
Figure 91 : Change in median monthly discharge and streamflow variability for all basins in the Moulouya (a), Sebou (b) and Tensift (c) basin for the periods 2010-2040 (left) 2040-2070 (middle) and 2070-2100 (right) for MPI-ESM-LR model and RCP4.5 scenario.....	160
Figure 92 : Change in median monthly discharge and streamflow variability for all basins in the Loukkos , Bouregreg, Souss Massa Draa and Oum Er rbia basins for the periods 2010-2040 (left) 2040-2070 (middle) and 2070-2100 (right) for MPI-ESM-LR model and RCP4.5 scenario.....	162
Figure 93 : Water balance Storage Compartments of the STREAM model (Aerts et al. 1999).....	164
Figure 94 : The pdf and cdf of the Gumbel distribution (Eq1 and Eq 2).The red and black line display the effect of a higher $\mu$ , the black and green line show the effect an increase in $\beta$ . Increase in magnitude is linked to in increase in $\mu$ , an increase of $\beta$ is associated with an increase in range.....	165

## List of tables

Table 1 : Percentage use of disk space per partition.....	19
Table 2: Climatic time series used in MOSAICC.....	21
Table 3: List of experiments used to interpolate the current climate variables (Tmin, Tmax and rainfall).....	26
Table 4 : Details of the experiment used for interpolating the dekadal rainfall.....	27
Table 5 : Details of the experiment used for interpolating the monthly rainfall.....	27
Table 6 : Details of the experiment used for interpolating the dekadal minimum temperature.....	28
Table 7 : Details of the experiment used for interpolating the monthly minimum temperature.....	29
Table 8 : Details of the experiment used for interpolating the dekadal maximum temperature.....	30
Table 9 : Details of the experiment used for interpolating the monthly maximum temperature.....	31
Table 10 : Filtering options used for each climate interpolated variable.....	32
Table 11 : CMIP5 list of models available in the SD portal.....	34
Table 12 : List of atmospheric variables available in the SD, in relation with CMIP5.....	35
Table 13 : List of identifiers of future climate time series imported from the SD portal to MOSAICC.....	36
Table 14: The format of a Social Accounting Matrix.....	52
Table 15: Commodities and activities in the 2010 SAM.....	53
Table 16: Climate Models in selected in MOSAICC.....	57
Table 17: Yield index for the year 2050 for different activities in two climate change scenarios elaborated by three climate models and the two trend approaches: linear (LIN) and 10-year average (MA).....	58
Table 18: The three parameters used in the STREAM model for calibration.	69
Table 19: List of species of the Maâmora forest and their parameters.....	83
Table 20: Rainfall trends for the two climate scenarios (Optimistic-RCP4.5 and Pessimistic-RCP8.5) and for the average of three climate models (CanESM2, MIROC-ESM, MPI-ESM-LR).....	114
Table 21: Maximum temperature trends for the two climate scenarios (Optimistic-RCP4.5 and Pessimistic-RCP8.5) for the average of three climate models (CanESM2, MIROC-ESM, MPI-ESM-LR).....	116
Table 22: Minimum temperature trends for the two climate scenarios (Optimistic-RCP4.5 and Pessimistic-RCP8.5) for the average of three climate models (CanESM2, MIROC-ESM, MPI-ESM-LR).....	118
Table 23: Simulations without disturbance for the Maâmora forest.....	130



Table 24: Summary results of the statistical analyses of the three climate scenarios (reference scenario, RCP4.5 and RCP8.5) for the three climate models.....	133
Table 25: Selected macro-economic results for RCP4.5 climate change scenario (MAD * 10 <sup>9</sup> ).....	141
Table 26: Selected macro-economic results for RCP4.5 climate change scenario (MAD * 10 <sup>9</sup> ).....	142
Table 27: Workshops and trainings organized during the MOSAICC project. .....	144

## Partner institutions



**Institut National de la Recherche Agronomique**



**Organisation des Nations Unies pour l'Alimentation et l'Agriculture**



**Direction de la Météorologie Nationale**



**Direction de la Stratégie et des Statistiques (MAPM)**



**Direction de la Recherche et de la Planification de l'Eau**



**Ecole Nationale Forestière des Ingénieurs**



**Haut Commissariat aux Eaux et Forêts et à la Lutte Contre la Désertification**



**Agence du Bassin Hydraulique du Souss Massa et du Draâ**



**Agence du Bassin Hydraulique du Loukous**



**Agence du Bassin Hydraulique du Tensift**



**Agence du Bassin Hydraulique de la Moulouya**



**Agence du Bassin Hydraulique de l'Oum Er Rbia**



**Agence du Bassin Hydraulique du Bouregreg et de la Chaouia**



**Agence du bassin hydraulique du Sebou**



**Université de Mons**



**Université Libre d'Amsterdam**



**Water Insight**



**UNICAN - Santander Meteorology Group**



**Union Européenne**

# I. INTRODUCTION

The strategy of the Government of Morocco for the agricultural sector, called "Green Morocco Plan" aims to stimulate agriculture and promote rural development. This strategy faces the challenge of climate change, because of its expected impact on crop productivity and the availability of irrigation water. Indeed, it is expected that climate change will lead decreased yields of major crops and increase the variability of agricultural production.

Metrics are primary data sources for policy makers and funder, who seek at monitoring the effects of adaptation measures to climate change. In recent years, scientists have developed a range of various models to monitor, evaluate and predict the effects of climate change on different economic sectors. For the agriculture and forestry sectors, this information is in general often limited to one scientific domain (crop yields, water balance, species distribution, economy, etc.). An innovative, multidisciplinary approach combining knowledge from different domains would therefore constitute an comprehensive means to evaluate impact of climate change.

Quantitative analyzes of the impact of climate change on the productivity of major crops in Morocco were undertaken by the Ministry of Agriculture and Maritime Fisheries (MAPM) in 2008, with technical support from FAO and in partnership with the National Institute of Agronomic Research (INRA-Morocco) and the National Department of Meteorology (DMN) (Gommes et al., 2008). From this first experience, and through the EU / FAO program on global governance and the reduction of hunger, FAO launched a pilot project for developing and implementing a simulation tool "Modelling System for Agricultural Impacts of Climate Change"<sup>1</sup> (MOSAICC), which aims to assess the impact of climate change on the agriculture, forestry and water sectors in Morocco.

The MOSAICC project was implemented through a Letter of Agreement signed in January 2013 between FAO and the National Institute for Agricultural Research (INRA), which provides project management. The partner institutions are the Directorate of Strategy and Statistics (MAPM), the National Meteorology Directorate, the Directorate of Research and Water Planning, the High Commission for Water, Forests and Combat Desertification, the National Forestry School of Engineers and the 7 Hydraulic Basin Agencies of Oum Er-Rbia Loukkos Sebou, Moulouya, Tensift, Souss-Massa-Draa and Bouregreg.

MOSAICC is a complex but powerful modelling system which allows users from various disciplines, including climatology, agronomy, hydrology, forestry and economics, to assess the impacts of climate change (Figure 1). It integrates a powerful data management system which allows users to upload data, as well as a flexible and configurable system to run multiple models. Its web-based interface is user-friendly. Users do not need to install any software

---

<sup>1</sup> <http://www.fao.org/climatechange/mosaicc/en/>



on their computers, as data and results are shared on a centralized server, acting as web server, data server and processing workstation.

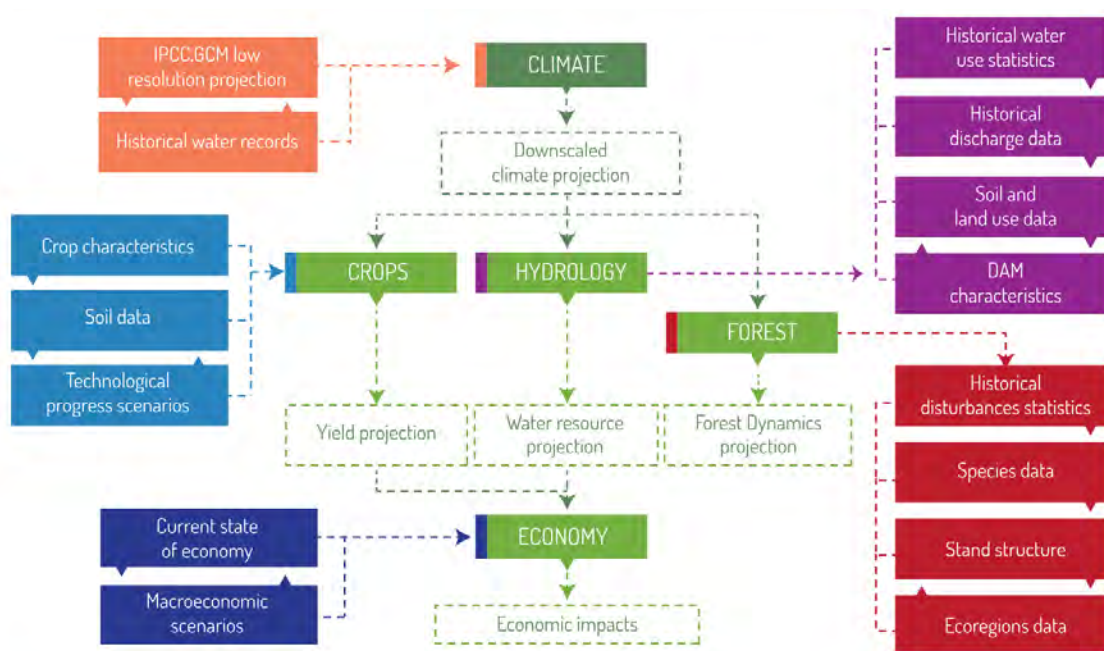


**Figure 1: Components of the MOSAICC system.**

In MOSAICC, models were all adapted to work on a centralized server with which users communicate through web interfaces (<http://81.192.163.58/>) (Figure 2). This type of architecture has several advantages :

- All models are connected to a unique spatial database. This significantly increases the interoperability among the models, solving notably data format issues and facilitating data transfer.
- Cross platform barriers are alleviated as any client using any operating system can run the models as long as it has a web browser.
- Defining a set of user profiles with different properties and permissions (including external user profiles) helps to track the experiments undertaken, to secure data and model uses and to make database management easier.

The user interface of MOSAICC is based on the WEB-GIS technology, which requires open source tools and libraries. It is a multi-user system which allows users to share data and results (i.e. other data generated from the models).The execution of the models is managed by a shell that

bridges the gap between the interfaces, the models and the database. The interfaces offer all the controls needed to perform the simulations and comprise functionalities to browse the database, to display and to download the data.

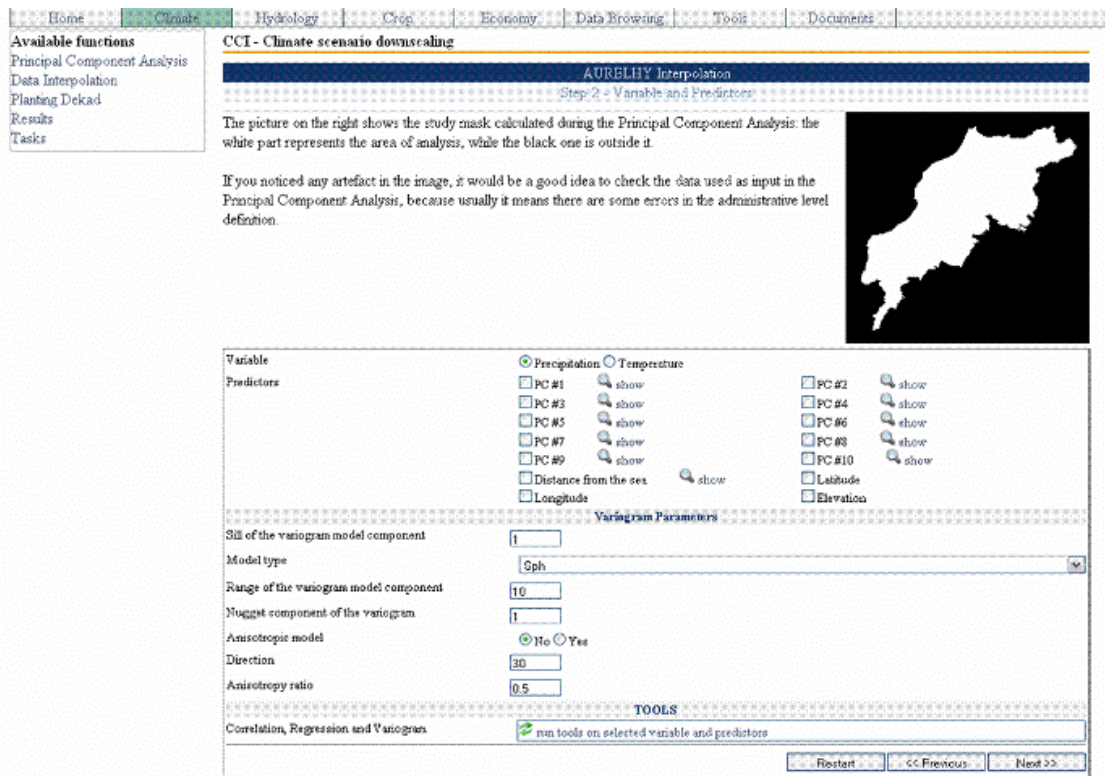


**Figure 2: User interface of the MOSAICC system.**

Also, a dedicated Web portal [www.changementclimatique.ma](http://www.changementclimatique.ma) has been developed for disseminating results performed by the MOSAICC tool to a wide audience of users (policymakers, scientists, students and NGOs) (Figure 3). The Web portal allows displaying impacts of climate change through various RCP and climate change models selections. Beside, all training material, video, flyers, technical notes and deliverables are available on the Web portal. The distribution of MOSAICC's results allows for the integration of scientific information in the design of agricultural development projects and, more generally, in economic decision-making and policy development. More information can be found at <http://www.fao.org/climatechange/mosaicc/en/>.



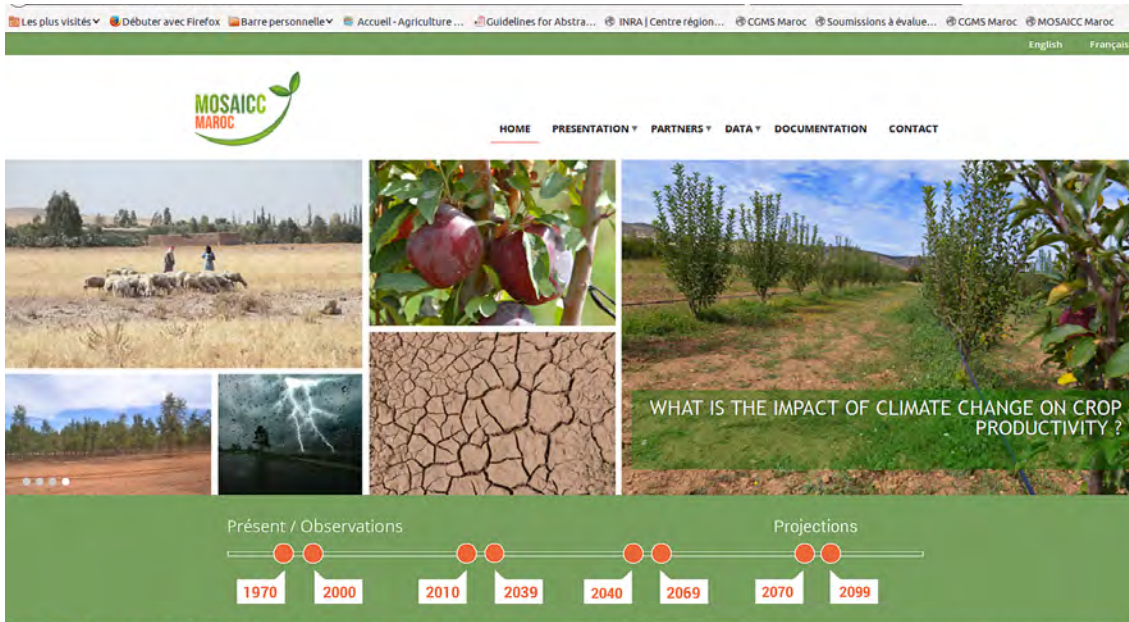


**Figure 3: Dissemination Web portal of the Mosaicc system.**

Climate impact assessment studies based on the Mosaicc system are being carried out in several countries by FAO outside Morocco, including Peru and the Philippines, and will soon be implemented in Malawi, Zambia and Indonesia. This innovative system has been developed to be transferred to interested countries, with training towards independent use by national experts provided. The climate impact assessments at country level constitute a pertinent response to the UNFCCC Least Developed Countries Expert Group’s request for country-specific climate information. Metrics derived from this system would also help decision makers and funder to monitor, verify and report outcomes of adaptation measures to climate change.

Experts who contributed to MOSAICC project in Morocco are :

<b>Experts from Morocco</b>	<b>International and FAO experts</b>
<ul style="list-style-type: none"><li>• Riad BALAGHI (coordination)</li><li>• Tarik BENABDELOUAHAB</li><li>• Tarik EL HAIRECH</li><li>• Meriem ALAOURI</li><li>• Redouane ARRACH</li><li>• Mustapha ABDERRAFIK</li><li>• Soundouce MOUTAOUAKKIL</li><li>• Fouad MOUNIR</li><li>• Laila TRIKI</li><li>• Mohamed BADRAOUI</li></ul>	<ul style="list-style-type: none"><li>• René GOMMES</li><li>• Michele BERNARDI</li><li>• Oscar ROJAS</li><li>• François DELOBEL</li><li>• Migena CUMANI</li><li>• Hideki KANAMARU</li><li>• Mauro EVANGELISTI</li><li>• Onno KUIK</li><li>• Ate POORTINGA</li><li>• Jose Manuel GUTIERREZ</li><li>• Dirk RAES</li><li>• Patricia MEJIAS MORENO</li><li>• Arjen VRIELINK</li><li>• Frederic REYNES</li><li>• Philip WARD</li><li>• Philippe GROSJEAN</li><li>• Daniel SAN MARTIN</li><li>• Patricia MEJIAS</li></ul>





## II. THE MOSAICC PLATFORM

81.192.163.58

Applications CGMS-MAROC E-Agr Département de l'ag... CGMS Maroc FAOSTAT Gateway W Connexion — Wikip... (INRA Mknnes) Home - Research Pa... Global Land Degrad... House Radio - Page 2 Abhtoo: EFFICIE...

FOOD AND AGRICULTURE ORGANIZATION OF THE UNITED NATIONS  
Helping to build a world without hunger

MOSAICC Morocco, v. 0.1

about contacts copyrights Log in

User login

Username: \*

Password: \*

Log in

Request new password

FAO Modelling System for Agricultural Impacts of Climate Change

Welcome to **FAO-MOSAICC** (for **MO**delling System for **AG**ricultural Impacts of **CL**imate Change), the system of models designed to carry out each step of the impact assessment from climate scenarios downscaling to economic impact analysis at national level.  
COMMIT;

FAO-MOSAICC is being developed in the framework of the EC/FAO Programme on "Linking information and decision making to improve food security" (GCP/GLO/243/EC), theme 3 "Climate change and food security". More information on [www.foodsec.org](http://www.foodsec.org).

The project manager and the expert users can take advantage of this system to carry on the following tasks:

- custom data management (upload, download, layout control and update)
- custom module management (upload and update)
- run the installed modules with the available data for multiple experiments
- geo-processing
- publish their experiments to be used from everybody

Logo of the Ministry of Agriculture, Rural Development and Fisheries  
Logo of the National Institute of Statistics  
Logo of the National Meteorology Directorate  
Logo of the National Directorate of Research and Water Purification

### 1. Description of the server

**M**OSAICC is a system based on the WEB-GIS technology. It has been developed to perform simulations on geo-referenced data of multiple type: raster, vector and scalar. MOSAICC requires "open-source" tools and libraries to execute queries from multiple users on one hand and for several other models. Therefore, MOSAICC requires minimal hardware configuration as follows :

#### **Cpu:**

- Xeon
- I7

#### **Ram:**

- 8 GB

#### **Disc space:**

- OS: 100 GB
- Data: 2 TB
- RAID: RAID 5

#### **Network:**

- LAN: Wide band line
- Internet : bandwidth of 2 Mbps

### **Safeguard:**

- NAS: at least as space as data
- Os :
- RHEL 6 : CentOS 5.4 or equivalent, MOSAICC is on RHEL6

## **2. Installation of the server computer in DMN**

Supercomputers of National Meteorology Directorate (DMN) are located in the Computer Center. This center enables operational IT systems to provide a favorable environment for their durabilities, with minimal dysfunction abnormalities. The center infrastructure meets the quality performance in terms of power, cooling and networking. DMN adopted simultaneously for architecture rack layout and MOSAICC server was installed in the Rack of the Climatological Applications Center (Figure 4). Preliminary consultations early in the project helped to equip a server that meets the requirements of this architecture.

### **2.1. Rack**

The Rack is a standard system (EIA 310-D, IEC 60297 and DIN 41494 SC48D) for mounting various electronic modules one above the other (Figure 4). The rack consists of two vertical walls in metal spaced 17.75 inches (450.85 millimeters). A rack is used to store more machines on the same floor area: The racks are used to stack some machines over others. At DMN, they are used for servers and supercomputers.



**Figure 4: Rack where MOSAICC is hosted, located at the Climatological Applications Centre of DMN.**

## **2.2. Power supply**

Two redundant arrays, and TDOV1 TDOV2 indoors, fed from the General table Inverters (TDHQ). The power of each painting is 60kVA (Figure 5).



**Figure 5 : Power redundancy board.**

### **2.2.1. Air conditioner**

Two air-conditioning cabinets, direct expansion of 60kW for cooling. The mode of operation is based on the principle of the redundancy (N + 1) (Figure 6). Blowing a 16°C and humidity 50% + or -5% are insured. Implementation for each cabinets system of its external processing unit "of all Tubing" with blowing ducts in false floors to the perforated tiles.



**Figure 6: Air-conditioning cabins.**

### **2.2.2. Networking**

Networking of MOSAICC server is performed by connection to two Eht0 interfaces to the LAN and Eht1 for the web. The latter will allow access the public by http protocol (Figure 7).



**Figure 7 : Cabin network connections: unifying LAN and WAN VPN Firewalls.**

#### **For interface 1:**

- IP 172.16.0.194
- MASK 255.255.255.0
- BRIDGE 172.16.0.254
- DNS1 172.16.0.16

- DNS2 212.217.0.1

**For interface 2:**

- IP 172.16.70.58
- MASK 255.255.255.0
- BRIDGE 172.16.70.254
- DNS1 172.16.0.16
- DNS2 212.217.0.1

To access MOSAIC server from outside, the following address should be used : <http://81.192.163.58/>.

## **3. Installing the MOSAIC software**

### **3.1. Installation prerequisites**

#### **3.1.1. NTP Client**

The MOSAICC system clock must be set according to UTC or local time. In general, the universal time is the most recommended, but be sure the clock is adjusted either vis-a-vis the local or universal time. For this purpose, an NTP client (Network Time Protocol) is implemented.

#### **3.1.2. HTTP Server and WEB**

MOSAICC was developed and tested under an Apache http server environment and MIIS 5.1. It is an adaptation of Drupal written in PHP. Thus a PHP support is installed.

#### **3.1.3. Serveur FTP**

For handling large files, the http protocol is not enough. Therefore an FTP server is recommended.

### 3.1.4. Database server

MOSAICC requires the DBMS PostgreSQL 8.x with its extension PostGIS GIS.

### 3.1.5. Software and base libraries

LIB/SOFT	Source	version
PROJ.4	<a href="http://trac.osgeo.org/proj/">http://trac.osgeo.org/proj/</a>	4.7
GEOS	<a href="http://trac.osgeo.org/geos/">http://trac.osgeo.org/geos/</a>	3.2.2
GD Graphics Library	Linux distribution	2.0
GDAL	<a href="http://www.gdal.org/">http://www.gdal.org/</a>	1.7.3
PostGIS	<a href="http://postgis.refractions.net/">http://postgis.refractions.net/</a>	1.5.1
libcurl	Linux distribution	
libxml2	Linux distribution	
libxslt	Linux distribution	
PAM	Linux distribution	
GNU readline	Linux distribution	
gdk-pixbuf	Linux distribution	
gtk2-devel	Linux distribution	
Lazarus	<a href="http://www.lazarus.freepascal.org/">http://www.lazarus.freepascal.org/</a>	0.9.28 (64-bits version for Linux)
FreeBasic	<a href="http://www.freebasic.net/">http://www.freebasic.net/</a>	0.20.0
GFortran	<a href="http://gcc.gnu.org/fortran/">http://gcc.gnu.org/fortran/</a>	2.4.0
R	<a href="http://www.r-project.org/">http://www.r-project.org/</a>	2.12.1
NumPy	<a href="http://www.scipy.org/">http://www.scipy.org/</a>	1.2.1
SciPy	<a href="http://www.scipy.org/">http://www.scipy.org/</a>	0.6.0
dateutil	<a href="http://labix.org/python-dateutil">http://labix.org/python-dateutil</a>	1.2.1
Pytz	<a href="http://pytz.sourceforge.net/">http://pytz.sourceforge.net/</a>	2010h-1
<b>agg (Anti-Grain Geometry)</b>	<a href="http://www.antigrain.com/">http://www.antigrain.com/</a>	2.5
matplotlib	<a href="http://matplotlib.sourceforge.net/">http://matplotlib.sourceforge.net/</a>	1.0.1
WEAVE	<a href="http://www.scipy.org/Weave">http://www.scipy.org/Weave</a>	n.a
GNU Octave	<a href="http://www.gnu.org/software/octave/">http://www.gnu.org/software/octave/</a>	3.0.5
Boostlib	<a href="http://www.boost.org/">http://www.boost.org/</a>	1.41
Dynare	<a href="http://www.dynare.org/">http://www.dynare.org/</a>	4.2.x
OpenLayers	<a href="http://www.openlayers.org/">http://www.openlayers.org/</a>	2.11
JPGGraph	<a href="http://jpgraph.net/">http://jpgraph.net/</a>	
NuSOAP	<a href="http://sourceforge.net/projects/nusoap/">http://sourceforge.net/projects/nusoap/</a>	0.9.5

### 3.1.6. General software and libraries

Software	Source	version
<b>MapServer</b>	<a href="http://www.mapserver.org/">http://www.mapserver.org/</a>	5.6.x
<b>TrueType fonts for MapServer</b>	<a href="http://www.mapserver.org/">http://www.mapserver.org/</a>	5.6.x
<b>Drupal CMS</b>	<a href="http://drupal.org/">http://drupal.org/</a>	6.2

## **3.2. Installation**

### **3.2.1. Download of tools and models**

MOSAICC is a set of PHP modules, tools developed in C ++ and also a range of models to download, build, install and configure.

#### **Themes and Drupal modules**

The graphic of MOSAICC is based on an ad hoc theme developed in 2011. It is called FAO\_MOSAICC\_2011. PHP modules developed to fit the Drupal core and create the MOSAICC system are:

- cci\_data\_mng: advanced utilities management database
- cci\_db\_mng, basic utilities for database management
- cci\_docs, documentaries database
- cci\_functions, user management features
- cci\_menu, menu management
- cci\_tools, advanced tools to manage the system (i.e. user management)

#### **C++ tools**

- ASC\_Threshold: Processing of the DEM for determining water systems;
- GridAnalysis: analysis tool and grid compatibility StarSpan;
- Grid\_Avg: calculating the average temperature from grids TMIN and TMAX;
- Multi\_StarSpan launches WABAL AQUACROP points and analysis grids or for a selection of points;
- PLD\_Grid launches PLD to grid points or stations

#### **Models**

The version of MOSAICC installed includes the following models and tools:

- AURELHY PCA: calculation of the main components of the relief;
- Preliminary interpolation: preliminary analysis of the interpolation;



- Aurelhy Interpolation: interpolation and production of grids by Aurelhy;
- Kriging interpolation: interpolation and production of grids by Kriging only;
- Planting Dekad: estimates cycle lengths and start dates;
- WABAL: calculation of water balance variables;
- AQUACROP: calculating crop growth variable;
- STREAM 1.1.3-1 - g646b2ea: STREAM 1.1.3-1 version (manual calibration);
- STREAM Version 1.1.3-1: STREAM 1.1.3-1 version (simulation method);
- PET Hargreaves calculation of Potential evapotranspiration by the simplified Hargreaves method.

### 3.2.2. Preparation of the database

The database created after the Drupal installation has 49 tables: 47 are Drupal tables with names starting with the prefix "Drupal\_" and 2 tables are from POSTGIS including: geometry\_columns and spatial\_ref\_sys. The owner of this database is changed to be "fao\_cc\_impact". A procedure for creating and initializing the database "fao\_cci\_db\_init.sql" is available for download in FAO-MOSAICC repository.

The following list enumerates the tables created during the initialization phase :

<ul style="list-style-type: none"> <li>• 1.aquacrop_out</li> <li>• 2.cci_basedata_downscaling</li> <li>• 3.cci_config</li> <li>• 4.cci_config_format</li> <li>• 5.cci_crop_library</li> <li>• 6.cci_data</li> <li>• 7.cci_data_downscaling</li> <li>• 8.cci_data_downscaling_mon</li> <li>• 9.cci_data_format</li> <li>• 10.cci_data_historical</li> <li>• 11.cci_data_historical_mon</li> <li>• 12.cci_data_parent</li> <li>• 13.cci_data_ref</li> <li>• 14.cci_data_source</li> <li>• 15.cci_data_station</li> <li>• 16.cci_data_type</li> <li>• 17.cci_data_variable</li> </ul>	<ul style="list-style-type: none"> <li>• 35.cci_layer_attributes</li> <li>• 36.cci_layer_layout</li> <li>• 37.cci_layer_order</li> <li>• 38.cci_layers_link</li> <li>• 39.cci_module_config</li> <li>• 40.cci_modules</li> <li>• 41.cci_module_run</li> <li>• 42.cci_module_type</li> <li>• 43.cci_plantation_time</li> <li>• 44.cci_profile_datatype</li> <li>• 45.cci_profile_function</li> <li>• 46.cci_roi</li> <li>• 47.cci_run_params</li> <li>• 48.cci_run_type</li> <li>• 49.cci_soil_data</li> <li>• 50.cci_stream_outlet</li> <li>• 51.cci_study_area</li> </ul>
--	--

<ul style="list-style-type: none"> <li>• 18.cci_dcge_act_com</li> <li>• 19.cci_dcge_group</li> <li>• 20.cci_dcge_out_pref</li> <li>• 21.cci_dcge_region_layer</li> <li>• 22.cci_dcge_regions</li> <li>• 23.cci_dcge_results</li> <li>• 24.cci_doc_cat</li> <li>• 25.cci_doc_dir</li> <li>• 26.cci_doc_doc</li> <li>• 27.cci_downscaling</li> <li>• 28.cci_field_type</li> <li>• 29.cci_file_type</li> <li>• 30.cci_files</li> <li>• 31.cci_function_datatype</li> <li>• 32.cci_function_mode</li> <li>• 33.cci_function_wizard</li> <li>• 34.cci_layer</li> </ul>	<ul style="list-style-type: none"> <li>• 52.cci_trace_act</li> <li>• 53.cci_trace_obj</li> <li>• 54.cci_user_function</li> <li>• 55.cci_user_profile</li> <li>• 56.cci_users_profiles</li> <li>• 57.cci_wizard_field</li> <li>• 58.cci_work_mode</li> <li>• 59.data_set</li> <li>• 60.ds_downscaling</li> <li>• 61.ds_downscaling_data</li> <li>• 62.ds_downscaling_method</li> <li>• 63.ds_gcm</li> <li>• 64.ds_predictand</li> <li>• 65.ds_predictor</li> <li>• 66.ds_run</li> <li>• 67.ds_scenario</li> <li>• 68.ds_stations</li> <li>• 69.db_translation</li> </ul>
---	---

### 3.2.3. Preparation of system files

The MOSAICC system requires specific directories:

- **\_LAYERS:** The geographic data is stored in subdirectories to facilitate the processing and use by MapServer;
- **\_LAYERS / FTP:** default directory of the FTP user;
- **\_MODULES:** Sub directories where the modules are lodged during an experiment;
- **\_RUNNER:** Directory that lists experiments launching;
- **\_SUPFILES:** Sub directories where files accompany each model;
- **\_WORKPATH:** Physical Hive results of each experiment.

The creation of these system files is made using an available script which also gives permissions and rights required for the Apache user.

### 3.2.4. Installation of Drupal

A detailed description of this part is in the installation guide, available in FAO-MOSAICC repository.

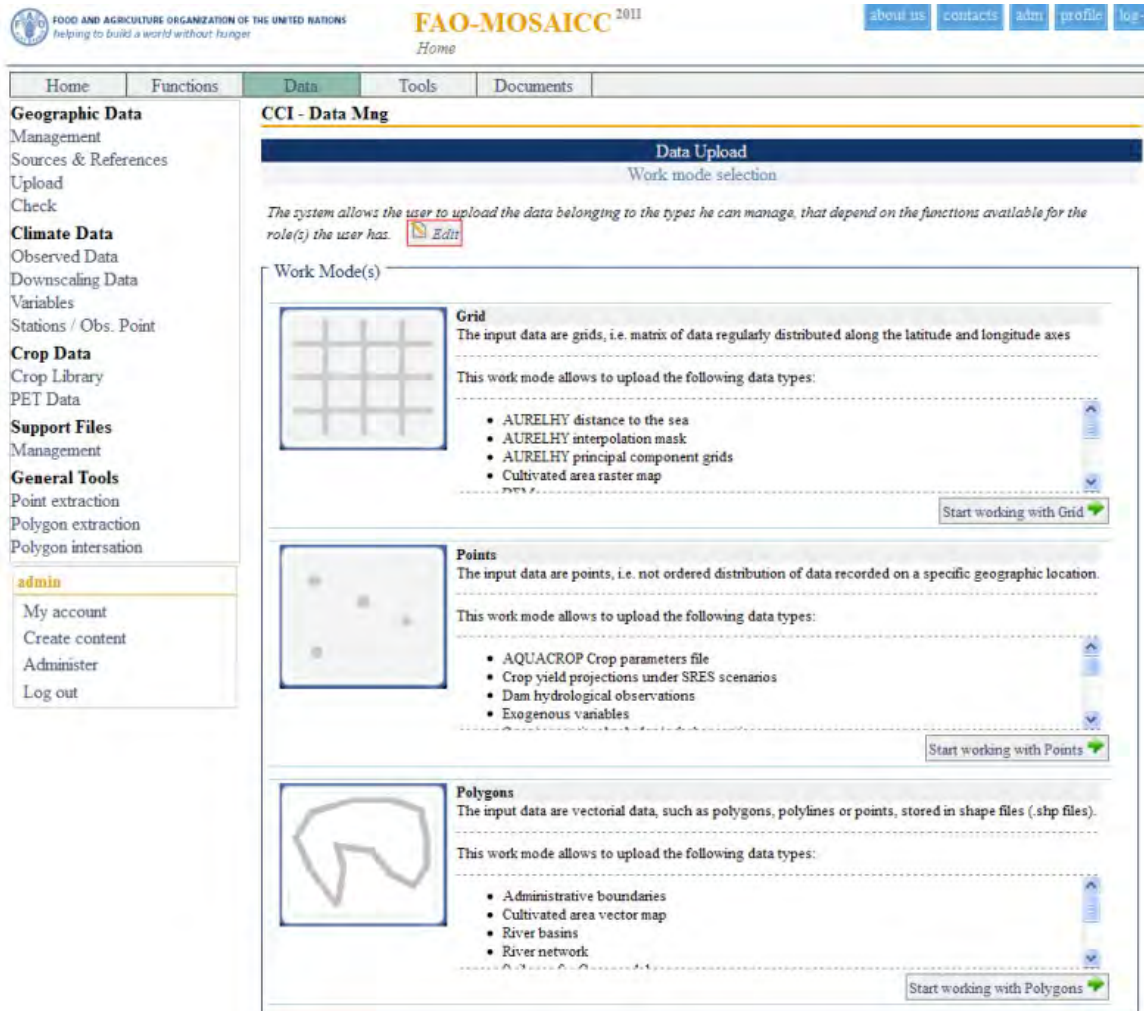


Figure 8 : Global view of the MOSAIC web page with different modules and functions.

## 3.3. Administration of the MOSAICC system

### 3.3.1. Users, roles and profiles

Creating new users to access the system utilities is a task entrusted to the administrator of MOSAICC. Each user is defined by a user name, a password, a role (Figure 9) and a profile (Figure 10). The uniqueness of a user is provided by the email address and account details. Three roles are predefined:

- Expert user;

- End user;
- Manager user.

The profiles are a combination of the following:

- climatologist
- Agronomist
- hydrologist
- Economist

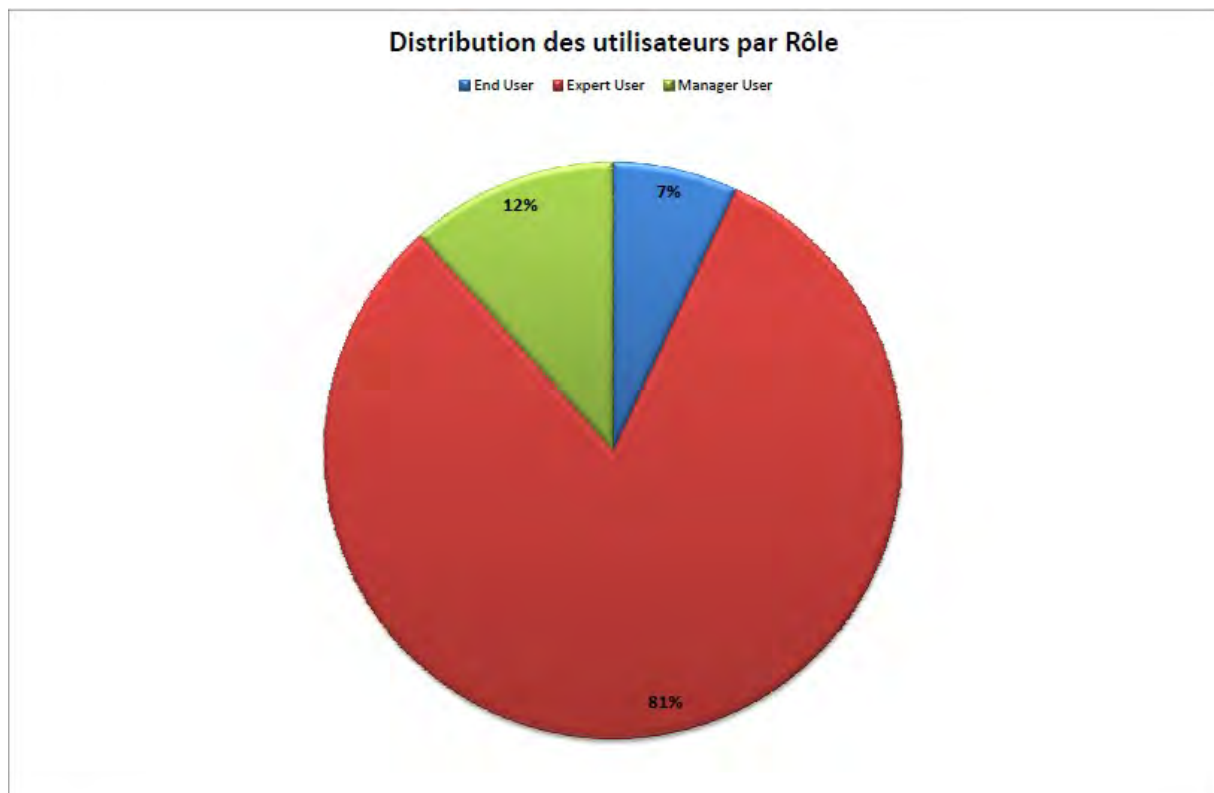


**Figure 9 : Distribution of users of MOSAICC by role.**

Distribution des utilisateurs par Profil

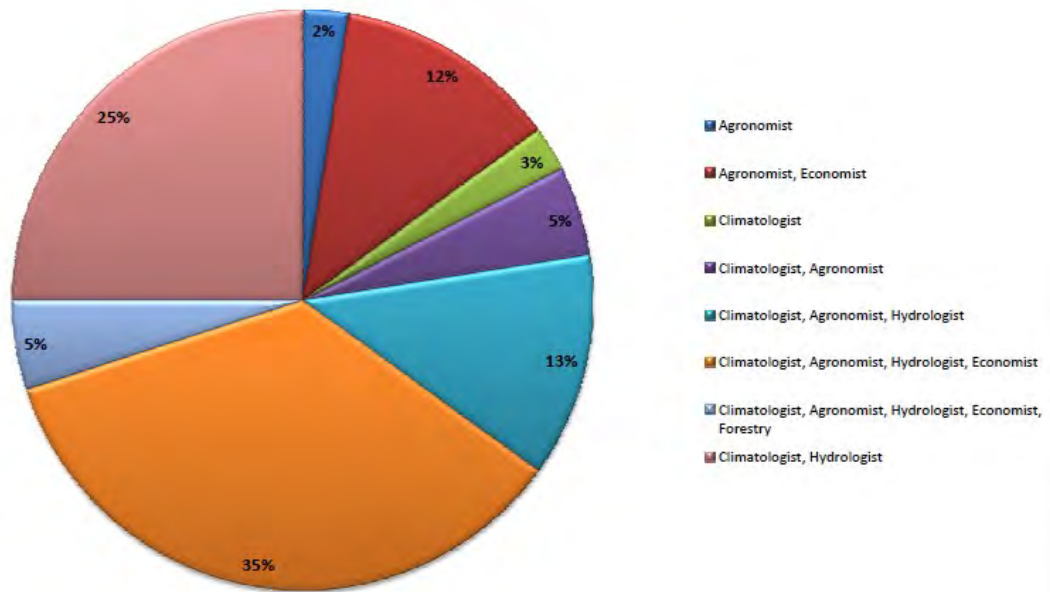
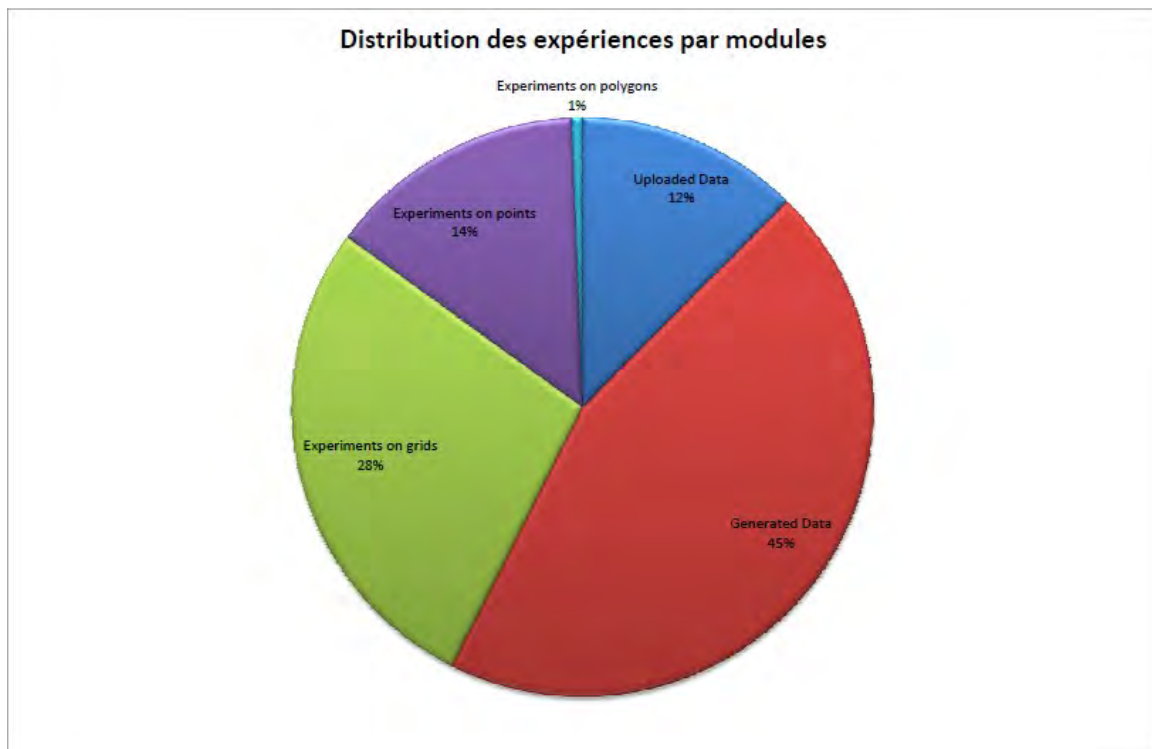
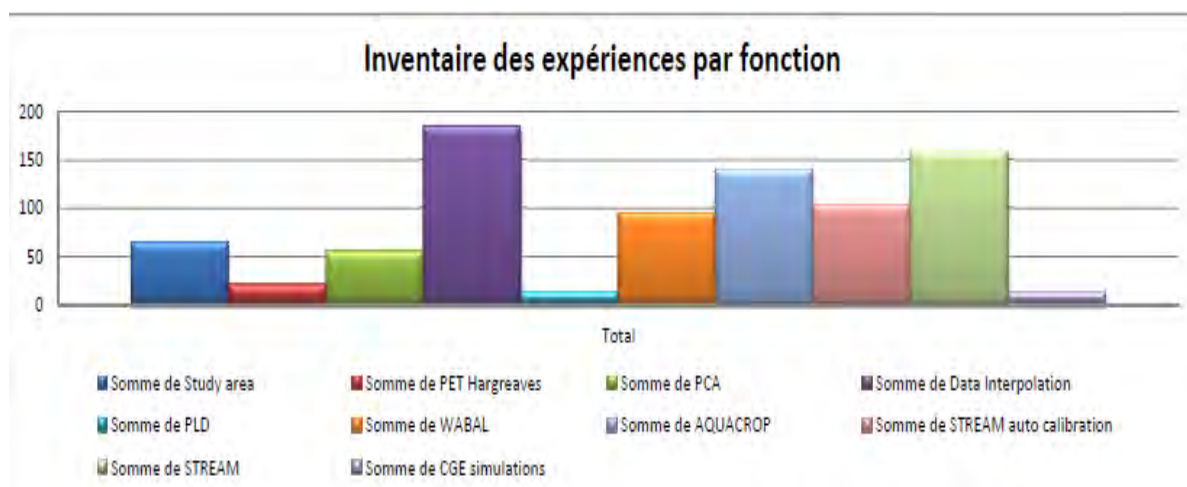


Figure 10 : Distribution of users of MOSAICC by profile.

### 3.3.2. Experiences



**Figure 11 : Distribution of experiments per module.**



**Figure 12 : Inventory of experiences by function.**

### 3.3.3. Management of disk space

Given the large amount of data that pass through the MOSAICC system, regular monitoring of disk space is paramount. Some features require special vigilance as to the STREAM model. To overcome the problem of saturation of the "System files", the administrator, in consultation with the users concerned, has to make cleaning actions of bulky temporary data,

unnecessary old data, or if appropriate to move these data to other partitions.

The current report disk space appears in Table 1:

**Table 1 : Percentage use of disk space per partition.**

<b>System file</b>	<b>% use</b>	<b>Mounting</b>
/dev/sda3	19%	/
/dev/sda2	67%	/data
/dev/sda1	33%	/boot
Tmpfs	1%	/dev/shm

#### **3.3.4. Security and backup**

Safeguarding the MOSAICC system consists in ensuring the continuity of activities of the system or, in case of failure, its quick restart. In general, and in case of serious disturbance, it is best to install the system from a backup version and recover data files from a reliable backup again.



### III. THE CLIMATIC COMPONENT



#### 1. Interpolation of reference climatic data

##### 1.1. Climate data used

The climate data used are from 39 meteorological Synoptic stations from the network of DMN (Figure 13). Synoptic stations work 24h/24h and produce hourly reports of the main meteorological variables: air pressure, temperature, relative humidity, wind speed and direction, cloud cover, quantity and intensity of precipitation, sunshine duration and radiation. The network is relatively small and covers mainly the coastal plains, whereas the mountainous regions and Sahara include less stations (Balaghi et al., 2012).



**Figure 13 : Location of the synoptic weather stations used.**

The data used are daily rainfall and maximum and minimum temperatures. The period used from 1980 to 2010, is taken as the current reference period.

**Table 2: Climatic time series used in MOSAICC.**

Station	Latitude	Longitude	Elevation (m)	Rainfall	Temperature	
					Minimum	Maximum
AGADIR AL MASSIRA	30.32	-9.40	72	1980 - 2010	1980 - 2010	1980 - 2010
AGADIR INEZGANNE	30.38	-9.57	177	1980 - 2010	1980 - 2010	1980 - 2010
AL-HOUCEIMA	35.18	-3.85	260	1980 - 2010	1980 - 2010	1980 - 2010
BENI MELLAL	32.37	-6.40	517	1980 - 2010	1980 - 2010	1980 - 2010
BOUARFA	32.57	-1.95	1285	1980 - 2010	1980 - 2010	1980 - 2010
CASABLANCA-ANFA	33.57	-7.67	68	1980 - 2010	1980 - 2010	1980 - 2010
CHEFCHAOUEN	35.08	-5.30	526	1980 - 2010	1980 - 2010	1980 - 2010
DAKHLA	23.72	-15.93	53	1980 - 2010	1980 - 2010	1980 - 2010
EL JADIDA	33.23	-8.52	43	1980 - 2010	1980 - 2010	1980 - 2010
ERRACHIDIA	31.93	-4.40	1146	1980 - 2010	1980 - 2010	1980 - 2010
ESSAOUIRA	31.50	-9.78	141	1980 - 2010	1980 - 2010	1980 - 2010
FES-SAIS	33.97	-4.98	518	1980 - 2010	1980 - 2010	1980 - 2010
GUELMIM	29.02	-10.05	338	1980 - 2010	1980 - 2010	1980 - 2010
IFRANE	33.50	-5.17	1496	1980 - 2010	1980 - 2010	1980 - 2010
KASBA-TADLA	32.87	-6.27	868	1980 - 2010	1980 - 2010	1980 - 2010
KENITRA	34.30	-6.60	44	1980 - 2010	1980 - 2010	1980 - 2010
KHOURIBGA	32.87	-6.97	784	1980 - 2010	1980 - 2010	1980 - 2010
LAAYOUNE	27.17	-13.22	30	1980 - 2010	1980 - 2010	1980 - 2010
LARACHE	35.18	-6.13	45	1980 - 2010	1980 - 2010	1980 - 2010

MARRAKECH	31.62	-8.03	454	1980 - 2010	1980 - 2010	1980 - 2010
MEKNES	33.88	-5.53	452	1980 - 2010	1980 - 2010	1980 - 2010
MIDELT	32.68	-4.73	1462	1980 - 2010	1980 - 2010	1980 - 2010
MOHAMMEDIA	33.72	-7.40	96	1980 - 2010	1980 - 2010	1980 - 2010
NADOR	35.15	-2.92	151	1980 - 2010	1980 - 2010	1980 - 2010
NOUASSEUR	33.37	-7.57	176	1980 - 2010	1980 - 2010	1980 - 2010
OUARZAZATE	30.93	-6.90	1202	1980 - 2010	1980 - 2010	1980 - 2010
OUJDA	34.78	-1.93	440	1980 - 2010	1980 - 2010	1980 - 2010
RABAT-SALE	34.05	-6.77	73	1980 - 2010	1980 - 2010	1980 - 2010
SAFI	32.28	-9.23	109	1980 - 2010	1980 - 2010	1980 - 2010
SETTAT	32.95	-7.62	413	1980 - 2010	1980 - 2010	1980 - 2010
SIDI IFNI	29.37	-10.18	320	1980 - 2010	1980 - 2010	1980 - 2010
SIDI SLIMANE	34.23	-6.05	50	1980 - 2010	1980 - 2010	1980 - 2010
SMARA	26.67	-11.67	233	1980 - 2010	1980 - 2010	1980 - 2010
TANGER-AERO	35.72	-5.90	49	1980 - 2010	1980 - 2010	1980 - 2010
TAN-TAN	28.17	-10.93	299	1980 - 2010	1980 - 2010	1980 - 2010
TAROUDANT	30.50	-8.82	300	1980 - 2010	1980 - 2010	1980 - 2010
TAZA	34.22	-4.00	593	1980 - 2010	1980 - 2010	1980 - 2010
TETOUAN	35.58	-5.33	179	1980 - 2010	1980 - 2010	1980 - 2010
TIZNIT	29.68	-9.73	231	1980 - 2010	1980 - 2010	1980 - 2010

## 1.2. Loading climate series in MOSAICC

Climate time series from 1980 to 2010 have been loaded into the MOSAICC database, for three time steps: daily, dekadal and monthly. Loading the climate series in MOSAICC happens in three steps:

- Creating the source and reference, using the **New reference** functionality;
- Preparing a file which contains the name of the stations, the WMO code, latitude, longitude and elevation and its load with the **geographic feature data / upload / dot /;**
- For each climatic parameter and for each time step, a csv file was created, containing the code, the date and the value of the measured variable. Then the WMO code has been replaced by the code generated by MOSAICC during the previous step.

## 1.3. Interpolation of current climate data

### 1.3.1. Inputs

The "PCA" function (Principal Component Analysis) allows the generation of the necessary interpolation grid, using the AURELHY<sup>2</sup>

<sup>2</sup> The AURELHY method uses the terrain to improve rainfall interpolation. The method is built around the following 3 points: (1) Automatic detection of existing statistical link between rainfall and the surrounding terrain; (2) Optimal use of this statistical link at the points where there is no measured value; (3) Generating a regional rainfall map,

(analysis using the relief for Hydro-meteorology) interpolation method. For this, the following files are generated:

- The interpolation mask;
- The grid of the digital elevation model (4.5x4.5 km);
- The grid of the distance from the sea;
- The grid of the main components of the topography.

The input data to perform this function are:

- Shapefile of the study area (geographic boundaries);
- The digital elevation model (<http://www2.jpl.nasa.gov/srtm/>) in Ascii format for Arcgis at 1x1 km spatial resolution.

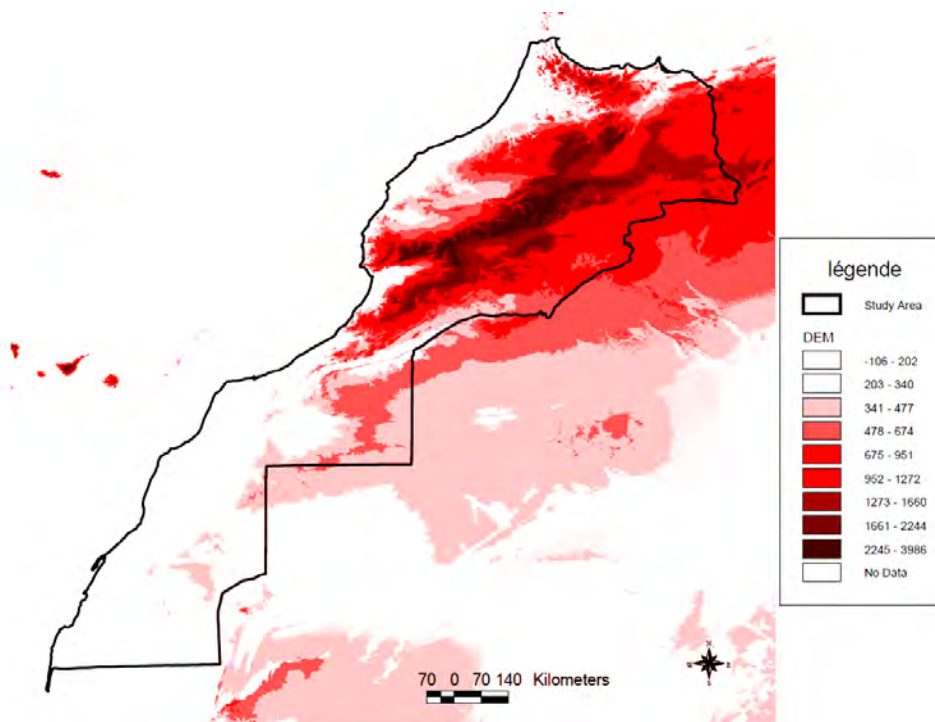


**Figure 14 : Digital terrain model and shapefile of the study area.**

To include the maximum number of synoptic stations in the database, the "experiments" function "pca\_tarik\_dmn\_step5, id = 3004" was executed. In this experiment, the digital terrain model step was set at a value of 5, which is equivalent to nearly 5 km in Morocco latitudes. This value was determined after a series of tests, checking the inclusion of synoptic stations in the interpolation field. The value of 5 is optimal

integrating the effects due to relief.

because only Mohammedia and Tangier port stations are excluded, which does not impact the quality of interpolation.

### 1.3.2. The main components of the topography and distance from the sea

The outputs of the execution of the PCA function are:

- 40 Principal Component, in ArcGIS grid Ascii , at a resolution of 0.04166667 degrees;
- The distance from the sea, in ArcGIS grid Ascii format, at a resolution of 0.04166667 degrees;
- The digital elevation model sampled at a resolution of 0.04166667 degrees;
- A text file "PCadiagnosis.txt" containing the standard deviation, the percentage of variance explained and the cumulative variance of each Principal Component.

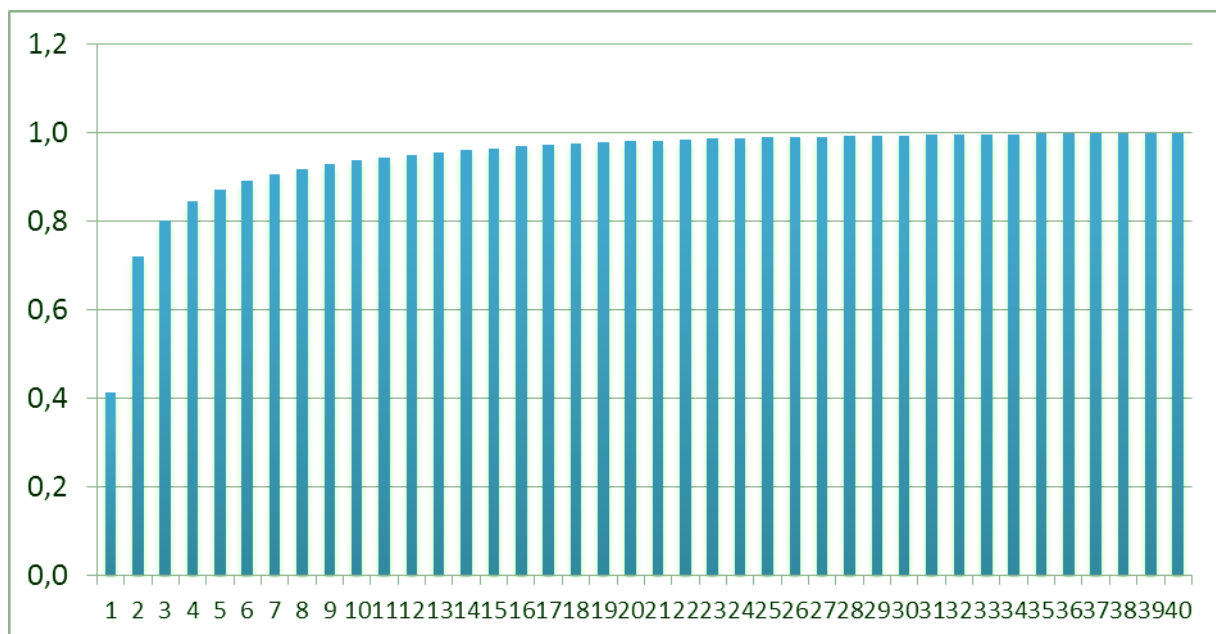


**Figure 15 : Cumulated contribution of the 40 Principal Components (%) to the total variance.**

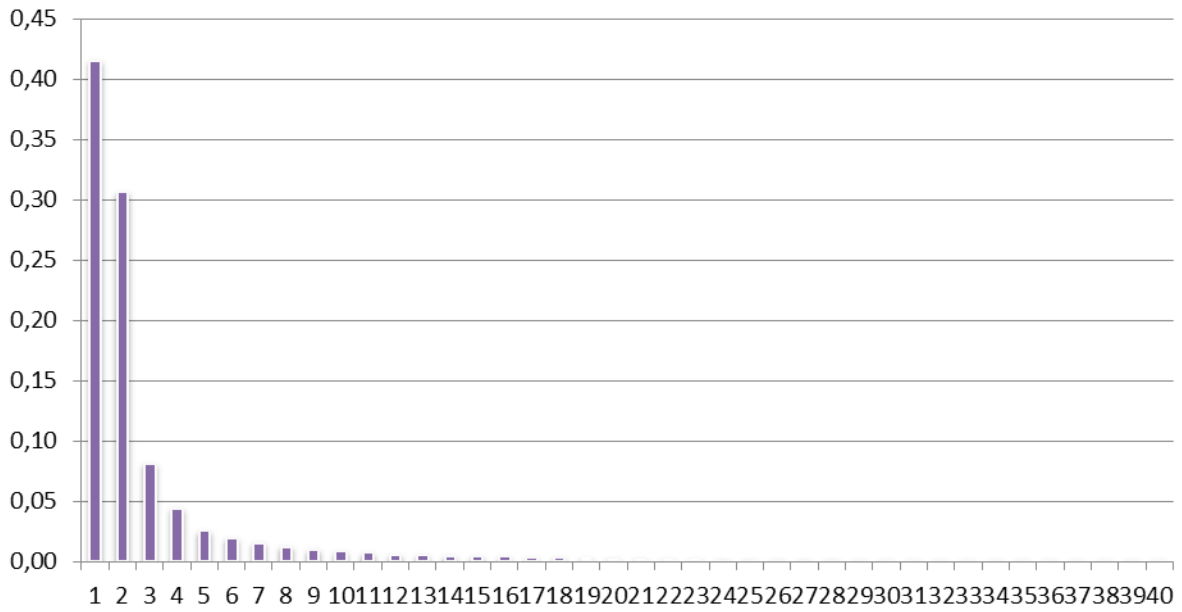


**Figure 16 : Contribution (%) of each Principal Component to the total variance.**

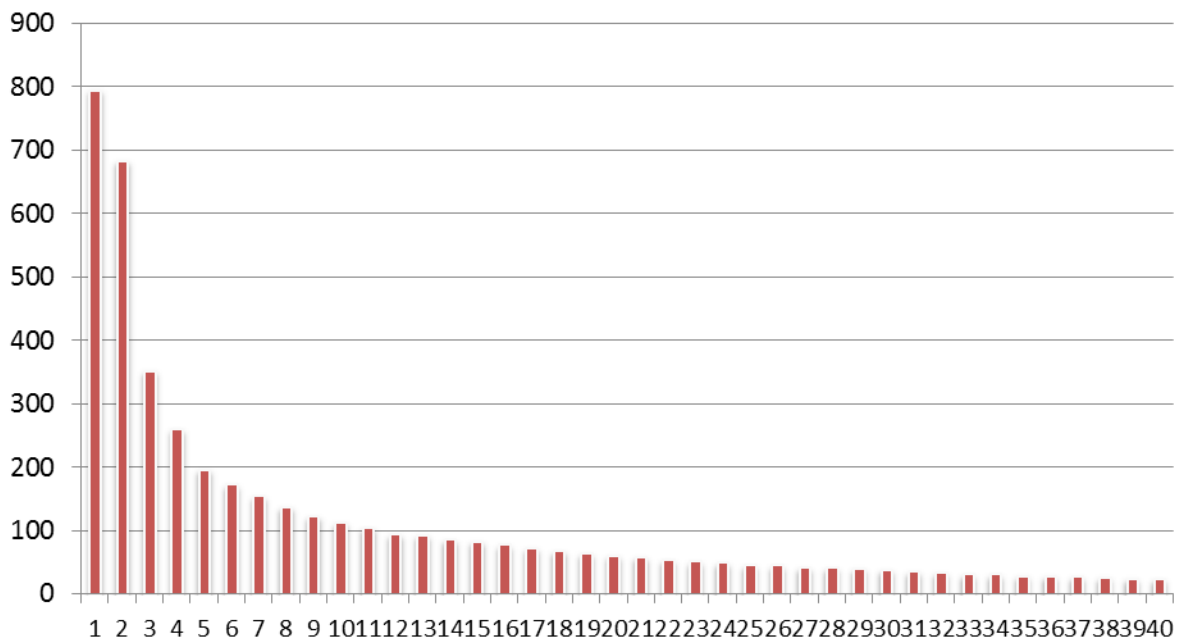








**Figure 17 : Standard deviation in (m) of each Principal Component.**



### 1.3.3. Preliminary analysis and interpolation

Several experiments were performed to adjust the regression models and the variogram. The following Table 3 lists the experiments used to interpolate the current climate variables : Tmin, Tmax and rainfall, at monthly and decadal time step. The variograms are listed in Table 4 to Table 9. It should be noted that during the preliminary analysis it was necessary to select the setting that allows for the best compromise between regression performance and the variogram. The difficulty was for Tmax and Tmin, when stations of Sidi Ifni and Casa Anfa which are close to Casablanca Nouacer and Guelmim, respectively, produce a noise on small distances.

**Table 3: List of experiments used to interpolate the current climate variables (Tmin, Tmax and rainfall).**

Name	parameter	Finished	
grid_precip_month_tarik_dmn_exp40pca_sill0.4r2.5n0.02_bis0	Monthly RR	21-11-2013 12:16	
grid_logprecip_tarik_dmn_exp40pca_sill1r4n0_bis01	Dekadal RR	21-11-2013 14:15	
grid_tmax_month_tarik_dmn_exp40pca_sill1r4n0_sidiifni_bis	Monthly Tmax	29-11-2013 17:34	
grid_tmin_month_tarik_dmn_exp40pca_sill1r4n0sidiifnicasanfa_bis	Monthly Tmin	02-12-2013 14:29	
grid_tmin_tarik_dmn_exp40pca_sill1r4n0outliersidiifnicasanfa_bis	Dekadal Tmin	03-12-2013 16:35	
grid_tmax_tarik_dmn_exp40pca_sill1r4n0outlier2sidiifnicasanfa_bis	Dekadal Tmax	04-12-2013 16:37	

**Table 4 : Details of the experiment used for interpolating the dekadal rainfall.**

Parameter	Experience	Performance of the regression	Variogram
<b>Dekadal RR</b>	step 5 varname "prec" log10 TRUE nbofPC 40 psill 1 type "Sph" range 4 nugget 0 anisotropy1 -9999 anisotropy2 -9999	"Percentage of significant model 98.3" "Percentage of non-significant model 1.7" "Percentage of normal residuals 66.2" "Percentage of non-normal residuals 33.8"	

**Table 5 : Details of the experiment used for interpolating the monthly rainfall.**

Parameter	Experience	Performance of the regression	Variogram
<b>Monthly RR</b>	step 5 log10 FALSE nbofPC 40 psill 1 type "Sph" range 4 nugget 0 anisotropy1 -9999 anisotropy2 -9999	""Fisher test: the model is significant if the p-value >= 5%)" "Percentage of significant model 99.7" "Percentage of non-significant model 0.3" "Shapiro-Wilk test of normality for	

		the residuals"	
		"Percentage of normal residuals	
		70.9"	
		"Percentage of non-normal residuals	
		29.1"	

**Table 6 : Details of the experiment used for interpolating the dekadal minimum temperature.**

Parameter	Experience	Performance of the regression	Variogram
<b>Dekadal Tmin</b>	step 5 varname "tmin" log10 FALSE nbofPC 40 psill 1 type "Sph" range 10 nugget 1 anisotropy1 -9999 anisotropy2 -9999 Sans SIDI IFNI et CASA ANFA	"Fisher test: the model is significant if the p-value $\geq 5\%$ " "Percentage of significant model 100" "Percentage of non-significant model 0" "Shapiro-Wilk test of normality for the residuals" "Percentage of normal residuals 89.4" "Percentage of non-normal residuals 10.6"	

**Table 7 : Details of the experiment used for interpolating the monthly minimum temperature.**

Parameter	Experience	Performance of the regression	Variogram
<b>Monthly Tmin</b>	step 5 varname "tmin" log10 FALSE nbofPC 40 psill 1 type "Sph" range 4 nugget 0 anisotropy1 -9999 anisotropy2 -9999 Sans casa anfa et sidi ifni	"Fisher test: the model is significant if the p-value $\geq 5\%$ " "Percentage of significant model 100" "Shapiro-Wilk test of normality for the residuals" "Percentage of normal residuals 94.1" "Percentage of non-normal residuals 5.9"	

**Table 8 : Details of the experiment used for interpolating the dekadal maximum temperature.**

Parameter	Experience	Performance of the regression	Variogram
<b>Dekadal Tmax</b>	step 5 varname "tmax" log10 FALSE nbofPC 40 psill 1 type "Sph" range 4 nugget 0 anisotropy1 -9999 anisotropy2 -9999 Sans SIDI IFNI	"Fisher test: the model is significant if the p-value $\geq 5\%$ "  "Percentage of significant model 99.9"  "Percentage of non-significant model 0.1"  "Shapiro-Wilk test of normality for the residuals"  "Percentage of normal residuals 92.6"  "Percentage of non-normal residuals 7.4"	

**Table 9 : Details of the experiment used for interpolating the monthly maximum temperature.**

Parameter	Experience	Performance of the regression	Variogram
<b>Monthly Tmax</b>	step 5 varname "tmax" log10 FALSE nbofPC 40 psill 1 type "Sph" range 4 nugget 0 anisotropy1 -9999 anisotropy2 -9999 Sans SIDI IFNI	"Fisher test: the model is significant if the p-value $\geq 5\%$ "  "Percentage of significant model 100"  "Percentage of non-significant model 0"  "Shapiro-Wilk test of normality for the residuals"  "Percentage of normal residuals 91.9"  "Percentage of non-normal residuals 8.1"	

The **"data interpolation / interpolation from a preliminary analysis"** function allows to generate the grids, based on the experiences and choices made during the preliminary analysis. The climatologist has to select some additional options such as filtering to mitigate the digital anomalies. The results are in ARCGIS ASCII format grids with a text file that describes the details of the interpolation for the entire current period. Table 10 list the details of the filtering options for each interpolated parameter.



**Table 10 : Filtering options used for each climate interpolated variable.**

<b>parameter</b>	<b>Filtering option</b>	
<b>Dekadal RR</b>	filter	TRUE
	factor	1.2
	threshold	200
	maxiter	3
	maxvalue	500
	minvalue	0.0
<b>Monthly RR</b>	filter	TRUE
	factor	1.2
	threshold	500
	maxiter	3
	maxvalue	1500
	minvalue	0.0
<b>Dekadal Tmin</b>	filter	TRUE
	factor	1.2
	threshold	-20.0
	maxiter	3
	maxvalue	50
	minvalue	-30.0
<b>Monthly Tmin</b>	filter	TRUE
	factor	1.2
	threshold	-20.0
	maxiter	3
	maxvalue	50
	minvalue	-30.0
<b>Dekadal Tmax</b>	filter	TRUE
	factor	1.2
	threshold	-1.0
	maxiter	3
	maxvalue	58
	minvalue	-20.0
<b>Monthly Tmax</b>	filter	TRUE
	factor	1.2
	threshold	-1.0
	maxiter	3
	maxvalue	58
	minvalue	-20.0

Figure 18 shows that the sample of the Principal Components, at the level of the 39 synoptic stations, represents only a relatively small part of the total distribution of these components. The regression equations used will be therefore extrapolated to areas where the values of the predictors exceed the ranges of data that were used to calibrate the model. Indeed, this numerical anomaly is often detected in the desert areas of the country.

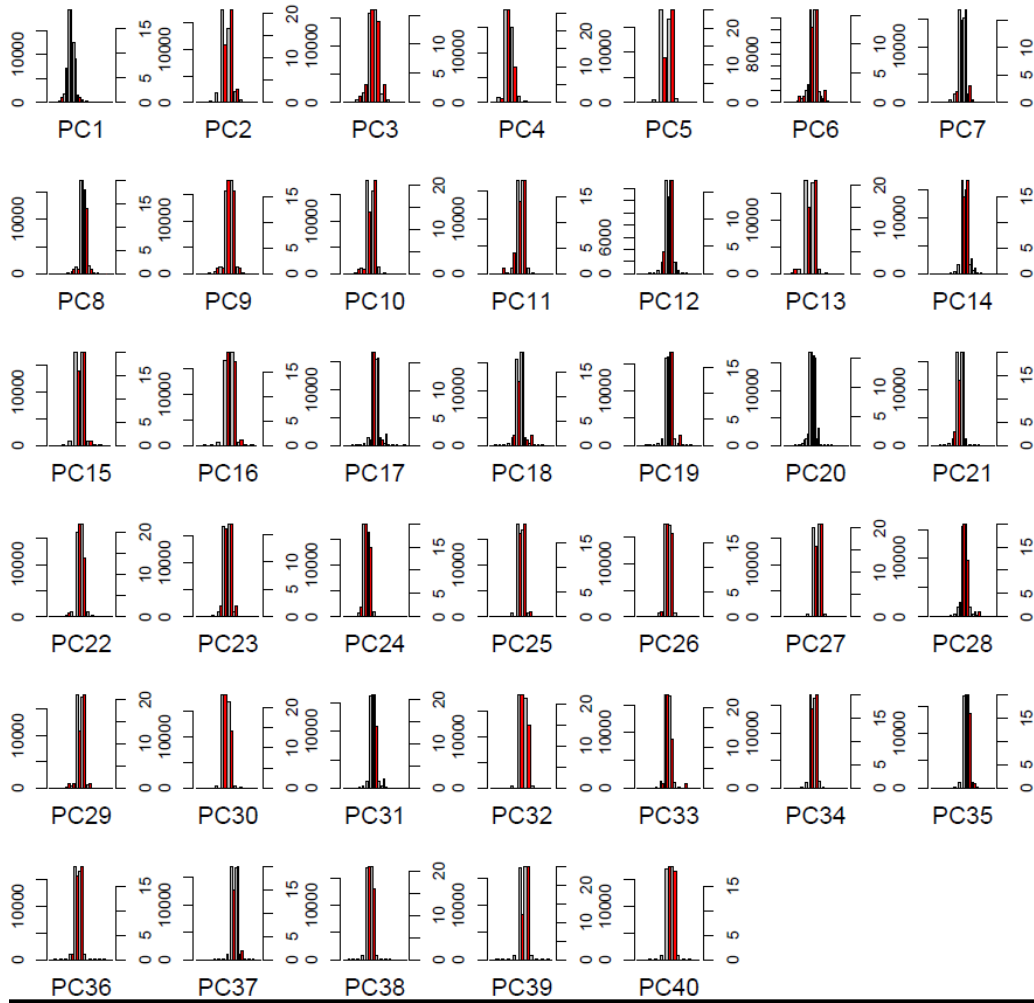


**Figure 18 : Distribution of PCA by synoptic station of DMN.**

### 1.3.4. Interpolation of PET

The potential evapotranspiration (PET) variable is calculated directly from the grids of Tmax and Tmin. The Hargreaves formula was used for this purpose. The function used is "**HAGREAVES PET / WORK MODE / GRID**".

## 2. Downscaling climate projections

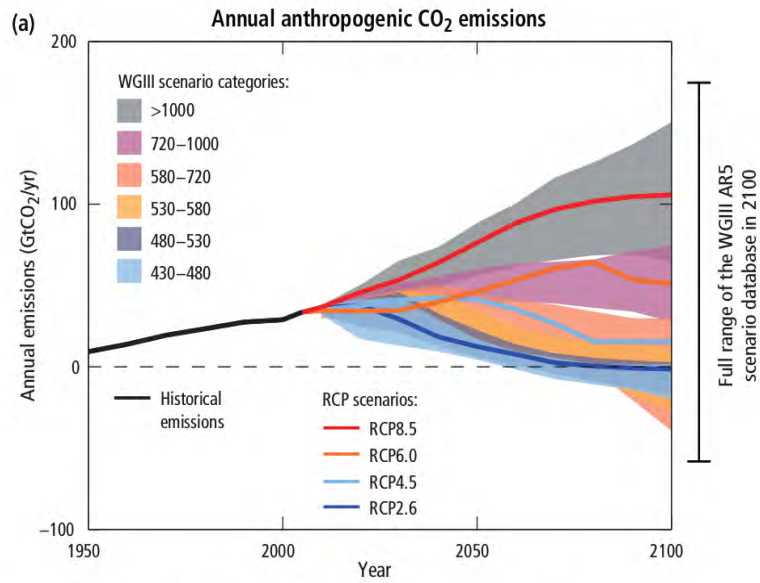
The statistical downscaling allows adapting the outputs of global climate models which are of very low resolution.

Following publication of the fifth report of the IPCC (2013), it was decided to use CMIP5 models available in the portal "Statistical Downscaling" (SD) (Table 11).

**Table 11 : CMIP5 list of models available in the SD portal.**

Model	Spatial resolution	Origin
<b>CanESM2</b>	2,8° x 2,8°	Canada
<b>CNRM-CM5</b>	1,4° x 1,4°	France
<b>HadGEM2-ES</b>	1,875° x 1,25°	UK
<b>IPSL-CM5-MR</b>	1,5° x 1,27°	France
<b>MIROC-ESM</b>	2,8° x 2,8°	Japan
<b>MPI-ESM-LR</b>	1,8° x 1,8°	Germany
<b>NorESM1-M</b>	1,5° x 1,9°	Norway

Another feature of the 5th IPCC report is the use of new scenarios for the trajectories of greenhouse gases emissions (Figure 19). In this report, the scientific community has developed a set of four new scenarios, called "Representative Concentration Pathways" (RCP). They are identified by their total radiative forcing approximate to the year 2100, compared to 1750: 2.6 W/m<sup>2</sup> for RCP2.6, 4.5 W/m<sup>2</sup> for RCP4.5, 6.0 W/m<sup>2</sup> for RCP6 and 8.5 W/m<sup>2</sup> for RCP8.5. These values should be taken as an indication. These four scenarios include a mitigation scenario leading to a very low level forcing (RCP2.6), two stabilization scenarios (RCP4.5 and RCP6.0), and a scenario with very high greenhouse gas emissions (RCP8.5). The global surface temperature change by the end of the 21<sup>st</sup> century is likely to exceed 1.5°C from 1850 to 1900 for all scenarios except for RCP2.6 scenario. It is likely to exceed 2°C and RCP6.0 and RCP8.5, and not likely to exceed 2°C for RCP4.5. The warming will continue beyond 2100 in all scenarios except for RCP2.6. The warming will continue to present a decadal variability and will not be uniform at the regional level. In the SD portal, two scenarios are available RCP8.5 and RCP4.5.



(b) Warming versus cumulative CO<sub>2</sub> emissions

**Figure 19 : Representative Concentration Pathways (RCP) scenarios (IPCC, 2015).**

The re-analysis model used is "ERA\_Interim\_DM". It offers the possibility of selecting atmospheric predictor variables aggregated to daily scale. The method chosen to perform downscaling is based on similarity analysis, of a selection of atmospheric variables that come from the re-analysis. It consists in finding the nearest weather situation (nearest' neighbors) to infer climate variables at stations level.

**Table 12 : List of atmospheric variables available in the SD, in relation with CMIP5.**

Variable	Levels	Times	Units	Temporal aggregation
<b>U velocity</b>	250 500 700 850 1000	-	m s <sup>-1</sup>	Daily Mean
<b>Specific humidity</b>	250 500 700 850 1000	-	kg kg <sup>-1</sup>	Daily Mean
<b>Mean Sea Level Pressure</b>	0	-	Pa	Daily Mean
<b>2m Temperature</b>	0	-	K	Daily mean
<b>V velocity</b>	250 500 700 850 1000	-	m s <sup>-1</sup>	Daily Mean
<b>Minimum Temperature</b>	0	-	K	Daily minimum value
<b>Geopotential</b>	250 500 700 850 1000	-	m <sup>2</sup> s <sup>-2</sup>	Daily Mean
<b>SSTd</b>	0	12		Instantaneous
<b>Maximum</b>	0	-	K	Daily maximum

<b>Temperature</b>				value
<b>Temperature</b>	250 500 700 850 1 000	-	K	Daily Mean
<b>Total Precipitation</b>	0	-	m	Daily accumulated value

## 2.1. Validation

Each downscaling experience is automatically associated with a validation procedure. The validation is based on the separation of the of the observed data, in two parts: a learning sample and a testing sample. The latter comprises 25% of the total data of the series. Needless to say, the series dedicated to the test is not used for calibration. Therefore, the model built is extrapolated to produce future projections. The SD portal traces the validation results of each validation experiment in an Excel file and a PDF report. The experience which leads the best compromise between "accuracy" and "reliability" at daily and dekadal time step is selected. To do this, several statistics are calculated and the experiences that give the highest scores based on the correlation coefficient of Pearson, the PDF score and KS-pvalue (priority to dekadal time step) is selected.

## 2.2. Loading future time series from SD portal to the MOSAICC system

The Table 13 lists the generated series, after execution of validated SD. The time step of the series is daily and the import to MOSAICC handles aggregation at dekadal and monthly time step.

**Table 13 : List of identifiers of future climate time series imported from the SD portal to MOSAICC.**

Period	Scenario	Predictor	CanES M2	CNR M-CM5	GFDL-ESM2M	IPSL-CM5A-MR	MIR-OC-ESM	MPI-ESM-LR
1971 - 1981	historical_r1-ilp1	cmip_5_tes_02_rr <sup>3</sup>	19773	19774	19777	19781	19785	19786
		cmip_5_test_Temp_Tmax <sup>4</sup>	20292	20049	20050	20051	20052	20307

3Cmip\_5\_tes\_02\_rr for rainfall

4cmip\_5\_test\_Temp\_Tmax for maximum temperature

		cmip_5_test_Temp_Tmin <sup>5</sup>	20054	20055	20058	20062	20063	20066
1981-1991		cmip_5_test_02_rr	19775	19778	19779	19782	19787	19790
		cmip_5_test_Temp_Tmax	20293	20294	20295	20296	20297	20298
		cmip_5_test_Temp_Tmin	20056	20059	20060	20064	20067	20068
1991-2001		cmip_5_test_02_rr	19776	19780	19783	19784	19788	19792
		cmip_5_test_Temp_Tmax	20300	20301	20302	20303	20304	20305
		cmip_5_test_Temp_Tmin	20057	20061	20053	20065	20069	20072
2010-2020	rcp45_r1i1p1	cmip_5_test_02_rr	19798	19803	19814	19818	19822	19826
		cmip_5_test_Temp_Tmax	20237	20238	20239	20240	20241	20242
		cmip_5_test_Temp_Tmin	20074	20082	20090	20175	20102	20103
	rcp85_r1i1p1	cmip_5_test_02_rr	19830	19834	19838	19842	19846	19850
		cmip_5_test_Temp_Tmax	20183	20184	20185	20186	20187	20188
		cmip_5_test_Temp_Tmin	20120	20121	20122	20123	20124	20125
2020-2030	rcp45_r1i1p1	cmip_5_test_02_rr	19799	19805	19815	19819	19823	19827
		cmip_5_test_Temp_Tmax	20243	20244	20245	20246	20247	20248
		cmip_5_test_Temp_Tmin	20075	20083	20091	20176	20104	20105
	rcp85_r1i1p1	cmip_5_test_02_rr	19831	19835	19839	19843	19847	19851
		cmip_5_test_Temp_Tmax	20189	20190	20191	20192	20193	20194
		cmip_5_test_Temp_Tmin	20126	20127	20128	20129	20130	20137
2030-2040	rcp45_r1i1p1	cmip_5_test_02_rr	19800	19807	19816	19820	19824	19828
		cmip_5_test_Temp_Tmax	20249	20250	20251	20252	20253	20254
		cmip_5_test_Temp_Tmin	20076	20084	20092	20177	20106	20107
	rcp85_r1i1p1	cmip_5_test_02_rr	19832	19836	19840	19844	19848	19852
		cmip_5_test_Temp_Tmax	20195	20196	20197	20198	20199	20200
		cmip_5_test_Temp_Tmin	20132	20133	20134	20135	20136	20137
2040-	rcp45_r1i1p1	cmip_5_test_02_rr	19801	19809	19817	19821	19825	19829

5cmip\_5\_test\_Temp\_Tmin for minimum temperature

205 0		cmip_5_test_Temp_	20255	2025	2025	2025	2025	202
		Tmax		6	7	8	9	60
		cmip_5_test_Temp_	20077	2008	2009	2017	2010	201
		Tmin		5	3	8	8	09
	rcp85_r1i1p	cmip_5_tes_02_rr	19833	1983	1984	1984	1984	198
			7	1	5	9	53	
		cmip_5_test_Temp_	20201	2020	2020	2020	2020	202
		Tmax		2	3	4	5	06
		cmip_5_test_Temp_	20138	2013	2014	2014	2014	201
		Tmin		9	0	1	2	43
205 0 - 206 0	rcp45_r1i1p	cmip_5_tes_02_rr	19977	1998	1998	1999	1999	200
				5	9	3	7	05
		cmip_5_test_Temp_	20261	2026	2026	2026	2026	202
				2	3	4	5	66
		cmip_5_test_Temp_	20078	2008	2009	2017	2011	201
		Tmin		6	8	9	0	11
rcp85_r1i1p	cmip_5_tes_02_rr	20013	2001	2002	2002	2003	200	
			7	1	5	3	37	
	cmip_5_test_Temp_	20207	2020	2020	2021	2021	202	
				8	9	0	1	12
	cmip_5_test_Temp_	20144	2014	2014	2014	2014	201	
	Tmin		5	6	7	8	49	
206 0 - 207 0	rcp45_r1i1p	cmip_5_tes_02_rr	19978	1998	1999	1999	2000	200
				6	0	4	1	06
		cmip_5_test_Temp_	20267	2026	2026	2027	2027	202
				8	9	0	1	72
		cmip_5_test_Temp_	20079	2008	2009	2018	2011	201
		Tmin		7	9	0	2	13
rcp85_r1i1p	cmip_5_tes_02_rr	20014	2001	2002	2002	2003	200	
			8	2	9	4	38	
	cmip_5_test_Temp_	20213	2021	2021	2021	2021	202	
				4	5	6	7	18
	cmip_5_test_Temp_	20150	2015	2015	2015	2015	201	
	Tmin		1	2	3	4	55	
207 0 - 208 0	rcp45_r1i1p	cmip_5_tes_02_rr	19979	1998	1999	1999	2000	200
				7	1	8	2	07
		cmip_5_test_Temp_	20273	2027	2027	2027	2027	202
				4	5	6	7	78
		cmip_5_test_Temp_	20080	2008	2010	2018	2011	201
		Tmin		8	0	1	4	15
rcp85_r1i1p	cmip_5_tes_02_rr	20015	2001	2002	2003	2003	200	
			9	6	0	5	39	
	cmip_5_test_Temp_	20219	2022	2022	2022	2022	202	
				0	1	2	3	24
	cmip_5_test_Temp_	20156	2015	2015	2015	2016	201	
	Tmin		7	8	9	0	74	
208 0 - 209 0	rcp45_r1i1p	cmip_5_tes_02_rr	19980	1998	1999	1999	2000	200
				8	5	9	3	08
		cmip_5_test_Temp_	20279	2029	2028	2028	2028	202
				1	1	2	3	84
		cmip_5_test_Temp_	20081	2008	2010	2018	2011	201
		Tmin		9	1	2	6	18
rcp85_r1i1p	cmip_5_tes_02_rr	20016	2002	2002	2003	2003	200	
			3	7	1	6	41	
	cmip_5_test_Temp_	20225	2022	2022	2022	2022	202	



209 0 - 210 0		Tmax		6	7	8	9	30
		cmip_5_test_Temp_Tmin	20161	20162	20163	20164	20165	201666
	rcp45_r1i1p1	cmip_5_test_02_rr	19984	19992	19996	20000	20004	20009
		cmip_5_test_Temp_Tmax	20285	20286	20287	20288	20289	202890
		cmip_5_test_Temp_Tmin	20094	20095	20096	20097	20117	20119
		rcp85_r1i1p1	cmip_5_test_02_rr	20020	20024	20028	20032	20040
		cmip_5_test_Temp_Tmax	20231	20232	20233	20234	20235	202336
		cmip_5_test_Temp_Tmin	20167	20168	20169	20170	20171	201772

## IV. AGRONOMIC COMPONENT

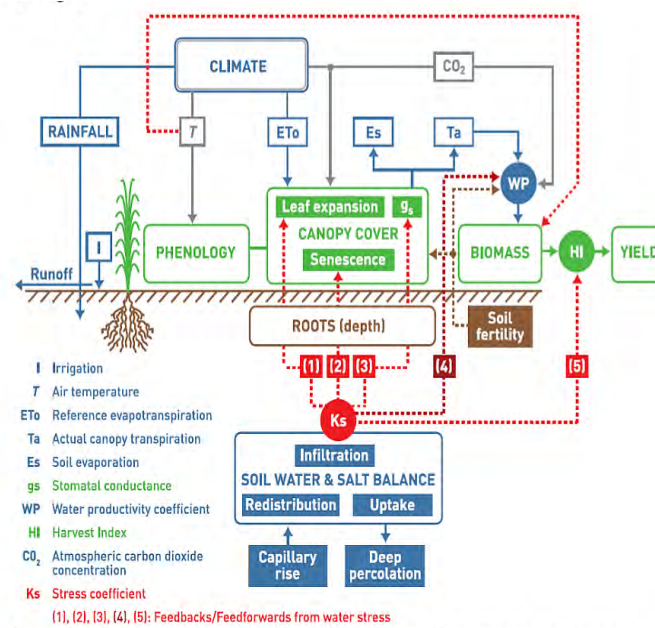


Photo INRA-Morocco

Cereals are produced in all over the country and, mainly in rainfed areas except in El Jadida province which is irrigated. Cereals occupy nearly two thirds of agricultural lands. They are grown on a wide range of environments: oasis (area insignificant), low rainfall (arid and semi-arid, 40% area), high rainfall (sub-humid and humid, 40% area), irrigated (10% area) and mountainous areas (10% area) and on a variety of soils and production systems. Cereals are part of almost all practiced rotations, in addition to cereals planted after cereals. Production is highly influenced by rainfall amount and distribution, varying from 1.7 million metric tons registered during 1995 cropping season to 9.7 registered the subsequent season.

The agronomic component allows the simulation of cereal yields based on FAO's AquaCrop model (version 4.0), using historical ( ) and projected (2010-2099) climatic data. AquaCrop was is an improvement of the previous Doorenbos and Kassam (1979) approach<sup>6</sup>, which assumes that yield (Y) is a factor of evapotranspiration (ET). In summary, in AquaCrop ET is divided into in soil evaporation (E) and crop transpiration (Tr), so as to avoid the confounding effect of the non-productive consumptive use of water (E). The biomass (B) is the product of water productivity (WP) and cumulated crop transpiration. Finally, yield (Y) is the product of B and Harvest Index (HI). The schematic representation of AquaCrop processes is in Figure 20.

6 See description: <http://www.fao.org/nr/water/docs/stedutoetal2008.pdf>



**Figure 20 : AquaCrop flowchart indicating the main components of the soil-plant-atmosphere continuum<sup>7</sup>.**

## 1. Calibration of AquaCrop for rainfed areas

### 1.1. Calibration of AquaCrop for rainfed wheat

AquaCrop has been calibrated for wheat in rainfed areas of Beni Mellal province of Morocco, using historical official survey data collected by the Ministry of Agriculture, from 1981 to 2010 (29 cropping seasons). These datasets are compiled from sub-province sample surveys and released in official documents as provincial averages (Balaghi, 2013<sup>8</sup>).

As reported in Figure 21, observed grain yields are highly variables across seasons, from 0.04 to 1.8 tons/hectare, mainly due to rainfall variability. The correlation between simulated (AquaCrop) and observed yields is satisfactory ( $R^2=0.51$ ). Correlation errors could be partially explained by inconsistencies in determining planting dates from the historical database.

<sup>7</sup> See: <http://www.fao.org/nr/water/aquacrop.html>

<sup>8</sup> See: <http://www.inra.org.ma/publications/ouvrages/prediction1113en.pdf>

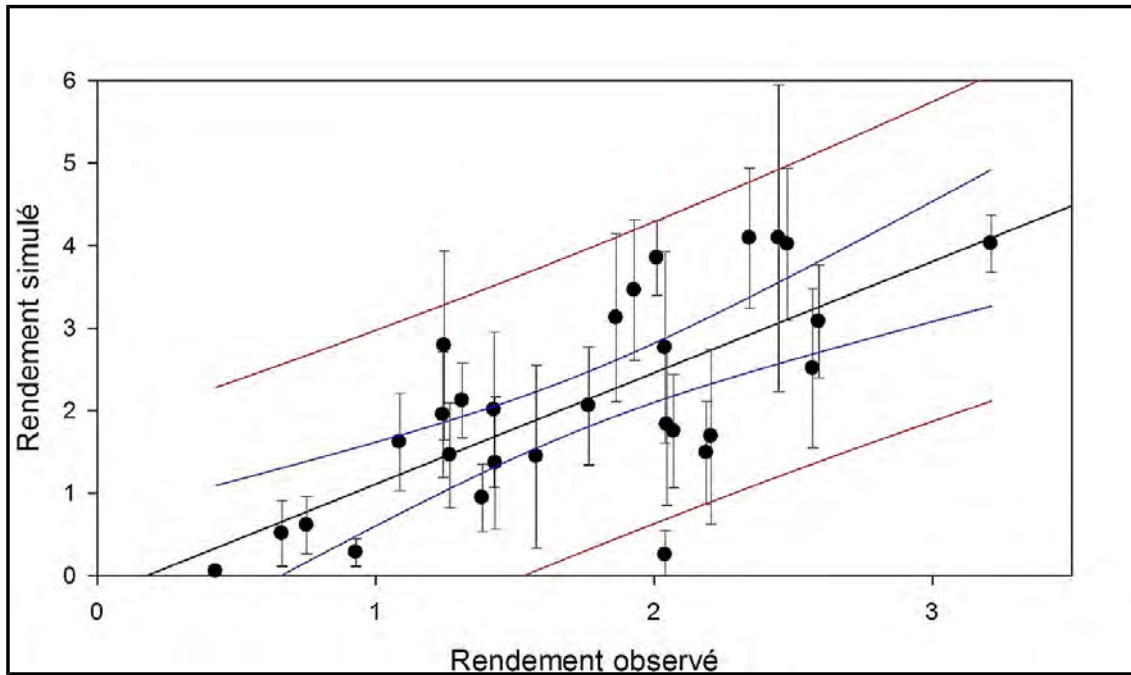


**Figure 21 : Simulated (AquaCrop) and observed official wheat grain yields (tons/ha), from 1981 to 2010 cropping seasons in Beni Mellal province.**

### **1.2. Calibration of AquaCrop for rainfed barley**

AquaCrop has been also calibrated for barley in rainfed areas of Fes, Safi and Meknes provinces of Morocco, using historical official survey data collected by the Ministry of Agriculture, from 1981 to 2010 (29 cropping seasons) (Figure 22). The correlation between simulated and observed yields is high ( $R^2=0.56$ ), but some outliers are persistent due to within-season rainfall variability and inconsistencies in determining planting dates from the historical database.

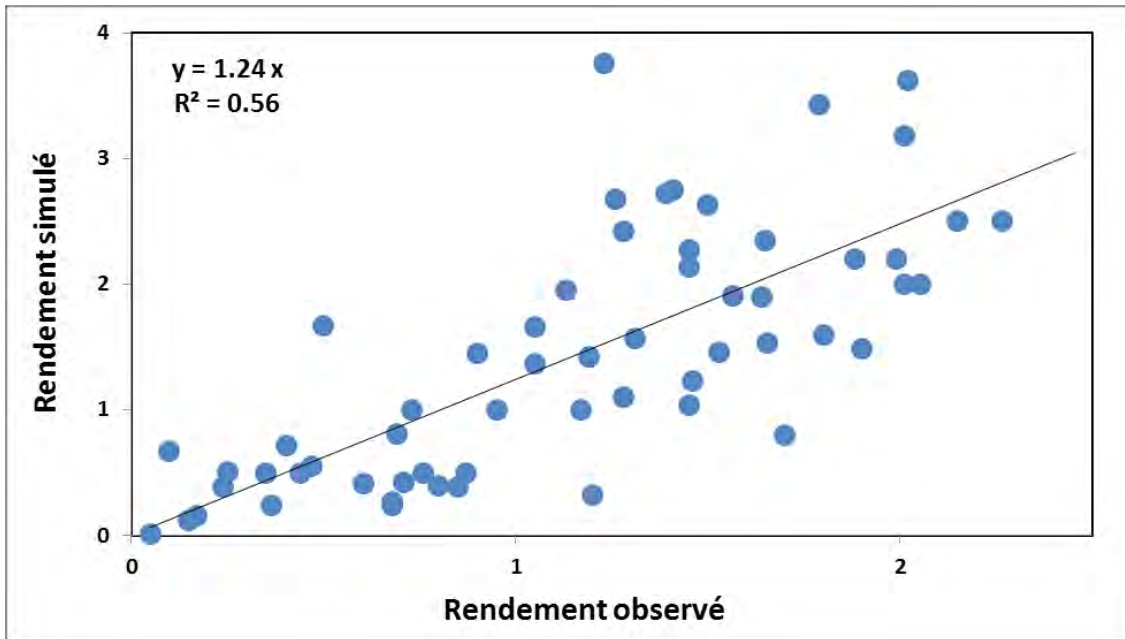


**Figure 22 : Simulated (AquaCrop) and observed official barley grain yields (tons/ha), from 1981 to 2010 cropping seasons in Fes, Safi and Meknes provinces.**

### **1.3. Prediction of wheat and barley yields in rainfed areas**

Based on the performed calibrations, AquaCrop has been used to simulate wheat and barley grain yields in rainfed areas at the level of all provinces of Morocco, for the period 2010-2099. Climatic models CanESM2, MIROC-ESM and MPI-ESM-LR and scenarios RCP4.5 and RCP8.5 has been considered. Simulations for the case of five of the main agricultural provinces (Chichaoua, Beni Mellal, Settat, Rabat and Fes) are presented below. These provinces can be representative of all agro-ecological zones of Morocco, ranging from arid to sub-humid climate.

#### **1.3.1. Prediction of wheat yields**

Predicted yields for the period 2010-2099 for the average of the three models CanESM2, MIROC-ESM and MPI-ESM-LR, and according to scenario RCP4.5 are presented in Figure 23. Simulations show decreasing wheat yields in rainfed areas for the five selected provinces of Morocco, especially in the two semi-arid and sub-humid provinces (Rabat and Fes), with high season to season variability (28 to 59%).

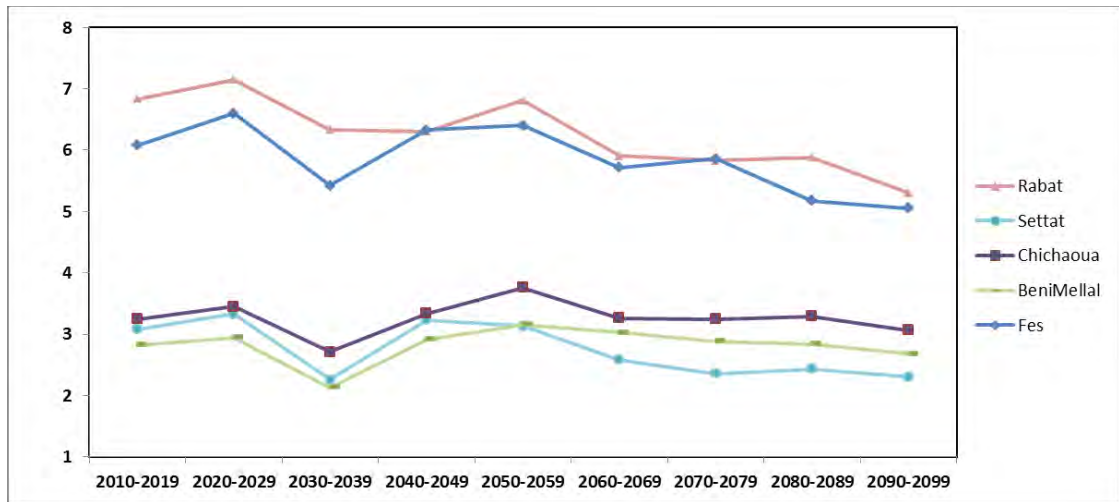


**Figure 23 : Predicted wheat yields (tons/ha) for the period 2010-2009, for the average of the models CanESM2, MIROC-ESM and MPI-ESM-LR, and according to scenario RCP4.5.**

Predictions for the average of the three models and for scenario RCP8.5 show accentuated decreasing wheat yields towards the end of the century, especially in the sub-humid provinces of Fes and Rabat (Figure 24). The season to season variability is higher than for RCP4.5 (30 to 100%).

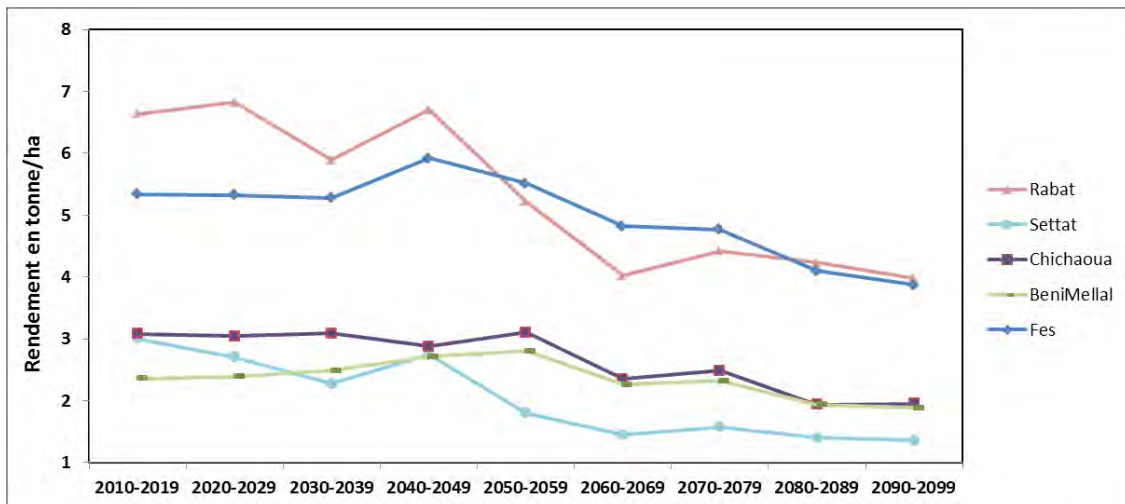


**Figure 24 : Predicted wheat yields (tons/ha) for the period 2010-2009, for the average of the models CanESM2, MIROC-ESM and MPI-ESM-LR, and according to scenario RCP8.5.**



### 1.3.2. Prediction of barley yields

Predicted yields for the period 2010-2099 for the average of the three models CanESM2, MIROC-ESM and MPI-ESM-LR, and according to scenario RCP4.5 are presented in Figure 25. Simulations show decreasing barley yields in rainfed areas for the five selected provinces of Morocco, especially in the two semi-arid and sub-humid provinces (Rabat and Fes), with high season to season variability (30 to 80%).

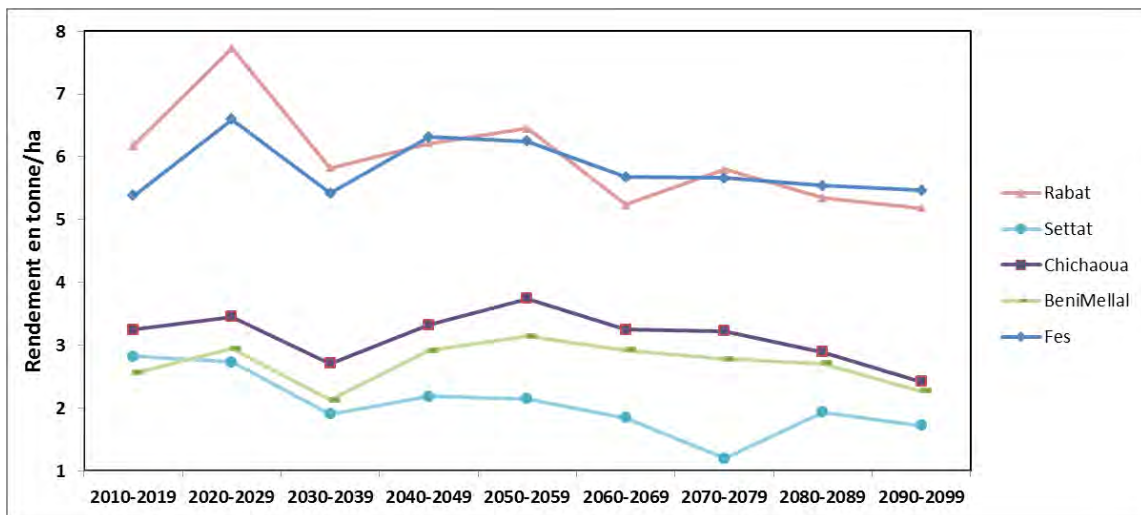


**Figure 25 : Predicted barley yields (tons/ha) for the period 2010-2099, for the average of the models CanESM2, MIROC-ESM and MPI-ESM-LR, and according to scenario RCP4.5.**

Predictions for the average of the three models and for scenario RCP8.5 show accentuated decreasing barley yields towards the end of the century, especially in the sub-humid provinces of Fes and Rabat (Figure 26). The season to season variability is higher than for RCP4.5 (44 to 120%).



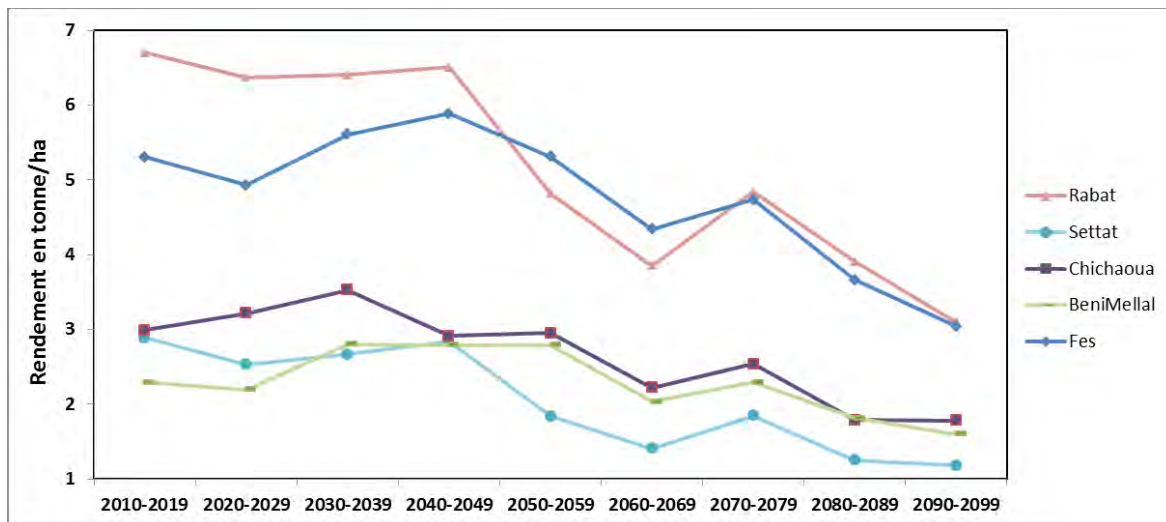


**Figure 26 : Predicted barley yields (tons/ha) for the period 2010-2009, for the average of the models CanESM2, MIROC-ESM and MPI-ESM-LR, and according to scenario RCP8.5.**

## 2. Calibration of AquaCrop for irrigated areas

AquaCrop has been calibrated also for irrigated durum wheat, using field sample data collected in the irrigated plain of Tadla region. Data collected are grain yield, biomass and soil water content (0-90cm), for the five cropping seasons from 2009 to 2012 (Figure 27).

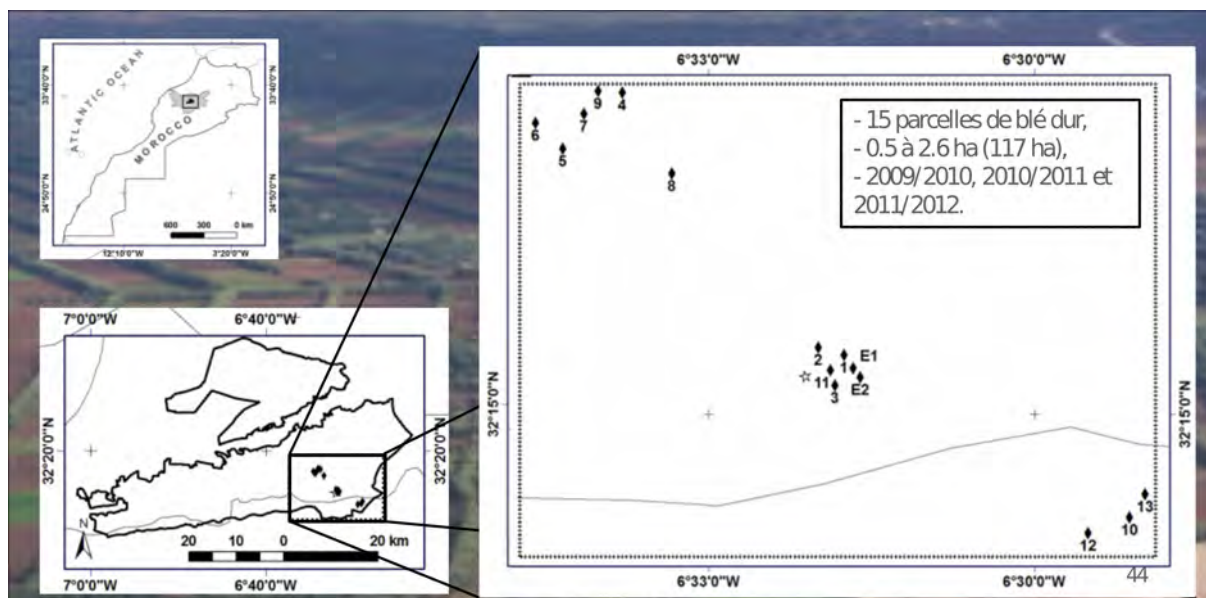


**Figure 27 : Location of experimental sites in the irrigated plain of Tadla.**

Results show high agreement between simulated and observed yield, with RMSE ranging from 4,06% (0.2 t.ha<sup>-1</sup>) to 5,71% (0.82 t.ha<sup>-1</sup>), respectively for grain and above biomass yields (Figure 28).

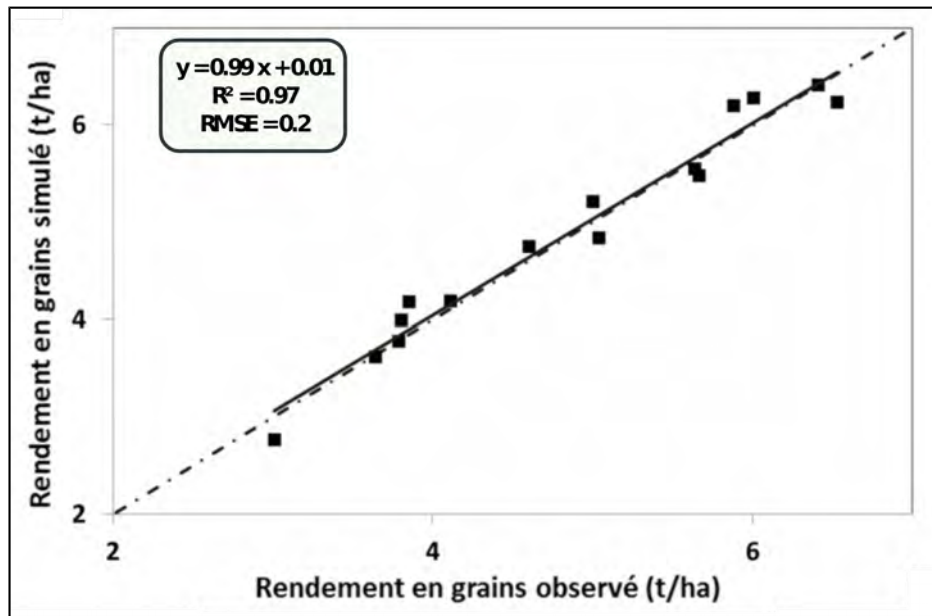
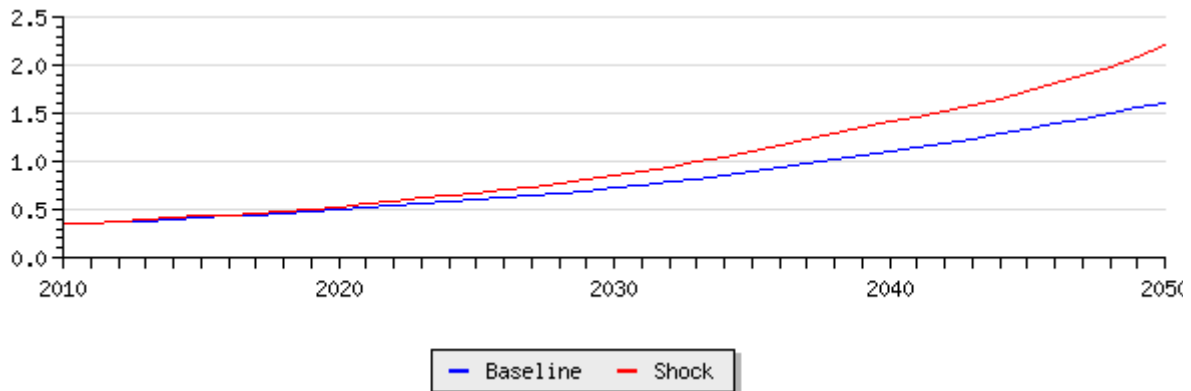


**Figure 28 : Simulated and observed durum wheat grain yields in irrigated area of Tadla plain.**

## V. ECONOMIC COMPONENT



The MOSAICC system comprises a set of components to carry out each step of the impact assessment from climate scenarios downscaling to economic impact analysis. The four main components of the methodology are a statistical downscaling method for processing GCM output data, a hydrological model for estimating water resources for irrigation, a crop growth model to simulate future crop yields and finally a Dynamic Computable General Equilibrium (DCGE) model to assess the effect of changing yields on national economies.

The software used to develop and run the DCGE model is open source and multi-platform. The model is programmed in the modelling language Dynare and can be solved with GNU Octave, a high-level language, primarily intended for numerical computations. GNU Octave provides a convenient command line interface for solving linear and nonlinear problems numerically, and for performing other numerical experiments using a language that is mostly compatible with Matlab. GNU Octave is freely redistributable software.

In this chapter, the DCGE model is described and an illustrative simulation on the macro-economic impacts of crop yield changes under climate change is presented with real data. Section 1 presents a non-technical description of the DCGE model, discussing its structure, parameterization and its key input and output data. Section 2 presents the simulation of the macro-economic effects climate-change induced changes in crop yields on the Moroccan economy. Section 3 concludes and gives recommendations for further research and development. The Annexes 7 and 8 provide additional technical detail.

## 1. The DCGE Model

The economic model that is developed in this study is inspired by the IFPRI dynamic CGE model (Lofgren et al 2002; Thurlow, 2004). Our economic model, like the IFPRI model, is designed to represent African agriculture and the wider African economy. IFPRI has applied its model on various occasions to assess the economy-wide effects of climate variability in African countries (Thurlow et al., 2009; Pauw et al., 2010). Specific features of both the IFPRI model and our economic model are their ability to account for the fact that a share of farm production is directly consumed at the farm and thus does not reach the market, and the division of demand between “subsistence” demand that is income-independent and “luxury” demand that grows with income. To account for spatial or other variations in yield effects of climate change, commodities, such as wheat, can be produced with several activities. Such activities could, for example, be “wheat produced in a favorable agro-ecological zone” and “wheat produced in an unfavorable agro-ecological zone”. There could even be more “activities” producing one “commodity”, so the economic model could distinguish between more agro-ecological zones (AEZ), if data were available. The economic model can also distinguish between different crops, to the extent allowed by the data.

The economic model is a dynamic computable general equilibrium model. The central concept of such a model is “equilibrium”. In economics, equilibrium relates to the condition that supply equals demand in all markets; in equilibrium there is no excess demand – all markets clear. The equilibrium force is the price system. When the supply of a commodity goes down (e.g. the supply of wheat because of adverse weather conditions), its price tends to go up, thereby stimulating additional supply and depressing demand, until supply and demand are equal again. Note that this mechanism does not only operate on product markets, but also on factor markets (labor, capital), saving markets (value of savings equals the value of investments) and on the foreign exchange markets (value of imports equals value of exports). An additional equilibrium constraint is that there are no excess profits, i.e., the sales’ revenues of a product are totally exhausted by competitive payments to the factors of production, expenditure for intermediate inputs, and, possibly, taxes paid to the government.

The diagram in Figure 29 presents a schematic overview of the links between production and consumption in the economic model. It is perhaps most illuminating to think of a small region with two farms and one village where consumers live. The farms both produce the same product; let’s call it “food”. The consumers in the village earn their income by renting out capital to the farms and spend this income on the consumption of food. A part of the produced food is exported to a neighboring village in exchange for, say, fertilizer.

At the bottom of Figure 29, both farms (Farm 1 and Farm 2) use land, labor, capital and fertilizer (and intermediate input) to produce “food”. Part of the food is withheld at the farms for own (home) consumption. The remaining part is offered on the market and is labeled “aggregate quantity of domestic output” in the diagram in Figure 29. Part of this aggregate output is exported to the neighboring village in exchange for fertilizer (import). The other part is sold on the domestic market (“domestic supply to domestic market”). This domestic supply of food is combined with imported food (in our example the import of food is null) to form the “composite supply to the domestic market”. This composite supply is purchased by households for consumption and savings, and also possibly by the government who has no role in our example.

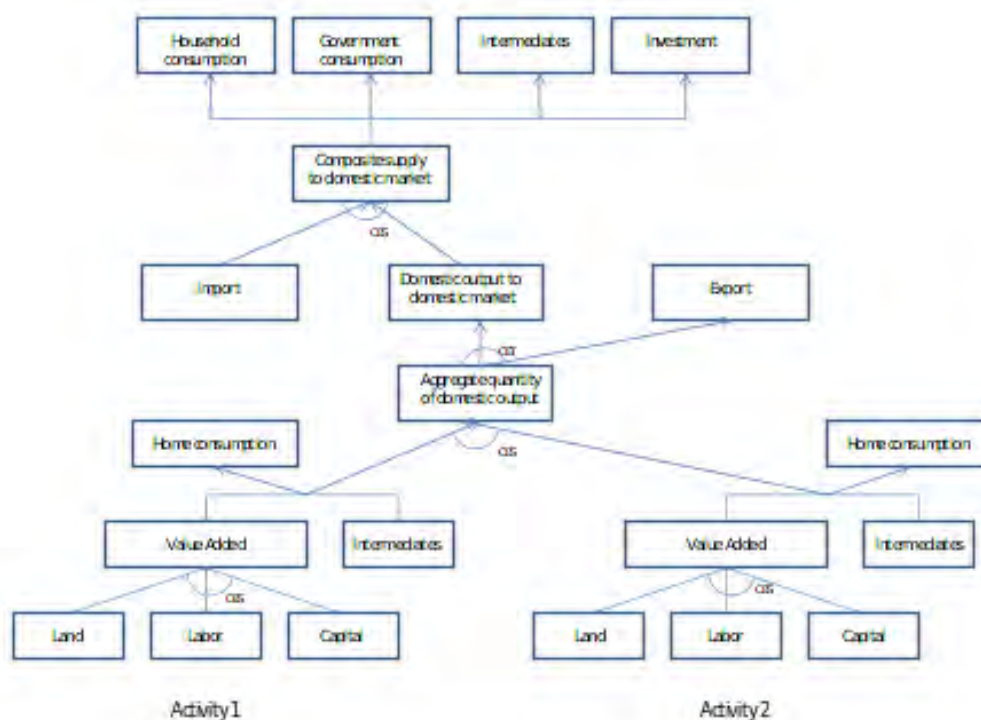


**Figure 29: Simplified production and demand structure of the economic model with one commodity produced by two activities.**

The production, consumption and exchange decisions of the different agents in the model (farms, households, government) are governed by relative prices. Throughout the mode it is assumed that agents are price-takers (the prices are “given” to them; they cannot influence them) and that, given the prevailing market prices, they aim to maximize their utility or profit. In Figure 1, important decision nodes are labeled by CES, CET, and LES. These acronyms refer to functions that specify by how much the

demanded or supplied quantity will change if the market price changes. For example, in the bottom of the diagram of Figure 29, a CES (Constant Elasticity of Substitution) function determines by how much the demand for labor will decrease by an activity when the price of labor increases relative to those of land and capital. A CET (Constant Elasticity of Transformation) function determines the share of the aggregate quantity of domestic output that is exported, based on the export price relative to the domestic market price. A LES (Linear Expenditure System) function determines the household demand, based on income and relative prices of the products that are offered for sale.

## 2. Input data

The economic model needs four types of input data:

- A specification of the **sets** of activities, commodities, institutions, and time periods;
- Benchmark data of all **variables** in the model;
- Parameter values for a number of **coefficients** of the model;
- Growth rates of **exogenous variables**;
- A spatial and temporal specification of the climate change **shocks** to yield productivity.

### 2.1. Sets and benchmark data of variables

The sets of activities, commodities, and institutions depend on the available benchmark data, so we discuss these two types of data in combination. The economic model has time steps of one year. The user is free to choose the number of years of the simulation.

The starting point for any CGE model is a set of benchmark data of the variables of the model in the form of a **Social Accounting Matrix (SAM)**. A SAM represents flows of all economic transactions in an economy over a specific period of time (usually a year). Table 14 below presents a simple and highly aggregated format of a SAM. The SAM is square. In its columns the SAM records how money is **spent**, in its rows it records how money is **earned**. Each entry should be read as a flow of money *from* the **column** header to the **row** header.



**Table 14: The format of a Social Accounting Matrix.**

	IMPORT	PROD ACTIVITY	DOM COMM	PROD FACTORS	TAXES	PRIV HOUSEH	GOVERNMENT	ROW	SAV/ INV	TOTAL
IMPORT										
PROD ACTIVITY										
DOM COMM										
PROD FACTORS										
TAXES										
PRIV HOUSEH										
GOVERNMENT										
ROW										
SAV/ INV										
TOTAL										

The rows of the SAM show how each activity and agents earns his money. For example imports are paid for by production activities (as intermediate goods), by private households and government (as final goods) and by the savings/investment sector (as investment goods). The other rows show how the other sectors earn money.

The 2010 SAM of Morocco for the MOSAICC DCGE model has been prepared by Moroccan experts in collaboration with IVM in March 2014. The monetary transactions in the SAM relate to the year 2010 and are expressed in billion (1,000 million) Dirham (MAD). The detailed SAM that is used for the calculations of the DCGE model has 50 rows and 50 columns.

The SAM includes data on 10 commodities: barley, wheat, legumes, olive, citrus, tomato, sugar, other agriculture, food, and other manufacturing and services. The SAM includes 15 activities, including wheat barley and olives produced in favourable and defourable regions, different qualities of tomatoes (*primeur* and *saison*), and sugar cane and beat. Table 15 below lists the commodities and activities included in the 2010 SAM.

The factors of production include ‘irrigation water’ whose volumes and values are based on Moroccan statistics. The valuation of irrigation water is based on tariffs for water abstraction that are applied in Moroccan agriculture.



**Table 15: Commodities and activities in the 2010 SAM.**

Commodities		Activities	
Name	Code	Name	Code
Barley	CBAR	Barley - Favorable Region	ABAR_FAV
		Barley - Unfavorable Region	ABAR_DEF
Wheat	CWHT	Wheat - Favorable Region	AWHT_FAV
		Wheat - Unfavorable Region	AWHT_DEF
Legumes	CLEG	Legumes	ALEG
Olive	COLV	Olive - Favorable Region	AOLV_FAV
		Olive - Irrigated	AOLV_DEF
Citrus	CCIT	Citrus	ACIT
Tomato	CTOM	Tomato Primeur	ATOMP
		Tomato Saison	ATOMS
Sugar	CSUG	Sugar beat	ASUGB
		Sugar cane	ASUGC
Other agriculture	CAGR	Other agriculture	AAGR
Food	CFOOD	Food	AFOOD
Other manufactures and services	COTH	Other manufactures and services	AOTH

## 2.2. Parameter values for coefficients

The economic model contains a number of coefficients that can be chosen by the user. These ‘free’ coefficients include:

- Substitution elasticity between primary factors (capital, labor and land) in activities. This substitution elasticity determines the rate at which the demand for primary factors adjusts to changes in their prices. The substitution elasticity is negative; that is, if the price of a primary factor increases, the demand for this factor in a particular activity will decrease. The rate of decrease depends on the magnitude of the elasticity. With a low absolute value, the decrease will be small; with a high absolute value the decrease in demand will be large. The user can determine the elasticity for each activity in the model, provided the elasticities are non-positive. The **default value** of this substitution elasticity is -0.1 for all activities<sup>9</sup>.

<sup>9</sup> The stability of the model, i.e. its ability to find a solution, decreases with higher absolute values of this substitution elasticity. Absolute values higher than about -0.4 can result in a failure to find a solution for large yield shocks.

- Substitution elasticity between sales to domestic and export markets. Whether it is more profitable for a domestic firm to export or to sell to the domestic market obviously also depends on relative prices. The rate at which export supply changes with a change in relative prices is determined by a positive elasticity. The **default value** of this (transformation) elasticity is + 0.5.
- Substitution elasticity between demand for imports and domestic production. If imports change in price relative to domestic substitutes, the relative demand for imports will change. The **default value** of this substitution elasticity is - 0.6.
- Private demand for goods is determined by a LES function with parameters  $\beta$  and  $\gamma$ .  $\beta_c$  is the marginal budget share for commodity  $c$  and is automatically derived from the SAM.  $\gamma_c$  is the subsistence minimum of commodity  $c$  (as perceived by the consumer). The **default value** for  $\gamma = 0$ .

### 2.3. Growth rates of exogenous variables

Some of the variables of the model are exogenous. That is, their value is not determined **within** the model, but is taken from sources **outside** the model. In a dynamic simulation, the user may wish that some of these variables change through time. The user can force these changes to the model by specifying growth rates for these variables. The growth rates can be constant or they can change over time.

Growth rates can be specified for subsistence demand of consumers, population and labor force, technical change (total factor productivity), investments, government spending and transfers. The **default growth rate** in the model is EXOG = 0.0.

In the simulations below, the exogenous growth rate of the economy is based on the Shared-Socioeconomic Pathways that are developed in the construction of the Representative Concentration Pathways (RCPs) that are used by MOSAICC. Information about the scenario process and the SSP framework can be found in [Moss et al. \(2010\)](#), [van Vuuren et al. \(2014\)](#) and [O'Neil et al. \(2014\)](#). The framework is built around a matrix that combines climate forcing on one axis (as represented by the Representative Concentration Pathways: [van Vuuren et al, 2011](#) ) and socio-economic conditions on the other. Together, these two axes describe situations in which mitigation, adaptation and residual climate damage can be evaluated.

On the basis of advice from IIASA, we have matched the RCP4.5 scenario with the SSP3 socioeconomic pathway and the RCP8.5 scenario with the SSP5 socioeconomic pathway. GDP projections for the region

«North Africa» are used for the exogenous projection of GDP in Morocco in the baseline simulations (the evolution of the Moroccan economy **without** climate change). Figure 30 shows the growth rates across the century.

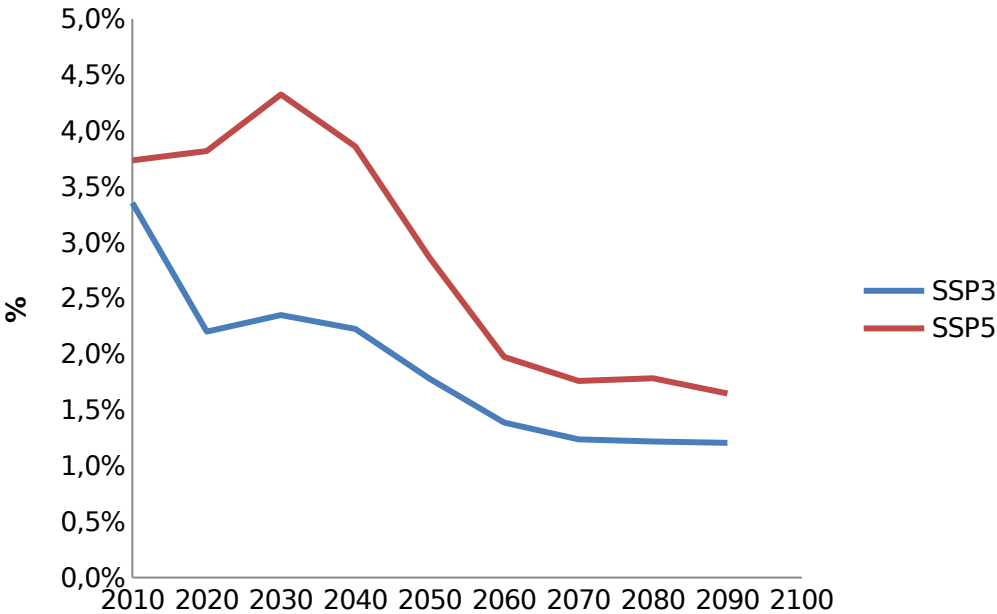


**Figure 30: Projected GDP growth rates in socioeconomic pathways SSP3 and SSP5. (Source: based on © SSP Database (Version 1.0) <https://secure.iiasa.ac.at/web-apps/ene/SSPDB>).**

### 2.4. Climate change shocks

The economic model is part of a series of models that together simulate the impacts of climate change on food production and food security. The models cover the entire **impact pathway** from climate scenario to hydrological and yield impacts to economic impacts (see Figure 31).

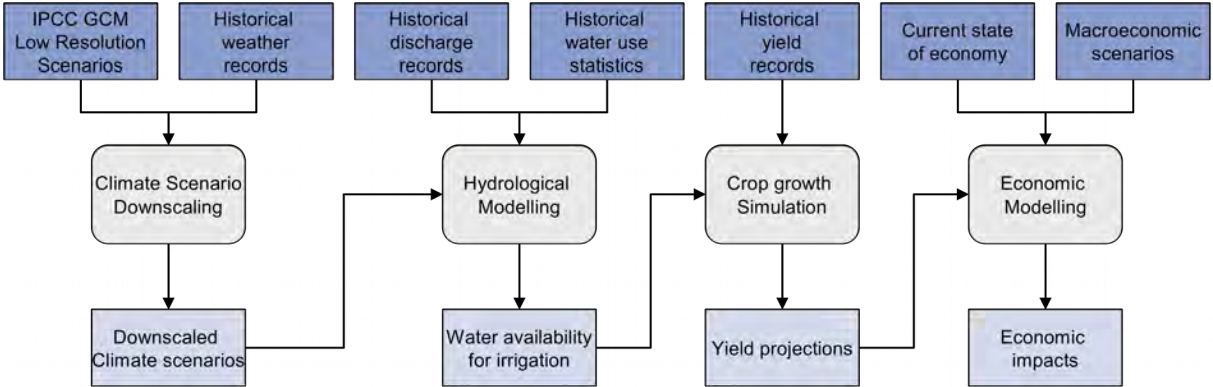


**Figure 31: Models and data flows.**

As can be seen from Figure 31, yield projections are the input to the economic model. In the economic model the percentage yield changes are transformed into technical shift parameters in the top level activity production functions. Figure 32 gives a graphical representation of the production function of one activity in the model (e.g. activity 1 in Figure 29). The output value of that activity is the value sum of value added and intermediates (say, fertilizer). The value added is multiplied by the technical shift parameter  $\theta$ . In the benchmark data this parameter is 1. An exogenous yield decrease can be simulated by proportional decreasing of the value of  $\theta$ . A five percent yield decrease gives a technical shift  $\theta$  of  $(1-0.05)= 0.95$ . Hence, with the same input of primary factors, output of the activity is now 5% less than in the benchmark. This seems an easy and obvious way to model a yield reduction.

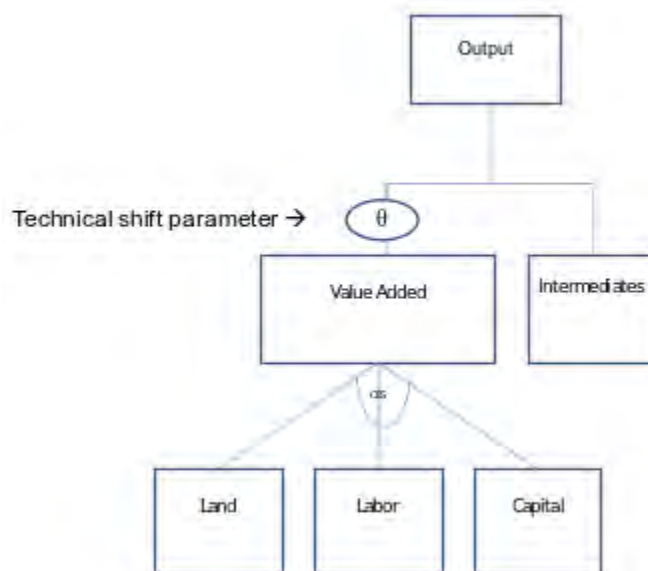


**Figure 32: Technical shift parameter  $\theta$  in the activity production function.**

For the current simulations, two RCPs are used (RCP4.5 and RCP8.5) that represent relatively optimistic and pessimistic climate change scenarios. Three different climate models for the Coupled Model Inter-comparison Project (CMIP5) are used to compute the evolution of climate variables (precipitation, minimum temperature, maximum temperature, and potential evapotranspiration) (see Table 16). These variables are downscaled to the Moroccan climate with statistical methods and fed into the AquaCrop model to project yield changes in wheat and barley for the period 2010-2100.

**Table 16: Climate Models in selected in MOSAICC.**

Name	Description	Institution
CanESM2	Canadian Earth System Model, 2nd generation	Canadian Centre for Climate Modelling and Analysis
MIROC-ESM	Model for Interdisciplinary Research on Climate - Earth System Model	Japan Agency for Marine-Earth Science and Technology, Atmosphere and Ocean Research Institute (The University of Tokyo), and National Institute for Environmental Studies
MPI-ESM-LR	Max Planck Institute for Meteorology - Earth System Model - Mixed Resolution	Max Planck Institute for Meteorology

It is not possible to do the economic simulations on the raw crop yield data. Therefore, the detailed crop yield data of AquaCrop have been preprocessed for use as exogenous inputs in the DCGE model in two ways:

- Detailed regional information of crop yield changes has been aggregated in two regions: the Favorable and the Unfavorable regions of Morocco. This is the regional level of detail that is allowed by the Moroccan SAM that was discussed in Section 2.1.
- The yield data contain rather large year-to-year shocks. The economic model cannot handle large year-to-year shock very well. Therefore, the data was smoothed in two alternative ways:
  - A simple linear yield index trend was calculated from the raw yield change data. In order that the slope of the trend would not be too much affected by the the yield in the starting year (2010), the starting year was calculated as the average of the first five years of the projection. The linearly smoothed data are referred to by the code «LIN».
  - A 10-year moving average has been fitted to the raw yield change data. The 10-year moving average smooths the time series. The moving average-smoothed data are referred to by the code «MA».

Figure 33 presents an example of the evolution of yield changes (of barley in one particular climate scenario) and the 10-year moving averages that were derived from the yield projections. A detailed overview of the projected changes in crop yields of wheat and barley for the two scenarios and the three climate models can be found in Annex 7.

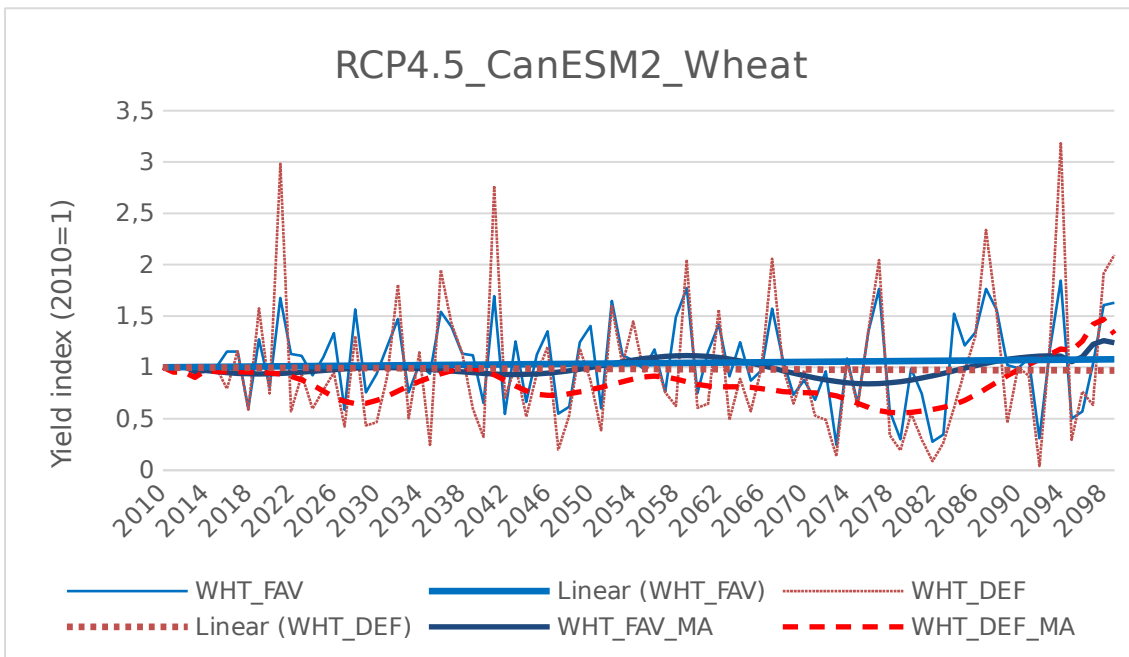


**Figure 33: Projected yield changes for barley in the favorable and unfavorable regions in the RCP4.5 climate change scenario as elaborated by the CanESM2 climate model .**

Table Table 17 shows the yield indexes of the two crops in the different regions in 2050 for the alternative data smoothing approaches (LIN and MA). Unfortunately there are a number of rather large difference in the shocks, depending on the smoothing method. For example for BAR\_FAV in the RPC4.5\_CanESM2 scenario, the shock differs between 1.01 (LIN) and 0.57 (MA). Hence, the method of data-preprocessing (smoothing) can have a relatively large impact on the results.

**Table 17: Yield index for the year 2050 for different activities in two climate change scenarios elaborated by three climate models and the two trend approaches: linear (LIN) and 10-year average (MA).**

Yield index 2050 (2010=1.00)								
	WHT FAV		WHT DEF		BAR FAV		BAR DEF	
	LIN	MA	LIN	MA	LIN	MA	LIN	MA*
RCP4.5_CanESM2	1.04	1.00	0.98	0.76	1.01	0.57	0.79	0.14
RCP4.5_MIROC-ESM	1.11	1.08	1.01	0.81	1.01	0.88	0.79	0.33
RCP4.5_MPI-ESM-LR	1.12	1.38	1.03	1.23	1.08	1.97	1.02	2.68
RCP8.5_CanESM2	0.84	0.97	0.85	1.197	0.69	0.77	0.56	0.98
RCP8.5_MIROC-ESM	0.77	0.87	0.74	1.07	0.56	0.78	0.44	0.30
RCP8.5_MPI-ESM-LR	0.97	0.99	0.91	0.82	0.69	0.62	0.55	0.49

\* MA could not be used for BAR\_DEF in the simulations. The year-to-year shocks were too big for the economic model.

## 2.5. Output data

The output data are annual values of all endogenous variables. The economic impact can be discerned by comparing the benchmark or baseline (no-shock) and the shocked variables over all years. The economic model produces graphical plots of selected variables and writes data of all variables and of selected variables to text files. The text files can be fed into specialized software (e.g. a spreadsheet program) for further processing.



# VI. HYDROLOGICAL COMPONENT



Photo INRA-Morocco

## 1. Introduction

**D**ue to economic growth and demographic development, water is becoming an increasingly valuable resource. Climate change poses an extra threat to water resources, as climate change is often associated with an increase in extreme precipitation events and a decrease in total precipitation [6]. A shift in precipitation poses a great risk on rainfed agricultural production systems [14], especially those that rely on areas with specific rainfall regimes. Mediterranean climates, such as found in Morocco, are especially vulnerable, as climate change might exacerbate the already variable precipitation regime [18]. Oftentimes, farmers lack the means to adapt to climate-induced shifts in water availability, compromising the food security of an entire nation. As such, it is important to gain insights into the plausible climate scenarios and their effects on water resources.

The goal of this study is to use high-resolution climate data to assess the impact of climate change on hydrological regimes and water resources for basins in Morocco. Three climate models CanESM2, MIROC-ESM and MPI-ESM-LR from a statistical regionalization were used to generate discharges in the historical period (1971-2000) and the future period (2010-2100) under two emission scenarios RCP4.5 and RCP8.5, and thereby obtain the volume of water that the basins can offer under potential effects of climate change.

This chapter describes the processes developed for hydrological modeling from distributed hydrological model STREAM (Spatial Tools for River basins and Environment and Analysis of Management options) implemented in the MOSAICC platform, including the calibration and the projection of future flows of each basin according to the general climate

model. The aim is to propose strategies to address the impacts of climate change on the availability of irrigation water for agriculture. For this purpose, it is important to quantify water resources in order to seek a balance between anthropogenic and natural ecosystem needs. Therefore, the need to meet current and future water availability under climate change scenarios, which will be useful for a better management of water resources including water resources strategies, construction and exploitation of hydraulic structures, planning agricultural production, in addition to research related to food security from the effects of climate change in the country.

## 2. Methodology

Three global climate models (GCM's) with a low and high emission scenario were used in this study. The coarse resolution precipitation and evaporation grids were downscaled to a resolution of approximately 4 km using a statistical downscaling method. These data were utilized in hydrological simulations.

### 2.1. Study area

Morocco is located in the northwestern part of Africa, with a population of approximately 34 million inhabitants. For the most part, the climate is Mediterranean, moving towards a more semi-arid climate in the interior regions. The geography of the country is characterized by the Rif Mountains in the northern and the Atlas mountains in the middle part of the country. Rainfall is concentrated from November to March, with a higher precipitation rates in the northern, coastal and mountainous zones. While Morocco has a strong industrial and service sector, still around 40% of the population live in the rural areas. The analysis was carried out for the Moulouya, Tensift and Sebou basin (Figure 34), as these basins cover important agricultural areas. The size of the upstream area of the different hydrological stations is shown in Figure 35.

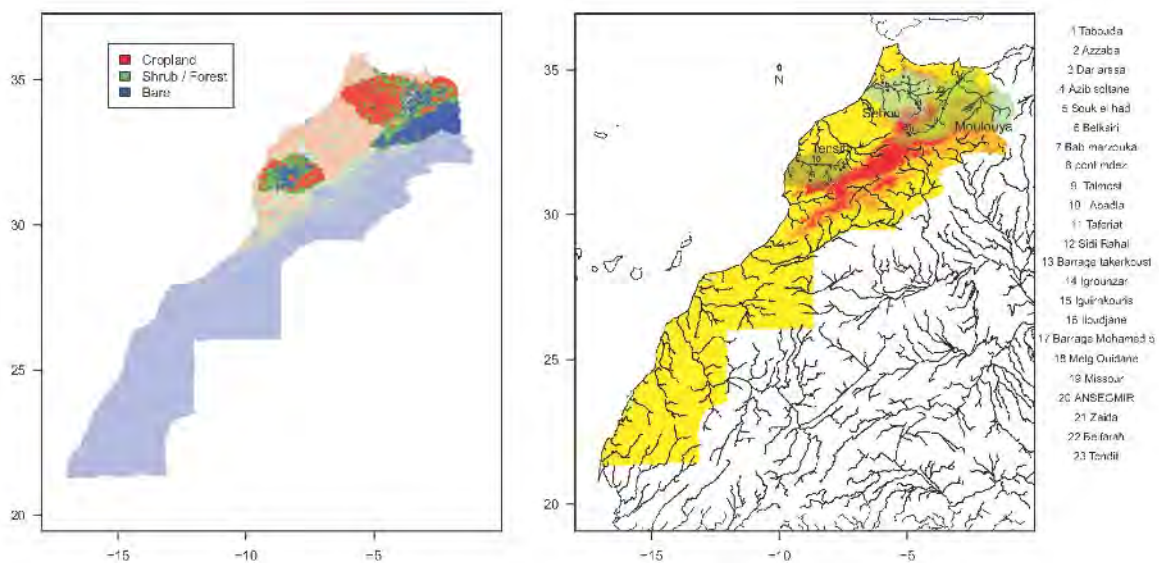


**Figure 34 : The Moulouya, Tensift and Sebou basin are highlighted on a land-use (left) and digital elevation map (right). The locations of the outlets used for model calibration are indicated with a dot and a number. The names corresponding to the numbers are shown right from the figures**

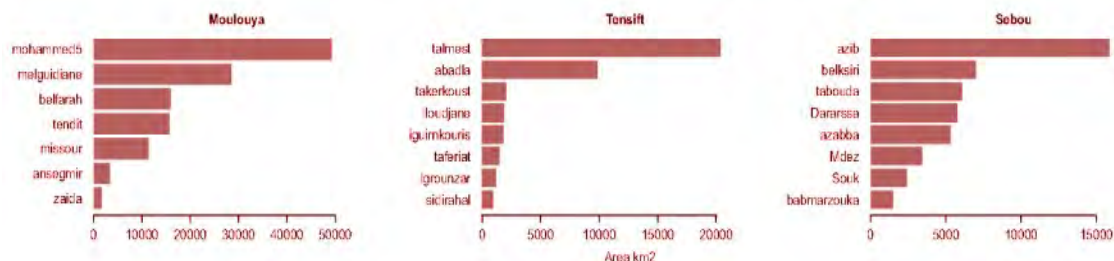


**Figure 35 : The size of the upstream basin corresponding to each outlet used for the Moulouya, Tensift and Sebou watersheds.**

## 2.2. Moulouya

Moulouya is a Mediterranean coastal basin, which covers an area of 74,000 km<sup>2</sup>. This Basin is characterized by arid climate with tendencies to a Mediterranean climate in the North-East (Low Moulouya and

Mediterranean coasts), continental on mean Moulouya and mountainous in High Moulouya. The average annual precipitation is 270mm, but shows a gradient from North to South. The plains of the basin receive water from the Eastern parts of the Rif Mountains and the middle Atlas. The predominant vegetation type is steppe, with in particular alfa in the high plateaus and natural forest, of which mainly the Thuja and the Holm oak in the mountainous areas. A large portion of the basin is non suitable for agriculture because of aridity, irregular rains and a lack of irrigation water. The areas are often used as pasture, especially in the high plateaus. The acreage is approximately 501.000 ha, of which 352.000 ha is dedicated to the cultivation of rainfed cereals. The small and medium hydraulics covers approximately 80.000 ha, whereas modern irrigated agriculture extends on approximately 70.000 ha, mostly used for citrus cultivation. Market gardening play a paramount role in the socio-economic development of the area, and this by the importance of their covered annual surface, the benefit created and the mass of labor employed. On the level of the small and medium hydraulics, the cultivation systems are different from upstream to downstream because of the importance of available irrigation water. Altitude, unfavorable especially for leguminous plants, but favorable to a broad range of rosacea (apple tree, peaches tree, pear tree, etc.), joins the enslavement which blocks the marketing of the perishable cultures with production (truck farming, apricots, apples, etc). The zone is known for snowfalls in the mountainous areas of the mean Atlas and Rif Eastern and rarely in the area of Eastern where the frequency doubles every ten years. During the last 30 years, the area knew 10 periods of accentuated drought: 1982-86, 1992-95, 1998-2000 and 2004-2005, during which the rain varied between 34 and 320 mm/year.

### **2.3. Tensift**

The Tensift basin situated in central of Morocco is located between 30.75E 32.40N and 7.05E 9.9W, occupying an expanse around 30,000 km<sup>2</sup>. The climate is semi-arid, typically Mediterranean, with an average annual precipitation of about 250 mm. However, the precipitation is characterized by big space-time variability. Rainfall annual average is about 250mm in Marrakech and can reach 800mm on the tops of the Atlas. The wet period from October to April accounts for 80 to 93% of the annual precipitation. The examination of the average distribution of the monthly rains also shows the two definitely differentiated seasons' existence.

Air temperature is very high in summer (38 °C) and low in winter (5 °C). In the Tensift basin, a large area is dedicated to agriculture. The Haouz plain covers around 6000 km<sup>2</sup>, and is delimited to the north by the "Jbilet" hills and to the south by the High-Atlas mountain range (that culminates up to 4,000 m). The Regional agriculture is characterized by the prevalence of the cultivation of cereals and tree crops. The area is an important olive producer with 123,000 ha, which is about 20% from the

national surface and 70% of olive national preserve exports. The area for cereal covers 800,000 ha, which is 16% from the national surface and 10% of the national production. The basin yield 57% of the national production of apricot. The region accounts for 20% of the national argan area, and 34% of the national surface in walnut trees.

## 2.4. Sebou

The Sebou basin has an area of around 40,000 km<sup>2</sup>. It is characterized by an agricultural and industrial economy that contributes significantly to the national economy. The climate prevailing in the whole basin is Mediterranean with an oceanic influence, and within the basin, the climate becomes more continental. It is manifested by westerly winds and rainy precipitation decreases away from the sea and in protected valleys such as the Beht or top Sebou before quickly increasing on the slopes of the Rif. These influences of altitude, latitude and exposure combine to form local micro-climates where cold, frost, snow and the winter rains may object to the summer heat and storms. These micro-climates are manifested by:

- Thunderstorms: the most affected region in the basin is the Sais (17-18 days / year) with two favorable periods: late summer and late spring. In the mountains, the frequencies are naturally higher, the Middle Atlas being more affected than the Rif.
- Hail: in the coastal regions, hail is totally absent in summer. The hills and interior shelves are primarily affected in 12 early winter and spring. In the mountains, the maximum is located in the spring but strong frequencies are extended in the summer.
- Snow: It affects the pool of altitudes of over 800 meters. These events are recorded between November and March (the Middle Atlas and Rif High).

The average annual rainfall of the basin is 600 mm, with a maximum of 1000 mm/year in the hills of the Rif and a minimum of 300mm on the top Sebou and the Beht valleys. The average annual rainfall across the Sebou basin, calculated over the period 1973-2008, is about 600 mm (640 mm over the period 1939- 2008). The minimum values of between 400 and 550 mm are observed on the basins of High Sebou and Middle Sebou (Fes region RDAT Wadi, Wadi R'dom, Beth wadi). They are slightly higher (500 to 600mm) in coastal border and far exceed these values (700 to 900 mm on the Middle Atlas lfrane, 1000 to 1500 mm on the reliefs of the Rif (upper basin wadi Ouergha).

In winter, warm and cold episodes or even warm periods alternate, but low minimum temperatures are never absent. These low temperatures undergo spatial variations resulted in few frosts in Meknes (protected by its bowl position) and frozen more likely to Fes. Finally, Taza located on the



continental airflow, is particularly affected. In summer, the temperature is characterized by two types of behavior, a beautiful weather at high or moderate maximum temperatures, but with night cooling and a hot weather with very high temperatures without appreciable night cooling. The temperatures are highest in July and August and minimum in January. Average annual temperatures vary according to altitude and continentality, between 10 and 20°C.

The average potential evaporation is quite strong in the basin. It varies between 1600 mm in the coast and 2000 mm inwards basin. It is highest in July-August with around 300 mm / month and minimum from December to January with less than 50 mm / month. On the coast and the center of the basin, high summer temperatures, the virtual absence of significant rainfall during this period, explain the high evaporation in the watershed (1500 mm on the coast and 2000 mm/ year inwards basin), explaining the unit needs important irrigation water.

The Sebou Basin is one of the most important regions of agriculture in Morocco, with nearly 20% of the irrigated agricultural area (i.e. 357,000 ha), and 20% of the UAA of Morocco (i.e. 1.8 million ha). The land use is relatively diverse with a dominance of cereals (60%), the rest is occupied by fruit plant (14.4%), legumes (6.6%), industrial beet and sugar-cane (4.2%), oleaginous cultures (3.6%), vegetable crops (3.1%), forage crops (1.7%).

Sebou watershed is one of the richest in water and is one of the most fortunate irrigation and industries areas. Cultivated potential amounts are estimated to 1,750,000 ha. Irrigable area is estimated at 375,000 ha, from which 269,600 are currently irrigated, divided between 114,000 ha of large irrigated areas and 155,600 ha of small and medium irrigated areas and private irrigation.

## **2.5. Loukkos**

The Loukkos Basin Agency covers an area of about 13 000 km<sup>2</sup>, bounded on nearly 260 km on the North by the Mediterranean Sea, and about 140km on the west by the ocean Atlantic, to the south by the Sebou basin and on the East by the Moulouya basin.

The basin is drained by many rivers forming everywhere very narrow valleys, excepting those of Loukkos to Hachef-Mharhar, Martil and Laou, which gives the region a rugged terrain, consisting of a succession of hills in the West (500 m to 1000 m) and high mountains in the East (1,500 m to 2,400 m, culminating at 2,456 m).

Under oceanic influence, the climate is wet in the watershed of Loukkos, the West Mediterranean Coastal and Tangiers. This influence gradually decreases and induces aridity increasingly pronounced from West to East to move towards a Mediterranean climate.

The canopy is characterized by the presence of plant species that vary according to the nature of the soil and altitude. Thus, oak and cork met on Tingitane Peninsula, while the people live oak central Rif Mountains in combination with pine itself relayed by the altitude fir or cedar. This canopy is constantly deteriorating because of land clearing which, combined with the rugged terrain of the area and land facies, favor erosion, considered among the strongest in Morocco, with the direct consequence of loss of agricultural land and siltation of dams. The area has significant economic advantages that helped boost its economic and social development. These potentials are noticeable through agriculture more modern and ever changing industry.

Agriculture is the dominant economic activity in the Loukkos plain that contains the largest irrigated area of large hydro in region with an area of over 30,400 ha, mainly fueled by the dam Oued El Makhazine. The land use is mainly shared between the industrial crops, market gardening, forage and cereals in addition to high-value crops, including strawberries, mostly for export.

The Mediterranean area, with the exception of a few privileged sectors irrigation (Laou, Neckor and Rhiss), has no agricultural use and is truly suitable as from the foothills of the Rif area and towards the West to the Atlantic, where the climate is mild and the soil is more suitable to the soil level.

## **2.6. Bouregreg and Chaouia**

The Bouregreg and Chaouia Basin covers a total area of 20,470 km<sup>2</sup>, which represent 3% of the territory of the Kingdom. It includes three distinct hydrologic units (from northeast to southwest): the watershed of Oued Bouregreg, the Atlantic Coastal basins and the endoreic basin of the Chaouia.

Administratively, it covers most of the regions of Casablanca and Rabat-Sale-Zemmour-Zaer, and part of the region of Chaouia-Ouardigha.

The watershed Basin includes the Bouregreg River and its tributaries and coastal rivers including N'Fifikh, Malleh, Cherrat, Ykem etc. The average total flow amounted is about 850 million m<sup>3</sup> / year, of which 675 million m<sup>3</sup> came from the single basin of Bouregreg, the remainder came mainly from small coastal basins.

## **2.7. Oum Er Rbia**

The action area of the Oum Er Rbia basin comprises the basin of Oum Er Rbia and the Atlantic coastal basin of El Jadida-Safi. With a total area of 48,070 km<sup>2</sup>, this basin covers nearly 7% of the total area of the country.



The Oum Er Rbia Basin, one of the largest basins in the country, covers an area of 35,000 km<sup>2</sup> with an extension of 550 km. It has its origin in the Middle Atlas at 1800 m, crosses the chain of the Middle Atlas, the Tadla plain and coastal Meseta and flows into the Atlantic Ocean near the city of Azemmour about 16 km North of the city of El Jadida. The Atlantic coastal basin El Jadida- Safi is located in the southwest of the Oum Er Rbia Basin and cover an area of approximately 13,070 km<sup>2</sup>.

In the basin of Oum Er Rbia, there is an increase in rainfall from Northwest to Southeast (from the ocean to the Middle Atlas), and a decrease in rainfall from Northeast to the Southwest in parallel to the chain of the High Atlas. As a result, in the basin of the Oum Er Rbia, the wettest region is not the highest chain of the High Atlas, but the Middle Atlas and specifically where Oum Er Rbia takes its sources: the rainfall there reaches 1000 mm per year on average.

The area has significant economic advantages that allowed it to occupy a distinguished place at the national level and contribute to economic and social development and the fight against social and regional disparities. These potentials are noticeable through agriculture increasingly modern, a constantly changing industry, especially in the mining and agribusiness and diversified tourism and especially in mountainous area.

Agriculture is the dominant economic activity in the plains of Tadla, Doukkala and Tessaout containing an area of over 300,000 ha irrigated modern and fed by a large water infrastructure so. The land use is mainly shared between the industrial crops, market gardening, fodder, citrus, olives and cereals.

## **2.8. Souss-Massa-Draâ**

The first zone of the Souss-Massa-Draa comprises the sub-basins of the Souss and Massa, the northern coastal basins of Tamri-Tamghart and the plain of Tiznit Sidi Ifni. The defined area thus covers 27,800 km<sup>2</sup> and is limited to the North by the Tensift basin, east and south by the Draa basin and in the West by its long Atlantic coastline of 200 km.

The second zone of the basin is the Draa basin, which is bounded to the north by the High Atlas, on the south of the river basin of the Sahara and the border with Algeria, to the east by the valleys of Toudgha and Rhris, and on the west by the hydraulic basin of Guelmim and Souss-Massa.

Land use in the study area is dominated by forests, rangelands and uncultivated lands which occupy 86.5%, while the agricultural area occupies only 13.5%.The potential irrigable land in the whole area is about 269 000 ha. Irrigated area, mainly located in the basins of the Souss and Chtouka, covers nearly 148,640 ha of which 60% is irrigated with modern amenities. In terms of gross value of production, market gardening for 34%, 25% for citrus fruits, 10% for cereals and 28% for livestock .The

production of citrus and early market gardens is the region most important activity. These two crops respectively account for 48% and 75% to domestic production and close to 50 and 67% of national exports.

## 2.9. Climate models

The new generation of General Circulation Models (GCMs) for the Coupled Model Comparison Project Phase 5 (CMIP5) was used in this study. The advantage of these Earth System Models (ESMs), in comparison to former GCMs, interactions with land-use and vegetation are incorporated as well as atmospheric chemistry, aerosols and the carbon cycle [16]. The models are driven by a newly defined atmospheric composition forcings for present climate conditions and representative concentrations pathways (RCPs) [11]. Three different ESMs with two different RCPs were included in the analysis. The name of each RCP refers to radiative forcing obtained from the path of concentration until 2100. The RCP4.5 [17] assumes that the total radiative forcing is stabilized due to the employment of a range of technologies that reduce the emission of greenhouse gasses (radiative forcing approximately 4.5 W/m<sup>2</sup> after 2100). The RCP8.5 [13] characterizes an increase in greenhouse emissions (radiative forcing reaches above 8.5W/m<sup>2</sup> in 2100, and continues to increase for a while).

Both RCPs were simulated in the Canadian Earth System Model (CanESM2) [3] Modelling and Analysis, the Model for Interdisciplinary Research on Climate (Miroc) [20] and the MPI Earth System Model running on medium resolution grid (MPI-ESM-LR) [12, 9], developed by the Max-Planck-Institute for Meteorology. The RCP4.5 and RCP8.5 were compared to the historical RCP. The historical data covered the period 1971-2000, and the future scenarios of 2010-2100.

## 2.10. Hydrological model

The Spatial Tools for River basins and Environment and Analysis of Management options (STREAM) model was used in this study. STREAM is a GIS-based rainfall and runoff model that calculates the water balance on a gridded landscape. The model, which was developed by Aerts (1999) [1] is extensively used to study streamflow on a relatively large spatial and temporal scale (e.g [10, 21, 19, 2, 8, 15]). The data on precipitation and evapotranspiration was used to determine the accumulated runoff for each outlet on a monthly basis. In order to do so, the basin of each outlet was derived from the Digital Elevation Model (DEM). To maintain important topological features in this DEM, the climate data was resized to the same spatial resolution of the DEM, approximately 2 km.

The STREAM model was calibrated to make sure the order of magnitude and monthly distributions of discharge data was in accordance with the

data measured in the field. Prior to do this, the available monthly observed discharge from 1980 till 2010 for the basins were collected, and prepared for use as input. The objective in running the model is to produce the naturalized streamflow response of the basins excluding anthropogenic influences in the basin as reservoirs, irrigation, and other river diversions. The historical Era-Interim [5] dataset was used for model calibration. The model calibration was done by manually adjusting three parameters (Table 18). The first parameter (GW) was used to define the amount of water flowing to the groundwater (as a fraction). The second parameter (WH) was used to determine the height of the water holding layer. The last parameter (C factor) was used to determine the groundwater flow velocity. The Era-interim data was used for model calibration. The monthly distributions of the measured and modelled discharge values were compared. The coefficient of determination and volumetric efficiency [4] were used as statistical measures to evaluate the performance of the model. The coefficient of determination or correlation, called  $R^2$ , assess the proportion of the variance of simulated discharges that can be attributed to the variance of the observed discharges. Volumetric efficiency is another indicator that evaluates the difference observed and calculated flow and was calculated using equation 2.1, where  $VE$  denotes the volumetric efficiency,  $Q_m$  and  $Q_o$  the modelled and observed discharge respectively.

$$VE = 1 - \frac{\sum (Q_m - Q_o)^2}{\sum Q_o^2} \quad (2.1)$$

**Table 18: The three parameters used in the STREAM model for calibration.**

Parameter	Range	Function
<b>GW</b>	0.0-1.0 (fraction)	Fraction of water owing to the groundwater
<b>WH</b>	0.5-3.0 (Parameter)	Water holding layer
<b>C Factor</b>	1.0-3.0 (Parameter)	flow velocity groundwater

## 3. Results and discussion

### 3.1. Spatial distribution of water resources

The monthly averaged water yield (P - PET) was calculated from the era-interim data (1980-2010). Figure 36 shows positive values for the northern part of the country for the months December -March, but year round ETP values exceeding P values for the southern part of the country. In the months April -November, PET values also exceed P values in the Northern part of the country. As such, evapotranspiration is limited by water availability for most part of the year. The coastal areas are relatively wet compared to the inland. The data was used in the stream flow calibrations.

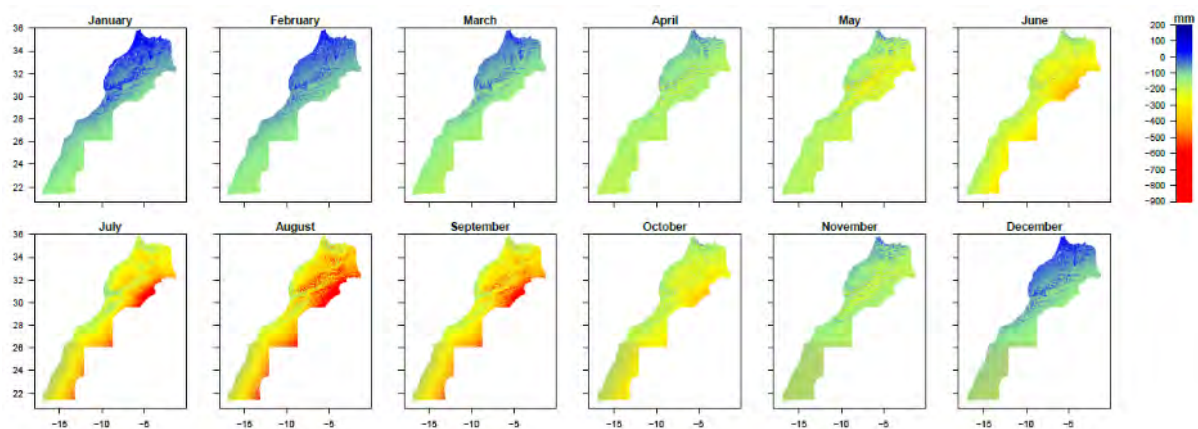


**Figure 36 : The monthly averaged water yield (P-PET) as calculated from the Era-interim data. This data was also used for model calibration**

### 3.2. Hydrological model calibration

In any hydrological modeling application, model calibration and validation are critical steps for credible modeling results. Calibration is an iterative comparison test of a model to fit simulated time series to observed time series data. These time series were compared for the same period at the same points and on a monthly time step.

The STREAM model was calibrated for each basin using ERA-Interim data and stream flow data on a monthly step from the period 1980 to 2010. The Figure 37, Figure 38, Figure 39 and Figure 40 show the results of the calibration for the basins. The blue line represents the monthly median of the measured runoff values, whereas the shaded areas the inter-quantile ranges. The box-plots indicate the distribution of the modeled runoff. The Volumetric Efficiency (VE) and the coefficient of determination ( $R^2$ ) were obtained and displayed for each station.

The calibration results of the Moulouya basin are shown in Figure 37. We observe higher discharge volumes measured for the Melgoudiane and Mohamed V stations, as for the other stations measured discharge volumes remained below 30 m<sup>3</sup>/s. It can be seen that there is a close agreement between simulated and measured runoff values in terms of magnitude but also seasonal streamflow patterns are well represented. The correlation between the monthly median measured and simulated runoff range between R<sup>2</sup>=0.65 and 0.90. There is a large variation in terms of volumetric efficiency which ranges from 0.23 for with a maximum of 0.73 for Belfarah. The model performed well in terms of quantity and seasonality important for future scenarios.

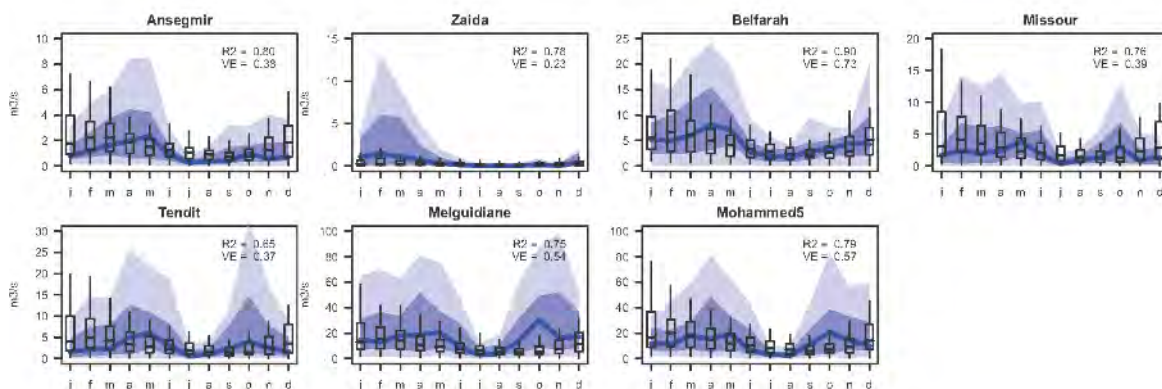


**Figure 37 : The monthly distributions in measured (blue) and modeled discharge volumes (box-plots) for the Moulouya basin. Each plot represents a different outlet. The STREAM parameters R<sup>2</sup> and VE for each outlet are displayed in the graphs.**

Likewise, for the Sebou basin, we observe a general good agreement between measured and modeled stream flows in terms of quantity and pattern (Figure 38). Water quantities are higher compared to the Moulouya basin, reaching up to 700 m<sup>3</sup>/s for the Belksiri station. For the Pont Mdez and Bab marzouka stations, there is an overestimation in terms of median stream flow, resulting in a negative VE, however, the pattern is well represented with R<sup>2</sup> = 0.71 and 0.84 respectively. For the other station, the VE and R<sup>2</sup> values were all above 0.13 and 0.75 respectively. For December, there is a general overestimation in total stream flow volume.



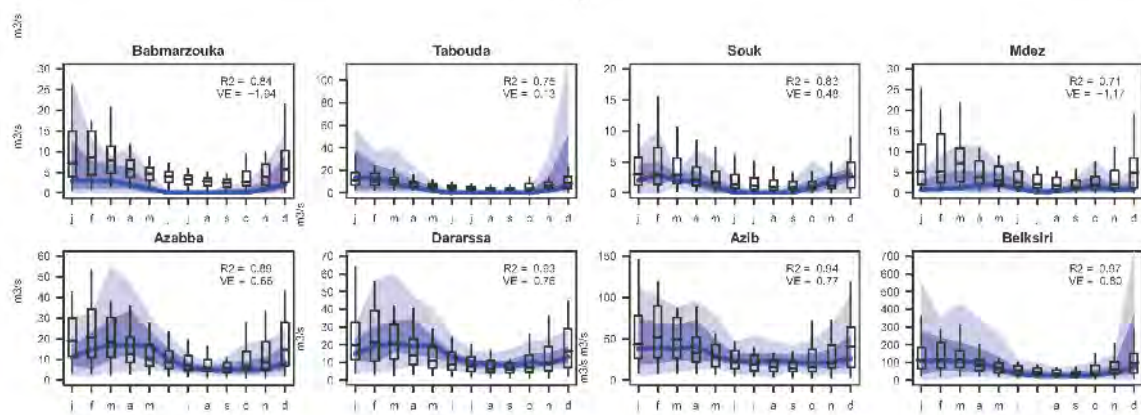


**Figure 38 : The monthly distributions in measured (blue) and modeled discharge volumes for the Sebou basin. Each plot represents a different outlet. The STREAM parameters, R<sub>2</sub> and VE for each outlet are displayed in the graphs.**

The calibration results of the Tensift basin are shown in Figure 39, we found a general underestimation in modeled streamflow. For the Igrounzar and Talmest stations, there is an overestimation in terms of median stream flow, resulting in a low VE. For the other station, the VE and R<sub>2</sub> values were all above 0.36 and 0.70 respectively. For the period from January to June, there is a general underestimation in total stream flow volume and an overestimation for the period from September to December.

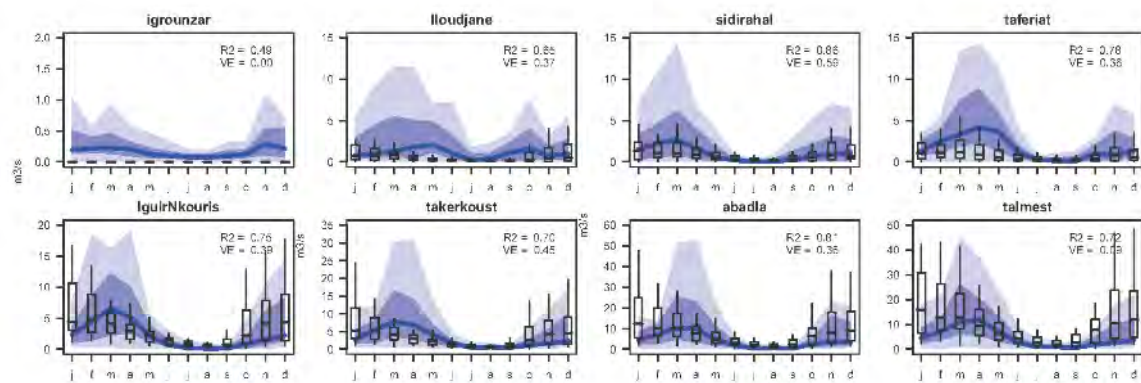


**Figure 39 : The monthly distributions in measured (blue) and modeled discharge volumes for the Tensift basin. Each plot represents a different outlet. The STREAM parameters, R<sub>2</sub> and VE for each outlet are displayed in the graphs.**

The calibration result of the Loukkos basin representing by the “Pont torreta” station is shown below (Figure 40). It is notable that there is a good agreement between measured and modeled stream flows in terms of quantity and pattern. The model performed well in terms of the magnitude but also the seasonal streamflow patterns are well represented which reflects with a correlation coefficient of 0.80 and a volumetric efficiency of 0.48.

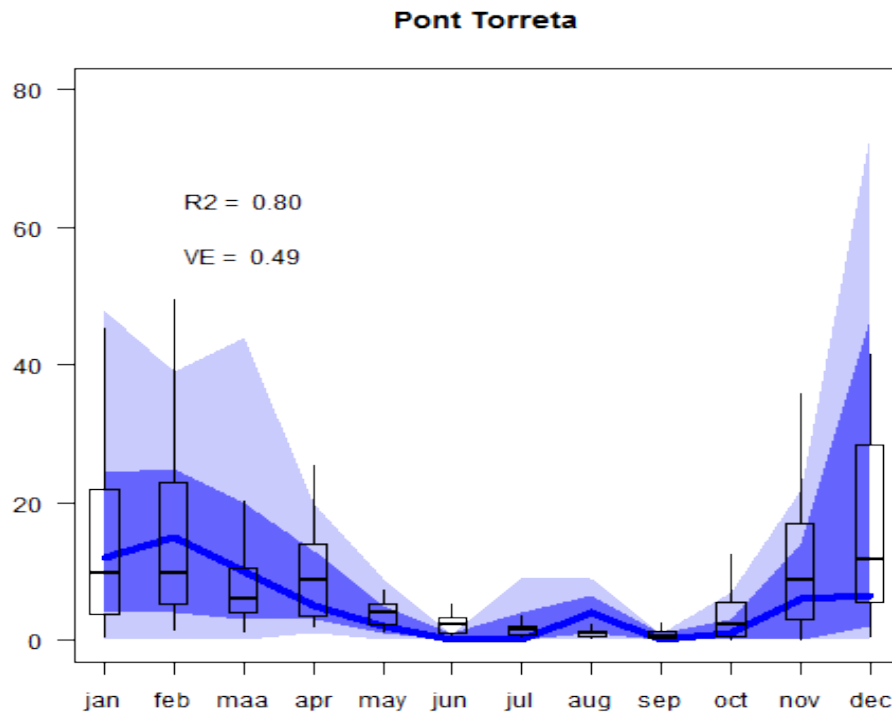


**Figure 40 : The monthly distributions in measured (blue) and modeled discharge volumes (box-plots) for the Loukkos basin. The plot represents the “Pont torreta” outlet. The STREAM parameters R2 and VE for the outlet are displayed in the graphs.**



# VII. FORESTRY COMPONENT



Photo INRA-Morocco

## 1. Introduction

Forests worldwide are affected by global changes such as climate change, changes in the atmospheric composition (Pitelka *et al.*, 1997; Thuiller *et al.*, 2008) and the introduction of exotic pests (Aukema *et al.*, 2010). These changes produce specific variations in landscape characteristics and dynamics on different spatial and temporal scales (Laughlin *et al.*, 2004; He and Mladenoff, 1999). Many of these changes are unprecedented, and their effects upon, and interactions with, other ecological processes are uncertain.

Past observations, experimental studies and simulation models based on current ecophysiological and ecological understanding show that forests are very sensitive to climate change. Over the past 30 years, the world has experienced significant temperature rises, especially in the northern hemisphere. Meanwhile, the variability of climatic conditions is expected to increase, with more precipitation in certain areas and extreme dry and hot periods in others. These events will have a significant impact on forests.

Rising temperatures force many living organisms to migrate to cooler areas, while new organisms take their place. These movements concern all species, including plants. Some species may seek higher altitudes, others may move poleward. In temperate areas, plant species may migrate naturally over 25 to 40 km over the course a century. If, however, the temperature in a region rises by – for example – 3 °C over a period of 100 years, the climatic conditions in the area will undergo a dramatic change equivalent in ecological terms to a displacement of several hundred kilometers (Jouzel and Debroise, 2007).

Over the past decades, scientists have observed the first signs of this process in the northern hemisphere, caused, apparently, by a rise in

temperature. Various studies have found that a number of species of birds, trees, bushes and herbs have moved an average of six kilometers every ten years, or have sought higher (between one and four meters) altitudes (Parmesan, 2003). Botanists have also noted that many trees and plants of the northern hemisphere tend to bloom earlier (by two days every ten years on average), which increases the risk of buds being killed by late frosts.

Slightly higher temperatures and a greater accumulation of CO<sub>2</sub> in the atmosphere accelerate the growth rate of species in forest ecosystems. It is estimated that the productivity of forests in temperate regions has increased by 15 percent since the early twentieth century (Medlyn *et al.*, 2000). In addition, increased CO<sub>2</sub>, nitrogen and soil moisture levels have all contributed to an increase in forest productivity over the course of the last century. Conversely, changes in climatic conditions may also cause a reduction in plant productivity. During the 2003 heat wave in Europe, plant productivity in continental Europe decreased by 30 percent.

Paradoxically, while increased CO<sub>2</sub> levels and other factors have led to increased plant productivity in some regions, changes in environmental conditions – strongly influenced by climate change – could lead to the massive destruction of forests and the extinction of many species.

Models using empirical relationships estimated under past conditions may fail to reliably predict the future dynamics of the forest under novel conditions (Gustafson, 2013; Williams *et al.*, 2007). Conversely, models using direct causal relations linking forest dynamics to fundamental variables such as temperature, precipitation and CO<sub>2</sub> concentrations may produce more robust estimates under novel conditions (Cuddington *et al.*, 2013; Gustafson, 2013).

In the case of Morocco, the impact of climate change on forest ecosystems is unclear. Moroccan forests suffer much more from human and animal constraints than from the impacts of climate change. Nevertheless, assessing the climate component is of paramount importance. Indeed, information on the potential impacts of climate change is crucial in the development of national adaptation policies. Given the great uncertainty about future climate change and its impacts on natural and human systems, simulation models offer the interesting possibility to test scenarios, explore potential impacts and understand how different processes interact with each other.

Under the joint EU and FAO “Improved Global Governance for Hunger Reduction” programme, FAO has developed an integrated system to conduct assessments of the impacts of climate change at the national level. This system, called MOSAICC (Modelling System of Agricultural Impacts of Climate Change), was built in collaboration with various scientific institutions in Europe, including universities and research centers. MOSAICC includes a model for the simulation of forest dynamics, named LANDIS-II.

One of the objectives of the project, and especially for the pilot area of the Maâmora forest, was to identify almost all factors that can influence the vulnerability of this ecosystem. Simulations of the evolution of forest stands under different climate scenarios were carried out to gain a better understanding of: time variations of biomass production; *Quercus suber* regeneration issues; issues linked to the production of non-timber forest products; the impacts of climate change on forests; and the influence of forest management techniques applied in Maâmora.

## 2. Method

### 2.1. Presentation of the study area

The forest of Maâmora was chosen as pilot area in order to test the model and decide on its use in the Moroccan context, primarily because of the availability of the data required by the model. Wide-ranging tests on all regional water and forestry directorates are planned in collaboration with regional planning services.

The Maâmora forest is one of the most important forests in Morocco because of its history and the goods and services it produces. It is used for fuelwood, livestock grazing, recreation etc. by more than a dozen municipalities.

Up to the period of the French Protectorate, the forest consisted entirely of cork oak (Mounir, 2002). At present, approximately half of the forest consists of other species such as acacia, pine and eucalyptus.

The Maâmora forest borders the Atlantic Ocean, stretching 68 km from east to west and 38 km from north to south (Mounir, 2002). It is located between the meridians 6° and 6° 45' West, and the parallels 34° and 34° 20' North (Figure 41).

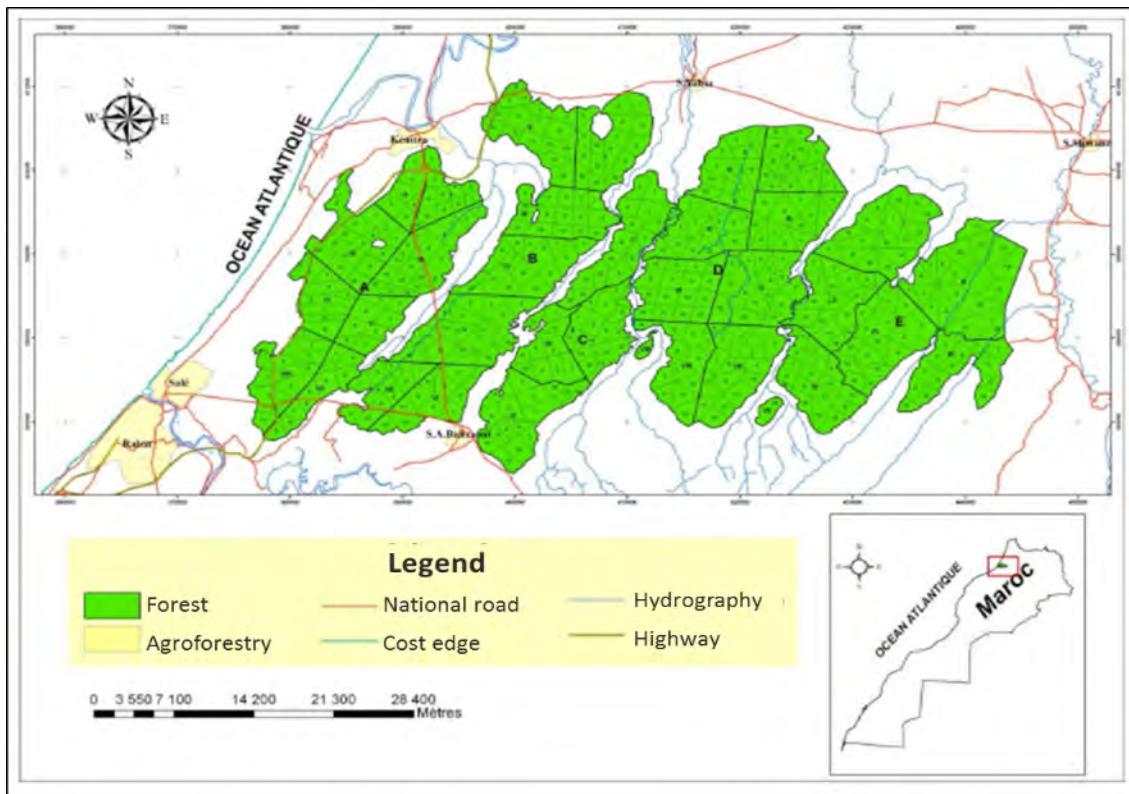


**Figure 41 : Location of the Maâmora forest (Bagaram, 2014).**

The forest is naturally divided into five parts by rivers, and is thus divided into five forest cantons labelled A to E from west to east. These five cantons are further subdivided into groups, resulting in a total of 33 groups throughout the forest. Each group is subdivided into plots. The forest has a total of 448 plots.

### **2.1.1. Climate**

The climate of the Maâmora forest is Mediterranean, with influence from the Atlantic Ocean. The lowest minimum temperature recorded to date is  $-6^{\circ}\text{C}$  (Kenitra) and the highest maximum temperature  $50.3^{\circ}\text{C}$  (Tiflet). The average minimum temperature of the coldest month (January) is always above  $0^{\circ}\text{C}$  and varies between  $4.5^{\circ}\text{C}$  (inland) and  $8.2^{\circ}\text{C}$  (along the coast). The average maximum temperature of the warmest month (July or August, depending on the location) ranges between  $27.3^{\circ}\text{C}$  (along the coast) and  $37.1^{\circ}\text{C}$  (inland). Visible precipitation takes the form of rain, with annual rainfall ranging from 350 to 650 mm (Mounir, 2002).

The bioclimate of the study area is semi-arid with temperate winters in the eastern part of the forest, and subhumid with warm winters in the western part (Aafi, 2007).



Figure 42 shows the ombrothermic diagrams of Bagnouls and Gausson (Bagnouls and Gausson, 1953) obtained for three stations from data from the National Direction of Meteorology (DMN) over the period 1980–2013.

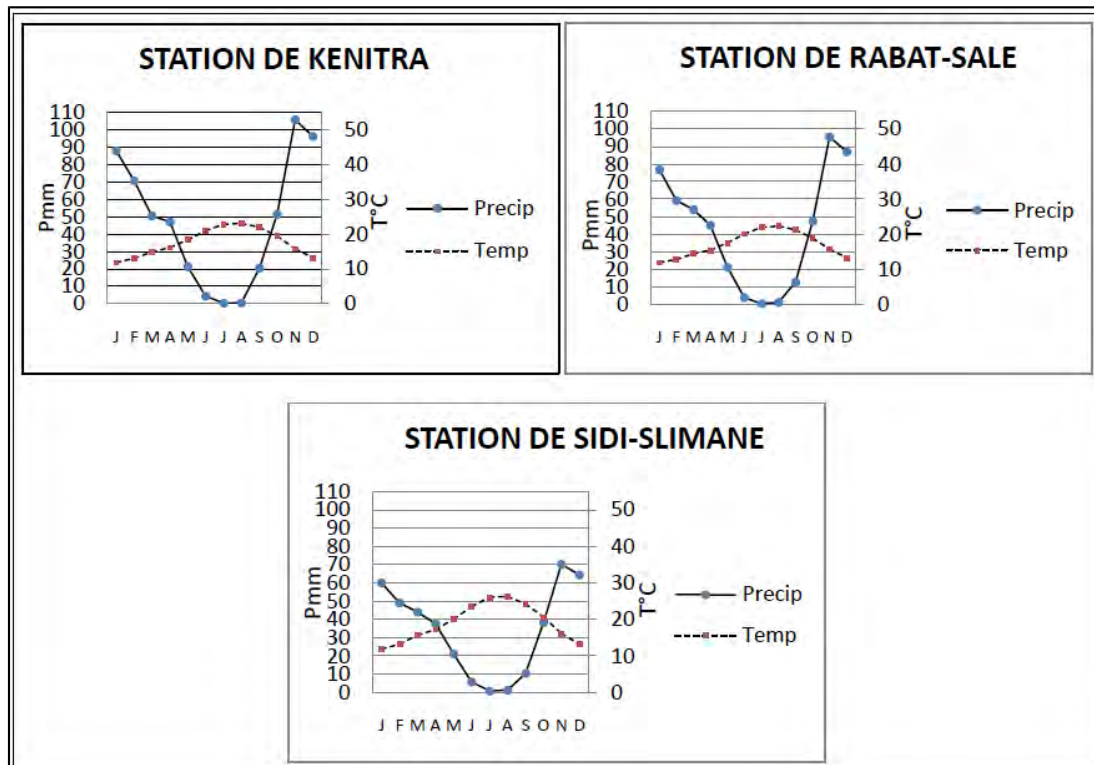


**Figure 42: Ombrothermic diagrams of Bagnouls and Gausson for the three stations in Maâmorâ, 1980–2013.**

These graphs show that the duration of the dry period ranges between 4.5 and 5 months in Kenitra and Rabat-Salé, and exceeds five months (5.5 months) in Sidi Slimane. This observation confirms the effect of continentality mentioned earlier, with dry periods lasting longer inland than on the coast.

### 2.1.2. Topography

Slope grades are generally very low. Slopes, gently inclined towards the Gharb plain, range from 0.6 to 0.8 percent on average, except in the eastern part of the Maâmorâ forest where slopes are strong enough to cause significant erosion (Abourouh *et al.*, 2005).

### 2.1.3. Pedology

The Maâmora soils are generally sandy clay type soils (Lepoutre, 1965 in Bagaram, 2014). Based on the nature and depth of the sands, Lepoutre (1965) distinguishes several types of soils including shallow beige sands on clay, common in the southern cantons C, D and E; deep sands on clay in the northern parts of cantons C, D and E; red sands on clay typical for dune landscapes; hydromorphic soils, present either in subhorizontal areas (northern part of canton D) where lateral drainage is low, or in the lowlands.

### 2.1.4. Forest vegetation

The cork oaks which originally formed the Maâmora forest have in large part been replaced by other species, including *Quercus suber* and *Pyrus mamorensis* (the only natural tree species); eucalyptus (*Eucalyptus camaldulensis* for the production of cellulose, *Eucalyptus gomphocephala* for timber production, *Eucalyptus grandis*, *Eucalyptus cladocalyx*, *Eucalyptus sideroxylon* and *Eucalyptus clonal*), pine (*Pinus pinaster*, *Pinus canariensis*, *Pinus halepensis*, *Pinus pinea*) and acacia (mainly *Acacia mollissima* for the production of tannin, but also *Acacia cyclops* for feeding livestock and *Acacia horrida* for the construction of hedges) (Mounir, 2002).

Meanwhile, shrub vegetation is composed of species such as *Citrus linifolia*, *Chamerops humilis*, *Thymelaea lythroides*, *Daphne gnidium* and *Solanum sodomium* (Mounir, 2002).

Any natural forest becomes vulnerable when degraded or replaced by other species. Indeed, the adaptability of natural species is often greater than that of reforested species. Climate change will further exacerbate the vulnerability of non-natural forest ecosystems.

### 2.1.5. Anthropic activities

For several decades, the Maâmora forest has been subjected to anthropic pressures with negative impacts on the natural regeneration of cork oak trees and thus on the dynamics and health of the Maâmora ecosystem. In 1993, the resident population of the forest stood at about 300,000 inhabitants, or 4.5 inhabitants per hectare of cork oak forest. Livestock numbers totaled 173,000 heads of sheep and 52,000 heads of cattle, representing a density of 6.4 heads per hectare (Abourouh *et al.*, 2005). Stocking rates are relatively high because the forest's forage productivity is only 400 forage units per hectare (FU/ha) at best. Stocking rates have increased over time: the latest HCEFLCD statistics (2012) indicate a population of 341,360 inhabitants (or five inhabitants per hectare of cork oak forest) and 336,518 heads of sheep and 90 553 heads

of cattle, representing an overall livestock density of 7.1 heads per hectare.

### **2.1.6. Forest management**

Various rescue and planning schemes have been applied to the Maâmora forest over the course of the twentieth century (HCEFLCD, 2012). After a number of failed attempts to protect the cork oak trees, the Danish planning scheme (1972–1992) adopted the goal of maintaining cork oak trees where they are vigorous, and replacing them by other, more profitable species such as acacia, pine or eucalyptus where the reconstitution of cork oak is difficult.

Inspired by the experience of the Iberian Peninsula in agrosylvopastoral management of cork oak forests, the sylvopastoral planning scheme that followed (A.E.F.C.S., 1992) set as its objectives the regeneration and reconstitution of cork oak stands by means of the artificial planting of cork oak trees (direct sowing of acorns and planting). This planning scheme was relatively successful in that the area regenerated with cork oak increased.

The current planning scheme (2014–2024) likewise sets as one of its important objectives the recovery of cork oak stands. The objectives are simple and achievable, and may, if realized, revitalize the Maâmora forest. This forest planning scheme was used in the simulation with harvest disturbance.

The assessment of the various planning schemes applied to the Maâmora forest demonstrates that they failed because managers had difficulties rebuilding the cork oak forest. However, over time, it appeared that even where site conditions are difficult, regeneration techniques (such as sowing acorns) give satisfactory results and may constitute, for now, the best way to regenerate the cork oak forest.

### **2.1.7. Climate data**

Climate data used in the forest model are derived from the climate component of the platform by statistical downscaling, prepared by climatologists from the DMN. Three models were selected for Morocco: CanESM2 (Canada), MIROC-ESM (Japan) and MPI-ESMMR (Germany). Two climate scenarios (IPCC, 2013) are available on the platform: RCP4.5 (optimistic) and RCP8.5 (pessimistic). A scenario with current climatic conditions (1971–2000) is also available to compare the simulation results under scenarios RCP 4.5 and RCP 8.5 with results obtained in the absence of climate change.

The model uses monthly data for five variables: the maximum temperature ( $T_{Max}$ ), the minimum temperature ( $T_{Min}$ ), precipitation,



photosynthetically active radiation (PAR) and the CO<sub>2</sub> concentration in the atmosphere. Values for  $T_{Max}$ ,  $T_{Min}$  and precipitation derive from the climate component of MOSAICC. Values for PAR are calculated in the MOSAICC platform according to several variables, including  $T_{Max}$ ,  $T_{Min}$ , latitude, distance from the sea and elevation. The values for CO<sub>2</sub> concentration are obtained from the RCP4.5 and RCP8.5 scenarios.

Figure 43 indicates maximum temperatures for all models and scenarios for the months of January, April, July and October from 2011 to 2099.

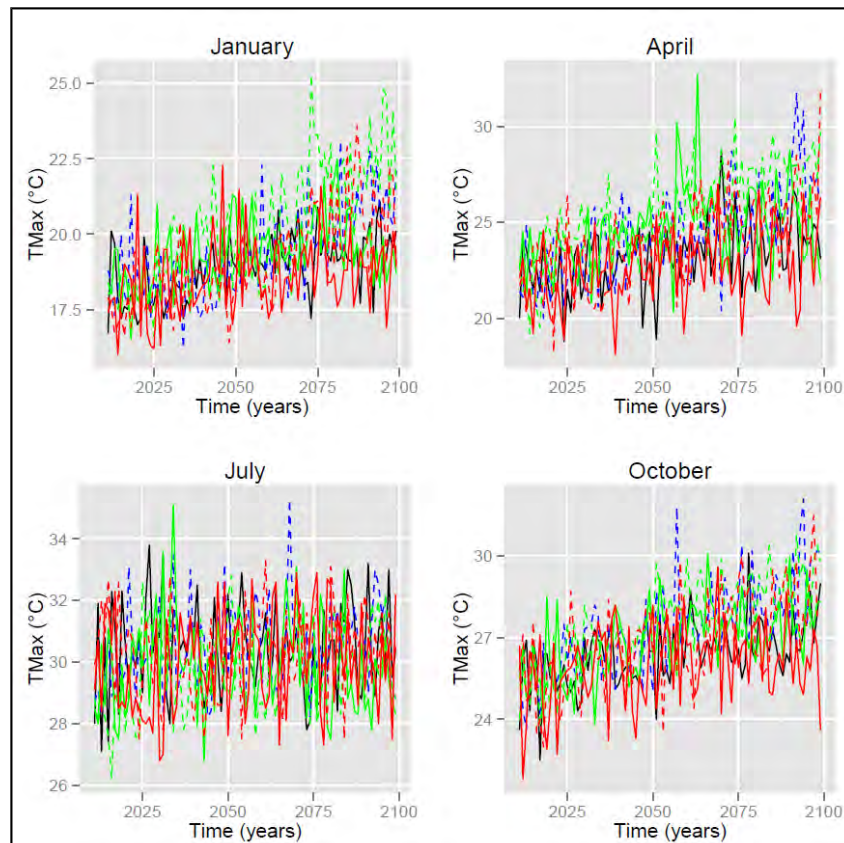


**Figure 43: Maximum temperatures in the Maãmore forest for three models and two scenarios, 2001–2099 (Blue solid line: model CanESM2 and scenario RCP4.5; blue dotted line: model CanESM2 and scenario RCP8.5 ; green solid line: model MIROC-ESM and scenario RCP4.5 ; green dotted line: model MIROC-ESM and scenario RCP8.5 ; red solid line: MPI-ESMLR model and scenario RCP 4.5 ; red dotted line: MPI-ESMLR model and scenario RCP8.5.**

### 2.1.8. Initial communities

The map of the initial communities constitutes a primary input to the LANDIS-II model. It was prepared based on the stand type layer developed

during the revision of the sylvopastoral planning scheme of the Maâmora forest for the period 1992–2012. Figure 44 shows the map of the initial communities.

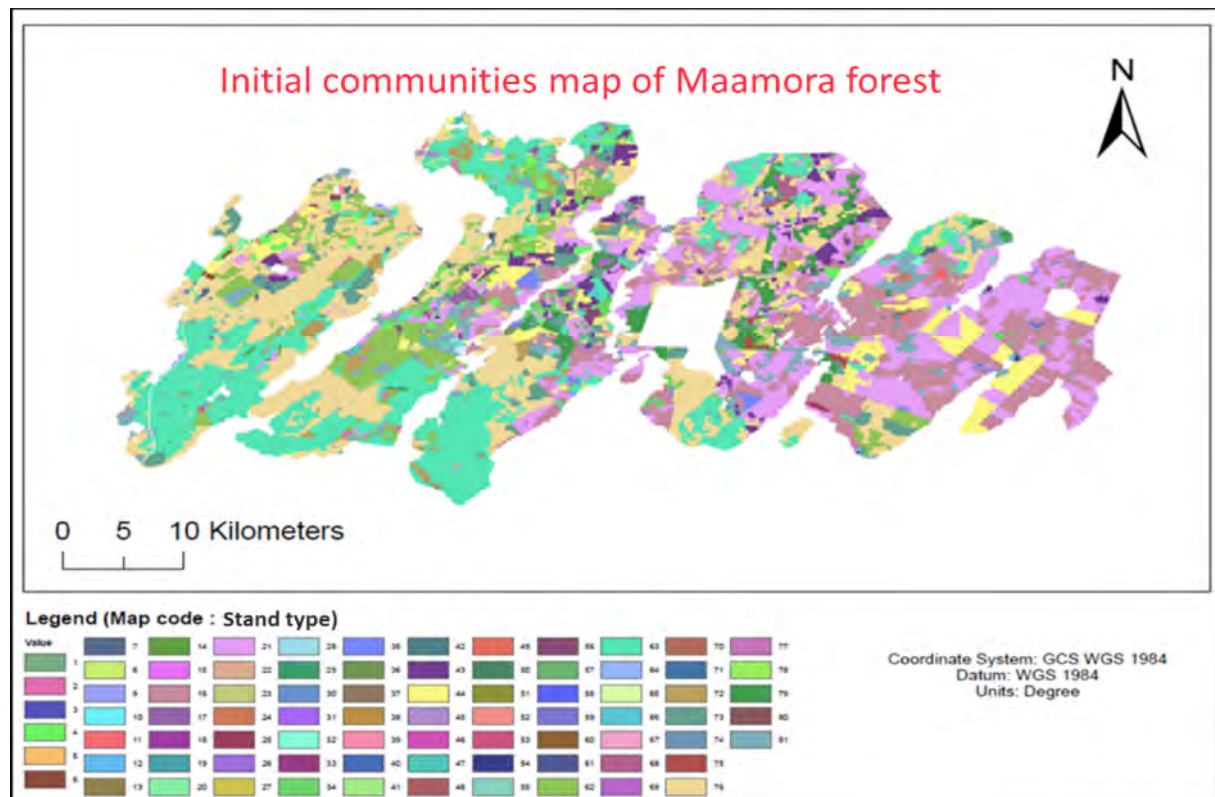


**Figure 44: Initial communities map of the Maâmora forest.**

### 2.1.9. Species parameters

Process-based modelling can be defined as a procedure whereby the behaviour of a system is derived from a set of functional components and their interactions with each other and the environment, using physical and mechanical processes that occur over time (Godfrey, 1983; Bossel, 1994). To describe each of the functional components, a set of variables or parameters is required. However, in most cases, the values of these parameters are unknown or difficult to measure.

For the pilot area of Maâmora, a literature review (Reich *et al.*, 2009; Kattge *et al.*, 2009; Kerkhoff *et al.*, 2006; Blonder *et al.*, 2011; Price *et al.*, 2007; Paula *et al.*, 2009; Ogaya and Penuelas, 2003; Milla and Reich, 2011; Wirth and Lichstein, 2009) complemented by interviews with experts in the ecology of Moroccan ecosystems allowed for the identification of values for certain species parameters that are necessary for the use of the model. Table 19 summarizes the values of the variables for each species.

**Table 19: List of species of the Maâmora forest and their parameters.**

Codes	Species	Longevity (year)	Sexual maturity (year)	Leaf type	Heliophilous (/5)	Fire tolerance (/5)	Drought tolerance (/4)	Effective seed dispersal (m)	Maximum seed dispersal (m)	Resprout probability	Min age to resprout (year)	Max age to resprout (year)
acaccycl	<i>Acacia cyclops</i>	30	5	Evergreen broadleaf	5	3	4	20	100	0.95	1	12
acacmoll	<i>Acacia mollissima</i>	40	5	Evergreen broadleaf	5	2	3	20	100	0.95	1	20
casucunn	<i>Casuarina cunninghamiana</i>	40	10	Other	5	2	2	50	100	0.95	1	40
eucacama	<i>Eucalyptus camaldulensis</i>	120	5	Evergreen broadleaf	5	1	3	50	100	0.95	1	120
eucaclad	<i>Eucalyptus cladocalyx</i>	120	5	Evergreen broadleaf	5	1	3	50	100	0.95	1	120
eucaclon	<i>Eucalyptus clonal</i>	40	5	Evergreen broadleaf	5	1	3	50	100	0.95	1	40
eucagomp	<i>Eucalyptus gomphocephala</i>	120	5	Evergreen broadleaf	5	1	4	50	100	0.95	1	120
eucagran	<i>Eucalyptus grandis</i>	120	5	Evergreen broadleaf	5	1	2	50	100	0.95	1	120
eucaside	<i>Eucalyptus sideroxylon</i>	120	5	Evergreen broadleaf	5	1	4	50	100	0.95	1	120
pinucana	<i>Pinus canariensis</i>	40	9	Pine	5	1	2	50	100	0.95	1	40
pinuhale	<i>Pinus halepensis</i>	40	10	Pine	5	1	3	5	28	0	0	0
pinupina	<i>Pinus pinaster</i>	40	9	Pine	5	1	3	10	100	0	0	0
pinupine	<i>Pinus pinea</i>	40	9	Pine	5	1	3	10	100	0	0	0
pinuradi	<i>Pinus radiata</i>	40	9	Pine	5	1	1	10	100	0	0	0
pyrumamo	<i>Pyrus communis var. mamorensis</i>	120	10	Evergreen broadleaf	3	1	3	5	10	0.95	1	120
quersube	<i>Quercus suber</i>	120	15	Evergreen broadleaf	4	1	3	5	10	0.95	1	120

## 2.2. Experimental design

The study was conducted using the MOSAICC platform, an integrated platform bringing together a set of models and tools to assess the impacts of climate change at the national level. MOSAICC was developed to allow various experts to collaborate remotely, regardless of their affiliation (ministries, universities, research institutions), using their own data. It is also a modelling and simulation capacity building tool.

The purpose of MOSAICC is to assess the impacts of climate change on agriculture, forest resources and the economy by combining interdisciplinary, spatially explicit models. Its results are used to support decision-making processes at the national level. MOSAICC is a system of models designed to complete each stage of the impact assessment process, from downscaling to the analysis of the economic impacts at the national level.

The model used for the forestry component of MOSAICC is called LANDIS-II. This model simulates forest succession and disturbance across large landscapes, ranging from thousands to millions of hectares, with spatial resolution generally ranging between 10 and 250 meter. Individual cells with homogeneous climatic and soil parameters are grouped to constitute the ecoregions. Consequently, the likelihood that tree species can successfully establish themselves varies across ecoregions (Scheller and Mladenoff, 2004). To reduce the complexity of the model and limit the need for computer memory capacity, LANDIS-II studies cohorts (species-age), rather than individual trees. The user chooses the succession extension to simulate the establishment, growth, aging and senescence of cohorts. Depending on the extension, the cohorts are represented by the presence-absence or by a continuous measurement of the abundance (e.g. biomass) for each cohort. The cohorts are discretized into separate classes that generally reflect the time integration unit (i.e. no time) used to model the succession (Scheller and Mladenoff, 2004). Optional disturbance extensions simulate destructive ecological processes such as logging (Gustafson *et al.*, 2000) used in this study.

The version of LANDIS-II integrated in MOSAICC is linked to the new PnET-Succession extension based on physiological processes (process-based model). PnET-Succession integrates components of spatially explicit forest biomass, the Biomass-succession extension of LANDIS-II (Scheller and Mladenoff, 2004; Scheller, 2012), and the one-dimensional model of ecophysiology PNET-II (Aber and Federer, 1992; Aber *et al.*, 1995) into a unique extension which dynamically simulates the most important ecophysiological processes determining the response of tree species to factors such as shading, climatic conditions and the chemical composition of the atmosphere.

The low resolution climate data from the statistical downscaling portal of MOSAICC's climate component are amongst the initial entries for the

overall structure of the model. The model's other main inputs are i) the types of stands (initial communities); ii) species' parameters; and iii) ecoregions representing land areas with a certain homogeneity in edaphoclimatic and topographic factors.

### 2.2.1. Calibration

Following Hofmann (2005), model calibration is the task of adjusting an already existing model to a reference system (or, if system data is not available, to a trusted reference model). This is usually done by adjusting the (internal) parameters of the model according to input-output sets of the system (or reference model).

Three parameters in Table 19– *Leaf type*, *Drought tolerance* and *Heliophilous* – group several subparameter values in MOSAICC to facilitate the use of the model. These subparameters are modifiable by the user on the platform and some of them are used during the calibration of species. MOSAICC allows users to integrate expected output values (e.g. from yield tables from the study area or from the literature). These outputs are used by MOSAICC to select parameter sets having outputs close to those expected (least squares method).

Maâmora yield tables were available for some species (*Eucalyptus sideroxylon*, *Eucalyptus camaldulensis*, *Quercus suber*, *Pinus pinaster*). For others, the data were derived from the literature (Sghaier and Ammari, 2012; Maseyk *et al.*, 2008; FAO, 1982; Theron *et al.*, 2004; Wieser *et al.*, 2002; Correia *et al.*, 2010). An example of calibration for *Quercus suber* is shown in .

The dots represent the actual data for biomass encountered in the Maâmora forest for deep and sandy soils (optimum growth). The curve represents the evolution of biomass over time in the LANDIS-II model after calibration in the MOSAICC platform.



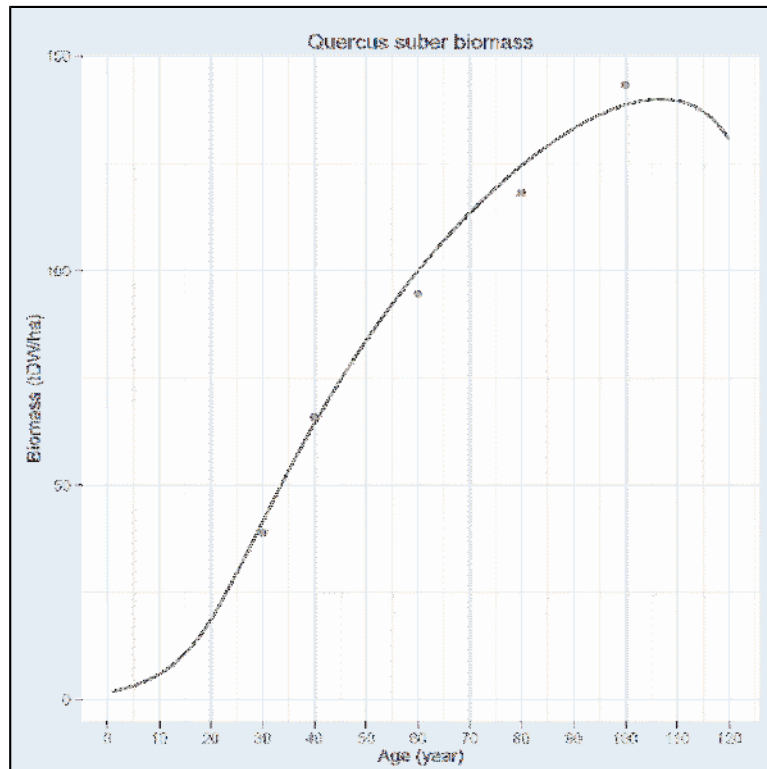


**Figure 45: Calibration of *Quercus suber* in the Maâmora forest.**

### 2.2.2. Ecoregions

An ecoregion is a geographical area distinguished by the uniqueness of its geomorphology, geology, climate, soil, water resources, fauna and flora. The LANDIS-II model simulates the development of cohorts by reference to the ecoregions of the study area. Ecoregions can be developed based on a number of factors which may be different from one zone to another.

In the context of the Maâmora forest, the factors that were considered in the development of the ecoregions map are the depth of the clay layer, the slope of the clay layer and the precipitation isohyets layer. A detailed analysis of the scientific literature on the Maâmora forest identified these factors as crucial to the development of forest species in the area. Figure 46 shows the eco-regions map of the Maâmora forest.

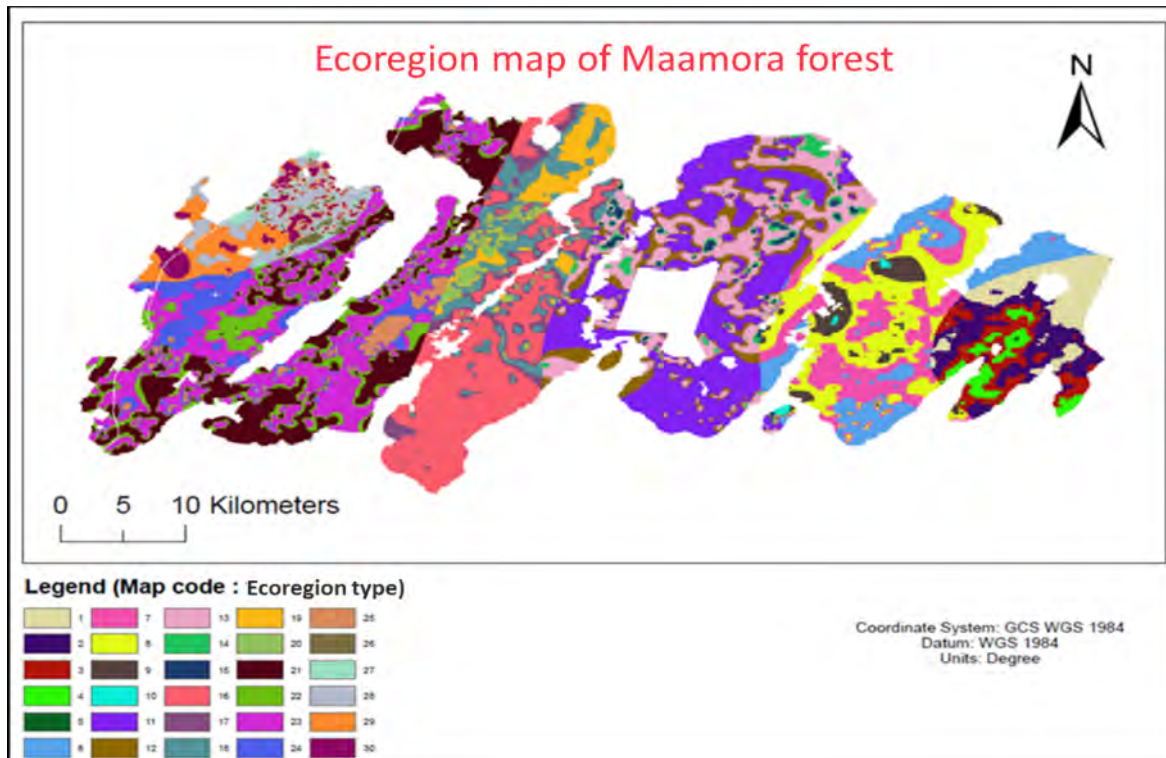


**Figure 46: Eco-regions map of the Maâmora forest.**

### 2.2.3. Forestry interventions

In the case of the Maâmora forest, forest fires are very rare and windfalls are almost nonexistent. For this reason, the only extension tested is the one related to forestry interventions (harvest). The data required for this extension are the plot maps, the stand maps per plot (management maps, stand maps) and the forestry interventions planned over time.

Forestry interventions are performed for each species individually. Eucalyptus trees are coppiced and subjected to release cutting, pine and acacia trees are coppiced with standards and planted after the final cut, and pine trees are thinned and pruned. *Quercus suber* undergoes several pruning and thinning operations prior to coppicing (50 percent of the stands between 75 and 100 years) or final cutting and planting (between 100 and 120 years). *Pinus radiata*, *Pyrus communis var. mamorensis* and *Casuarina cunningamiana* do not undergo any intervention.

Through the harvest disturbance extension, a success rate for the regeneration of *Quercus suber* of only 15 percent was introduced, to capture existing pressures on the natural regeneration of cork oak in the Maâmora forest (collection of acorns, livestock grazing, etc.).



# VIII. THE MOSAICC WEB-GIS PORTAL



## 1. Introduction

An interactive WEB-GIS portal has been developed for disseminating data generated by the MOSAICC tool to a wide audience of users (students, researchers, policy makers, extension services, NGOs, etc.). The portal is installed on server at the National Institute for Agronomic Research (INRA) and is freely accessible via the address: [www.changementclimatique.ma](http://www.changementclimatique.ma) (Figure 47). It contains documents of the project, training and dissemination material, list of partners and two didactic tools which are the core and innovative component of the portal, i.e. the “CC Impact” and “Simulator” tools. These tools gives hand for displaying maps and graphs of climate change projections, and impacts of climate change on agriculture, water and forests. The two RCP4.5 and RCP8.5 of the latest IPCC report (IPCC, 2013), for CanESM2, MIROC-ESM, MPI-ESM-LR climate models, and for the following three time periods: 2010 – 2039, 2040 - 2069 and 2070 – 2099 are available. Besides, climate change projections are available for “average” RCP and models.

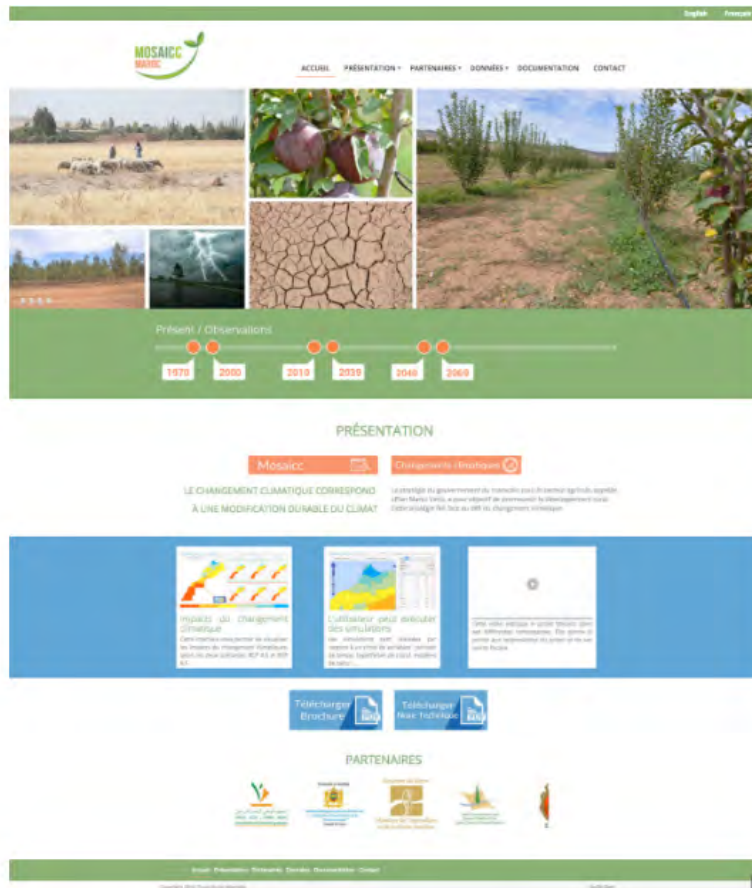


**Figure 47: The MOSAICC Web-GIS portal**  
[www.changementclimatique.ma](http://www.changementclimatique.ma).

The interface portal is designed to be easily used. The home page appears as follows:

- Home
- Presentation
  - MOSAICC
  - Climate Change
  - Technical Architecture
  - Exchange Workshops
  - Resources
- Partners
  - National
  - International
- Data
  - CC Impact
  - Simulator
- Documentation

- Contacts

Most of the contents is static, except the Data section:

- **CC Impact** - Simple point-and-click interface with three views on the data: Variable Overview, Single Variable Mode and Comparison Mode. Built-in PDF generation facility.
- **Simulator** - WEB-GIS based interface for advanced users that offers highly configurable query system for detailed analysis

## 2. Technology overview

The MOSAICC WEB-GIS portal can be displayed in any Web browser (Chrome, Firefox, Internet Explorer, etc.). The portal was written in Drupal<sup>10</sup>, which is a free and open source content management system (CMS). CMS can manage the content of a website, without resorting to a programmer. Drupal is a tool dedicated to both beginners and experts programmers. Due to its flexibility, Drupal is tailored for various market needs: corporate websites, blog, directory, community, merchant or intranets, etc.. Drupal is fully programmed in PHP. The set consists of modules orbiting a lightweight core. Each module is a kind of function library which enriches the application and increases its possibilities. One of Drupal's strengths is the ability of the modules to interact. The counterpart of this flexibility is complexity and, Drupal often proposes one or more solutions to solve the same problem. On the other hand, sometimes it is difficult to find "the" module that best answers particular needs. Another point that distinguishes Drupal from other CMS, is that the site and its administration interface are intertwined: Administrators publish their content in the same graphics context or nearly that of the visitor. This can be confusing at first, but by the very productive and intuitive suite.

## 3. The CC Impact tool

The Climate Change Impact tool ("CC Impact") gives hand for displaying maps and graphs of impacts of climate change impacts on agriculture, water and forests (see configuration and installation details in annex 9). Additionally, it also, displays climate change projections in a multiple windows menu (in comparison mode), for minimum and maximum temperature, rainfall and potential evapotranspiration. All generated maps can be printed in a pdf file format for dissemination purposes.

10 See: <https://www.drupal.org/>

The CC Impact tool can display with three views on the data (Figure 48) :

- Variable Overview
- Single Variable Mode
- Comparison Mode.

The CC Impact tool provides the results displayed as simple maps (static or interactive) in a printer-friendly version that can be download and printed. The PDF file contains maps, data and charts. It adapts to the user's selection: therefore, each page provides a different content.

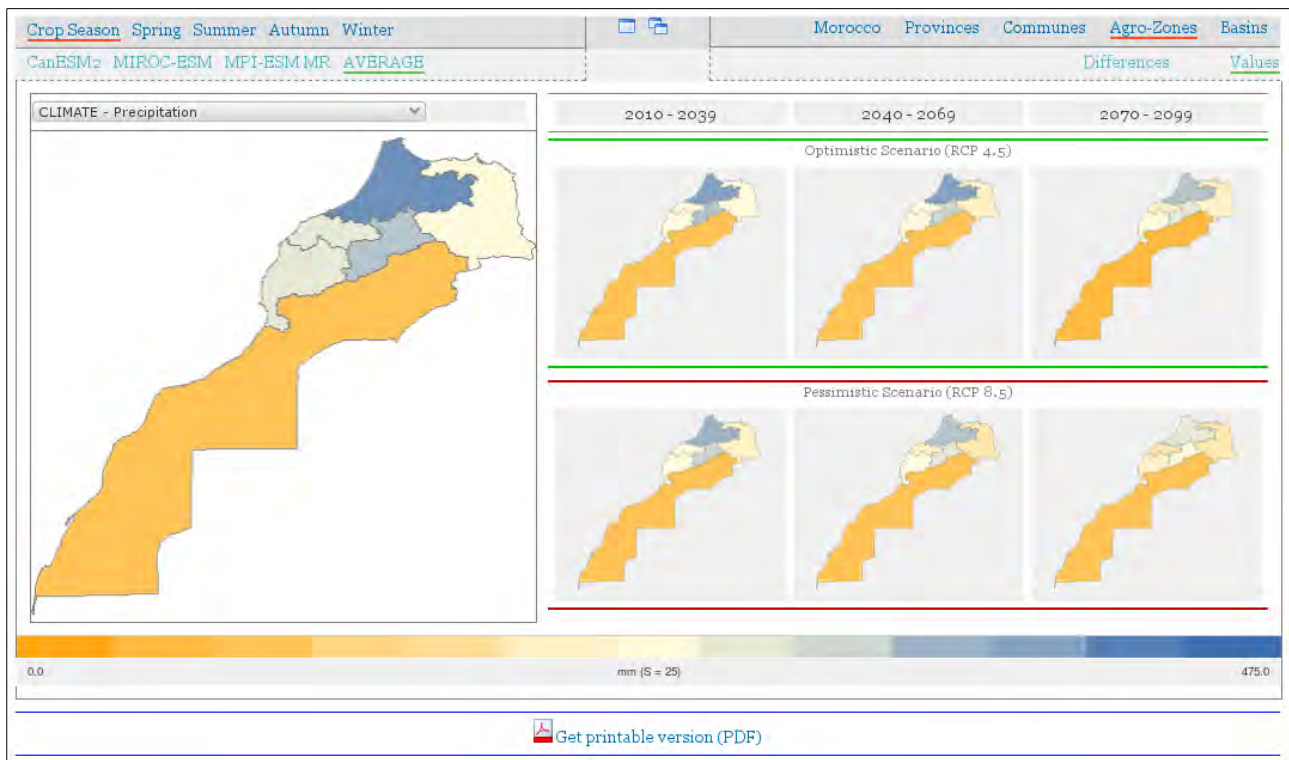


**Figure 48: The CC Impact tool.**

More precisely, the page layout has 6 parts:



**Period Selector**  
It allows the user to select the period to display with a simple click on one of them:

- Crop Season (September-August)
- Spring
- Summer
- Autumn
- Winter

**Aggregation Level Selector**  
It allows the user to select the level of aggregation of the data with a simple click on one of them:


- Morocco
- Provinces
- Communes
- Agro-zones
- Basins

**Model Selector**  
It allows the user to select the model to display with a simple click on one of them:

- CanESM2
- MIROC-ESM
- MPI-ESM-MR
- AVERAGE

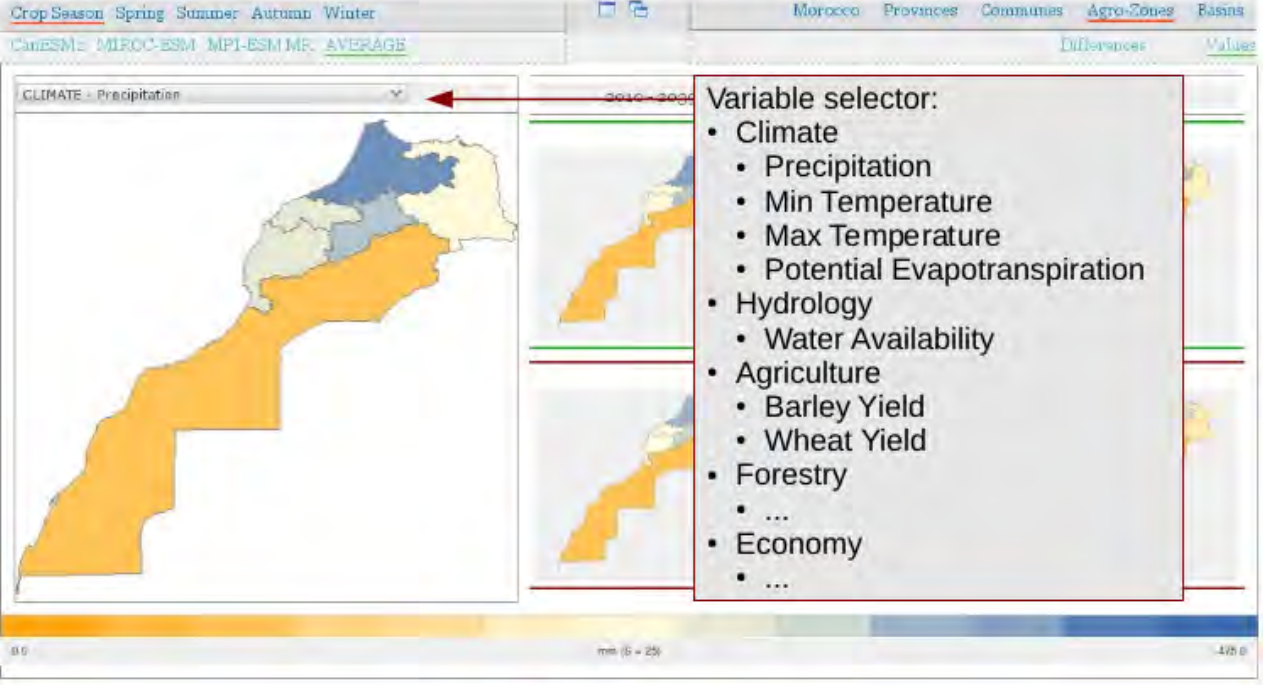
**Data Visualization Mode Selector**  
It allows the user to select the mode to display the data with a simple click on one of them:

- Difference
- Values



Single Variable Mode Icon      Compare Mode Icon

The variable selector allows the user to display a specific one (Figure 49).



**Variable selector:**

- Climate
  - Precipitation
  - Min Temperature
  - Max Temperature
  - Potential Evapotranspiration
- Hydrology
  - Water Availability
- Agriculture
  - Barley Yield
  - Wheat Yield
- Forestry
  - ...
- Economy
  - ...

Get printable version (PDF)

**Figure 49: The variable selector of the CC Impact tool.**

Currently the following variables are available:

- CLIMATE
  - Precipitation
  - Min Temperature
  - Max Temperature
  - Potential Evapotranspiration
- HYDROLOGY
  - Water Available
- AGRICULTURE
  - Barley Yield
  - Wheat Yield
- FORESTRY
  - Eucalyptus camaldulensis
    - No Harvest
    - Harvest
  - Quercus suber
    - No Harvest
    - Harvest
  - Leaf Area Index
- ECONOMY
  - Production of
    - Barley
      - in favorable areas
      - in Unfavorable areas
    - Wheat
      - in favorable areas
      - in Unfavorable areas
  - Import of
    - Barley
    - Wheat
  - Price of
    - Barley
    - Wheat
    - Food
  - GDP

The overview page usually display 7 images (reference plus future in two scenarios), that give access to single variable view, but there are two exceptions:



- Forestry component shows the evolution of the Maâmora forestry every 5 years because the data are available at grid cells and can't be aggregated at any administrative level (Figure 50).
- Economy component shows the evolution of the selected variable as chart because makes no sense to map the data as they are very aggregated (Figure 51).

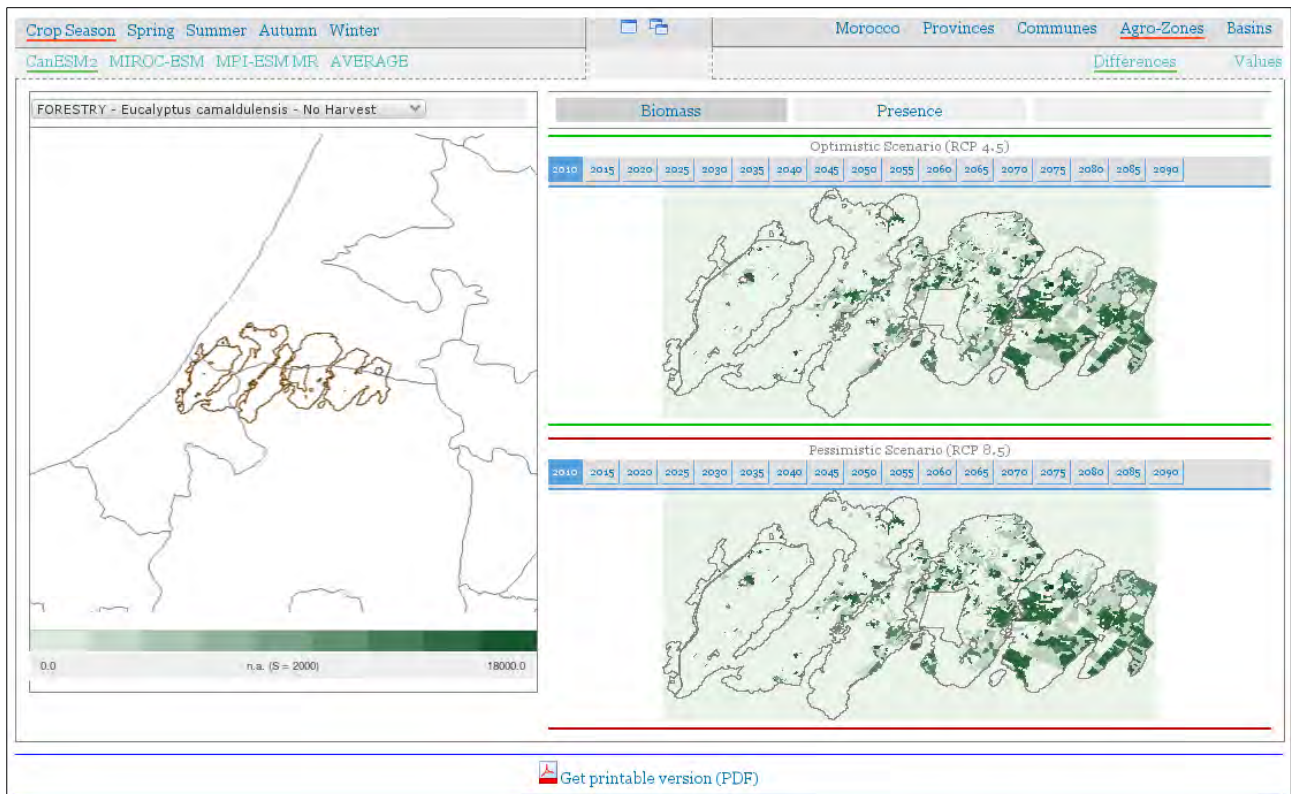


**Figure 50: The forestry component of the CC Impact tool.**



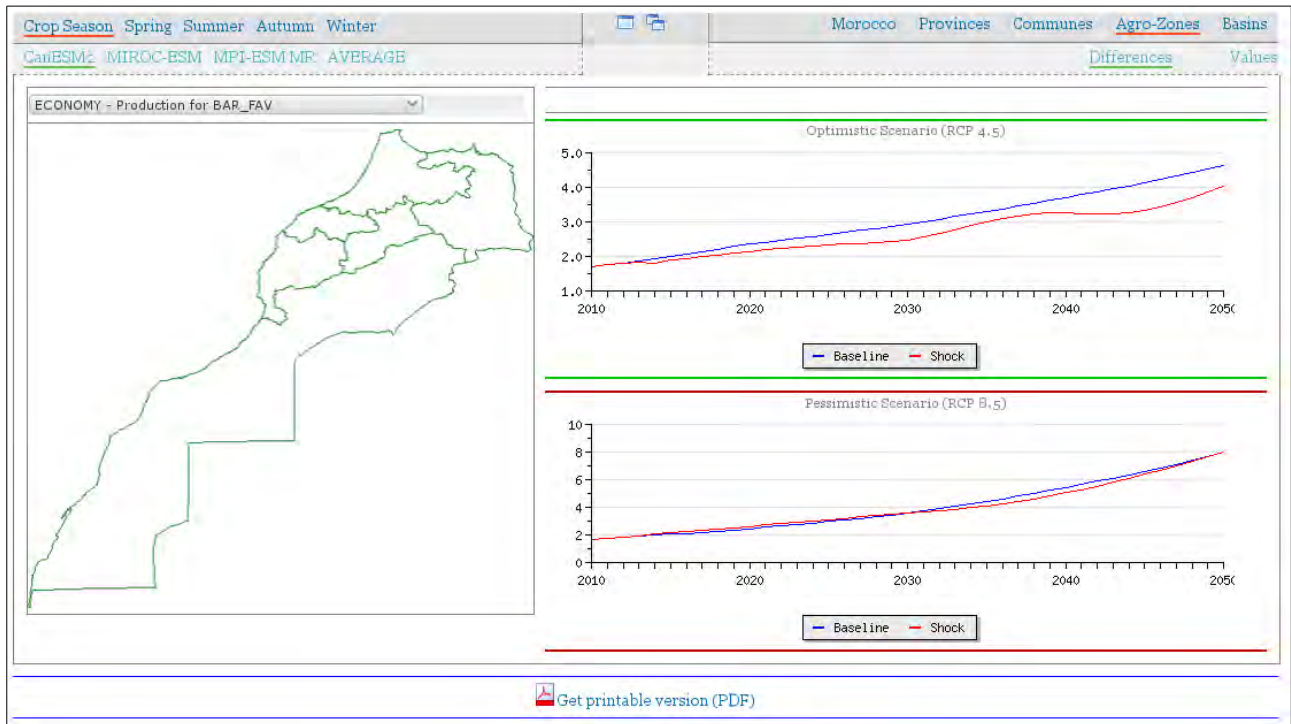


**Figure 51: The economy component of the CC Impact tool.**

### 3.1. The single mode of the CC Impact tool

The single variable mode has two parts (Figure 52): on the left the Web-GIS interface allows the user to inspect the map, and on the right the system displays the data related to the place where the user clicks. The right panel provides two views of the data: as chart and as table. The next pictures show an example:

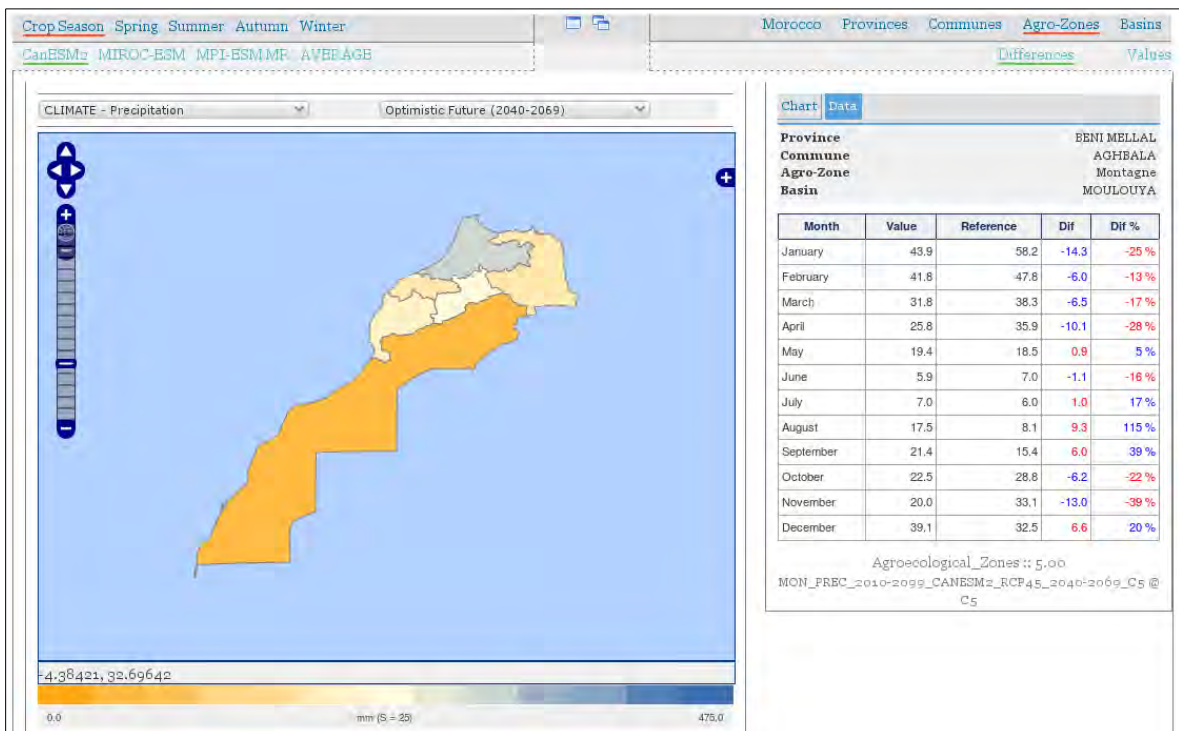
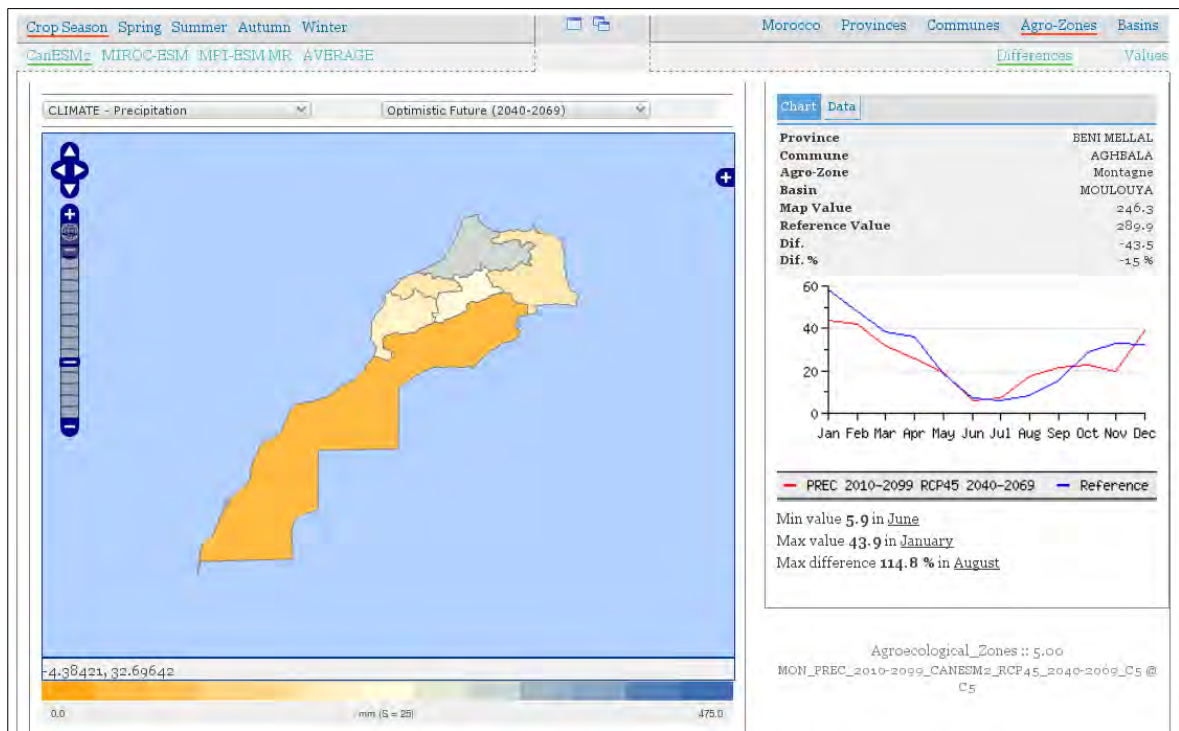
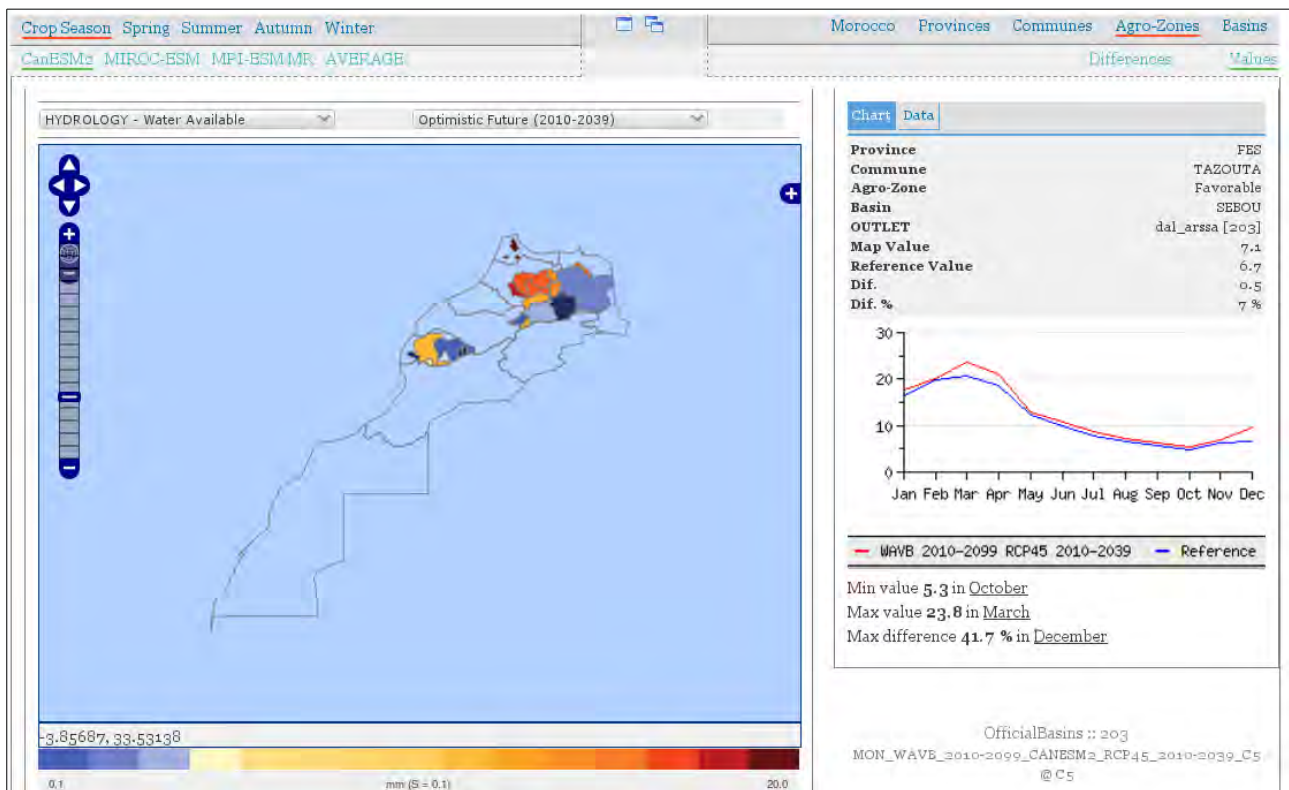


Figure 52: The CC Impact tool, in single variable mode.

The hydrology component displays maps the water availability, and charts and tables of discharge (Figure 53).



**Figure 53: The Hydrology component of CC Impact tool, displaying maps the water availability (left), and charts and tables of discharge (right).**

The water availability (WA) is calculated from the discharge as “WA=D/A”, where D is the discharge at the outlet of a basin and A is its area.

Four basins have been fully studied: Tensift, Sebou, Moulouya and Loukkos. For each basin, several hydrological stations were available with sufficient data to perform the calibration of the model. That operation allowed the experts to define a reliable way to estimate the water naturally available for each basin that each station represents. The basin of the Moulouya river is a good example to explain the idea. Seven stations were available, but the discharge recorded for some of them depend on the discharge measured in previous stations along the river. Each station is identified by a number and they are related as follows:

- 101, that is the last one, depends on
  - 102, but it depends on
    - 103
    - 104, that depends on
      - 105, that depends on

- 106
- 107

The hydrological model estimates the discharge for each station then we need to calculate the net value for each on considering how the water flows through the river.

The four basins have been studied using 23 stations, that define 23 sub-basins (Figure 54).

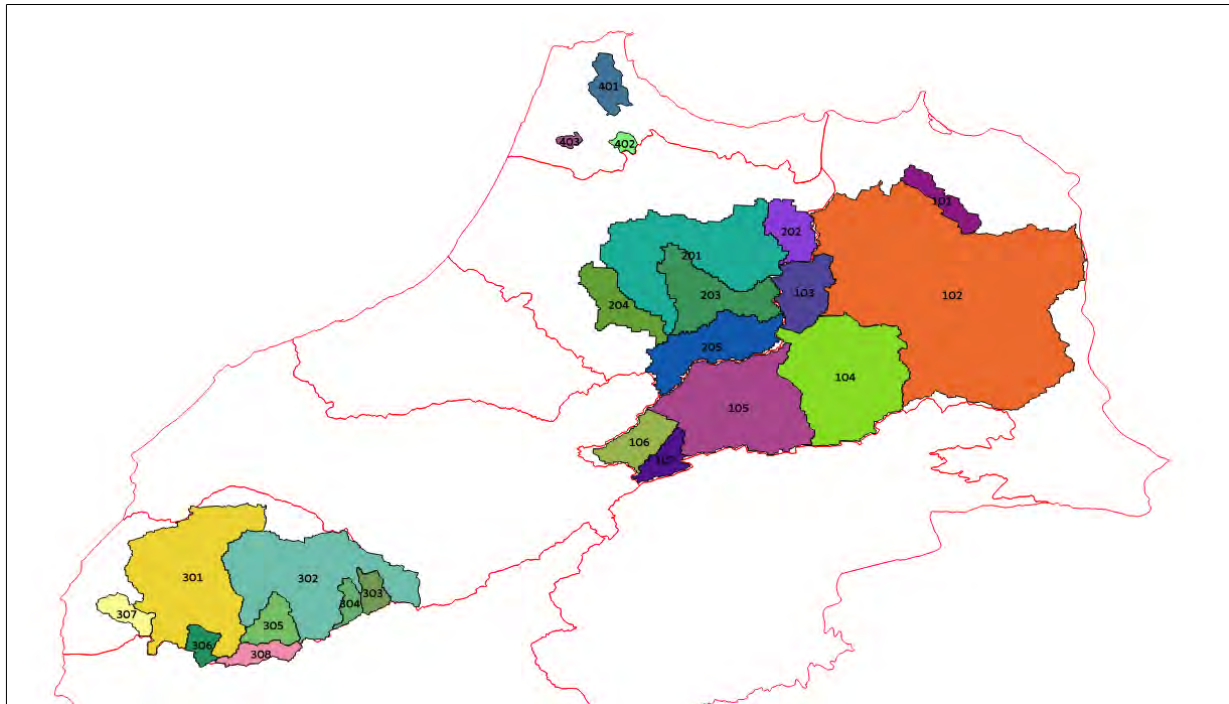


**Figure 54: Location of the four studied basins.**

The Figure 55 displays rivers, stations with their ID and related sub-basin in the Moulouya basin.



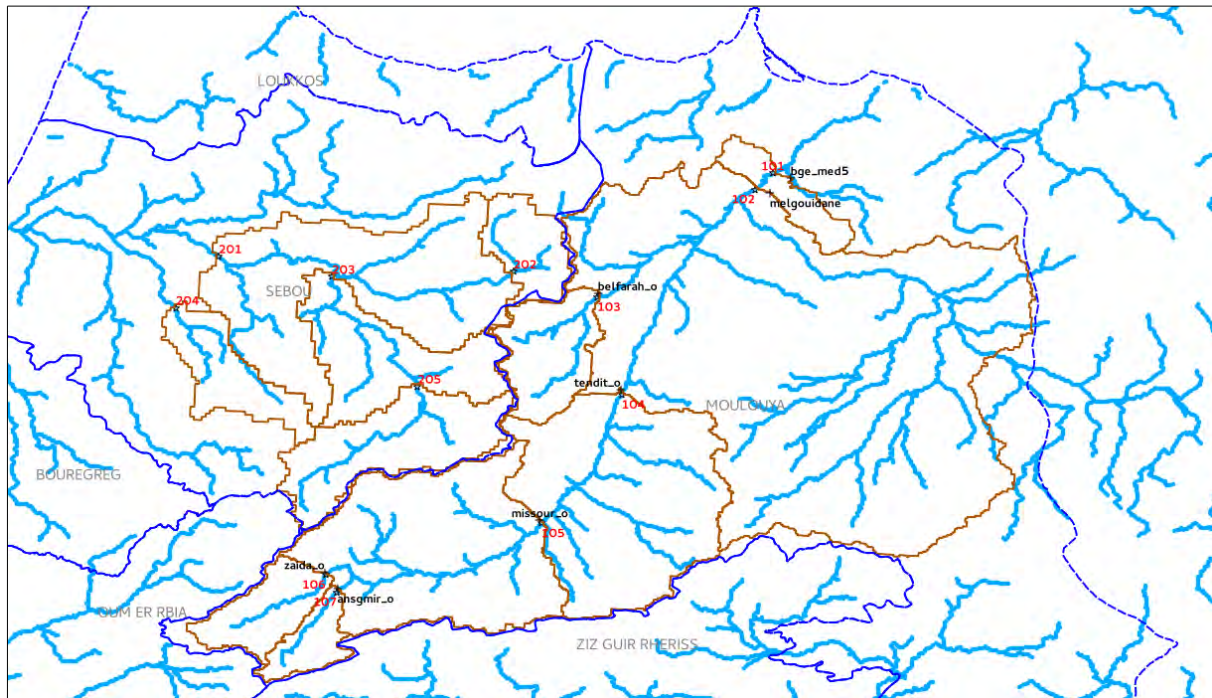


**Figure 55: Water discharge in the Moulouya basin.**

### **3.2. The comparison mode of the CC Impact tool**

The comparison mode is organized in three parts: on the top the user can select the variables he wants to compare (Figure 56).

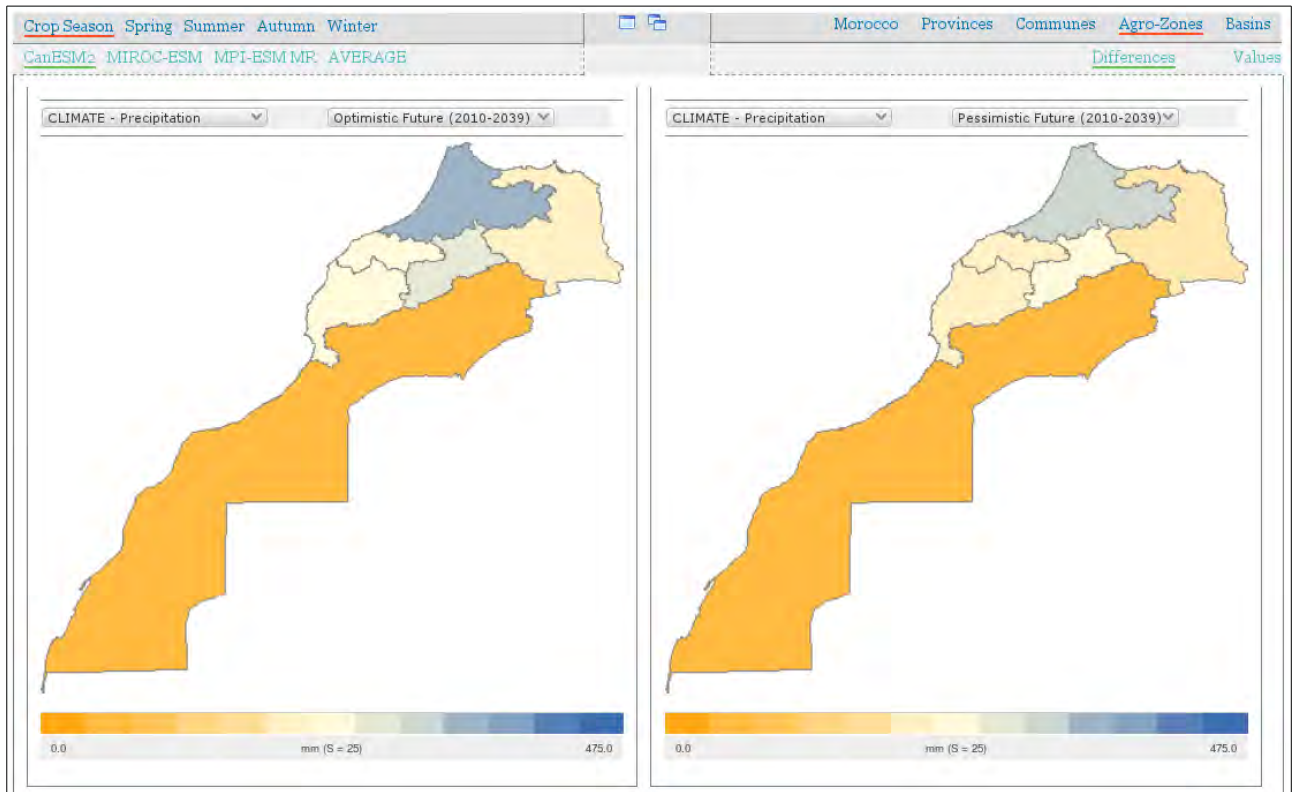


**Figure 56: The comparison mode of the CC Impact tool.**

Below the maps, the system displays two tables: the first one shows the data for each polygon, while the second provides details month by month (Figure 57).



NAME	LEFT	RIGHT	DIF	% DIF
Defavorable Oriental	200.3	197.4	2.9	1.5 %
Defavorable Sud	231.1	216.7	14.3	6.2 %
Favorable	351.1	323.7	27.4	7.8 %
Intermediaire	229.3	204.4	24.9	10.9 %
Montagne	283.1	266.4	16.7	5.9 %
Saharienne	67.4	71.0	-3.6	-5.3 %

### Monthly average comparison

Name	Jan	Feb	Mar	Apr	May	Jun	Jul	Aug	Sep	Oct	Nov	Dec
Defavorable Oriental	33.2	26.0	30.9	25.4	13.0	5.0	4.4	11.7	14.2	20.7	20.7	29.2
	33.4	27.6	23.7	26.8	16.3	4.8	4.5	9.4	19.5	23.0	18.6	24.8
	0.2	1.6	-7.2	1.4	3.3	-0.2	0.1	-2.3	5.3	2.3	-2.1	-4.4
	0.6 %	6.2 %	-23.3 %	5.5 %	25.4 %	-4.0 %	2.3 %	-19.7 %	37.3 %	11.1 %	-10.1 %	-15.1 %
Defavorable Sud	46.2	32.2	37.8	25.8	11.5	3.1	3.8	9.4	9.4	20.1	26.4	33.0
	40.8	34.0	28.1	25.1	13.0	3.8	3.6	7.9	13.9	20.6	22.2	31.9
	-5.4	1.8	-9.7	-0.7	1.5	0.7	-0.2	-1.5	4.5	0.5	-4.2	-1.1
	-11.7 %	5.6 %	-25.7 %	-2.7 %	13.0 %	22.6 %	-5.3 %	-16.0 %	47.9 %	2.5 %	-15.9 %	-3.3 %
Favorable	70.4	48.5	55.3	39.5	16.8	4.3	3.6	8.3	11.4	32.4	38.1	55.5
	66.3	50.6	39.3	41.5	18.1	4.6	3.4	7.0	15.5	30.3	35.4	44.9
	-4.1	2.1	-16.0	2.0	1.3	0.3	-0.2	-1.3	4.1	-2.1	-2.7	-10.6
	-5.8 %	4.3 %	-28.9 %	5.1 %	7.7 %	7.0 %	-5.6 %	-15.7 %	36.0 %	-6.5 %	-7.1 %	-19.1 %
Intermediaire	50.7	32.0	39.6	23.9	7.9	1.6	1.5	4.1	4.4	15.9	27.3	35.5
	45.5	33.7	25.8	22.4	9.5	1.8	1.2	2.9	7.0	16.4	21.4	32.1
	-5.2	1.7	-13.8	-1.5	1.6	0.2	-0.3	-1.2	2.6	0.5	-5.9	-3.4
	-10.3 %	5.3 %	-34.8 %	-6.3 %	20.3 %	12.5 %	-20.0 %	-29.3 %	59.1 %	3.1 %	-21.6 %	-9.6 %
Montagne	53.0	40.8	45.3	32.6	18.0	5.2	6.7	15.7	15.7	27.2	29.0	39.5
	45.5	41.1	34.8	33.8	19.8	6.2	6.7	14.1	22.6	25.8	26.8	36.1
	-7.5	0.3	-10.5	1.2	1.8	1.0	0.0	-1.6	6.9	-1.4	-2.2	-3.4
	-14.1 %	0.7 %	-23.3 %	3.7 %	10.0 %	11.5 %	0.0 %	-23.3 %	43.9 %	-4.8 %	-7.8 %	-8.6 %

**Figure 57: Tables displayed by the comparison mode of the CC Impact tool.**

The monthly data comparison displays 4 rows for each month: left value, right value, absolute difference and percentage difference.

If the selected variables can't be compared, just the values of each one is displayed, as in Figure 58 where precipitation and temperature were compared:



**Figure 58: Monthly data comparison displayed by the comparison mode of the CC Impact tool.**

## 4. The Simulator tool

The “Simulator” tool can display climate change projections in terms of climatic data trends (Maximum and minimum temperature, rainfall, Reference evapotranspiration, and Rainfall Deficit i.e.  $\Sigma P/\Sigma ET_0$ ), comparatively to a reference period (1980-2010) or any other reference period which can be specified by the user. On the first tab “MOSAICC” of the Simulator tool, all maps can be displayed at any administrative level of Morocco (region, province, commune), or at grid level (4.5x4.5 km), all over the country (Figure 59). For any displayed map, corresponding data can be exported to Excel file, by clicking the “Results” button on the left side of the tool. Maps of climate change projections, can be displayed on various basemaps (OpenStreetMap, Terrain OSM, Mapquest, and Google Maps) and overlaying administrative boundaries. The Simulator tool has also the usual features of GIS (zoom, pan, length and area calculation, image export, etc.).

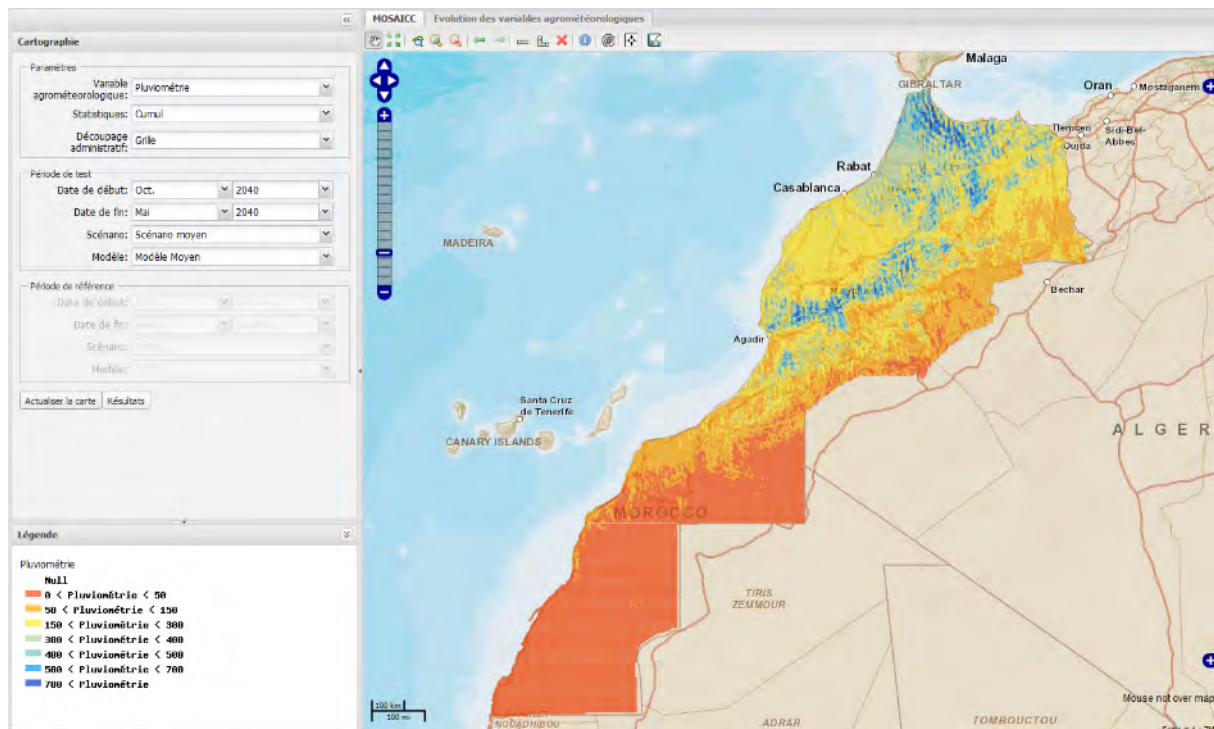


**Figure 59: The MOSAICC WEB-GIS portal, showing cumulated rainfall by 2040, at grid level (4.5x4.5 km).**

Using the «Evolution of agrometeorological variables» tab of the Simulator tool, charts and tables of the evolution of all climatic variables can be displayed and exported, at any administrative level, and for any RCP, climate model and time period (Figure 60).

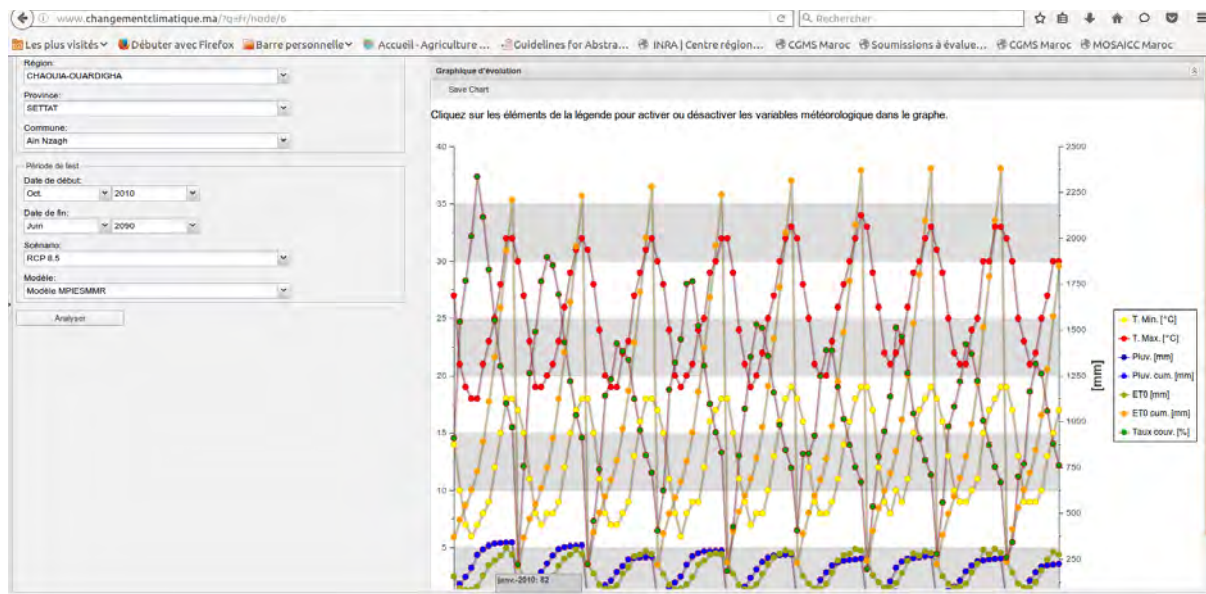


**Figure 60: Evolution of the climatic variables by 2090, according to RCP8.5, MPI-ESM-LR model in the district of Ain Nzagh (province of Settat).**

#### 4.1. Functionalities

The application has an interface that can be used both on a personal computer with a web browser or on the latest generation of mobile devices (tablet or smartphone) (Figure 61).



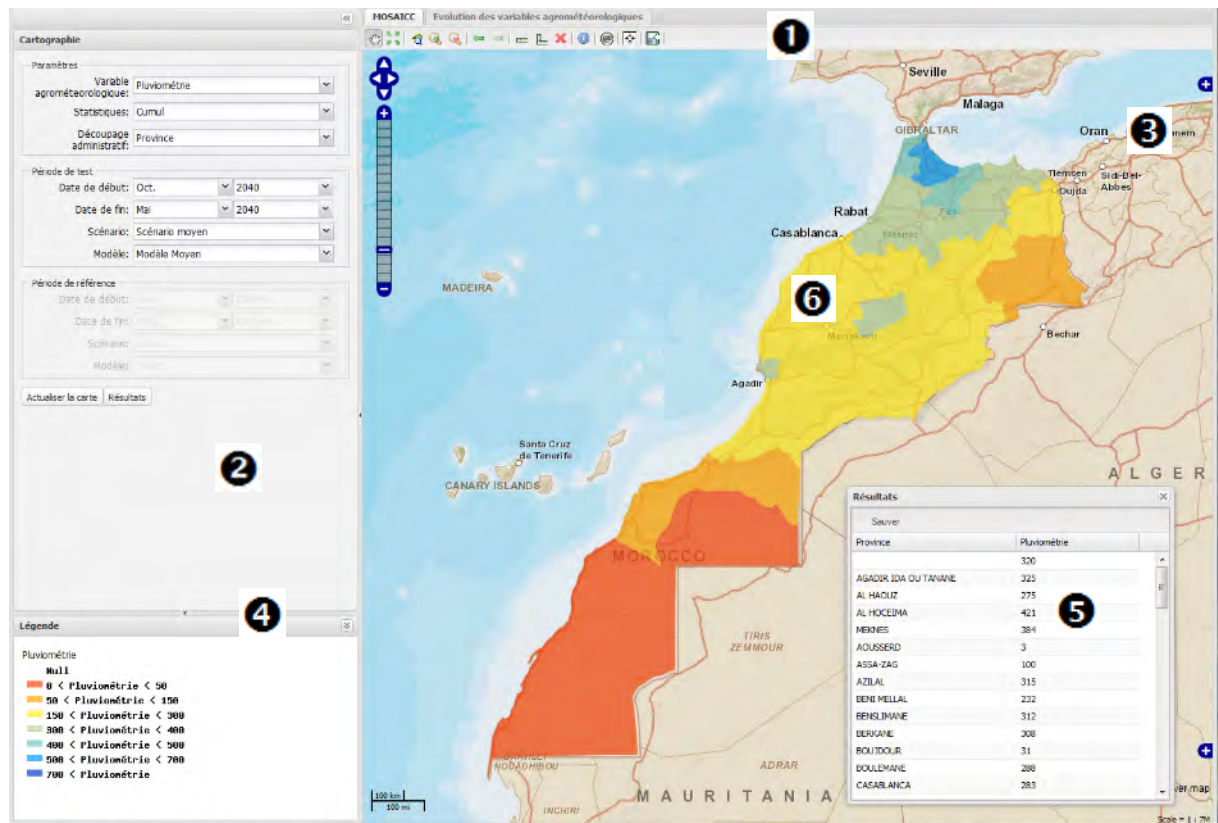


**Figure 61 : Functionalities of the Simulator tool.**

The various interface elements are: (1) Navigation tools, (2) query selector, (3) layers selector (4) Legend window, (5) Results window, and (6) the main window for displaying maps.

The Simulator tool has the following features:

- Display of climatic data;
- GIS type features such as zoom, move on map, calculating distance or surface and export image format for editing;
- Extraction of graphics and data, from current data and records for any period and administrative level.
- Access to external data and open source map sources, such as Open Street Map, Google Maps and Bing Maps.

#### 4.1.1. Chart display function

Figure 62 and Figure 63 show examples of chart display function. To obtain such a result the user must:

1. Login to the portal [www.changementclimatique.ma](http://www.changementclimatique.ma) and selected the Simulator tool tab.
2. Select the agro-meteorological variable to be displayed. In our case it is the maximum temperature "Tmax".
3. Select the statistic to perform on this variable. In our case it is the average.
4. Select the level of administrative aggregation. In our case it is the region.
5. Select the date of the beginning of the test period. In our case it is the month of June and the decade 2060.
6. Select the end date of the test period. In our case it is the month of August and the decade 2070. This will be interpreted as the period from June to August for two decades in 2060 and 2070.
7. Select the climate change scenario. In our case it is the RCP8.5.
8. Select the simulation model of climate change. In our case it is MIROC-ESM.
9. Once all these items selected, simply click on the button "Refresh map" to display the map.
10. To retrieve digital data click on the "Results" button to open a window for this purpose.

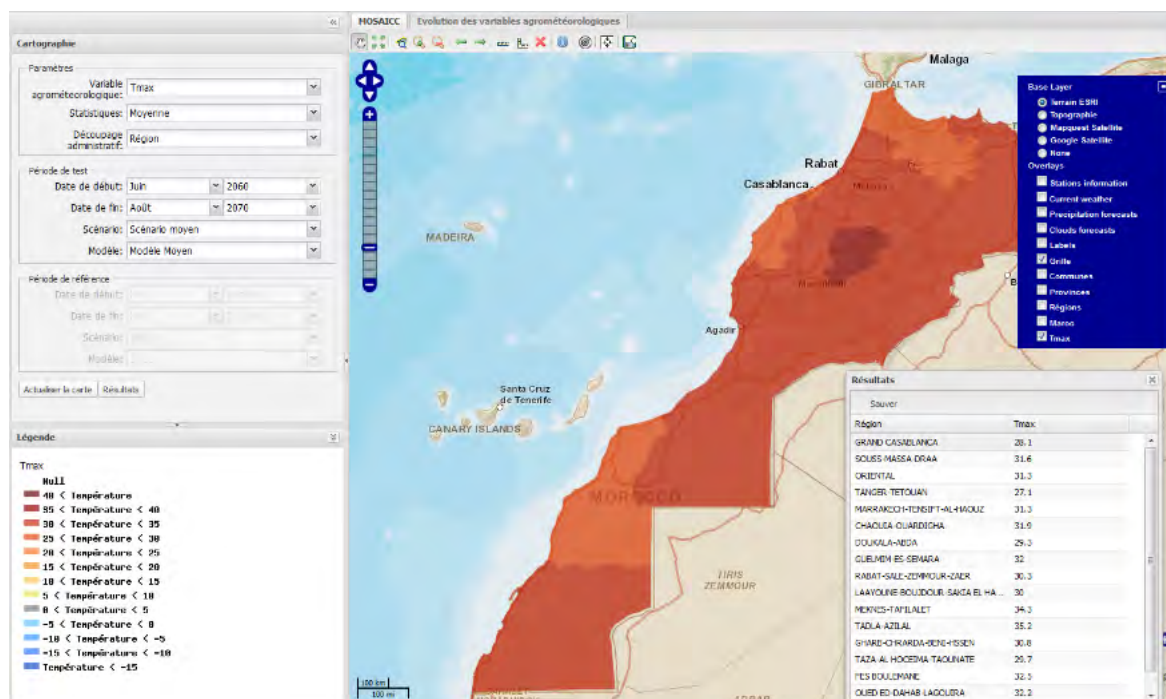




**Figure 62 : Regional average maximum temperatures between June and August, estimated in the decades 2060 and 2070, according to scenario RCP8.5 and using the MIROC-ESM model displayed with OpenStreetMap basemap.**

The "Results" window displays the numerical results and offers the possibility to export data in Excel format.

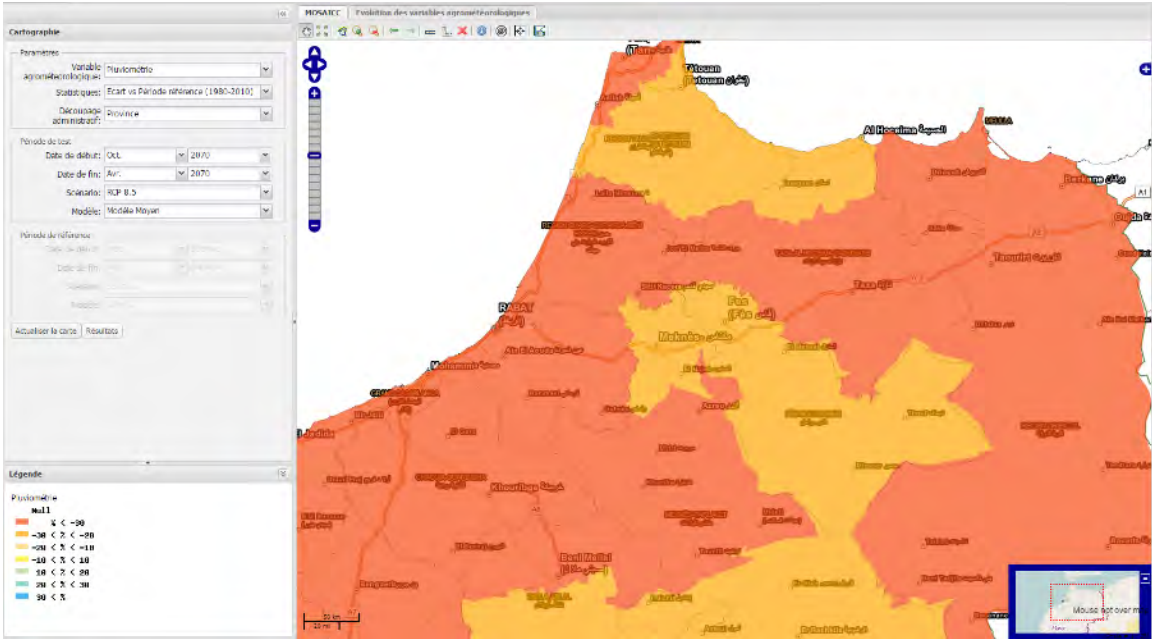


**Figure 63 : Deviation from the reference period (1980-2010) of cumulative rainfall between October and April, estimated in decade 2070 , according to RCP8.5 scenario and using the average climatic model.**

**4.1.2. Evolution of agro-meteorological variables function**

This feature displays a table and a chart of the evolution of agro-meteorological variables. In Figure 64, an example is shown for Meknes-Tafilalet region, between October and April, estimated in the 2070 decade according RCP8.5 scenario and using average climatic model. Once the selections are made, the button "Analyze" displays data as a table and a graph, both can be exported.

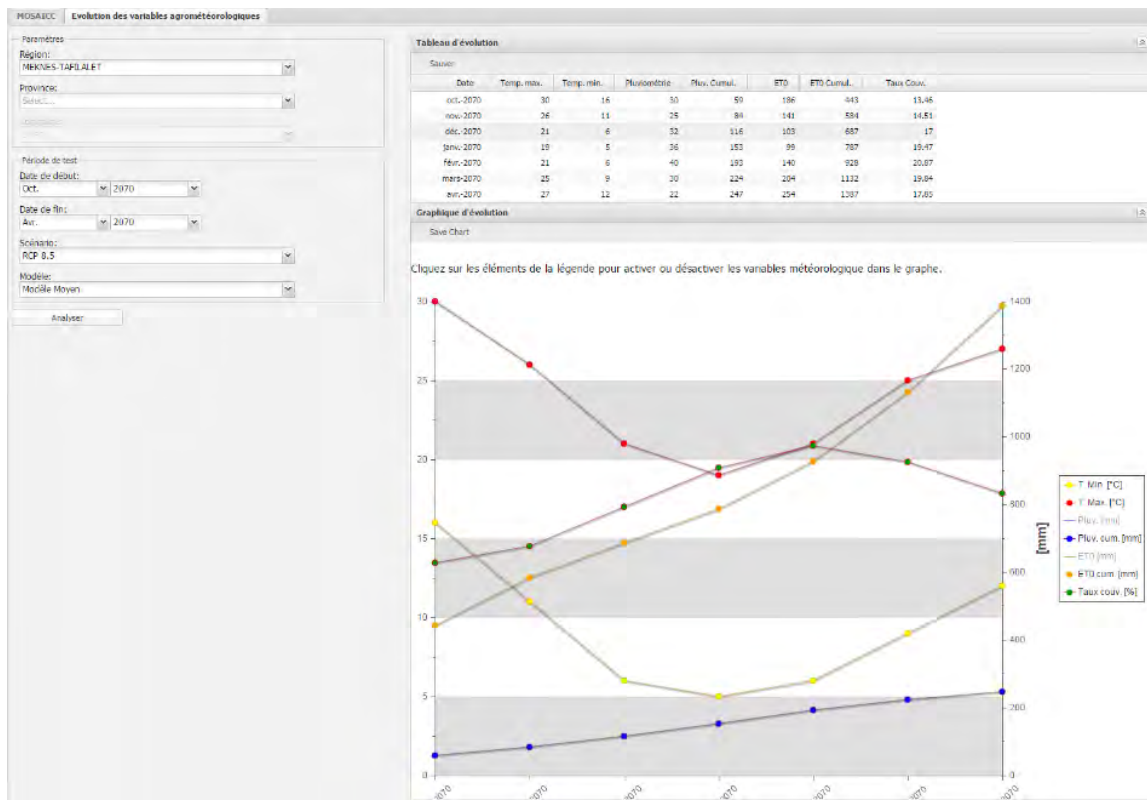


**Figure 64: Tabular and graphic evolution of the agro-meteorological variables for Meknes-Tafilalet region, between the months of October and April, estimated in decade 2070, according to RCP8.5 scenario and using average climatic model.**

## 4.2. Architecture of the system

The Simulation Tool include a database, from where climate data and results of the simulations are displayed.

### 4.2.1. Conceptual diagram of the data

The conceptual diagram of the data shows the internal structure of the data. Figure 65 shows the description of the different parts of the data flow and the objects forming each party.

### 4.2.2. Database tables

The database consists of two types of tables: the tables of geographical references (reference grids, administrative boundaries and watersheds) and tables of simulation data generated by the MOSAICC tool. The following statements in SQL describe the various objects and also will recreate them.

The following statements in SQL, describe the various objects and also allow to recreate them.

**Table `Grille`**

```
CREATE TABLE IF NOT EXISTS `GRILLE` (
  `GRID_NO` INT NOT NULL,
  `GÉOMÉTRIE` GEOMETRY NULL,
  PRIMARY KEY (`GRID_NO`));
```

**Table `Météo`**

```
CREATE TABLE IF NOT EXISTS `MÉTÉO` (
  `GRILLE_GRID_NO` INT NOT NULL,
  `DÉCÉNIE` INT NOT NULL,
  `MOIS` INT NOT NULL,
  `MODEL` VARCHAR(45) NOT NULL,
  `SCÉNARIO` VARCHAR(45) NOT NULL,
  `TEMPÉRATURE MIN` DOUBLE NULL,
  `TEMPÉRATURE MAX` DOUBLE NULL,
  `ETP` DOUBLE NULL,
  `PRÉCIPITATION` DOUBLE NULL,
  PRIMARY KEY (`GRILLE_GRID_NO`, `DÉCÉNIE`, `MOIS`, `MODEL`, `SCÉNARIO`));
```

**Table `National`**

```
CREATE TABLE IF NOT EXISTS `NATIONAL` (
  `IDNATIONAL` INT NOT NULL,
  `GÉOMÉTRIE` GEOMETRY NULL,
  PRIMARY KEY (`IDNATIONAL`));
```

**Table `Région`**

```
CREATE TABLE IF NOT EXISTS `RÉGION` (
  `RÉGION_ID` INT NOT NULL,
  `NOM RÉGION` VARCHAR(45) NULL,
  `GÉOMÉTRIE` GEOMETRY NULL,
  `NATIONAL_IDNATIONAL` INT NOT NULL,
  PRIMARY KEY (`RÉGION_ID`));
```

**Table `Province`**

```
CREATE TABLE IF NOT EXISTS `PROVINCE` (
  `PROVINCE_ID` INT NOT NULL,
  `NOM PROVINCE` VARCHAR(45) NULL,
  `GÉOMÉTRIE` GEOMETRY NULL,
  `RÉGION RÉGION_ID` INT NOT NULL,
  PRIMARY KEY (`PROVINCE_ID`));
```

**Table `Commune`**

```
CREATE TABLE IF NOT EXISTS `COMMUNE` (
  `Commune_Id` INT NOT NULL,
  `Géométrie` GEOMETRY NULL,
  `Nom Commune` VARCHAR(45) NULL,
  `Province_Province_Id` INT NOT NULL,
  PRIMARY KEY (`COMMUNE_ID`));
```

**Table `Commune\_has Grille`**

```
CREATE TABLE IF NOT EXISTS `COMMUNE_HAS_GRILLE` (
  `COMMUNE_COMMUNE_ID` INT NOT NULL,
  `GRILLE_GRID_NO` INT NOT NULL,
  PRIMARY KEY (`COMMUNE_COMMUNE_ID`, `GRILLE_GRID_NO`));
```

**Table `Productions agricoles`**

```
CREATE TABLE IF NOT EXISTS `Productions agricoles` (
  `PROVINCE_PROVINCE_ID` INT NOT NULL,
  `DÉCÉNIE` INT NOT NULL,
  `CULTURE` VARCHAR(45) NOT NULL,
  `MODEL` VARCHAR(45) NOT NULL,
  `SCÉNARIO` VARCHAR(45) NOT NULL,
  `RENDEMENT` DOUBLE NULL,
  PRIMARY KEY (`PROVINCE_PROVINCE_ID`, `DÉCÉNIE`, `CULTURE`, `MODEL`, `SCÉNARIO`));
```

**Table `Bassins versants`**  
CREATE TABLE IF NOT EXISTS `BASSINS VERSANTS` (  
 `BASSIN\_ID` INT NOT NULL ,  
 `GÉOMÉTRIE` GEOMETRY NULL ,  
 `NOM BASSIN` VARCHAR(45) NULL ,  
 PRIMARY KEY (`BASSIN\_ID`)) ;

**Table `Bassins versants\_has\_Grille`**  
CREATE TABLE IF NOT EXISTS `BASSINS VERSANTS\_HAS\_GRILLE` (  
 `BASSINS VERSANTS\_BASSIN\_ID` INT NOT NULL ,  
 `GRILLE\_GRID\_NO` INT NOT NULL ,  
 PRIMARY KEY (`BASSINS VERSANTS\_BASSIN\_ID`, `GRILLE\_GRID\_NO`)) ;

**Table `Apports Eau`**  
CREATE TABLE IF NOT EXISTS `APPORTS EAU` (  
 `BASSINS VERSANTS\_BASSIN\_ID` INT NOT NULL ,  
 `DÉCÉNIÉ` INT NOT NULL ,  
 `MODEL` VARCHAR(45) NOT NULL ,  
 `SCÉNARIO` VARCHAR(45) NOT NULL ,  
 `APPORTS EAU` DOUBLE NULL ,  
 PRIMARY KEY (`BASSINS VERSANTS\_BASSIN\_ID`, `DÉCÉNIÉ`, `MODEL`, `SCÉNARIO`)) ;

**Table `Revenus`**  
CREATE TABLE IF NOT EXISTS `REVENUS` (  
 `RÉGION RÉGION\_ID` INT NOT NULL ,  
 `DÉCÉNIÉ` INT NOT NULL ,  
 `MODEL` VARCHAR(45) NOT NULL ,  
 `SCÉNARIO` VARCHAR(45) NOT NULL ,  
 `REVENU` DECIMAL(10,2) NULL ,  
 PRIMARY KEY (`RÉGION RÉGION\_ID`, `DÉCÉNIÉ`, `MODEL`, `SCÉNARIO`)) ;

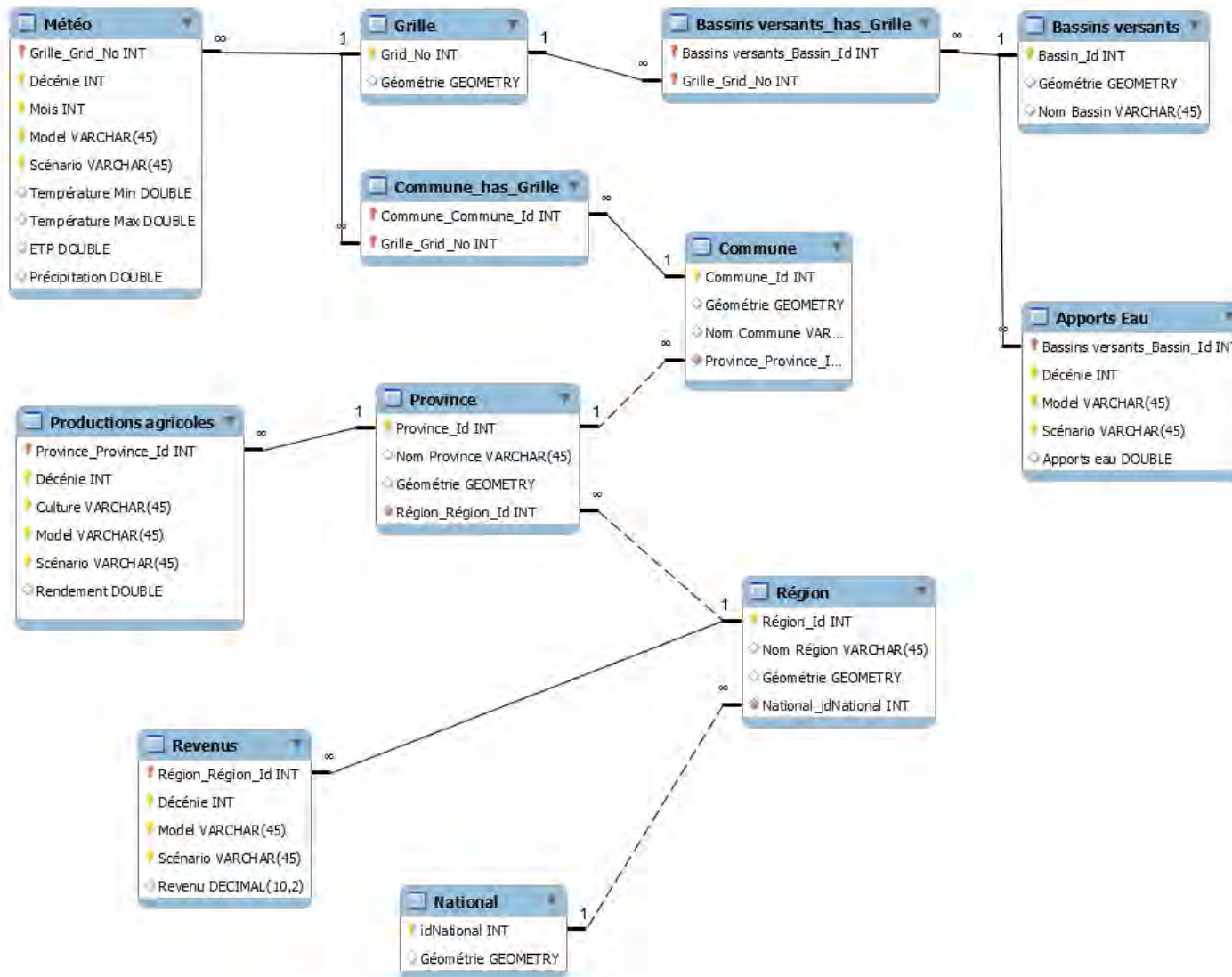


Figure 65: Data flow chart.

### 4.2.3. Software architecture

The software architecture was defined to satisfy the following services (see details in Annex 10) :

- Navigation on a simple map interface ;
- Display of the data, by selecting :
  - The climate data to be displayed (maximum and minimum temperature, rainfall, reference evapotranspiration and the water satisfaction ratio  $\Sigma P/\Sigma ET$ ).
  - Statistics to be displayed (long term average, sum, minimum, maximum, deviation from reference period 1980-2010, deviation from 2010-2039 projection, deviation from 2040-2069 projection, deviation from 2070-2099 projection, deviation from a specified period).
  - Spatial aggregation: Reference grid (4.5x4.5 km), district, province, region, whole country.
  - Start and end selected month of the cropping season.
  - Start and end selected decade.
  - Scenario (RCP4.5, RCP8.5), or average of the two scenario.
  - Climate model (CanESM2, MIROC-ESM, MPI-ESM-LR) or average of the three models.
- Data (Excel format) and maps export (jpg format), at any selected spatial aggregation.



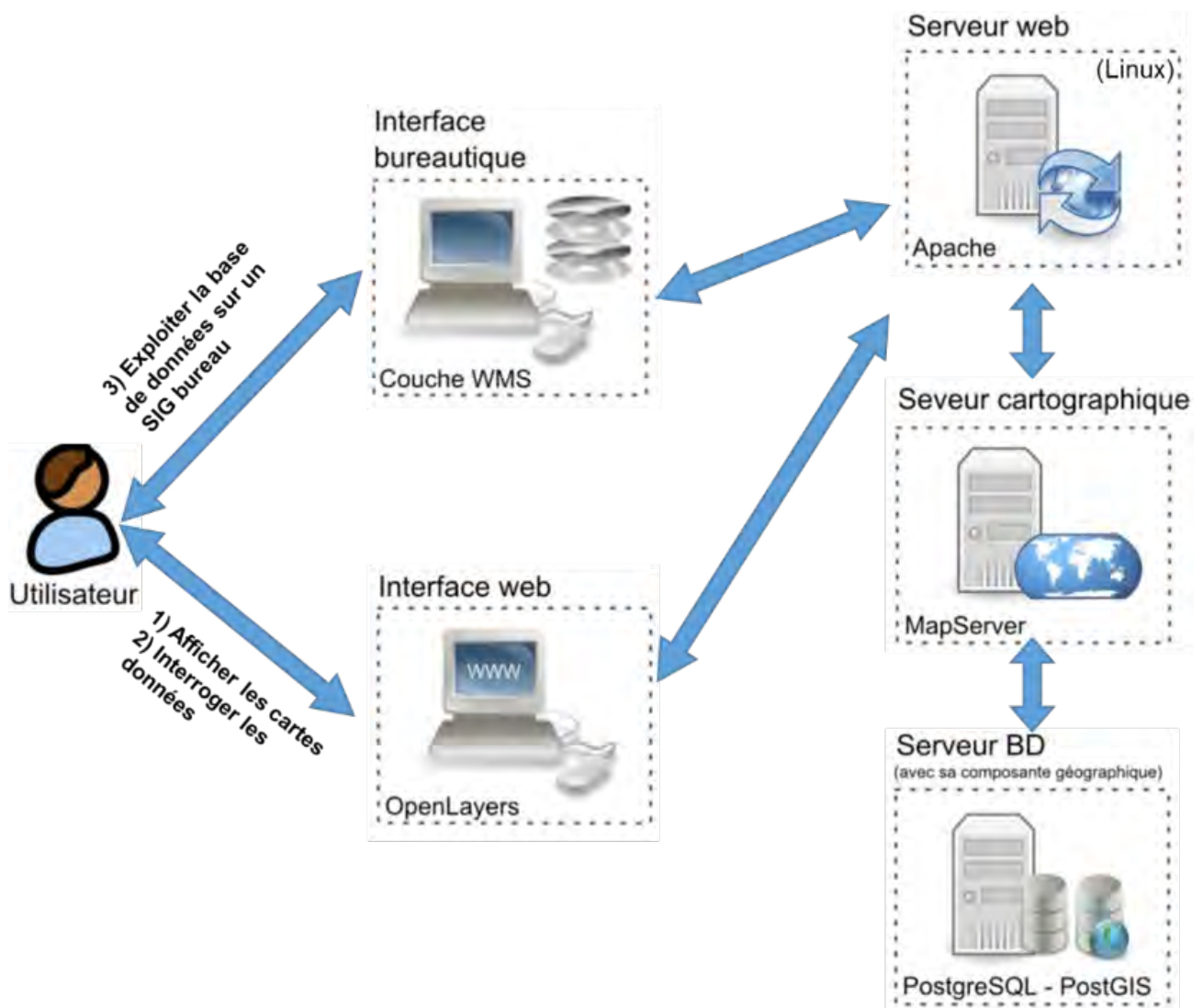


Figure 66: General architecture of the Simulator tool.

# IX. CLIMATE CHANGE TRENDS IN MOROCCO

## 1. Precipitations

Climate change would lead to a continuous decrease of rainfall in all agricultural areas of Morocco toward the end of the century, comparatively to reference period (1971-2000). Countrywide, rainfall would decrease by 17 and 20% toward the period 2040-2069, for scenarios RCP4.5 (optimistic) and RCP8.5 (pessimistic) respectively. However, the deficit is predicted to be marked over the rainy season, from October to April, i.e. 23 and 34% for scenarios RCP4.5 and RCP8.5 respectively (Table 20). These results are in accordance with the previous study realized in Morocco (Gommes et al., 2008), by FAO in collaboration with the Ministry of Agriculture and Maritime Fisheries and the National Institute of Agronomic Research.

**Table 20: Rainfall trends for the two climate scenarios (Optimistic-RCP4.5 and Pessimistic-RCP8.5) and for the average of three climate models (CanESM2, MIROC-ESM, MPI-ESM-LR).**

Month	Reference	Optimistic Scenario			Pessimistic Scenario		
		2010-2039	2070-2099	2040-2069	2010-2039	2070-2099	2040-2069
January	52.5	39.3	40.9	32.3	44.1	35.3	32.9
February	51.0	46.8	45.5	42.7	41.4	37.9	36.7
March	43.1	42.1	38.8	30.6	36.5	33.4	29.5
April	35.0	37.1	27.8	31.3	31.9	25.4	17.9
May	16.2	16.3	15.2	13.8	15.6	15.7	14.2
June	6.4	5.7	6.3	6.9	5.6	5.8	7.6
July	3.4	3.9	4.8	5.0	3.5	5.2	6.9
August	5.4	7.9	9.2	11.5	7.6	12.3	18.9
September	11.5	13.4	15.1	16.6	14.2	18.3	26.2
October	31.9	36.2	32.3	28.9	28.1	26.6	27.0
November	36.4	33.7	31.4	28.2	34.0	30.6	26.4
December	43.5	37.8	38.0	31.9	39.4	34.4	23.5

Color legenda: blue values are lower than the reference values and red values are higher than the reference values.

At subnational level, climate projections show that agricultural areas of Morocco (northwestern) will suffer more from rainfall deficit than other areas, up to -50% relatively to reference period, except for the Saharan part of the country (Figure 67). The increase in rainfall in this latter area could be explained by inconsistencies of climate change rainfall projections, since very few weather stations are available for downscaling. For example, the rainfall decrease would reach 37% in El Jadida, 36% in Settat, 33% in Sidi Kacem and Kelâa des Sraghna, 32% in Meknes, and 23% in Khenifra, for scenario RCP8.5 and toward the period 2070-2099.

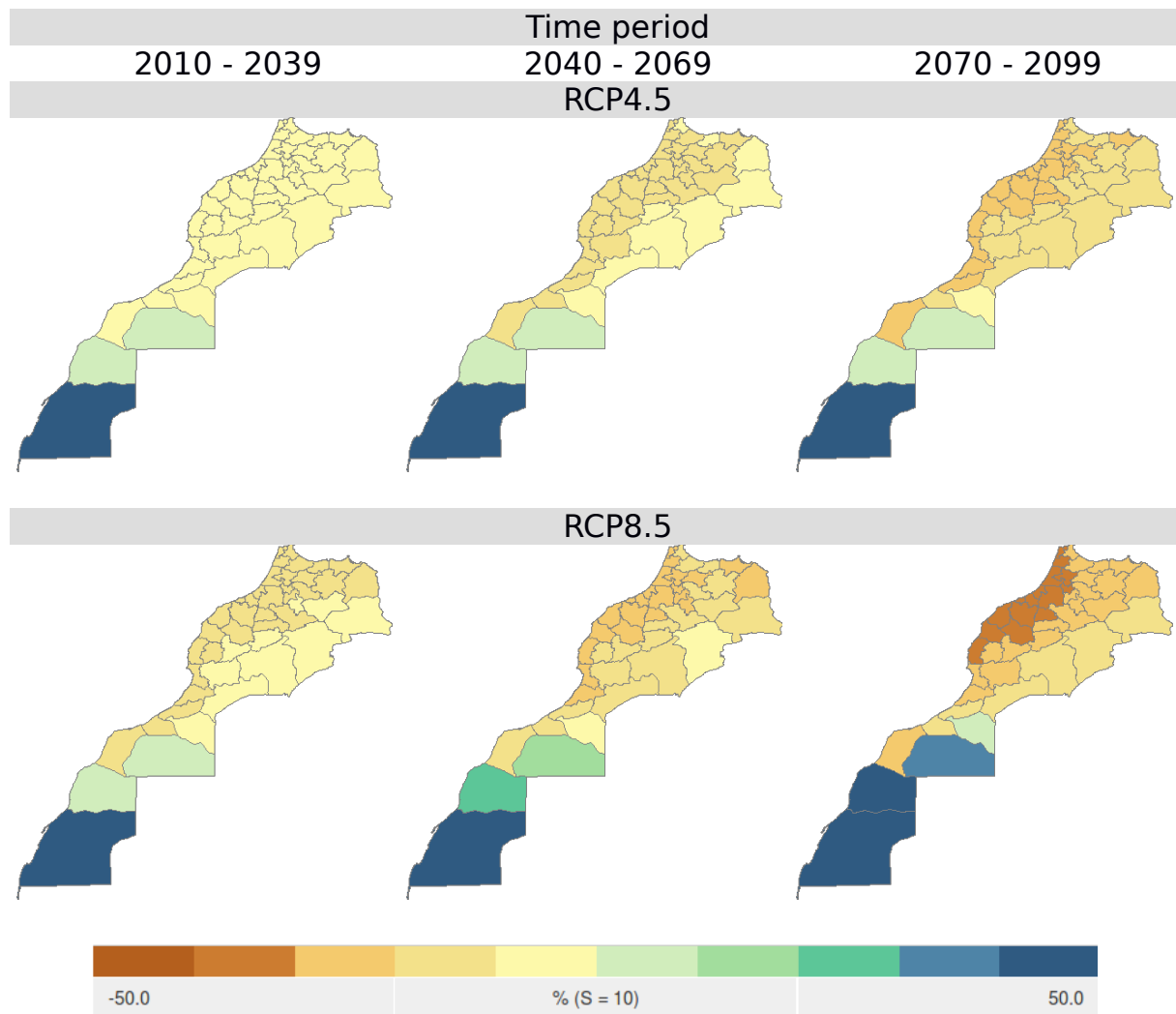


**Figure 67: Rainfall change (%), compared to reference period (1971-2000), at province administrative level, according to RCP4.5 and RCP8.5 scenarios and for average climate model.**

## 2. Maximum temperature

Climate change would lead to a continuous increase of maximum temperature (Tmax) in all Morocco toward the end of the century, comparatively to reference period (1971-2000). Tmax would increase by 1.9°C (+8%) and 3.4°C (+14%) toward the period 2040-2069, for scenarios RCP4.5 and RCP8.5 respectively. However, Tmax increase is predicted to be marked over the rainy season, from October to April, i.e. +2.4°C (+11%) and 4.4°C (+21%) for scenarios RCP4.5 and RCP8.5 respectively (Table 21). This temperature increase would exacerbate the expected rainfall deficit during this period of the cropping season.

**Table 21: Maximum temperature trends for the two climate scenarios (Optimistic-RCP4.5 and Pessimistic-RCP8.5) for the average of three climate models (CanESM2, MIROC-ESM, MPI-ESM-LR).**

	Reference	RCP4.5			RCP8.5		
		2010-2039	2040-2069	2069-2099	2010-2039	2040-2069	2069-2099
January	17,9	18,7	19,6	19,6	18,7	19,8	21,7
February	18,4	19,5	20,0	20,8	19,7	21,0	22,7
March	20,7	22,1	22,7	23,3	22,4	23,7	25,3
April	22,5	23,7	24,7	25,0	24,1	25,4	26,9
May	25,1	26,0	27,1	27,6	26,3	27,5	29,0
June	28,2	29,0	29,5	30,0	29,2	30,0	30,6
July	31,8	32,1	32,2	32,3	32,0	32,2	32,4
August	32,1	32,3	32,5	32,3	32,5	32,3	32,4
September	29,2	30,1	30,5	30,5	30,1	30,9	31,5
October	26,1	27,3	28,0	28,4	27,5	28,6	29,8
November	21,4	23,0	24,0	24,4	23,1	24,9	27,0

At subnational level, climate projections show that eastern arid areas of Morocco will be more impacted by Tmax rise, more than 5°C relatively to reference period (Figure 68). For example, the Tmax increase would reach 5.3°C in Azilal and Khenifra, 4.9°C in Ouarzazate, 4.8°C in Errachidia, 4.5°C in Oujda, 4.3°C in Kelâa des Sraghna, for scenario RCP8.5 and toward the period 2070-2099.

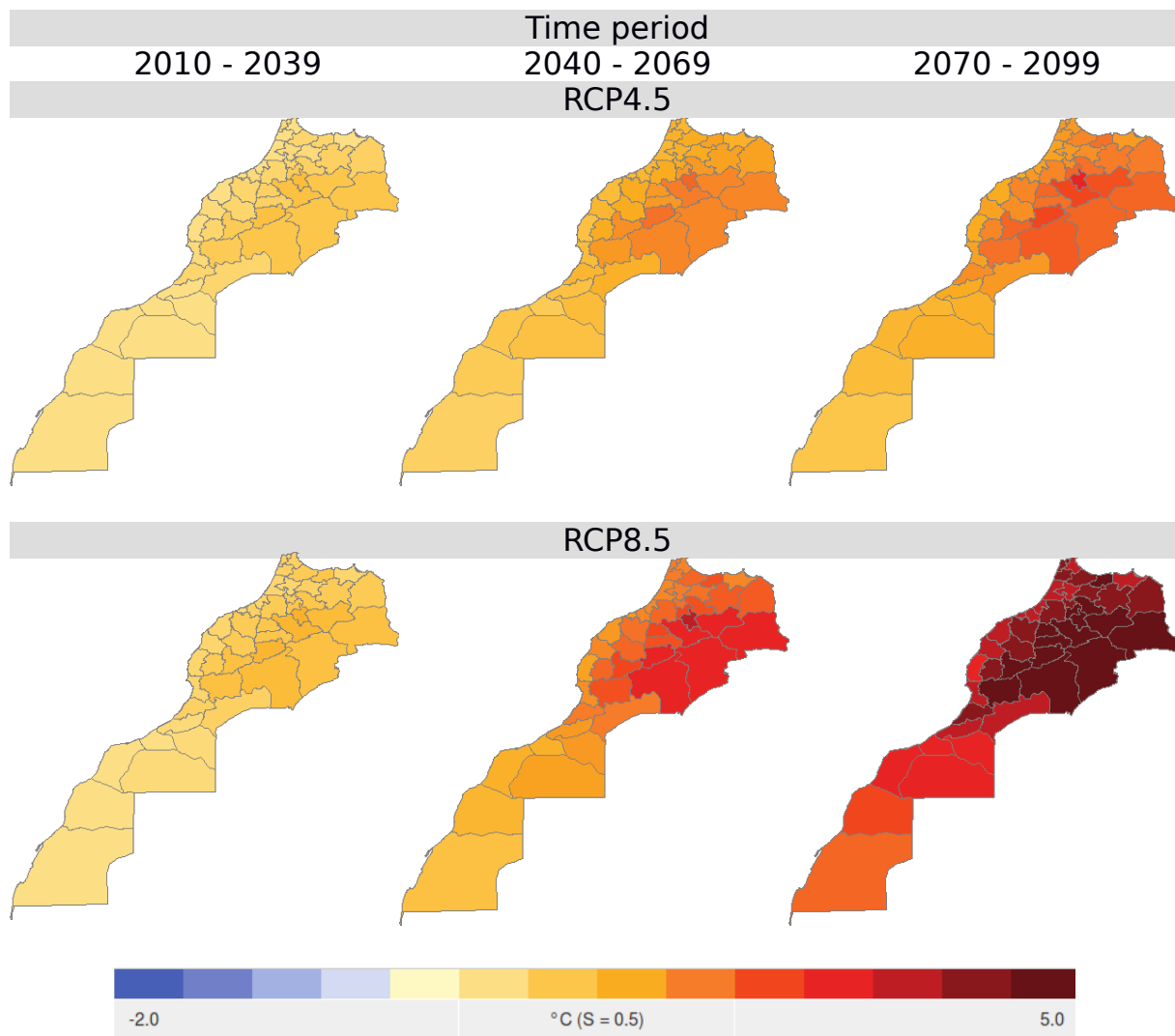


**Figure 68: Maximum temperature change (°C), compared to reference period (1971-2000), at province administrative level, according to RCP4.5 and RCP8.5 scenarios and for average climate model.**

### 3. Minimum temperature

Climate change would lead to a continuous increase of minimum temperature (Tmin) in all Morocco toward the end of the century, comparatively to reference period (1971-2000). Tmin would dramatically increase by +2.1°C (+18%) and +3.2°C (+27%) toward the period 2040-2069, for scenarios RCP4.5 and RCP8.5 respectively. However, Tmin would even increase more over the rainy season, from October to April, i.e. +2.4°C (+27%) and +3.8°C (+44%) for scenarios RCP4.5 and RCP8.5 respectively (Table 22). This temperature increase would exacerbate the expected rainfall deficit during this period of the cropping season.

**Table 22: Minimum temperature trends for the two climate scenarios (Optimistic-RCP4.5 and Pessimistic-RCP8.5) for the average of three climate models (CanESM2, MIROC-ESM, MPI-ESM-LR).**

	Reference	RCP4.5			RCP8.5		
		2010-2039	2040-2069	2069-2099	2010-2039	2040-2069	2069-2099
January	6,2	6,7	7,6	7,6	6,7	7,4	9,0
February	6,6	7,5	8,0	8,6	7,5	8,5	9,8
March	8,0	8,9	9,7	10,1	9,2	10,3	11,7
April	9,7	11,0	12,4	12,7	11,0	12,6	14,1
May	12,4	13,9	14,9	15,4	13,9	15,1	16,8
June	15,6	16,4	17,1	17,5	16,5	17,5	18,3
July	18,4	19,0	19,3	19,3	18,9	19,2	19,7
August	18,9	19,3	19,9	20,0	19,6	19,9	20,1
September	16,9	18,0	18,9	19,1	18,0	19,0	19,7
October	13,8	15,3	16,4	16,9	15,2	16,6	18,0
November	9,5	11,0	11,8	12,4	10,9	12,3	14,1
December	6,8	7,6	8,9	8,8	7,7	8,8	10,3

At subnational level, climate projections show that eastern arid areas of Morocco will be more impacted by Tmin rise, more than 5°C relatively to reference period (Figure 69). For example, the Tmin increase would reach 5.0°C in Azilal, 4.6°C in Khenifra, 4.6°C in Ouarzazate, 4.5°C in Errachidia, 3.9°C in Oujda, 3.6°C in Kelâa des Sraghna, for scenario RCP8.5 and toward the period 2070-2099.





# X. CLIMATE CHANGE IMPACTS ON AGRICULTURE, WATER AND FORESTS

## 1. Impacts on wheat and barley yields

Climate change would lead to a decrease in wheat yields in all main agricultural areas of Morocco toward the end of the century, comparatively to reference period (1971-2000) (Figure 70 and Figure 71). Yield decrease is the direct consequence of rainfall deficit and temperature rise. The effect of climate change will be more pronounced in semi-arid and arid lands, whereas in mountainous zones, yields will increase due to more favorable temperatures.

## 1.1. Impacts on wheat yields

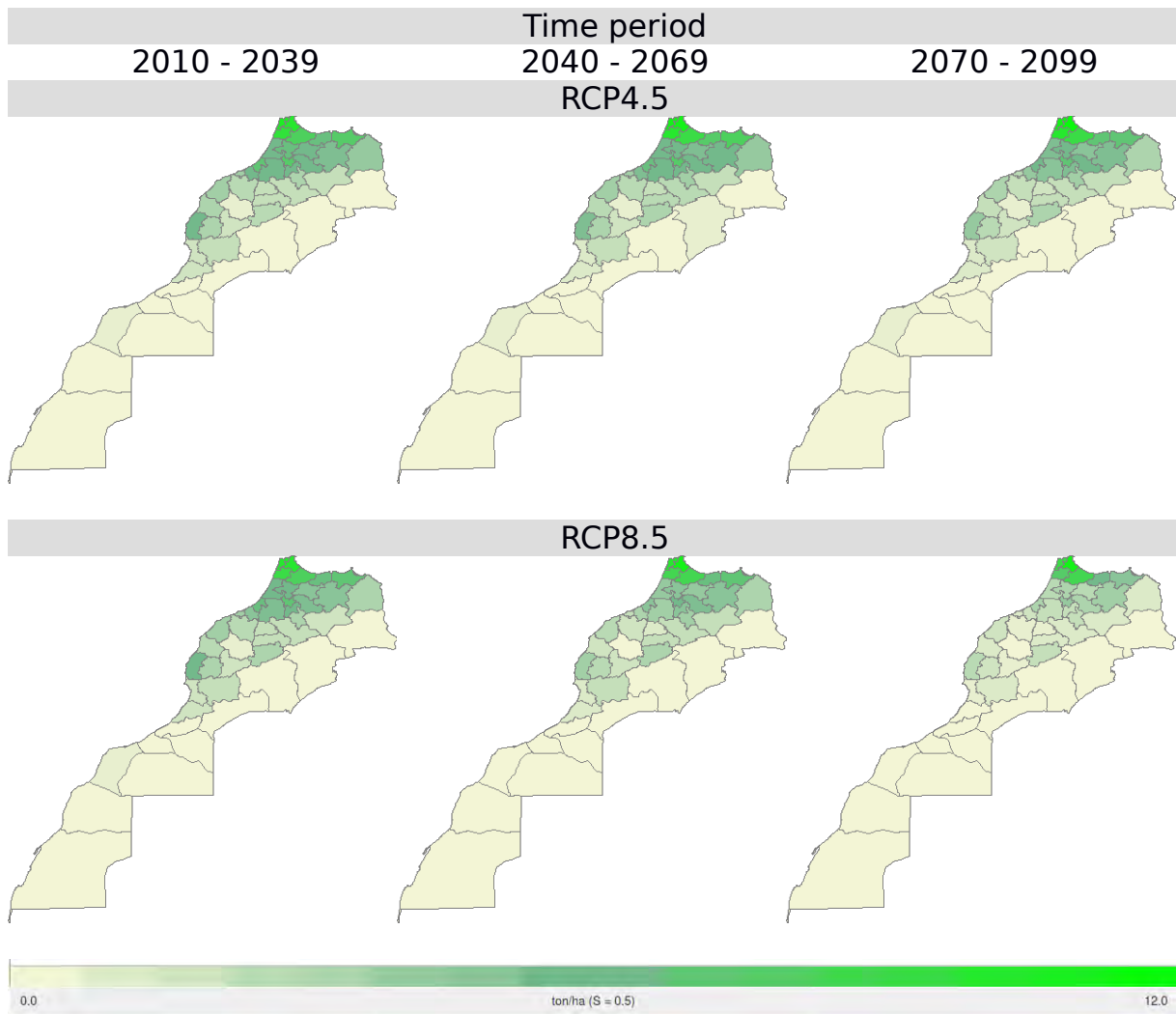


**Figure 70: Wheat yield (t/ha) projections, according to RCP4.5 and RCP8.5 scenarios and for average climate model.**

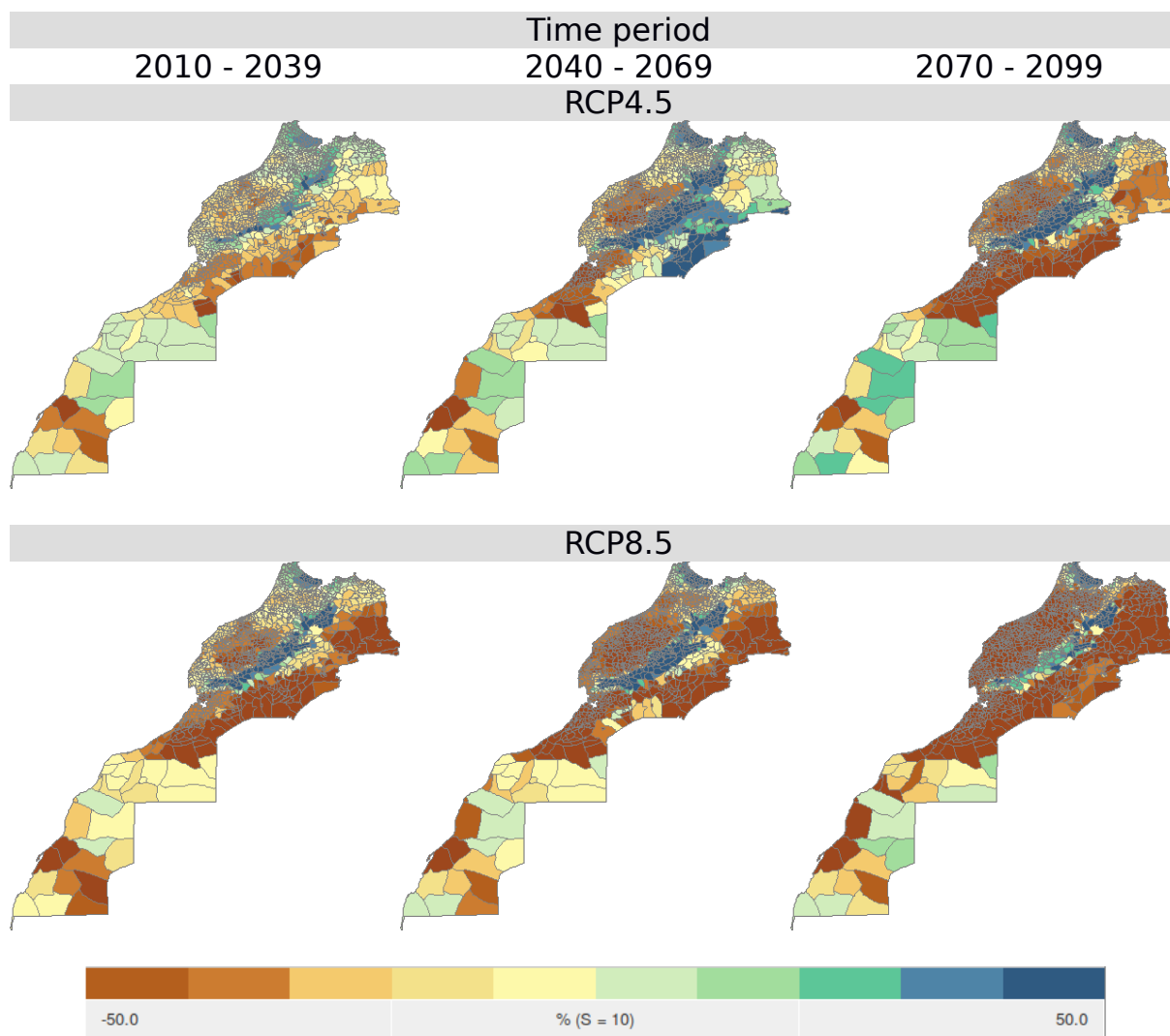


**Figure 71: Wheat yield change (%) projections, according to RCP4.5 and RCP8.5 scenarios and for average climate model.**

## 1.2. Impacts on barley yields

Climate change would lead to a decrease in barley yields in all main agricultural areas of Morocco toward the end of the century, comparatively to reference period (1971-2000) (Figure 72 and Figure 73). Yield decrease is the direct consequence of rainfall deficit and temperature rise. The effect of climate change will be more pronounced in semi-arid and arid lands, even in mountainous zones to the contrary of wheat.

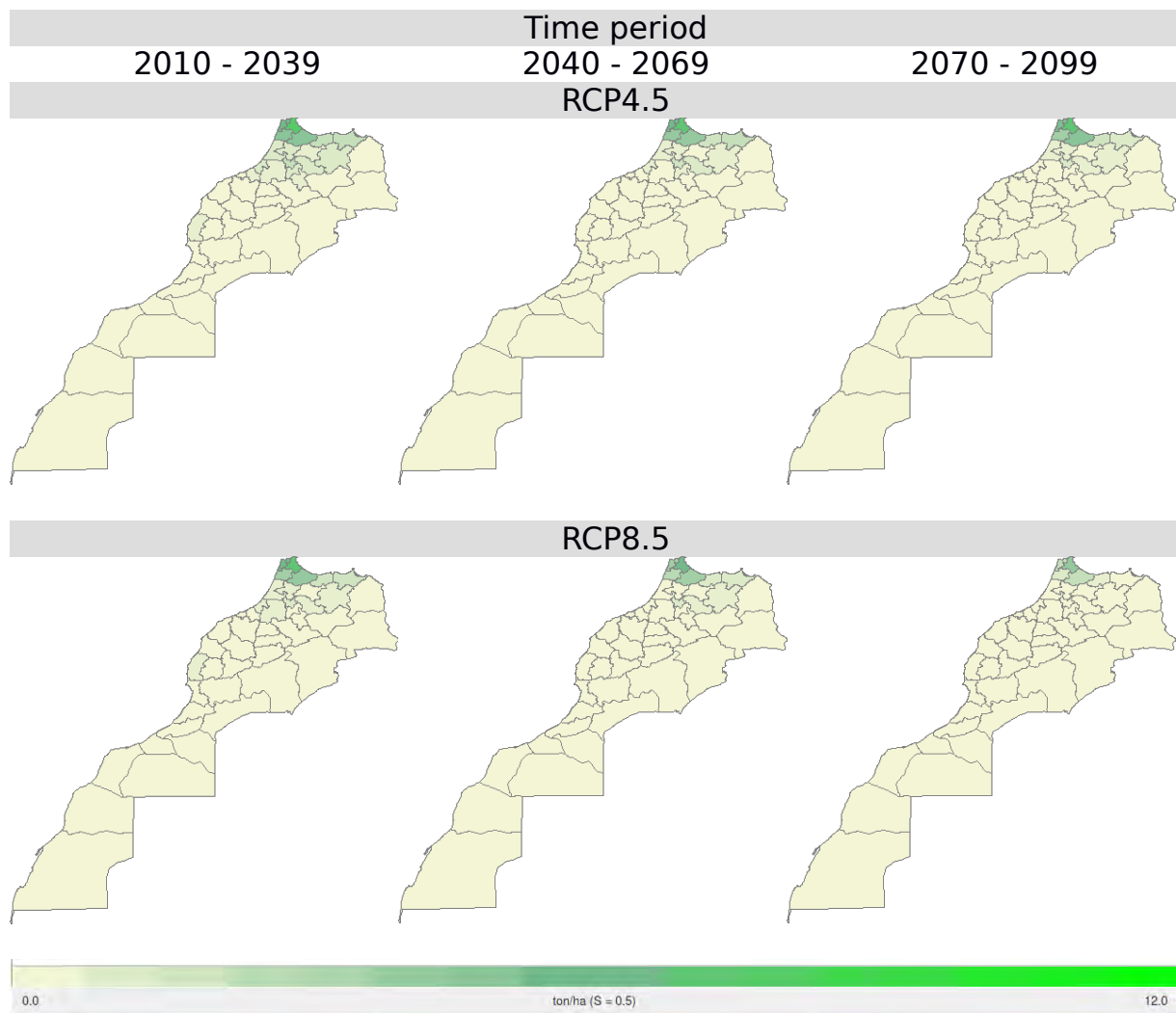


**Figure 72: Barley yield (t/ha) projections, according to RCP4.5 et RCP8.5 scenarios and for average climate model.**

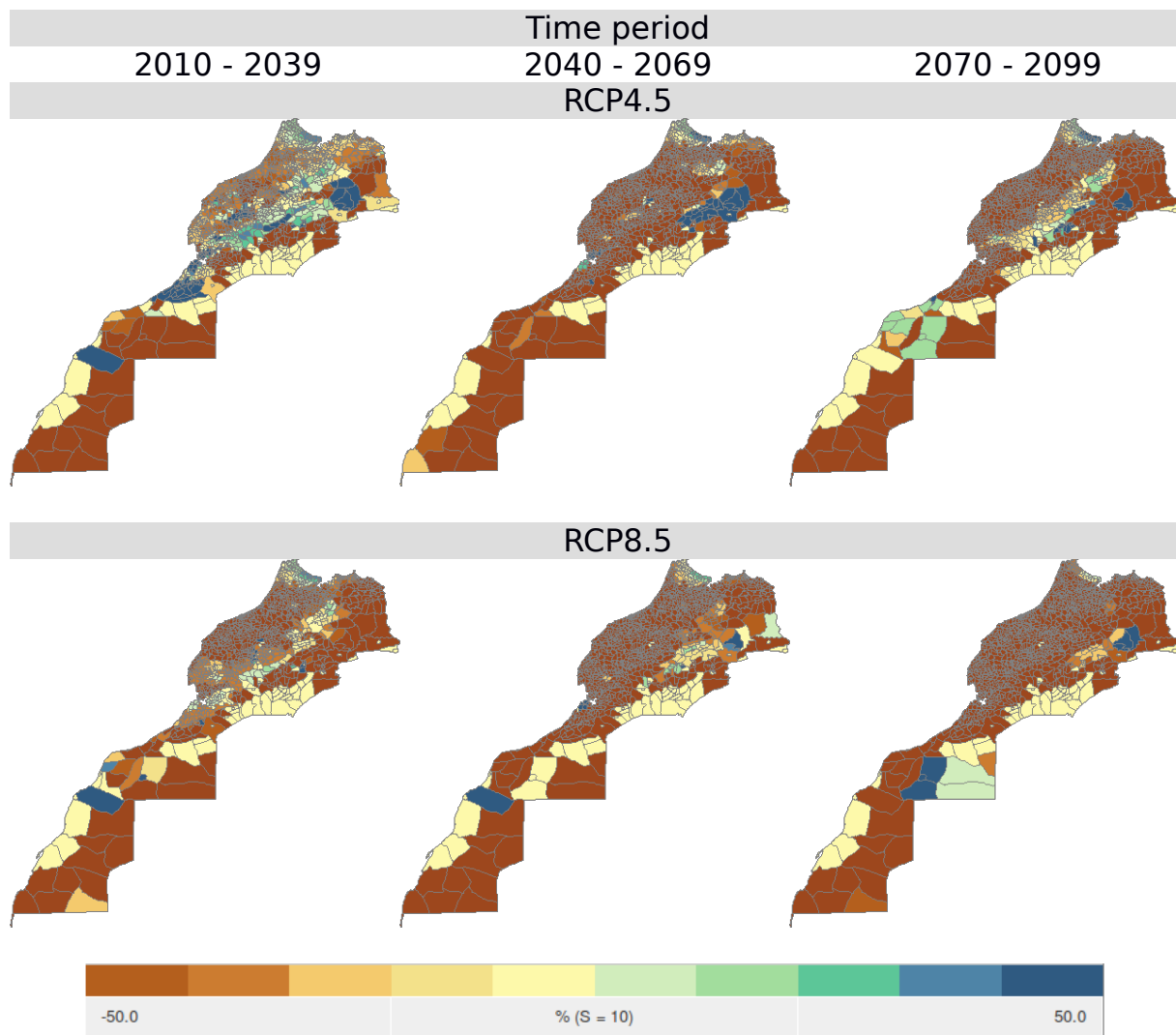


**Figure 73: Barley yield change (%) projections, according to RCP4.5 and RCP8.5 scenarios and for average climate model.**

## 2. Impacts on water

Changes in the spatio-temporal distribution of water resources were calculated by comparing the historic data with the scenarios. The RCP4.5 and the RCP8.5 scenarios of the MIROC-ESM, CanESM2 and MPI GCMs were analyzed in batches of 30 years. Figure 74 shows the water balance in comparison to the historic runs for the wet (October-May) (three left images) and dry (June-September) (three right images) season.



Positive values indicate an excess of water compared to the historical runs of each model whereas negative values indicate a decrease in water.

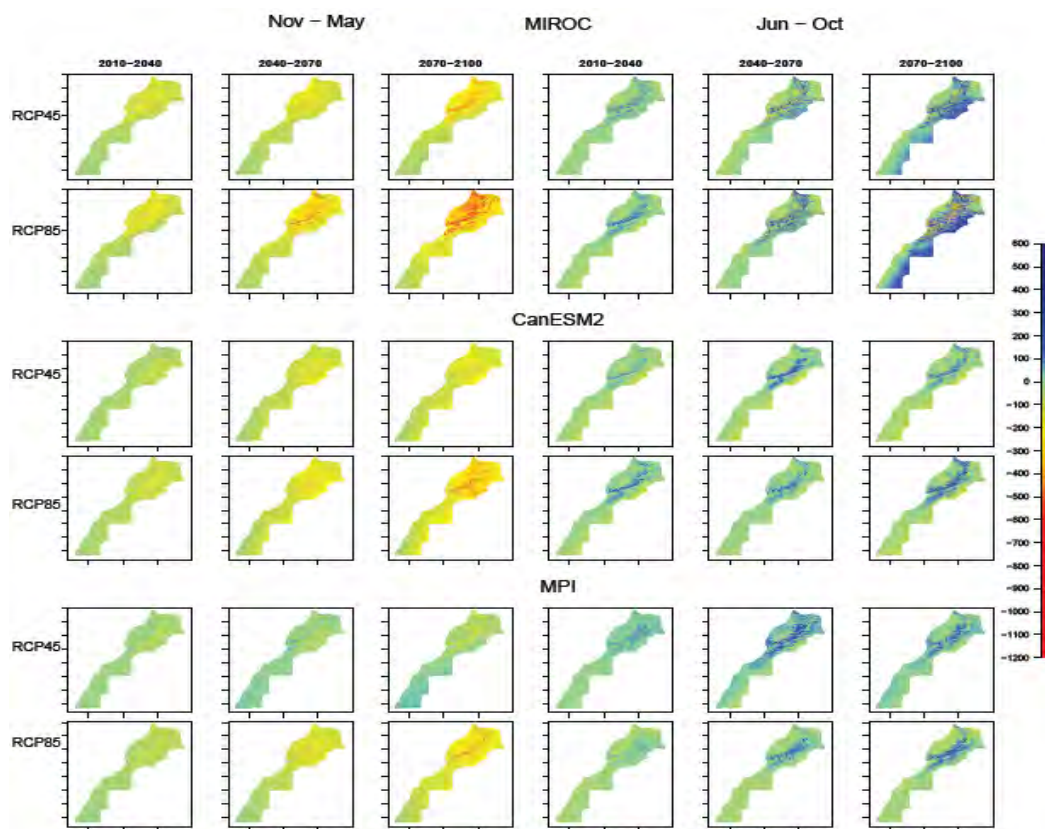


**Figure 74 : The water balance for the MIROC-ESM (top), CanESM2 (middle) and MPI-ESM-LR (bottom) for the RCP4.5 (top of each GCM) and the RCP8.5 (bottom of each GCM) scenarios for the periods 2010-2040, 2040-2070 and 2070-2100. The data were compared to the historical data of each GCM. Positive values indicate an increase in water availability compared to the 1971 - 2000 period, negative values a decrease.**

As shown, all GCM/RCP project a general decrease compared to the historical data during the wet season (October-May) and an increase during the dry season (June-October). For CanESM2 and MPI they provide generally similar results, moreover the two RCPs lead to similar projections up to 2070, differences start growing this moment onward specially on the mountains part with a more accentuate decrease for the RCP8.5 of CanESM2 during the wet season and more increase during the dry season for the RCP4.5 of MPI-ESM-LR. Whereas MIROC-ESM provides more accentuate changes, with a maximum decrease during the wet season generally on the northern part of the country for the RCP8.5 for the period

(2070-2100), and also the maximum increase during the dry season on the inland part.

The results of the RCP4.5 and RCP8.5 for the three models are shown below. The projected period was split up in three periods of 30 years. For brevity, the results of the most downstream point are shown, which represents the averaged situation for the whole basin. For more details, the graphs representing the results for all the stations of each basin are in Annexes 1, 2, 3, 4 and 5.

For Mohamed V station (Figure 75), representing the most downstream station in the Moulouya basin, we can observe clearly that all the models agree on a decrease of the monthly discharge, either for the scenario RCP4.5 or RCP8.5. This decrease starts from 20% and becomes more accentuated on the period 2070-2100, reaching up to 80% for the RCP8.5 of the Canadian model Canesm2.

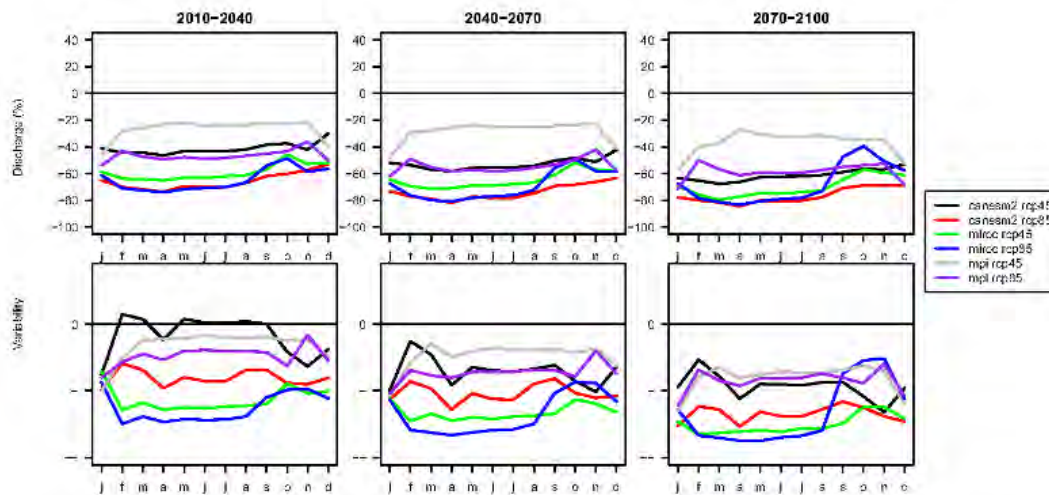


**Figure 75 : Scenarios for Mohamed V, the most downstream point in the Moulouya basin.**

Further, we notice for Belksiri station on the Sebou basin (Figure 76), a general decrease on the monthly discharge clearly for all the models. This decrease reaches up to 50% on the period 2010-2040 becoming a slightly more accentuated on the period 2070-2100.

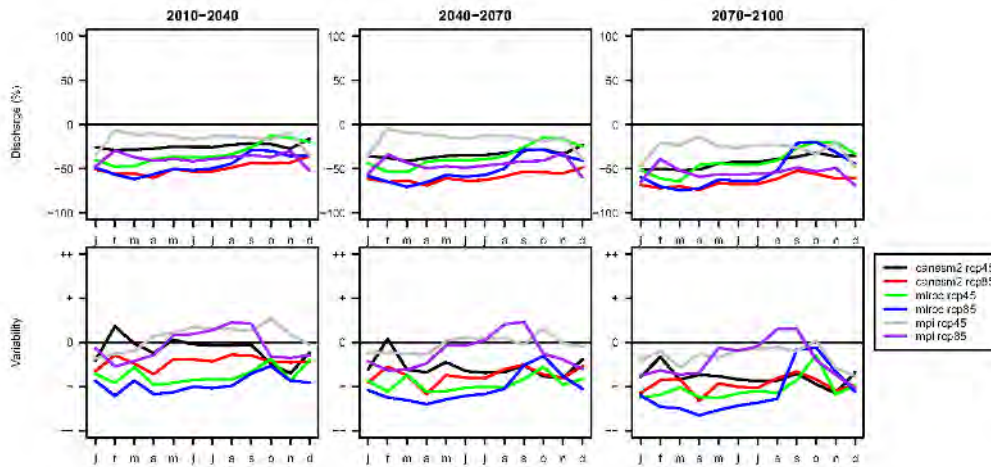


**Figure 76 : Scenarios for Belksiri, the most downstream point in the Sebou basin.**

Referring to Tensift basin represented by its most downstream station Talmest (Figure 77), we note that the RCP4.5 scenario of the MPI-ESM-LR model is giving a different configuration with an increase on the discharge at November on the periods 2010-2040 and 2040-2070. For the rest, all the models agree on a decrease of the discharge starting from almost 50%, this decrease reaches up to 100% for the RCP8.5 of the MIROC-ESM model.

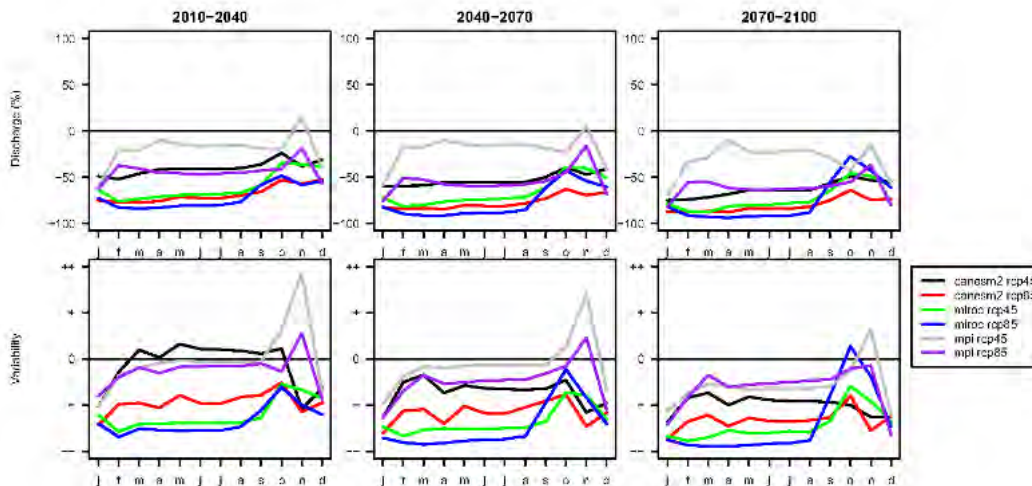


**Figure 77 : Scenarios for Talmest, the most downstream point in the Tensift basin.**

For Pont Torreta station (Figure 78), representing the most downstream station in the Mediterranean side of the Loukkos basin, we observe clearly that all the models agree on a general decrease of the monthly discharge. This is the case for both scenarios RCP4.5 and RCP8.5, except for the months September-October where we can see an increase in discharge. The minimum of decrease is observed for the RCP4.5 of the MPI-ESM-LR model on all the period from 2010 till 2100, in which we barely observe a decrease in discharge. For the other models, the decrease is generally estimated about 50% becoming a little more accentuated on the period 2070-2100, reaching up to 80% for the RCP8.5 of the Canadian model CanESM2.

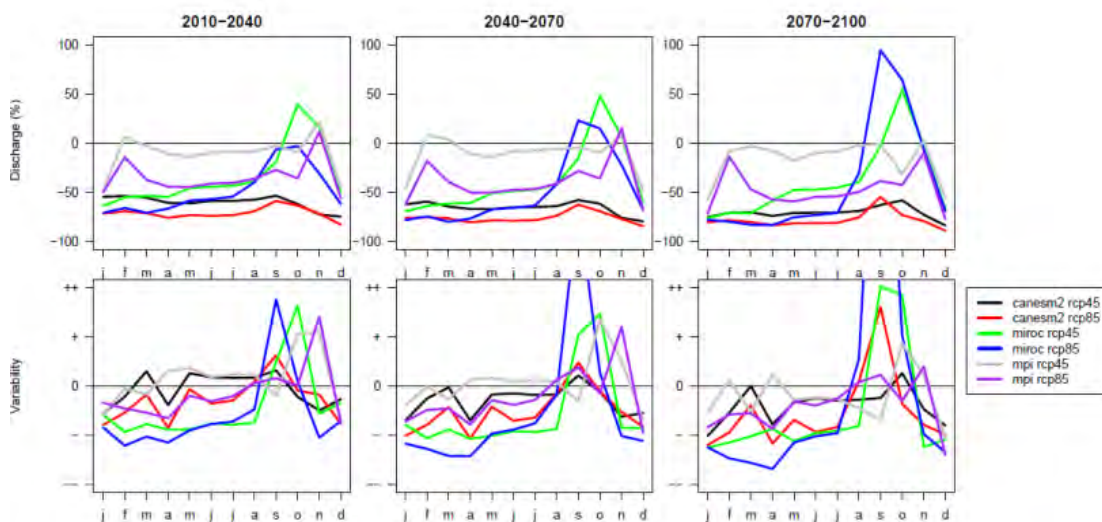
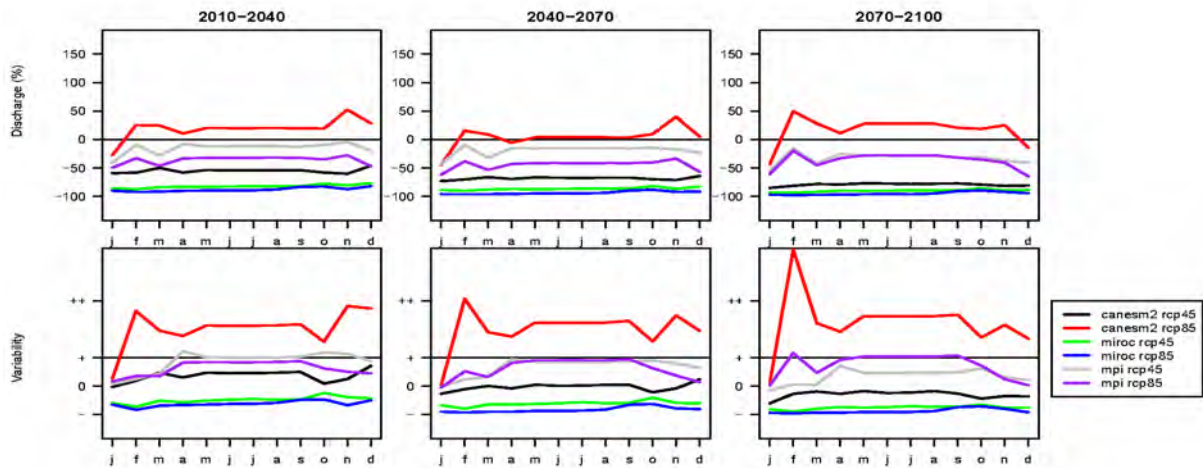


**Figure 78 : Scenarios for Pont torreta station, the most downstream point in the Loukkos basin.**

For Rass fathia station (Figure 79), we clearly observe that all the models agree on a general decrease of the monthly discharge except for the scenario RCP8.5 of the canadian model CanESM2 which predict an increase in discharge for the two periods 2010-2040 and 2070-2100 whereas the discharge is not going change significantly for the period 2040-2070 .The maximum of decrease is observed for the RCP8.5 of the MIROC-ESM model on all the period from 2010 till 2100 reaching up to 100% on all the months. For the other models, the decrease is lower.

**Figure 79 :Scenarios for Rass fathia station in the Bouregreg basin.**





Further, we notice for Ait Ouchen station on the Oum Er rbia basin (Figure 80) that all the models agree on a general decrease of the monthly discharge for both scenarios RCP4.5 and RCP8.5. The minimum of decrease is observed for the RCP4.5 of the MPI-ESM-LR model on all the period from 2010 till 2100. For the three models CanESM2 RCP8.5, MIROC-ESM RCP4.5 and MIROC-ESM RCP8.5, the value of decrease is almost the same, becoming a little more accentuated on the period 2070-2100, reaching up to 80% for the RCP8.5 of the Canadian model CanESM2.

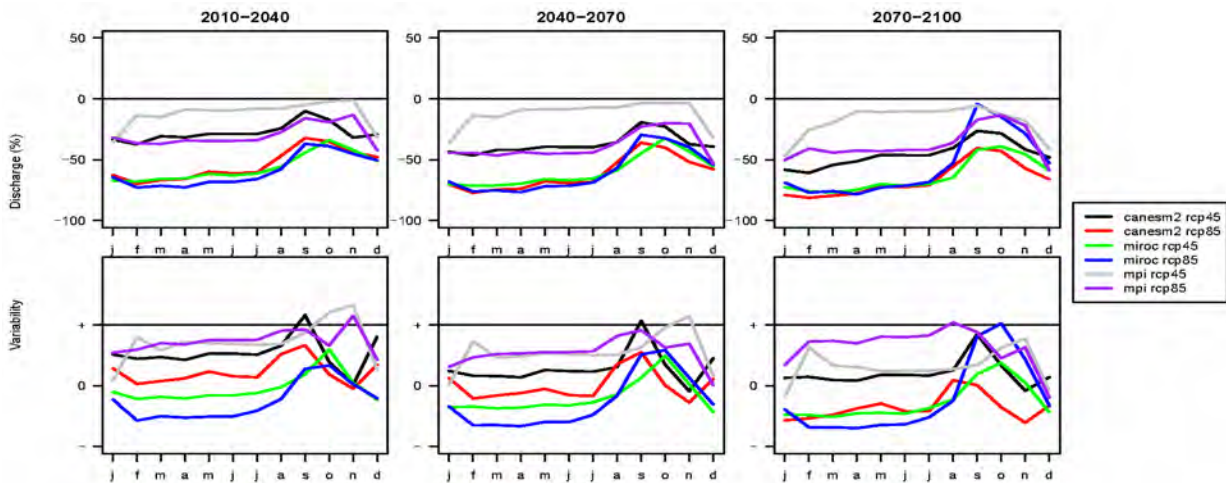


**Figure 80 : Scenarios for Ait ouchen station in the Oum Er rbia basin.**

Finally, for the Agouilal station located on the Draa basin (Figure 81) we observe that the models respond in different ways to the future scenarios.

The scenario RCP4.5 of the MPI model is predicting a decrease for the months December to March and an increase for all the rest of the year and for all the periods. For the CanESM2 RCP4.5 and MPI-ESM-LR RCP8.5 models, they agree on an increase on the two months September and November during all the period from 2010 till 2100. And for the other models , they predict a general decrease on all the months except for the RCP8.5 of the MIROC-ESM model where the discharge on September and October is going to increase significantly reaching up to 150% during the last period of 2070-2100.

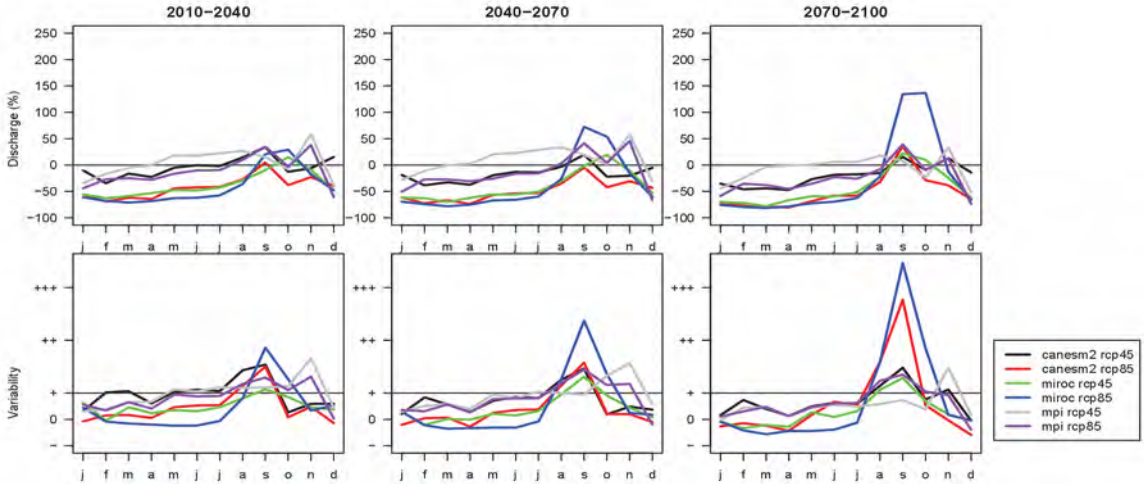


**Figure 81 : Scenarios for Agouilal station in the Souss-Massa-Draa basin.**

### 3. Impacts on forests

#### 3.1. Impacts without disturbance

Six simulations were carried out to cover different scenarios and to use the three climate models chosen for Morocco. Table 23 summarizes the six combinations.

**Table 23: Simulations without disturbance for the Maâmora forest.**

Models\Scenarios	RCP4.5	RCP8.5
CanESM2	✓	✓
MIROC-ESM	✓	✓
MPI-ESMLR	✓	✓



In addition to these six combinations, a simulation with current climatic data (1971–2000) was performed to compare the results and assess the impact of climate change on the Maâmora forest. Two dates were selected for comparison: 2050 for the near future, and 2090 for the distant future.

### 3.1.1. Impacts on species distribution

The presentation of the distribution of a species in map format allows users to spatially visualize where the species is most present. In addition, cartographic visualization allows users to identify the sites where species are most likely to establish naturally according to the climatic scenario. Figure 82 shows that the number of sites with *Quercus suber* decreases over time. This decrease is more pronounced in the pessimistic scenario (RCP8.5) than in the optimistic one (RCP4.5). The natural regeneration of the cork oak shows a strong preference for the western part of the forest. Only for eucalyptus trees does the distribution proportion increase. Overall, the forest area decreases in the absence of forestry interventions.

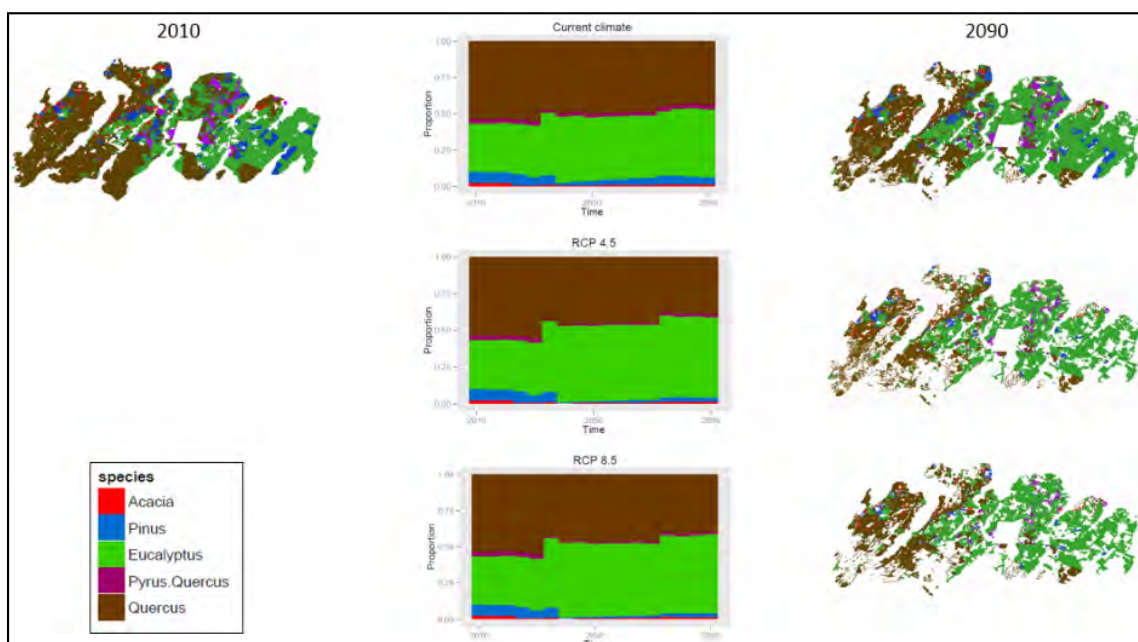


**Figure 82: Comparison of species distribution in the forest of Maâmora without disturbance, 2010/2090 (Model CanESM2).**

### 3.1.2. Impacts on total biomass

The aggregation in a chart of the evolution of the average total biomass for the three scenarios (reference scenario, RCP4.5 and RCP8.5) produces an overview of the impact of climate change on each species. Figure 83 shows total biomass averaged at site level for the CanESM2 model.

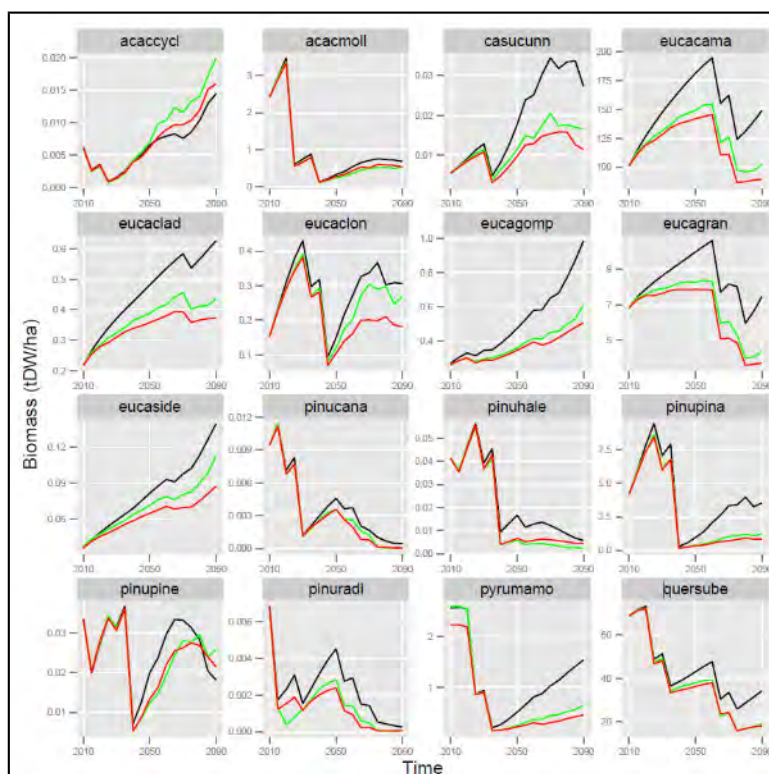


**Figure 83: Total biomass (in tons of dry matter per hectare) for each species in the Maâmora forest without disturbance, 2010–2090 (model CanESM2). Black curve: reference scenario; Green curve: RCP4.5 scenario; Red curve: RCP8.5 scenario.**

In all three models, climate change has a negative impact on most species. Except for *Pinus pinea* reaching 2090 and *Acacia cyclops* from 2050, the curve for the RCP8.5 scenario (in red) is below the reference curve, indicating that total biomass is lower than under current climatic conditions. *Eucalyptus clonal* and *Pinus canariensis* are only marginally affected under the optimistic scenario (RCP4.5).

The results of each simulation, grouped by model for all three scenarios, were subjected to a complete statistical analysis (Table 24). The focus was on the two most common species in the Maâmora forest, *Eucalyptus camaldulensis* and *Quercus suber*.

**Table 24: Summary results of the statistical analyses of the three climate scenarios (reference scenario, RCP4.5 and RCP8.5) for the three climate models.**

Time	Scenario	Species	MPI-ESM- LR	CanESM2	MIROC-ESM
2010	RCP4.5	<i>Eucalyptus camaldulensis</i>	NS	NS	NS
		<i>Quercus suber</i>	NS	NS	NS
	RCP8.5	<i>Eucalyptus camaldulensis</i>	NS	NS	NS
		<i>Quercus suber</i>	NS	NS	NS
2050	RCP4.5	<i>Eucalyptus camaldulensis</i>	NS	NS	NS
		<i>Quercus suber</i>	NS	NS	NS
	RCP8.5	<i>Eucalyptus camaldulensis</i>	NS	NS	NS
		<i>Quercus suber</i>	NS	NS	NS
2090	RCP4.5	<i>Eucalyptus camaldulensis</i>	NS	NS	NS
		<i>Quercus suber</i>	NS	S	HS
	RCP8.5	<i>Eucalyptus camaldulensis</i>	NS	S	HS
		<i>Quercus suber</i>	NS	S	HS

NS: non-significant ( $p > 0.05$ ); S: significant ( $p < 0.05$ ); HS: highly significant ( $p < 0.01$ )

For the base year 2010, analyses of variance to a single classification criterion, whose criterion is that of the scenarios for each of the three climate models, reveals that there is no difference between the three models for the two dominant species, eucalyptus and cork oak. This result is normal since the three models provide the same levels of production as they are based on historical data.

For the two other periods, 2050 and 2090, the results for each model are as followed:

- The CanESM2 model shows significant differences for *Eucalyptus camaldulensis* between the RCP8.5 scenario and the reference scenario. In addition, the analysis reveals significant differences between the two projected scenarios and the reference scenario in 2090 for cork oak.
- The MIROC-ESM model does not show any significant differences for *Eucalyptus camaldulensis* between the RCP4.5 scenario and the reference scenario. Conversely, the RCP8.5 scenario presents highly significant differences with the reference scenario in 2090. For cork

oak, both scenario RCP4.5 and scenario RCP8.5 show highly significant differences with the reference scenario by the year 2090.

- The MPI-ESMLR model did not reveal any differences between the three scenarios for both species and for all projections.

### 3.2. Impacts with forestry interventions

As for the simulations without disturbance, six simulations were performed applying the harvest disturbance extension in order to cover the different climatic scenarios and use the three climate models (Figure 84).

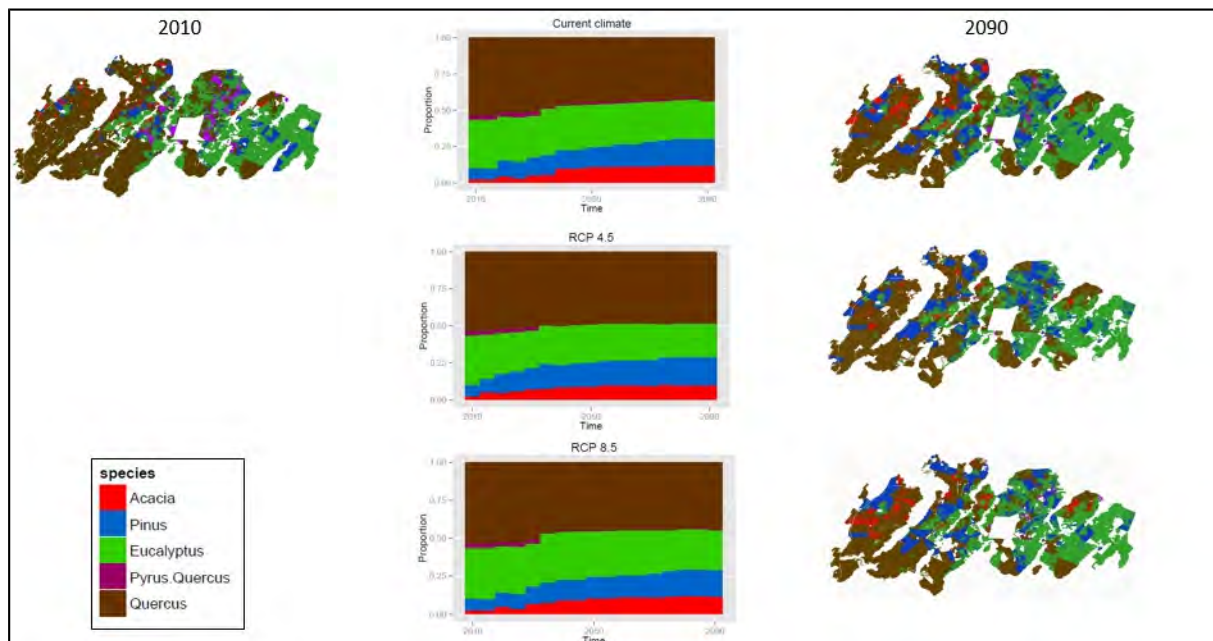


**Figure 84: Comparison of species distribution in the Maâmore forest in 2090 with forestry interventions (Model CanESM2).**

The simulation with forestry interventions shows that the area under *Quercus suber* remains stable. With artificial regeneration i.e. planting in plots where trees become too old (100 to 120 years), the proportion of distribution for *Quercus suber* decreases slightly as compared to other species in the early years, and reaches a more or less stable level already by 2035. The distribution proportion for eucalyptus is stable under all three scenarios. The proportion of pine and acacia trees increases markedly over the period 2010–2090.



### 3.3. Comparison of results with and without forestry interventions

#### 3.3.1. Distribution

For each species, the simulations with and without forestry interventions show differences in the number of sites where that species is present (Figure 85). Where the curve is below the dotted line (representing the 2010 baseline), the number of sites where the species is found decreases.

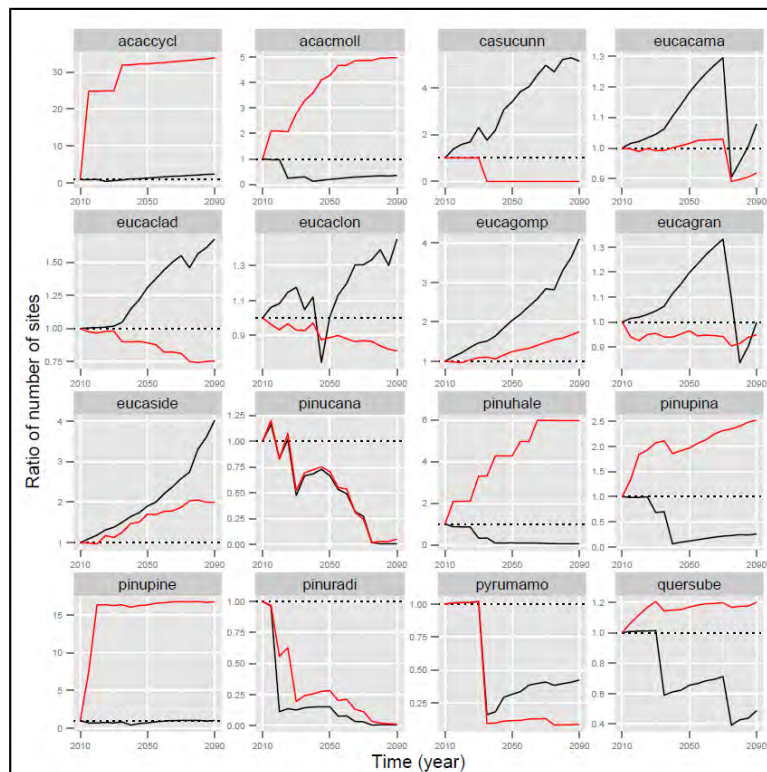


**Figure 85: Comparison of the number of sites where each species is present with (red curve) and without (blue curve) forestry interventions, as compared with the number of sites where each species occurs in 2010 (CanESM2 model and RCP4.5 scenario).**

Without forestry interventions, the number of sites for most pine species decreases, while the number of sites for eucalyptus increases or remains stable. As shown on the map, a decrease in sites for *Quercus suber* can also be noticed over time without forestry interventions.

With forestry interventions, the number of sites for *Acacia cyclops* increases significantly compared with the situation in 2010. The distribution of eucalyptus remains fairly stable overall, with a greater

increase in sites for *Eucalyptus sideroxylon* and *Eucalyptus gomphocephala* resulting from natural regeneration, in addition to coppicing. The number of sites for *Quercus suber* increases slightly. Figure 10 shows that without forestry interventions, *Casuarina cunninghamiana* is doomed to see its surfaces decrease significantly or even disappear from the Maâmora forest by 2090. The areas under *Pyrus mamorensis*, *Pinus radiata* and *Pinus Canariensis* decrease considerably as compared with 2010, without however completely disappearing by 2090.

### 3.3.2. Average biomass

The simulation with the Canadian model and the optimistic climate scenario shows that without forestry interventions, most species will undergo a decrease in total average biomass over the period 2010–2090. Certain species, such as *Acacia cyclops* and *Eucalyptus cladocalyx*, show an increase in biomass (Figure 86).

With forestry interventions, *Quercus suber* (bottom right graph) experiences a decrease in average total biomass in 2050 as compared with 2010, and an increase by 2090. The initial decrease for eucalyptus is due to cuts in older stands to transform them into coppices, as suggested by the Maâmora forestry management. In fact, the curve stabilizes by 2070.



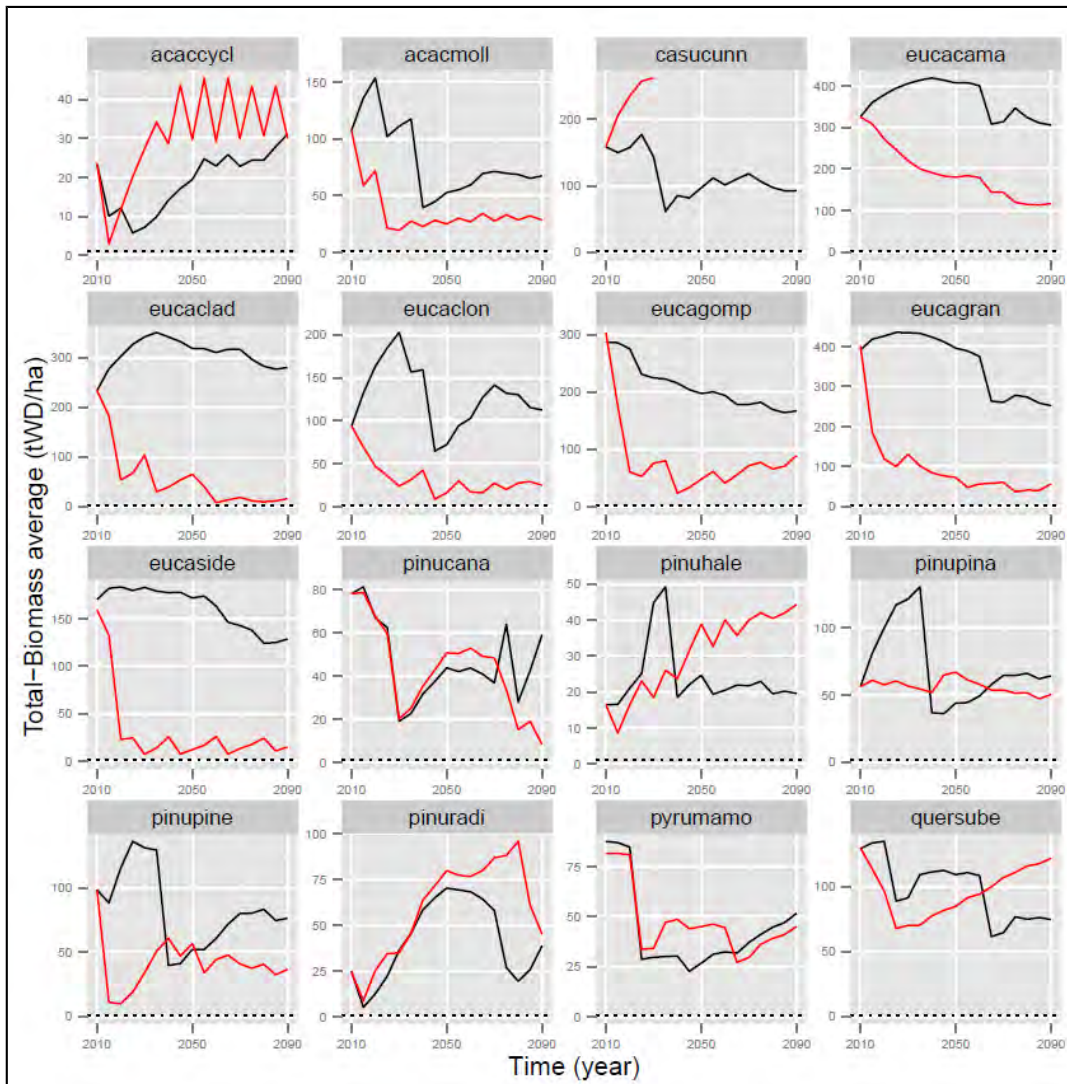


**Figure 86: Comparison of the evolution over time of average total biomass of each species with (red curve) and without (blue curve) forestry interventions in the Maâmora forest (tonnes of dry matter per hectare) (CanESM2 model and RCP4.5 scenario)**

### 3.3.3. *Quercus suber*

The comparison of the simulation results for total biomass for *Quercus suber* with and without forestry interventions (Figure 87) illustrates the importance of these interventions for forest cover. The red dotted curve represents the standing and living biomass plus the biomass collected in the scenario with harvest disturbance (CanESM2 model and RCP4.5 scenario).

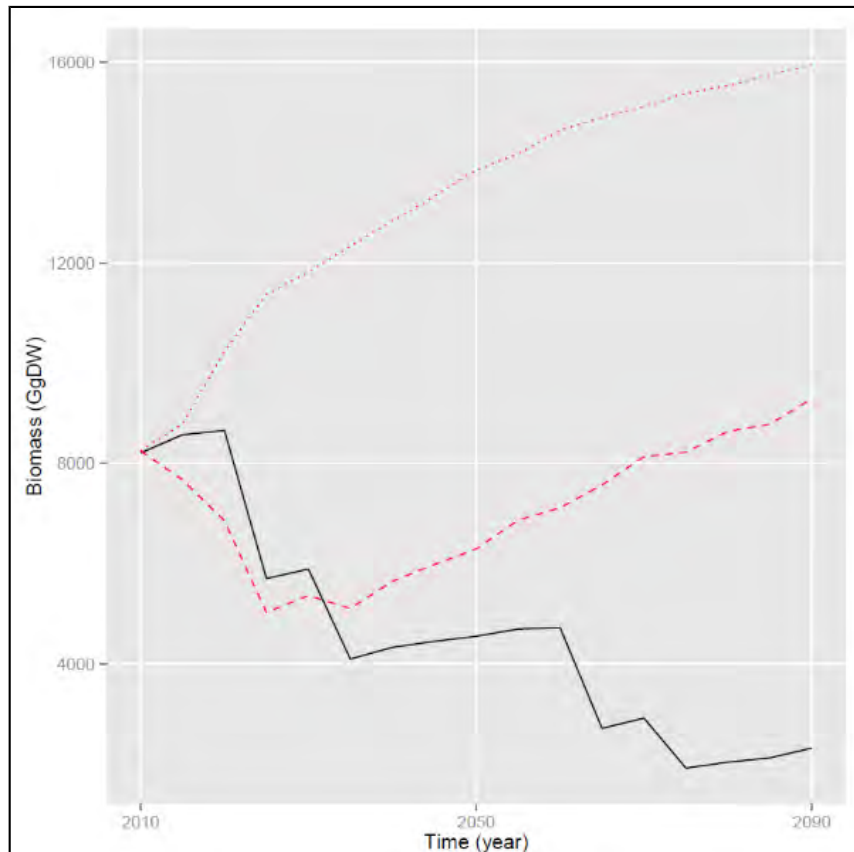


**Figure 87: Total standing and living biomass in gigagrammes of dry matter for *Quercus suber* with (red dashed curve) and without (black curve) forestry interventions for the entire Maâmora forest.**

Without artificial regeneration, the standing and living biomass of *Quercus suber* decreases without real recovery. Starting from the twenty-fifth year of the simulation, total biomass in the scenario with forestry interventions exceeds that in the scenario without interventions. In 2090, standing biomass is almost four times higher with interventions than without interventions, and surpasses standing biomass in 2010.

### 3.3.4. Cork production

The production of cork is a very important activity in the Maâmora forest. Without a known relationship between the biomass of cork oak and cork production, the production of cork cannot be directly simulated. Figure 87 shows how the number of cohorts within the age range for cork production (26 to 75 years in the case of the Maâmora forest) evolves over time.

The simulation without forestry interventions shows that the number of these cohorts decreases from 2010 to 2090. Conversely, with forestry interventions, the simulation shows that after a drop in the number of

cohorts over 25 years (until 2035, when they reach a low of 12.5 percent of the number in 2010), the number of cohorts increases almost continuously, and exceeds the 2010 level by 2070.

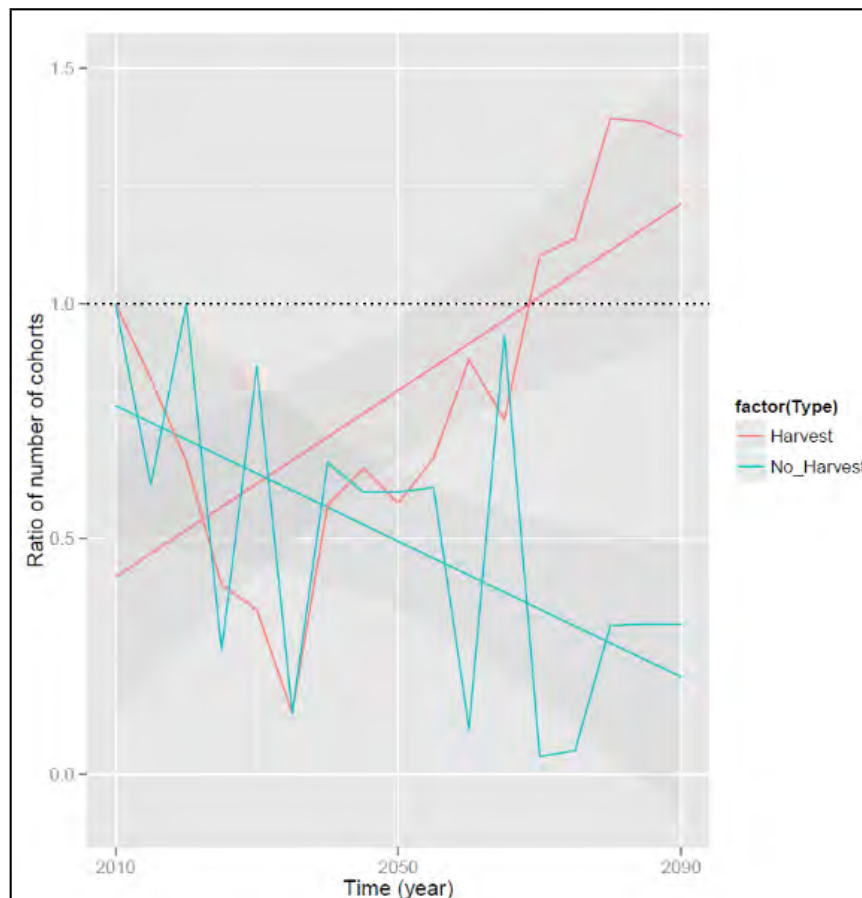


**Figure 88: Ratio of the number of cohorts within the age range to produce cork, with (red curve) and without (blue curve) harvest in the Maâmora forest, 2010–2090 (CanESM2 model and RCP 4.5 scenario).**

#### 4. Impacts on agricultural economy

The simulations with crop yield changes of wheat and barley under the two climate change scenarios (RCP4.5 and RCP8.5) are discussed below, respectively. The AquaCroP projections of the yield shocks cover the period 2010-2100, but for the economic projection, the period 2010-2050 is chosen. There are three reasons for this choice of projection period. In the first place there is a technical reason. It appeared that the magnitude of some of the (trended) yield shocks become so large in the second half of this century that the economic model did not find an equilibrium solution. Second, even if technically possible, it can be

questioned whether the projection of the Moroccan economy so far into the future with this simple model makes much sense. Third, many analyses of the economic impacts long-term climate change focus on mid-century.

The yield shocks that are simulated are for wheat and barley. According to the 2010 SAM of Morocco, the market supply of wheat is predominantly demanded by the sector “food”, i.e. the processing industry. Any changes in the supply of wheat may have an effect on the sector “food”. Minor shares of wheat supply are demanded by private households and are used as intermediate consumption (e.g. for seeds). There are no exports of wheat. The market supply of barley is predominantly demanded by the sector “other agriculture” that includes livestock. Minor shares of supply are demanded by private households and are used as intermediate consumption. There are no exports of barley. The other sectors and commodities included in the model are not significantly affected by the yield shocks, so they are not discussed in this section<sup>11</sup>.

The presentation of the simulation results in Table 25 and Table 26 start with the effect of the yield shock on the production (QA\_) of wheat and barley in the favourable (FAV) and defavourable (DEF) regions in 2050 (in constant 2010 Dirham), respectively. After that, volumes of imports (QM\_) are presented that may partially cover for a decline in domestic production. Domestic production and imports make up the total domestic supplies (QQ\_) of wheat and barley. The next variables present the effects on the demand of wheat, barley, other agriculture, and food by private households (QH\_). The market price indices (PQ\_) of wheat, barley, other agriculture, and food are presented next. The tables conclude with aggregate indicators of self-sufficiency of wheat and barley (SS\_) and economic activity (GDP).

Table Table 25 presents selected results of the yield shocks under the RCP4.5 climate change scenario elaborated by the three climate models (CanESM2, MIROC-ESM, and MPI-ESMMR) and by the two data smoothing methods (LIN and MA). As is already clear for the signs and magnitudes of the yield shocks, the economic impacts are small. Production of wheat and barley is around baseline values, with only significant decreases in the production of barley in the defavourable region in two of the three climate models. Consequently, the effects on imports and household consumption are therefore also small. The market price of barley increases by 60% to 111% in the CanESM2 scenario, but decreases in the MPI-ESMMR scenario. The market price of wheat is little affected (with the exception of the CanESM2\_MA scenario), and so are the market prices of other agriculture and food. Finally, self-sufficiency and GDP are little affected.

<sup>11</sup>The full suite of results can be inspected on the MOSAICC platform.

**Table 25: Selected macro-economic results for RCP4.5 climate change scenario (MAD \* 10<sup>9</sup>).**

Variable	Dimension	2010	2050						
			Baseline (SSP3)	CanESM2		MIROC-ESM		MPI-ESMLR	
				LIN	MA	LIN	MA	LIN	MA
QA_ABAR_FAV	MAD	1.76	4.62	4.51	4.02	4.77	4.53	4.76	5.55
QA_ABAR_DEF	MAD	3.04	7.99	7.15	7.22	7.60	7.59	8.05	8.03
QA_AWHT_FAV	MAD	6.33	16.65	15.80	14.49	17.17	16.43	17.70	19.93
QA_AWHT_DEF	MAD	3.67	9.66	9.11	7.68	9.72	8.79	10.02	11.25
QM_CBAR	MAD	0.36	0.94	1.18	1.30	1.00	1.03	0.91	0.83
QM_CWHT	MAD	7.65	20.11	20.37	21.19	19.93	20.38	19.77	19.09
QQ_CBAR	MAD	5.21	13.71	12.95	12.60	13.51	13.32	13.87	14.40
QQ_CWHT	MAD	19.35	50.91	49.79	47.77	51.25	50.07	51.85	53.89
QH_CBAR_HSH	MAD	0.47	1.23	0.76	0.62	1.08	0.99	1.33	1.64
QH_CWHT_HSH	MAD	2.86	7.53	7.11	6.24	7.72	7.17	7.97	9.01
QH_CAGR_HSH	MAD	60.67	159.59	156.5	155.0	158.8	158.4	159.8	160.7
QH_CFOOD_HSH	MAD	119.15	313.45	310.0	304.5	313.9	311.1	315.4	319.6
PQ_CBAR	Index	1.00	1.00	1.60	2.11	1.14	1.24	0.93	0.76
PQ_CWHT	Index	1.00	1.00	1.05	1.46	0.97	1.05	0.95	0.84
PQ_CAGR	Index	1.00	1.00	1.01	1.02	1.00	1.00	1.00	1.00
PQ_CFOOD	Index	1.00	1.00	1.01	1.02	1.00	1.00	1.00	0.99
SS_CBAR	fraction	0.93	0.93	0.91	0.90	0.91	0.92	0.93	0.94
SS_CWHT	fraction	0.57	0.57	0.55	0.51	0.57	0.55	0.58	0.62
GDP	MAD	789	2077	2072	2067	2076	2074	2079	2083

*N.B. It was not possible to use the MA shocks for BAR-DEF in the economic model; for this crop-area combination the linearized shocks have been used in all scenarios.*

The yield shocks under the RCP8.5 climate change scenario are larger and therefore the economic impacts are also larger. Table 26 presents selected results of the RCP8.5 scenario. Production of wheat and barley declines in all regions in (almost) all climate scenarios, relative to the baseline. The largest relative declines are for wheat in both regions. The MIROC-ESM climate has the largest declines. Consequently, the imports of wheat and barley increase, but not enough to prevent negative impacts on household consumption of wheat, barely, other agriculture and food. The



market price of barley increases by 112-170% in the MIROC-ESM scenario, and also increases in the other two scenarios (by 60-89% and 84-95%, respectively). The market price of wheat also increases, between 8% and 64%, relative to the baseline price. The market prices of other agriculture and food also increase. The market price of food increases between 1% and 4%, relative to the baseline. Self-sufficiency of wheat and barley decrease. The overall effect on GDP is negative but small.

**Table 26: Selected macro-economic results for RCP4.5 climate change scenario (MAD \* 10<sup>9</sup>).**

Variable	Dimension	2010	2050						
			Baseline (SSP5)	CanESM2		MIROC-ESM		MPI-ESMLR	
				LIN	MA	LIN	MA	LIN	MA
QA_ABAR_FAV	MAD	1.76	7.96	7.31	8.03	6.87	7.84	7.46	7.20
QA_ABAR_DEF	MAD	3.04	13.75	12.13	12.12	11.49	11.49	12.13	12.18
QA_AWHT_FAV	MAD	6.33	28.68	23.68	27.34	20.88	24.05	25.54	25.27
QA_AWHT_DEF	MAD	3.67	16.63	13.95	14.66	12.22	15.13	14.70	13.99
QM_CBAR	MAD	0.36	1.61	2.20	2.03	2.64	2.34	2.18	2.24
QM_CWHT	MAD	7.65	34.63	36.83	35.39	38.59	36.16	35.86	36.19
QQ_CBAR	MAD	5.21	23.60	21.76	22.29	20.84	21.59	21.90	21.73
QQ_CWHT	MAD	19.35	87.67	81.63	85.04	77.39	82.71	83.69	82.89
QH_CBAR_HSH	MAD	0.47	2.12	1.11	1.32	0.77	0.99	1.14	1.08
QH_CWHT_HSH	MAD	2.86	12.96	10.45	11.91	8.89	11.00	11.36	11.02
QH_CAGR_HSH	MAD	60.67	274.8	267.6	269.7	261.5	265.5	267.7	266.9
QH_CFOOD_HSH	MAD	119.1	539.7	522.9	532.1	508.8	525.3	528.4	526.1
PQ_CBAR	Index	1.00	1.00	1.89	1.60	2.70	2.12	1.84	1.95
PQ_CWHT	Index	1.00	1.00	1.23	1.08	1.43	1.17	1.13	1.64
PQ_CAGR	Index	1.00	1.00	1.02	1.01	1.03	1.02	1.02	1.02
PQ_CFOOD	Index	1.00	1.00	1.02	1.01	1.04	1.02	1.01	1.02
SS_CBAR	fraction	0.93	0.93	0.90	0.93	0.87	0.89	0.90	0.90
SS_CWHT	fraction	0.57	0.57	0.51	0.57	0.46	0.52	0.53	0.52
GDP	MAD	789	3577	3560	3566	3547	3559	3563	3561

QA<sub>a</sub> : Level of domestic activity a (quantity of output produced by activity a)

QM<sub>c</sub> : Quantity of imports of commodity c

QQ<sub>c</sub> : Composite supply to domestic market of commodity c

QH<sub>h</sub> : Quantity of consumption of marketed commodity c for household h

PQ<sub>c</sub> : Market price of commodity c



*SS\_ : Self-sufficiency indicator*  
*GDP\_ : Gross Domestic Product*  
*\_ABAR: Activity barley production*  
*\_AWHT: Activity wheat production*  
*\_CBAR : Commodity barley*  
*\_CWHT : Commodity wheat*  
*\_CAGR : Commodity other agriculture*  
*\_CFOOD : Commodity processed food*  
*\_HSH : Private household*  
*\_FAV : Favorable region*  
*\_DEF : Unfavorable region*

# XI. TRAINING AND DISSEMINATION MATERIAL

In the framework of the MOSAICC project a series of workshops and training sessions (Table 27) have been organized. All related materials, dissemination technical notes, brochures and videos (in English, French and Arabic) are freely available on the dissemination portal [www.changementclimatique.ma](http://www.changementclimatique.ma). More than 30 national experts have been training during these sessions.

**Table 27: Workshops and trainings organized during the MOSAICC project.**

2011/02/17	<a href="#">Workshop 17-18 Feb 2011 Provisional agenda</a>
2011/02/17	<a href="#">Workshop on FAO-MOSAICC - Main lessons from the discussions</a>
2011/04/06	<a href="#">FAO-MOSAICC - Module Integration Requirements and Skills</a>
2011/04/08	<a href="#">List of minimum requirements for the deployment of MOSAICC</a>
2012/09/13	<a href="#">CROP MODEL INTRODUCTION</a>
2012/09/13	<a href="#">CROP MODEL TRENDS</a>
2012/09/13	<a href="#">CROP MODEL WABAL</a>
2012/09/21	<a href="#">TRAINING ON CROP YIELD MODELLING IN THE FRAME OF THE AMICAF</a>
2013/04/05	<a href="#">MAN_Tutorial on Wabal</a>
2013/05/01	<a href="#">Introduction Maroc tutorial</a>
2013/05/07	<a href="#">Composante climatique et hydrologique in Morocco</a>
2013/05/08	<a href="#">Deploiement de MOSAICC a la DMN au Maroc</a>
2013/05/27	<a href="#">WABAL</a>
2013/12/14	<a href="#">Developing capacities on climate change</a>
2013/12/14	<a href="#">Integrating multi-disciplinary models</a>
2014/10/07	<a href="#">Development of the forestry component of MOSAICC</a>
2015/02/16	<a href="#">Guide pratique pour réaliser des simulations dans le modèle STREAM</a>
2015/04/07	<a href="#">The Economic Module lecture_1_French</a>
2015/04/07	<a href="#">The Economic Module lecture_2_French</a>
2015/04/07	<a href="#">The Economic Module_lecture_3_French</a>
2015/04/07	<a href="#">The Economic Module lecture_4</a>
2015/04/07	<a href="#">The Economic Module lecture_5_French</a>
2015/04/07	<a href="#">The Economic Module lecture_6_French</a>
2016/05/17	<a href="#">FAO Modelling System for Agricultural Impacts of Climate Change</a>
2016/05/17	<a href="#">Portail Mosaicc</a>

2016/05/17 [Formation sur le Modèle Mosaicc](#)  
2016/06/01 Formation administration du site Web

Below, some photos of the workshops and training sessions.



## XII. CONCLUSION AND RECOMMENDATIONS

Climate change would lead to a continuous decrease in rainfall and increase in temperature (max and min) in all agricultural areas of Morocco toward the end of the century, comparatively to reference period (1971-2000). Countrywide, rainfall would decrease by 17 and 20% toward the period 2040-2069, for scenarios RCP4.5 (optimistic) and RCP8.5 (pessimistic) respectively. However, the deficit is predicted to be marked over the rainy season, from October to April, i.e. 23 and 34% for scenarios RCP4.5 and RCP8.5 respectively. At subnational level, climate projections show that agricultural areas of Morocco (northwestern) will suffer more from rainfall deficit than other areas, up to -50% relatively to reference period, except for the Saharan part of the country. Besides, climate change would lead to a continuous increase of temperature all over the country toward the end of the century. Tmax would increase by 1.9°C (+8%) and 3.4°C (+14%) toward the period 2040-2069, for scenarios RCP4.5 and RCP8.5, respectively. Tmin would dramatically increase by +2.1°C (+18%) and +3.2°C (+27%) toward the period 2040-2069, for scenarios RCP4.5 and RCP8.5, respectively. Consequently, climate change is expected to affect cereal production in Morocco.

Simulation of yield trends using AquaCrop model show that climate change would lead to a decrease in wheat and barley yields in all main agricultural areas of Morocco toward the end of the century, comparatively to reference period (1971-2000). Yield decrease is the direct consequence of rainfall deficit and temperature rise. The effect of climate change will be more pronounced in semi-arid and sub-humid lands. In opposite, wheat yields will increase due to more favorable temperatures in mountainous zones whereas for barley they will still decrease.

The STREAM model was run to produce the naturalized stream-flow response of the basins to future climate change scenarios, excluding anthropogenic influences. The RCP4.5 and the RCP8.5 scenarios of the MIROC-ESM, CanESM2 and MPI GCMS were analyzed in batches of 30 years. The results of the hydrologic modeling based on data from the basins of Moulouya, Sebou, Tensift, Loukkos, Bouregreg and Chaouia, Oum Er rbia and Souss-Massa-Draa show a general decrease of the monthly discharge for both scenarios RCP4.5 and RCP8.5. This decrease is pronounced toward the period 2070-2100, ranging between 20% to almost 100%. An increase in climatic variability is and a reduction in the natural flow of rivers may bring pressure on existing water resources or exacerbate the challenges associated with water supply already under pressure. Adaptation to climate change should be thought of in terms of



planning, infrastructure development and ongoing management of water resources through improved planning and assessment alternatives to identify the most effective and efficient solutions.

Economic simulations using a Dynamic Computable General Equilibrium (DCGE) model show that especially in the more extreme climate change scenario, yields of wheat and barley will decline and their market prices will go up. The shortfall in production is to some extent counteracted by increasing imports, but the simulations suggest that food consumption of households will decrease compared to baseline consumption. The overall impacts of the shortfall in wheat and barley on food consumption, including meat and dairy, is limited. The overall impact on GDP is limited across all scenarios. It should be noted that the current analysis *only* considers the impacts of climate change on the yields of wheat and barley, not on other crops not on other sectors of the economy. The current analysis also does explicitly consider the potential impact of climate change on the availability of irrigation water, which is a critical resource in the more productive areas of Moroccan agriculture. On a methodological note, the current study shows that yield output data that are simulated in MOSAICC can be used as inputs to the economic model, but it also shows that the linkage between the models is not easy and that more research should be carried out to improve this linkage. The simulated crop yield data show large volatility and large absolute changes. At the moment, the economic model has limitations in dealing with both the large volatility and the large absolute crop yield changes. Further study is needed to increase the flexibility of the economic model for these kind of data and for the best way to pre-process the data. Finally, it would be interesting to test the economic model for variations in irrigation water availability and for yield changes of more crops, including critical commercial crops such as tomatoes and citrus. Additionally, it would be interesting to let the model compute more aggregate indicators, such as, for example, agricultural GDP.

Forest simulations for the Maâmora forest, show that climate change will have a negative impact on *Quercus suber* by 2099, considering average total biomass per site (significant for two out of three models). In the future, and under changing climatic conditions, cork oak will therefore not only experience a decrease in distribution area, but also a fall in the production of biomass per hectare. It appeared that it is difficult to determine the production of cork without a relationship between this production and the standing biomass of *Quercus suber*. This relationship is currently being studied and will be incorporated into the platform in the future. It has been simulated that over time, and under changing climatic conditions: the number of sites where *Quercus suber* is present will decrease and its production of biomass per hectare will diminish; and the number of cohorts within the age range for cork production (26–75 years for the Maâmora forest) will fall. Another widely distributed species in the Maâmora forest is *Eucalyptus camaldulensis*. The model does not show

any significant variations in the area under this species; however, its biomass production per hectare appears to suffer a negative impact under the least optimistic scenario, RCP8.5. A comparison between total biomass simulations with and without forestry interventions illustrates the fact that it takes 25 years for forestry interventions to start having a positive impact on the species. The currently applied forest management scheme seems appropriate for the conservation of *Quercus suber*. Future forest management schemes should take into consideration several species such as *Acacia cyclops*, *Eucalyptus sideroxylon*, *Eucalyptus gomphocephala* and *Pinus pinea*. Indeed, these species show good resilience to climate change and could be more suitable for production in the coming century.



## XIII. REFERENCES

- [1] JCJH Aerts, MKriek, and MSchepel. Stream (spatial tools for river basins and environment and analysis of management options): set up and requirements. *Z. Physics and Chemistry of the Earth, Part B: Hydrology, Oceans and Atmosphere*, 24(6):591-595, 1999.
- [2] LM Bouwer, JCJH Aerts, P Droogers, and AJ Dolman. Detecting the long-term impacts from climate variability and increasing water consumption on runoff in the krishna river basin (india). *Hydrology and Earth System Sciences Discussions*, 3(4):1249-1280, 2006.
- [3] S Brands, S Herrera, J Fernández, and JoseMGutiérrez. How well do cmip5 earth system models simulate present climate conditions in europe and africa? *Climate dynamics*, 41(3-4):803-817, 2013.
- [4] Robert E Criss and William E Winston. Do nash values have value? discussion and alternate proposals. *Hydrological Processes*, 22(14):2723, 2008.
- [5] DP Dee, SM Uppala, AJ Simmons, P Berrisford, P Poli, S Kobayashi, U Andrae, MA Balmaseda, G Balsamo, P Bauer, et al. The era-interim reanalysis: Configuration and performance of the data assimilation system. *Quarterly Journal of the Royal Meteorological Society*, 137(656):553-597, 2011.
- [6] Filippo Giorgi and Piero Lionello. Climate change projections for the mediterranean region. *Global and Planetary Change*, 63(2):90-104, 2008.
- [7] Emil J Gumbel. The return period of flood flows. *The annals of mathematical statistics*, 12(2):163-190, 1941.
- [8] RTWL Hurkmans, H De Moel, JCJH Aerts, and PA Troch. Water balance versus land surface model in the simulation of rhine river discharges. *Water resources research*, 44(1), 2008.
- [9] JH Jungclaus, SJ Lorenz, C Timmreck, CH Reick, V Brovkin, K Six, J Segschneider, MA Giorgetta, TJ Crowley, J Pongratz, et al. Climate and carbon-cycle variability over the last millennium. *Climate of the Past*, 6:723-737, 2010.
- [10] Matti Kummu, Philip J Ward, Hans de Moel, and Olli Varis. Is physical water scarcity a new phenomenon? global assessment of water shortage over the last two millennia. *Environmental Research Letters*, 5(3):034006, 2010.
- [11] Richard H Moss, Jae A Edmonds, Kathy A Hibbard, Martin R Manning, Steven K Rose, Detlef P Van Vuuren, Timothy R Carter, Seita Emori, Mikiko Kainuma, Tom Kram, et al. The next generation of scenarios for climate change research and assessment. *Nature*, 463(7282):747-756, 2010.
- [12] TJ Raddatz, CH Reick, Wolfgang Knorr, Jens Kattge, E Roeckner, Reiner Schnur, K-G Schnitzler, P Wetzler, and J Jungclaus. Will the tropical land biosphere dominate the climate-carbon cycle feedback during the twenty-first century? *Climate Dynamics*, 29(6):565-574, 2007.
- [13] Keywan Riahi, Shilpa Rao, Volker Krey, Cheolhung Cho, Vadim Chirkov, Guenther Fischer, Georg Kindermann, Nebojsa Nakicenovic, and Peter Rafaj. Rcp

8.5âˆA ˆTa scenario of comparatively high greenhouse gas emissions. *Climatic Change*, 109(1-2):33-57, 2011.

[14] Janpeter Schilling, Korbinian P Freier, Elke Hertig, and Jürgen Scheffran. Climate change, vulnerability and adaptation in north africa with focus on morocco. *Agriculture, Ecosystems& Environment*, 156:12-26, 2012.

[15] Julia Stürck, Ate Poortinga, and Peter H Verburg. Mapping ecosystem services: The supply and demand of flood regulation services in europe. *Ecological Indicators*, 38:198-211,2014.

[16] Karl E Taylor, Ronald J Stouffer, and Gerald A Meehl. An overview of cmip5 and the experiment design. *Bulletin of the American Meteorological Society*, 93(4):485-498, 2012.

[17] AllisonMThomson, Katherine V Calvin, Steven J Smith, G Page Kyle, April Volke, Pralit Patel, Sabrina Delgado-Arias, Ben Bond-Lamberty,Marshall AWise, Leon E Clarke, et al.Rcp4. 5: a pathway for stabilization of radiative forcing by 2100. *Climatic Change*, 109(1-2):77-94, 2011.

[18] Yves Trambly,Wafae Badi, Fatima Driouech, Salaheddine El Adlouni, Luc Neppel, and Eric Servat. Climate change impacts on extreme precipitation in morocco. *Global and Planetary Change*, 82:104-114, 2012.

[19] PJWard, H Renssen, JCJH Aerts, RT Van Balen, J Vandenberghe, et al. Strong increases in flood frequency and discharge of the river meuse over the late holocene: impacts of long-term anthropogenic land use change and climate variability. *Hydrology and Earth System Sciences Discussions*, 12(1):159-175, 2008.

[20] S Watanabe, T Hajima, K Sudo, T Nagashima, T Takemura, H Okajima, T Nozawa,H Kawase, M Abe, T Yokohata, et al. Miroc-esm 2010: Model description and basic results of cmip5-20c3mexperiments. *GeoscientificModel Development*, 4:845-872, 2011.

[21] HCWinsemius, HHG Savenije, AMJ Gerrits, EA Zapreeva, and R Klees. Comparison of two model approaches in the zambezi river basin with regard to model reliability and identifiability. *Hydrology and Earth SystemSciences*, 10(3):339-352, 2006.

Lofgren, H., Thoams, M. and El-Said, M. (2002). A Standard Computable General Equilibrium (CGE) Model in GAMS, Microcomputers in Policy Research 5, International Food Policy Research Institute.

Moss,R. H., Edmonds, J. A., Hibbard,K. A., Manning, M. R.; Rose,S. K., van Vuuren, D. P; Carter,T. R., Emori,S., Kainuma, M., Kram,T., Meehl, G. A., Mitchell, J. F.B., Nakicenovic, N., Riahi,K., Smith, S. J., Stouffer,R. J.; Thomson, A. M., Weyant, J.P., Wilbanks,T. J. (2010). The next generation of scenarios for climate change research and assessment. *Nature*, 463 (7282): 747-756.

O'Neill,B. C., Kriegler,E., Riahi,K., Ebi,K. L., Hallegatte,S., Carter,T.R., Mathur,R., van Vuuren,D. P. (2014). A new scenario framework for climate change research: the concept of shared socioeconomic pathways. *Climatic Change*, 122 (3): 387-400.

Pauw, K., Thurlow, J. and van Seventer, D (2010). Droughts and Floods in Malawi: Assessing the Economywide Effects, IFPRI Discussion Paper 00962,

Development Strategy and Governance Division, International Food Policy Research Institute.

Thurlow, J. (2004). A Dynamic Computable General Equilibrium (CGE) Model for South Africa: Extending the Static IFPRI Model, Trade and Industrial Policy Strategies, International Food Policy Research Institute.

Thurlow, J. Zhu, T, and Diao, X. (2009). The Impact of Climate Variability and Change on Economic Growth and Poverty in Zambia, IFPRI Discussion Paper 00890, Development Strategy and Governance Division, Environment and Production Technology Division, International Food Policy Research Institute.

van Vuuren,D.P.; Edmonds,J., Kainuma,M., Riahi,K., Thomson, A., Hibbard,K., Hurtt,G. C., Kram,T., Krey,V., Lamarque,J. F., Masui,T., Meinshausen, M., Nakicenovic, N., Smith,S. J. (2011). The representative concentration pathways: an overview. *Climatic Change*, 109 (1): 5-31.

van Vuuren,D.P.; Kriegler,E., O'Neill,B. C., Ebi,K. L., Riahi,K., Carter,T.R., Edmonds,J., Hallegatte,S., Kram,T., Mathur,R., Winkler,H. (2014). A new scenario framework for Climate Change Research: scenario matrix architecture. *Climatic Change*, 122 (3): 373-386.

Aafi, A. 2007. *Étude de la diversité floristique de l'écosystème de chêne-liège de la forêt de la Maâmora*. Institut Agronomique et Vétérinaire Hassan II, Rabat (doctoral thesis).

Aber, J.D. & Federer, A.C. 1992. A generalized, lumped-parameter model of photosynthesis, evapotranspiration and net primary production in temperate and boreal forest ecosystems. *Oecologia*, 92: 463-474.

Aber, J.D., Ollinger, S.V., Federer, A., Reich, P.B., Goulden, M.L., Kicklighter, D.W., Melillo, J.M. & Lathrop, R.G. 1995. Predicting the effects of climate change on water yield and forest production in the northeastern United States. *Climate Research* 5: 207-222.

Abourouh, M., Taleb, M., Makhloufi, M., Boulmane M., & Aronson, J., 2005.- Biodiversité et dynamique dans la subéraie de la Maâmora (de la durée de clôture). *Forêt méditerranéenne*, 4, 275-278.

A.E.F.C.S., 1992. Forêt de la Maâmora. Procès-verbal d'aménagement 1992-2011, Tome I, Rabat.

Aukema, J.E., McCullough, D.G., Von Holle, B., Liebhold, A.M. & Britton, K.O. 2010. Historical accumulation of nonindigenous forest pests in the continental US. *BioScience*, 60: 886-897.

Bagaram, B.M. 2014. *Elaboration d'une base de données géographiques et catalogue des stations de la subéraie de la Maâmora*. Ecole Nationale Forestière d'Ingénieurs, Salé (mémoire de 3ième cycle).

Bagnouls, F. & Gausson H. 1953. Saison sèche et indice xérothermique. *Bulletin de la Société d'histoire naturelle*, 88: 193-239.

Belinda, E., Medlyn, R., McMurtrie, R., Dewar, M. & Jeffreys, P. 2000. Soil processes dominate the long-term response of forest net primary productivity to increased temperature and atmospheric CO<sub>2</sub> concentration. *Canadian Journal of Forest Research*, 30(6): 873-888.

Blonder, B., Violle, C., Patrick, L. & Enquist, B. 2011. Leaf venation networks and the origin of the leaf economics spectrum. *Ecology Letters*, 14(2) : 91–100.

Bossel, H. 1994. *Modeling and simulation*. A.K. Peters Ltd., Wellesley, MA, 484 p.

Correia, A. C., Tomé, M., Pacheco, C. A., Faias, S., Dias, A. C., Freire, J., Carvalho, P. O. & Pereira, J. S. 2010. Biomass allometry and carbon factors for a Mediterranean pine (*Pinus pinea* L.) in Portugal. *Forest Systems*, 19 (3): 418–433.

Cuddington, K., Fortin, M.-J., Gerber, L.R., Hastings, A., Liebhold, A., O'Connor, M. & Ray, C. 2013. Process based models are required to manage ecological systems in a changing world. *Ecosphere* 4(2), Article 20.

Dzotsi, K. 2002. *Application du modèle CERES-Maize de DSSAT à l'analyse des stratégies de semis pour le maïs (Zea mays) dans les conditions de Sévè-Kpota*. École Supérieure d'Agronomie, Université de Lomé (Mémoire d'ingénieur agronome).

FAO. 1982. *Les eucalyptus dans les reboisements*. Collection FAO: Forêts, 11. Rome.

Foster, J.R. 2011. *Forest insect defoliation patterns and carbon dynamics: Linking remote sensing with simulation models*. University of Wisconsin (PhD dissertation).

GIEC. 2007. *Bilan 2007 des changements climatiques: rapport de synthèse*. Geneva.

Godfrey, K. 1983. *Compartmental models and their applications*. Academic Press, New York.

Gustafson, E.J., Shifley, S.R., Mladenoff, D.J., Nimerfro, K.K. & He H.S. 2000. Spatial simulation of forest succession and timber harvesting using LANDIS. *Canadian Journal of Forest Research*, 30: 32–43.

Gustafson, E.J. 2013. When the past can't be used to predict the future: using mechanistic models to predict landscape ecological dynamics in a changing world. *Landscape Ecology*, 28: 1429–1437.

HCEFLCD. 2012. *PV d'aménagement de la forêt de Maâmora*. Bureau d'études TTOBA. Rabat.

Hofmann M. 2005. On the Complexity of Parameter Calibration in Simulation Models. *JDMS*, Volume 2, Issue 4, October 2005 Pages 217–226.

IPCC. 2013: *Climate Change 2013: The Physical Science Basis*. Contribution of Working Group I to the Fifth Assessment Report of the Intergovernmental Panel on Climate Change [Stocker, T.F., D. Qin, G.-K. Plattner, M. Tignor, S.K. Allen, J. Boschung, A. Nauels, Y. Xia, V. Bex and P.M. Midgley (eds.)]. Cambridge University Press, Cambridge, UK and New York, NY, USA, 1535 pp, doi:10.1017/CBO9781107415324.

Jouzel, J. & Debroise, A. 2007. *Le climat: jeu dangereux – Dernières nouvelles de la planète*. Dunod.

Kattge, J., Knorr, W., Raddatz, T. & Wirth, C. 2009. Quantifying photosynthetic capacity and its relationship to leaf nitrogen content for global-scale terrestrial biosphere models. *Global Change Biology*, 15: 976–991.

Kerkhoff, A.J., Fagan, W.F., Elser, J.J. & Enquist, B.J. 2006. Phylogenetic and growth form variation in the scaling of nitrogen and phosphorus in the seed plants. *American Naturalist*, 168: E103–E122.

Laughlin, D.C., Bakker, J.D., Stoddard, M.T., Daniels, M.L., Springer, J.D., Gildar, C.N., Greena, A.M. & Covington, W. 2004. Toward reference conditions: wildfire effects on flora in an old-growth ponderosa pine forest. *Forest Ecology and Management*, 199: 137–152.

Lepoutre, G. 1965. Régénération artificielle du chêne-liège et équilibre climatique de la subéraie en forêt de la Mâamora. *Annales de la Recherche Forestière au Maroc*, IX, 1–149.

Liu, F., Mladenoff, D.J., Keuler, N.S. & Moore, L.S. 2011. Broadscale variability in tree data of the historical Public Land Survey and its consequences for ecological studies. *Ecological Monographs*, 81(2): 259–275.

Lin T., M.L., E., J.M., A. & D. 2008. Physiology-phenology interactions in a productive semi-arid pine forest. *New Phytologist*, 178: 603–16.

Milla, R. & Reich, P.B. 2011. Multi-trait interactions, not phylogeny, fine-tune leaf size reduction with increasing altitude. *Annals of Botany*, 107: 455–465.

Ogaya, R. & J. Penuelas. 2003. Comparative field study of *Quercus ilex* and *Phillyrea latifolia*: photosynthetic response to experimental drought conditions. *Environmental and Experimental Botany*, 50: 137–148.

Paula, S., Arianoutsou, M., Kazanis, D., Tavsanoglu, Ç., Lloret, F., Buhk, C., Ojeda, F., Luna, B., Moreno, J. M., Rodrigo, A., Espelta, J. M., Palacio, S., Fernández-Santos, B., Fernandes, P. M. & Pausas, J. G. 2009. Fire-related traits for plant species of the Mediterranean Basin. *Ecology*, 90: 1420.

Price, C.A. & Enquist, B.J. 2007. Scaling of mass and morphology in Dicotyledonous leaves: an extension of the WBE model. *Ecology*, 88: 1132–1141.

Reich, P.B., Oleksyn, J. & Wright, I.J. 2009. Leaf phosphorus influences the photosynthesis-nitrogen relation: a cross-biome analysis of 314 species. *Oecologia*, 160: 207–212.

Scheller, R.M., Mladenoff, D.J., 2004. A forest growth and biomass module for a landscape simulation model, LANDIS: Design, validation, and application. *Ecological Modelling* 180, 211–229.

Scheller, R.M., 2012. LANDIS-II Biomass Succession v. 3.1: Extension user's guide. Published online by Portland State University (<http://www.LANDIS-II.org/exts/biomass-succession>).

Sghaier, T. & Ammari, Y. 2012. Croissance et production du pin d'Alep (*Pinus halepensis* Mill.) en Tunisie. *Ecologia mediterranea*, Vol. 38(1): 39–57.

Theron, J.M., Van Laar, A., Kunneke, A. & Bredenkamp, B.V. 2004. A preliminary assessment of utilizable biomass in invading *Acacia* stands on the Cape coastal plains. *South African Journal of Science*, 100: 123–125.

Wieser, G., Peters, J., Luis, V.C., Morales, D. & Jimenez, M.S. 2002. Ecophysiological studies on the water relations in a *Pinus canariensis* stand, Tenerife, Canary Islands. *Phyton*, 42, 291-304.

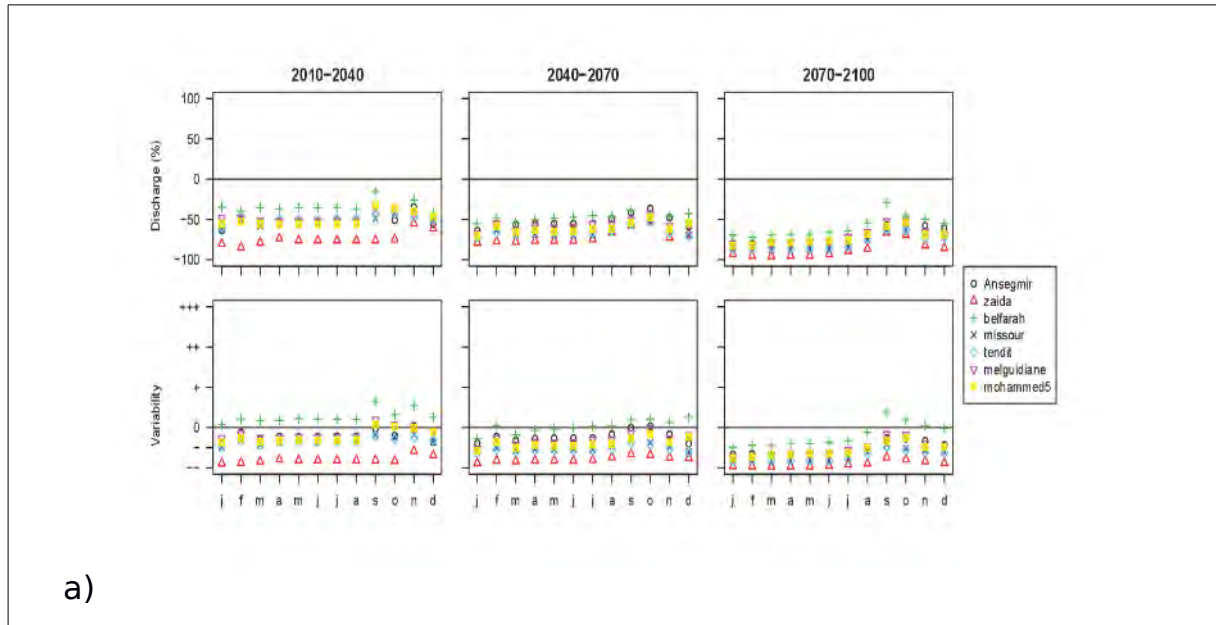
Williams, J.W., Jackson, S.T., 2007. Novel climates, no-analog communities, and ecological surprises. *Frontiers in Ecology and the Environment* 5, 475-482.

Wirth, C. & Lichstein, J.W. 2009. The imprint of species turnover on old-growth forest carbon balances – insights from a trait-based model of forest dynamics. In C. Wirth, G. Gleixner and M. Heimann, eds. *Old-growth forests: function, fate and value*, pp. 81–113. Springer, New York, Berlin, Heidelberg.

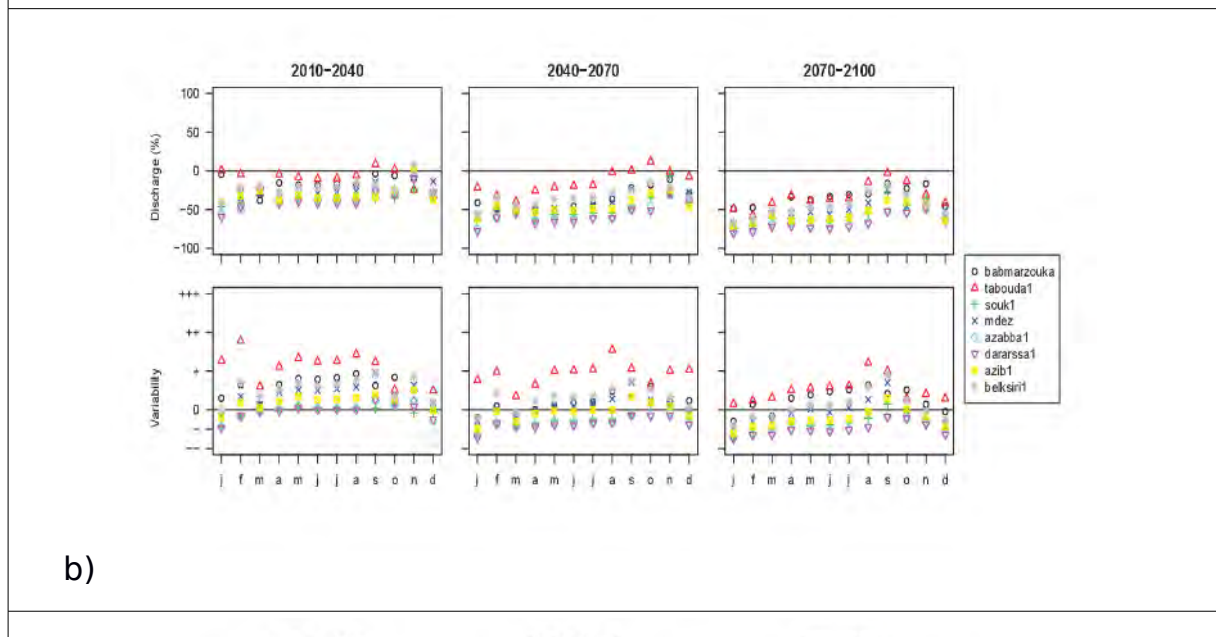


# XIV. ANNEXES

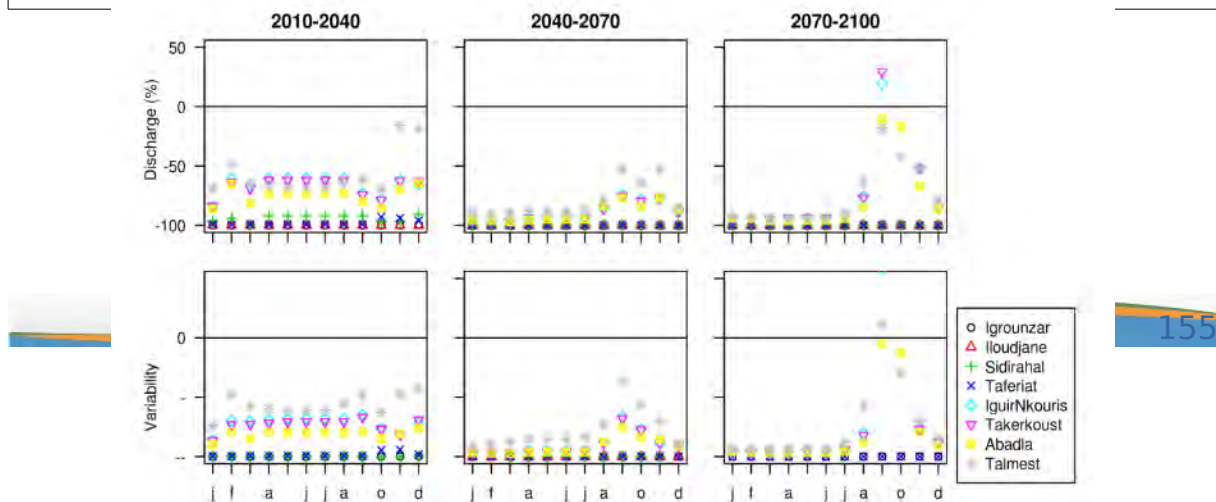
## 1. Annex 1



a)



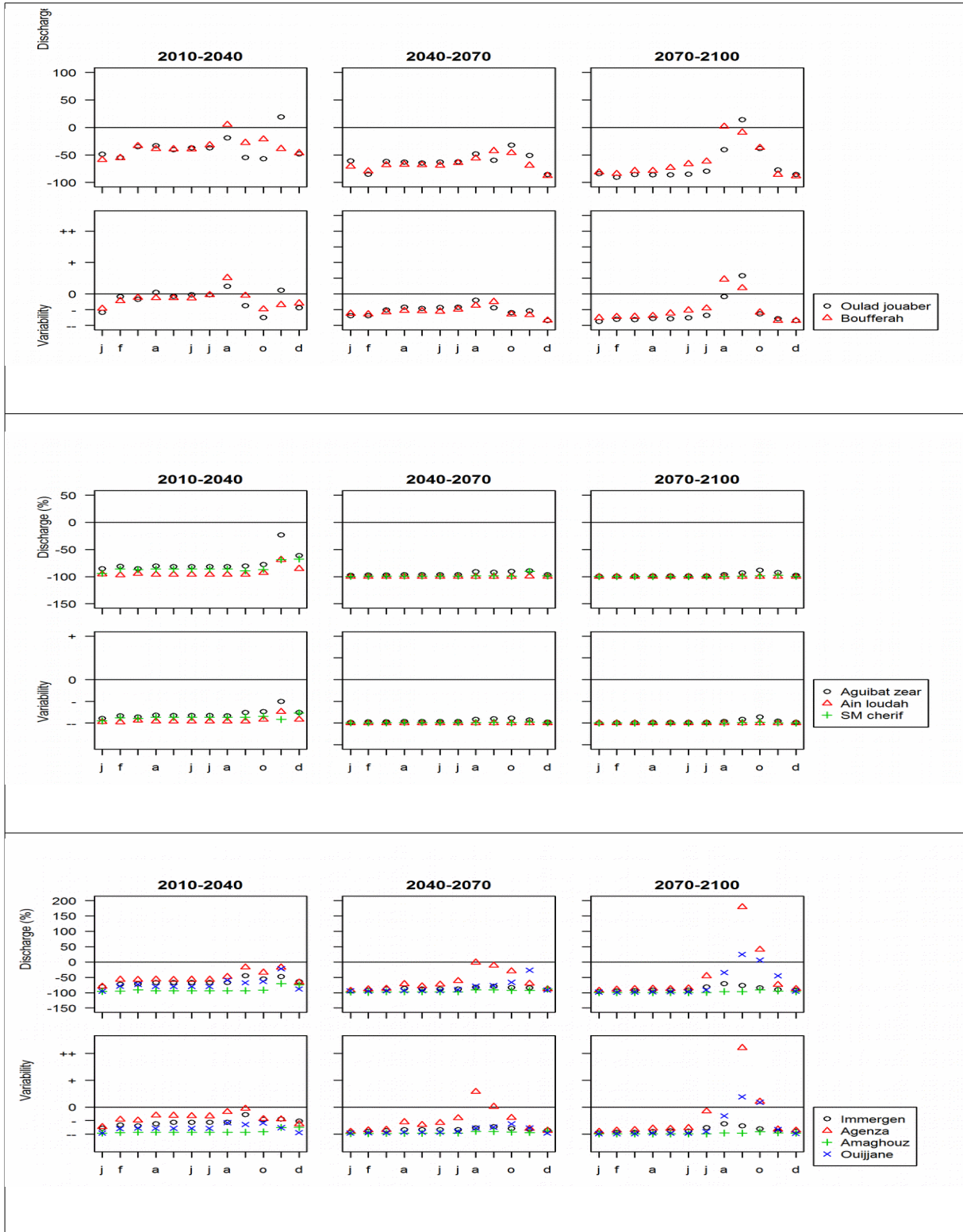
b)



c)

**Figure 89 : Change in median monthly discharge and streamflow variability for all basins in the Moulouya (a), Sebou (b) and Tensift (c) basin for the periods 2010-2040 (left) 2040-2070 (middle) and 2070-2100 (right) for MIROC-ESM model and RCP8.5 scenario.**

## 2. Annex 2



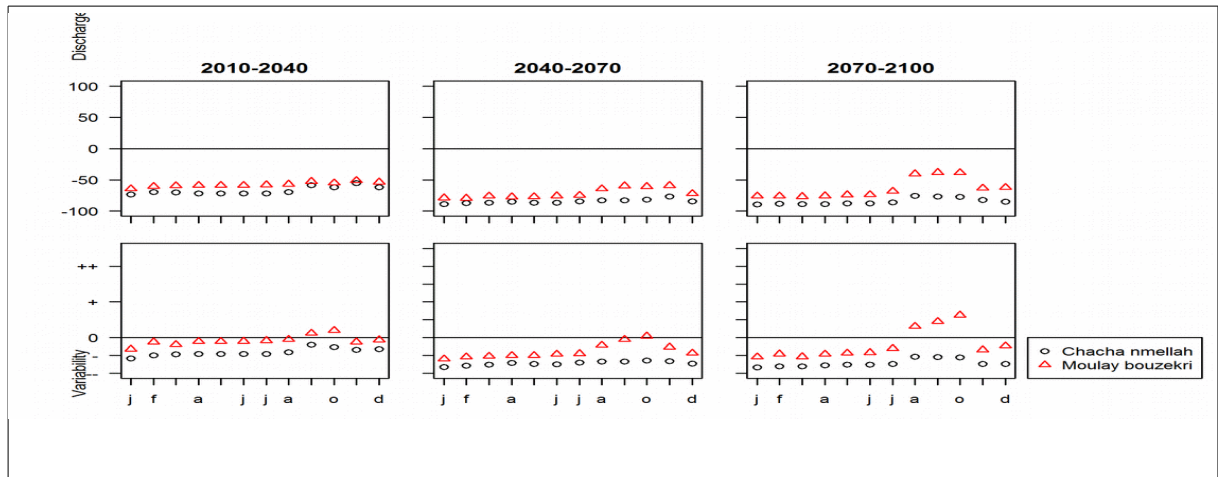
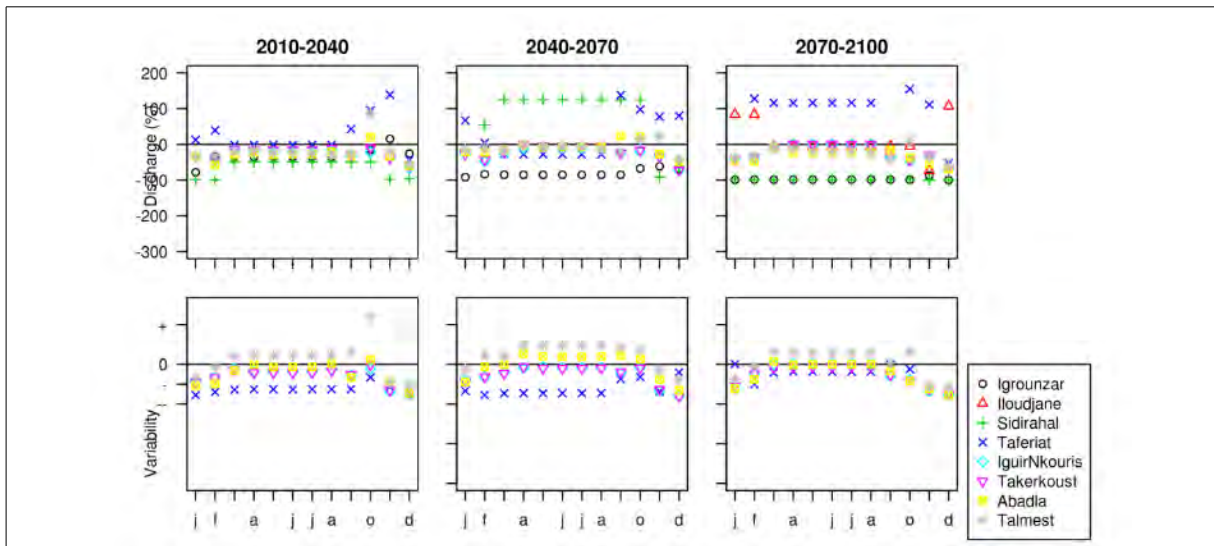
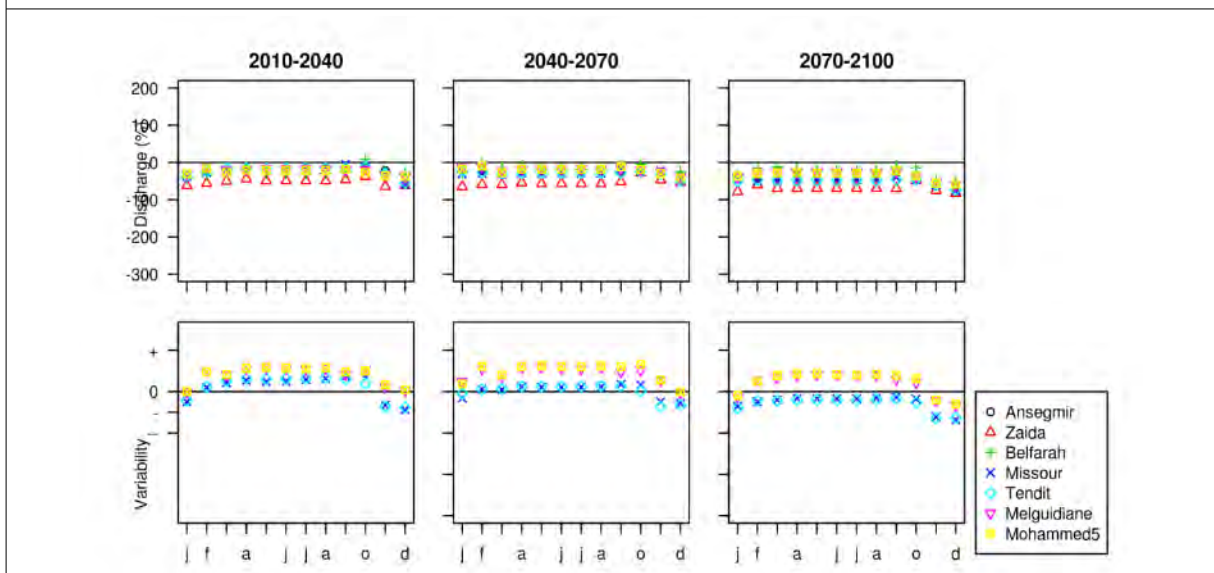


**Figure 90 : Change in median monthly discharge and streamflow variability for all basins in the Loukkos , Bouregreg, Souss Massa Draa and Oum Er rbia basins for the periods 2010-2040 (left) 2040-2070 (middle) and 2070-2100 (right) for MIROC-ESM model and RCP8.5 scenario.**

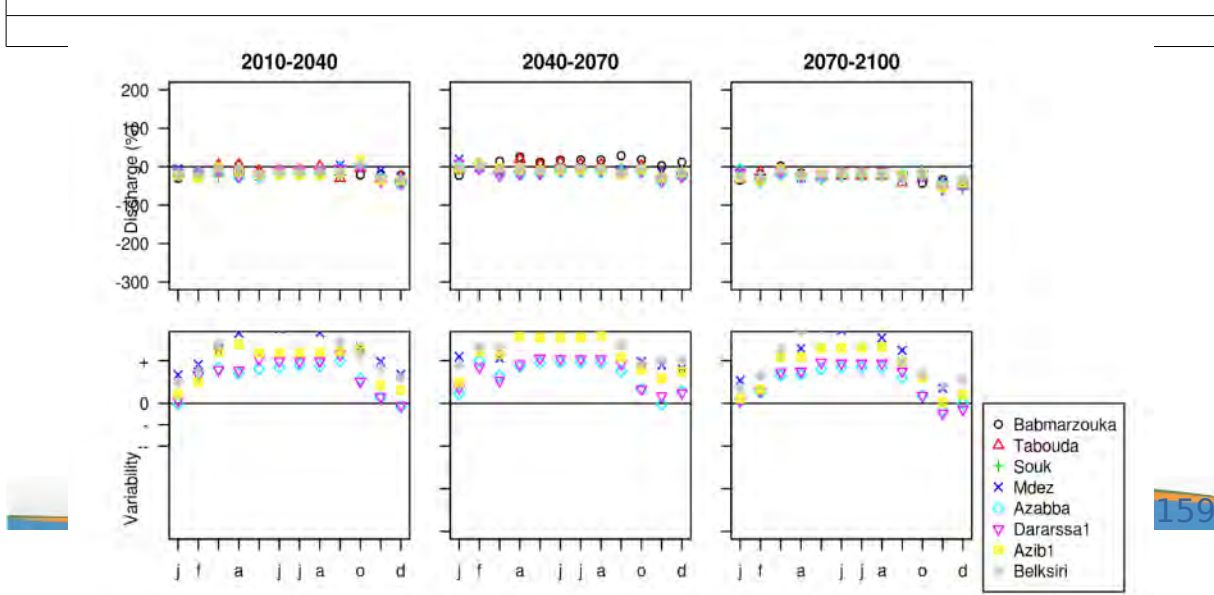
### 3. Annex 3



a)



b)

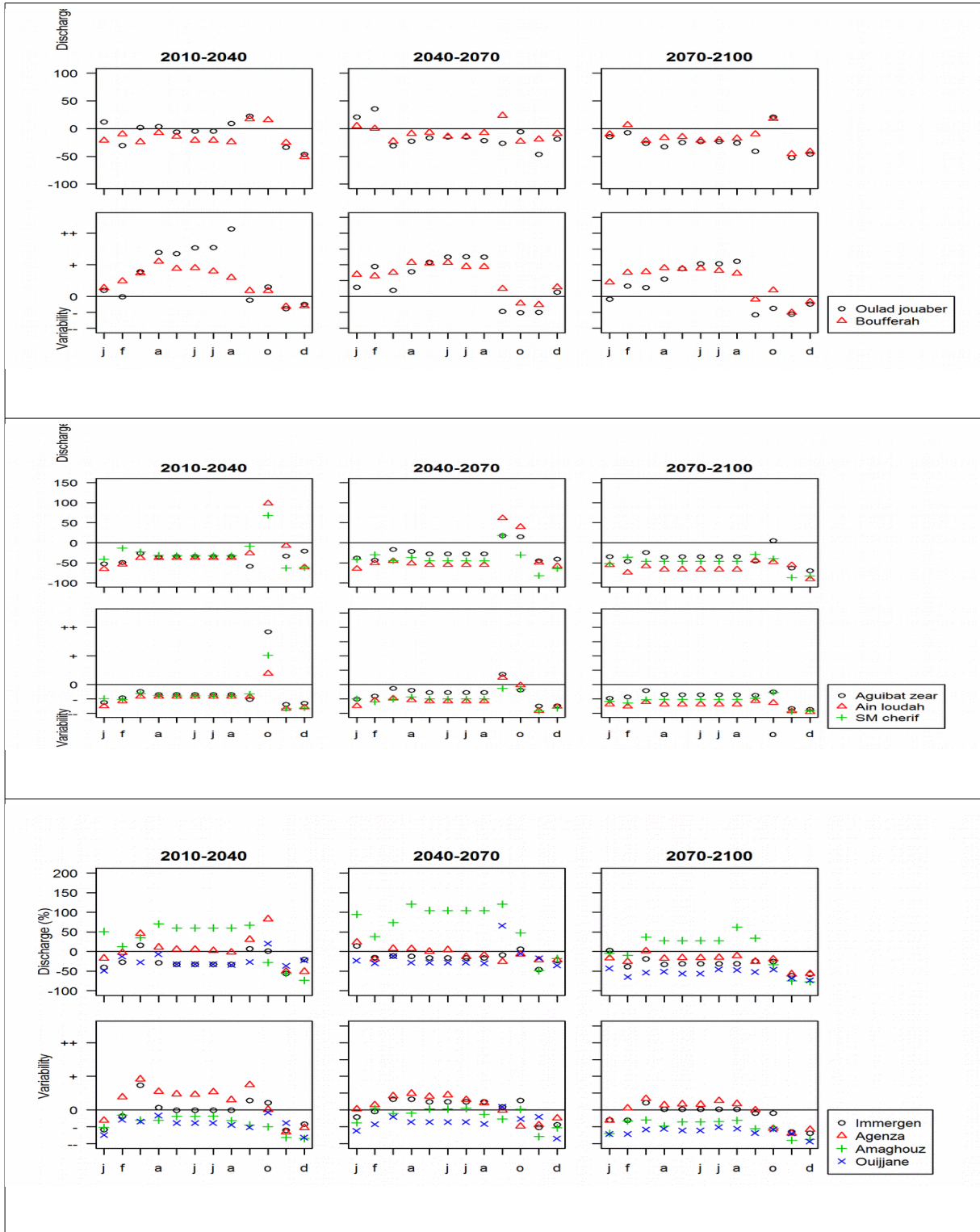


c)

**Figure 91 : Change in median monthly discharge and streamflow variability for all basins in the Moulouya (a), Sebou (b) and Tensift (c) basin for the periods 2010-2040 (left) 2040-2070 (middle) and 2070-2100 (right) for MPI-ESM-LR model and RCP4.5 scenario**



# 4. Annex 4



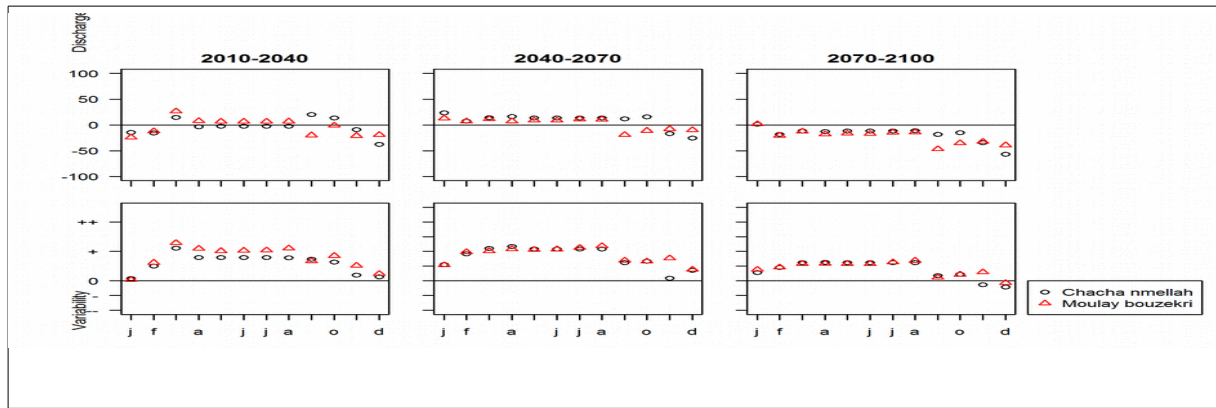


**Figure 92 : Change in median monthly discharge and streamflow variability for all basins in the Loukkos , Bouregreg, Souss Massa Draa and Oum Er rbia basins for the periods 2010-2040 (left) 2040-2070 (middle) and 2070-2100 (right) for MPI-ESM-LR model and RCP4.5 scenario.**

## 5. Annex 5 : Distributed hydrological model STREAM

Hydrological modeling allows the quantification of water resources for planning and management of water, develops water balances, evaluate the behavior of extreme events (droughts and floods), simulate future scenarios and assess the dynamics of the basin to potential effects of climate change. In this context, the application of the STREAM model (Spatial Tools for River Basin Environmental Analysis and Management) allows to represent the impacts of climate change and land use on river flows and the model can simulate anthropic activities in the basin, such as reservoirs (Aerts et al 2011). This model represents the past, present and future about the effects of water availability, climate change and land use.

The STREAM model is a distributed rainfall-runoff based on the use of GIS (Geographical Information System) which allows the simulation of river discharges for obtaining the availability of water in river basins. The STREAM model allows calculation of water balance from the water balance of each grid cell River basin under study, which accumulates in the local direction of drainage, derived from digital elevation model (DEM) to the point of exit (where the measurement station is located). The model structure consists of a series of reservoirs, where surface flows are routed to rivers (Aerts et al 1999). STREAM model consists of three storage tanks: snow storage, storage soil moisture and groundwater storage, dividing the outflow component in a fast and a slow component. The fast component is affected by soil moisture storage and the slow component soil water storage, both behave as linear reservoirs (Hurkmans, Troch & Uijlenhoet, 2005) (Hurakmans et al. 2008). The model uses Hargreaves equation in the MOSAICC, to calculate potential evapotranspiration or reference evapotranspiration, FAO (2006), which takes into account temperature and precipitation as the main input parameters.

The water balance is calculated at position (x, y) in the month (t) by the following equations (Aerts et al 1999).

$$\text{Eq 1 : } R_{x,y,t} = P_{x,y,t} - \Delta E_{x,y,t} +$$

$dS_{x,y,t}$

$$\text{Eq 2 : } S_{x,y,t} = SS_{x,y,t} - GWS_{x,y,t} + SNS_{x,y,t}$$

Where: R: Runoff (mm / month);

P: precipitation (mm / month);

S: Volume of water stored in the soil, snow and groundwater (mm / month);

$\Delta E$ : Loss of water due to actual evapotranspiration (mm / month);

dS: Change in the volume of water stored (mm / month);

SS: Water stored in the soil as shallow groundwater (mm / month);

GWS: water stored in aquifers and groundwater deep (mm / month);

SNS: the amount of water stored in the snow (mm / month).

The spatial nature of the model allows the analysis of patterns of water availability and changes in these patterns, according to the artificial measures (ie, changes in land use such as deforestation and irrigation) and external influences, such as climate change. Figure 93 shows the main storage compartments and water flows model STREAM, which together determine water availability for each grid cell obtained from Digital Elevation Model - MED (Aerts et al 1999), and the end result, which is the runoff, discharge of each river.

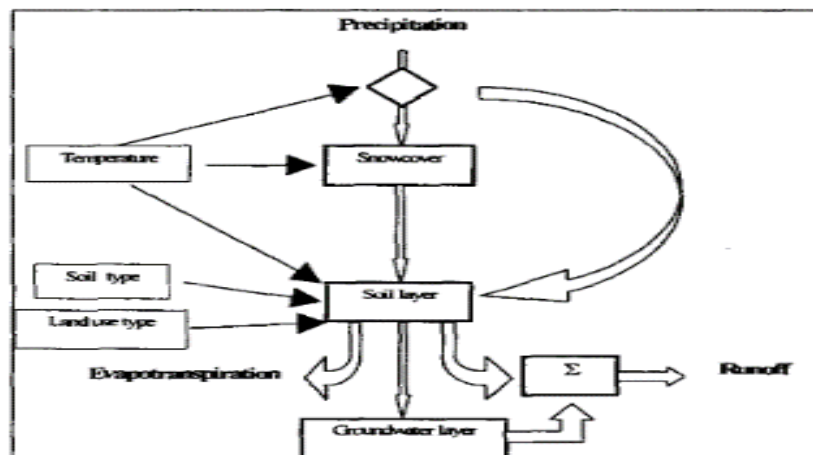


**Figure 93 : Water balance Storage Compartments of the STREAM model (Aerts et al. 1999).**

The STREAM allows rapid assessment studies for watersheds, especially when they are large. Data entry required to run space are five: the land use map, the map of soil types, the map of rainfall and monthly temperatures; and digital elevation model.

## 6. Annex 6: Data analysis method

Climate change induced differences were investigated by comparing the modeled discharge series with the baseline. Comparison between the baseline and scenarios was done by fitting a Gumbel distribution through the modeled riverflow (Q) and then extracting the Gumbel parameters [7]. Figure 94 shows the probability density function (cdf) and cumulative distribution function (pdf) of three Gumbel distribution functions. The cdf was calculated using Eq. 1 (cdf ) and 2 (pdf), where  $\mu$  represents the mode,  $\beta$  a scale parameter and the median ( $\mu_{1/2}$ ) is given by  $\mu - \beta \ln(\ln(2))$ . The curves in Figure 94, show that an increase in  $\mu$  gives in higher (discharge; Q), while an increase in  $\beta$  results in a larger range. Thus, a change in  $\mu_{1/2}$  or  $\beta$  indicates a change in river flow magnitude or river flow variability, respectively.

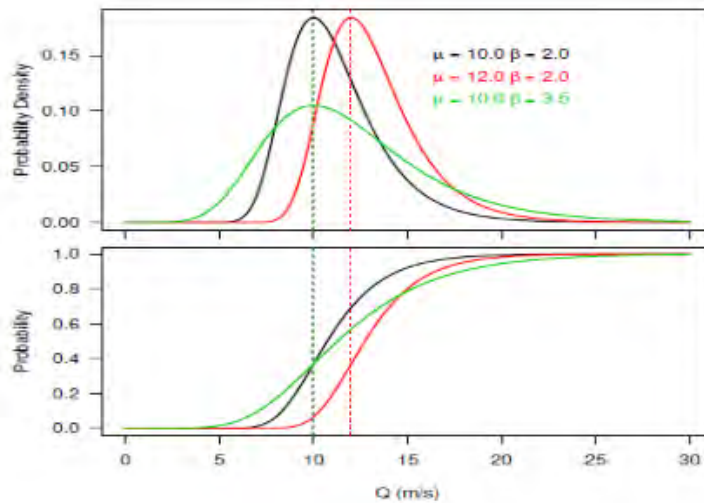


**Figure 94 : The pdf and cdf of the Gumbel distribution (Eq1 and Eq 2).The red and black line display the effect of a higher  $\mu$ , the black and green line show the effect an increase in  $\beta$ . Increase in magnitude is linked to in increase in  $\mu$ , an increase of  $\beta$  is associated with an increase in range**

$$f(Q) = \frac{1}{\beta} e^{-\frac{Q-\mu}{\beta}} + e^{-\frac{Q-\mu}{\beta}} \quad (.1)$$

$$F(Q) = e^{-e^{-\frac{x-\mu}{\beta}}} \quad (.2)$$

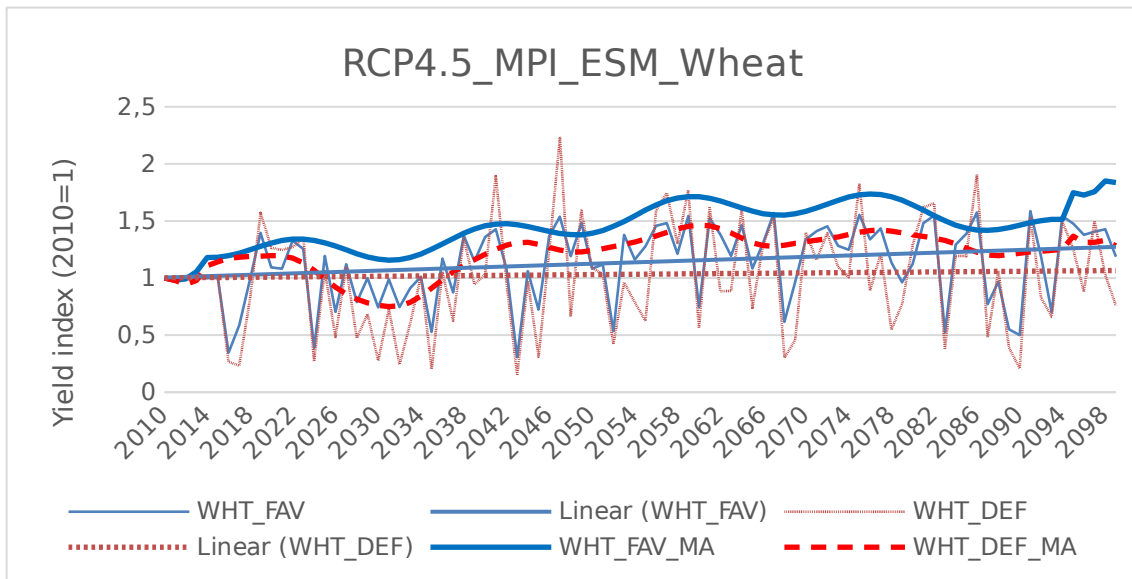
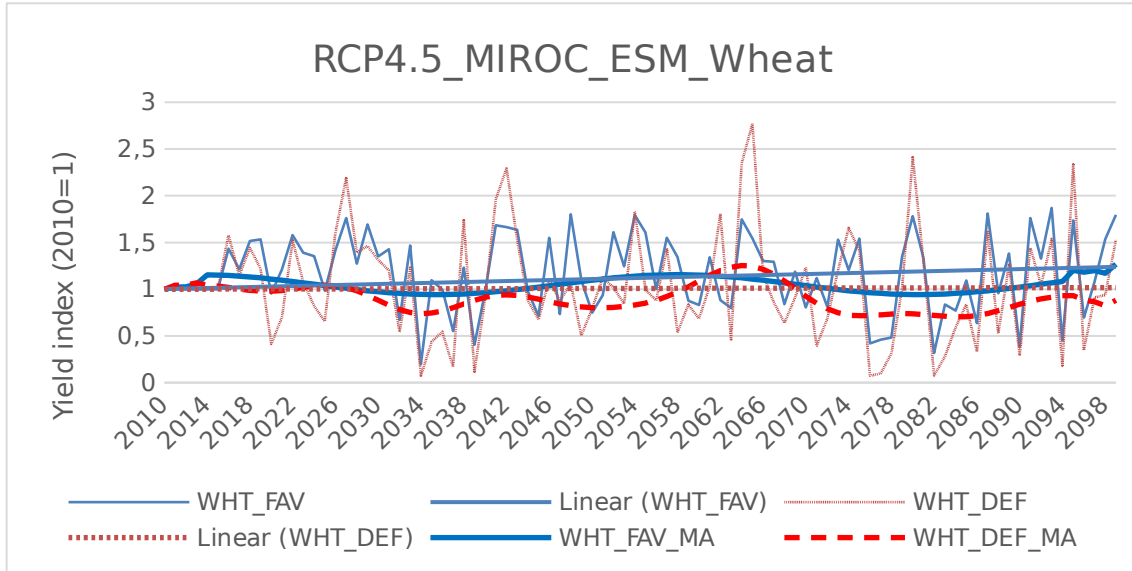
The probability of a specific extreme event can be calculated using the cumulative probability ( $F(Q)$ ): Eq. 2) can be expressed by in its return period  $y$  (Eq. 3.). As such, the maximum flood ( $Q$ ) to be expected within a given number of years ( $y$ ) can be expressed by Eq. 4.

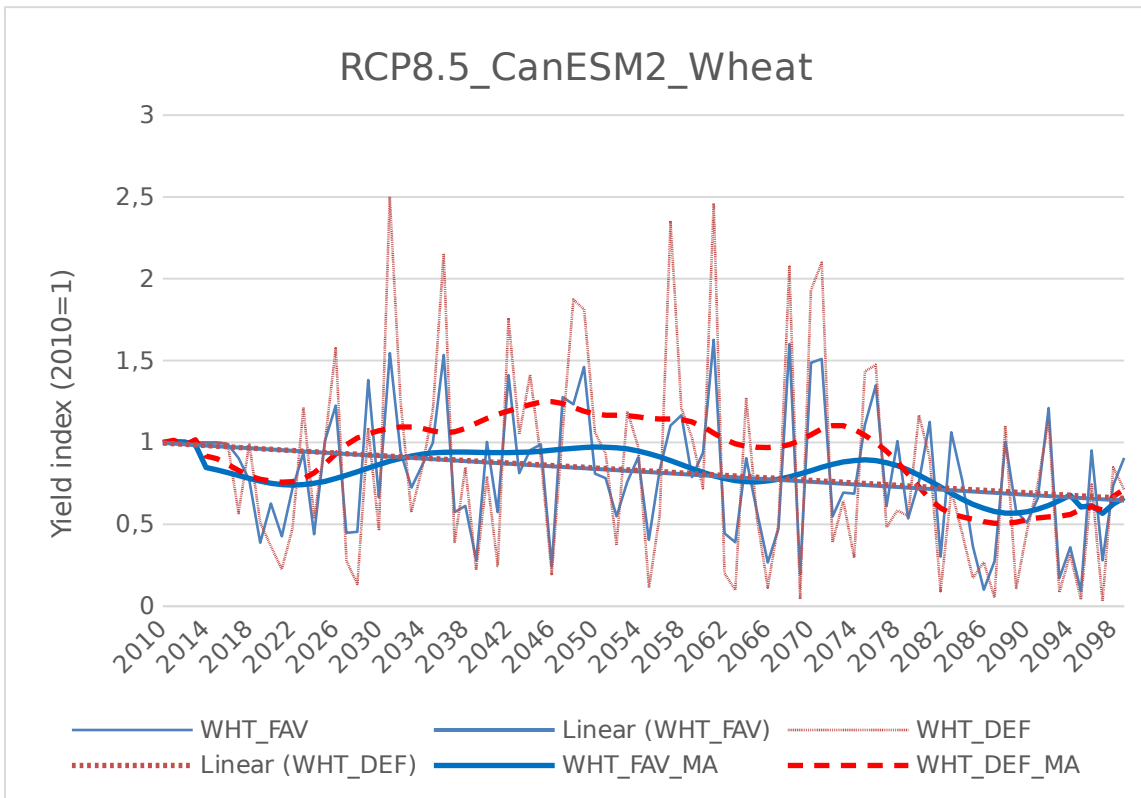
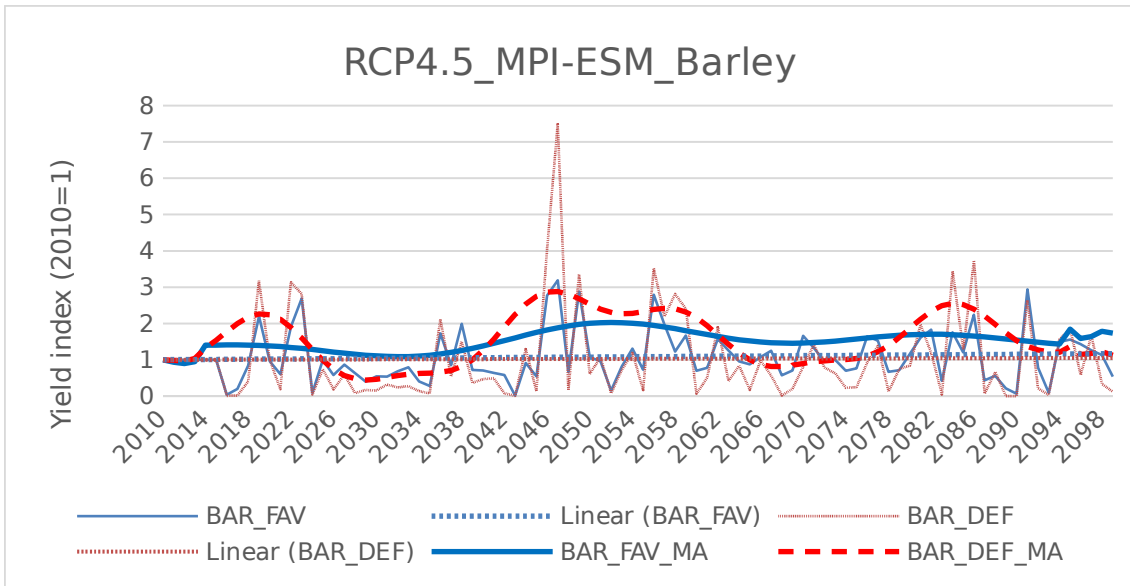
$$y = \frac{1}{1 - F(Q)} \quad (.3)$$

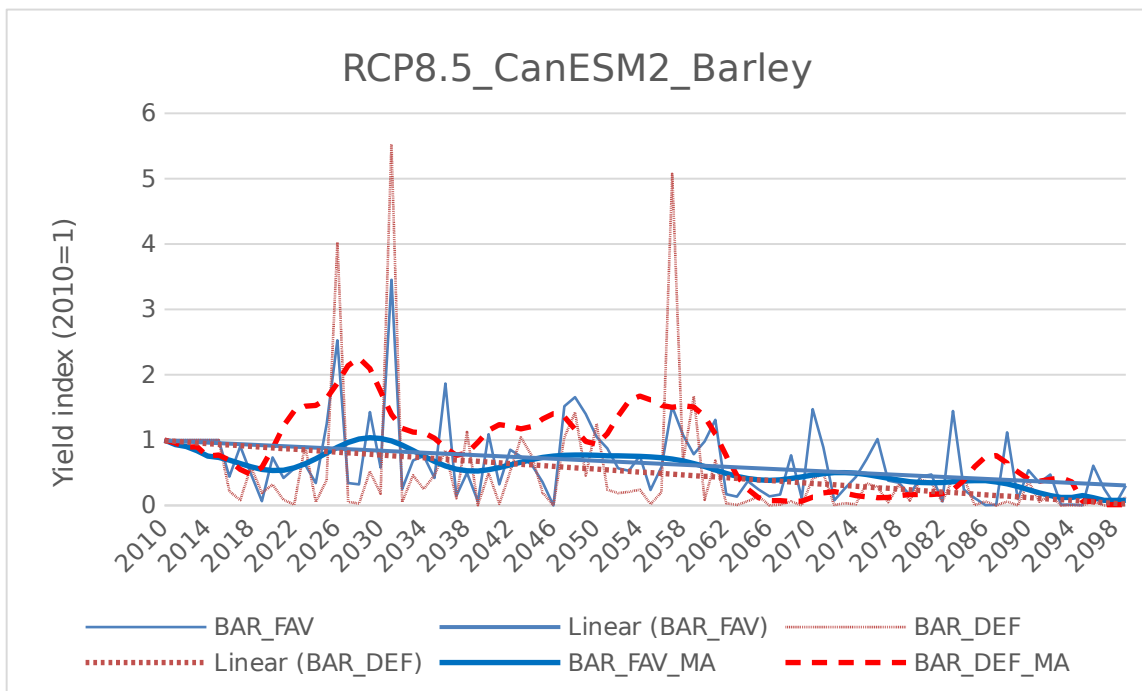
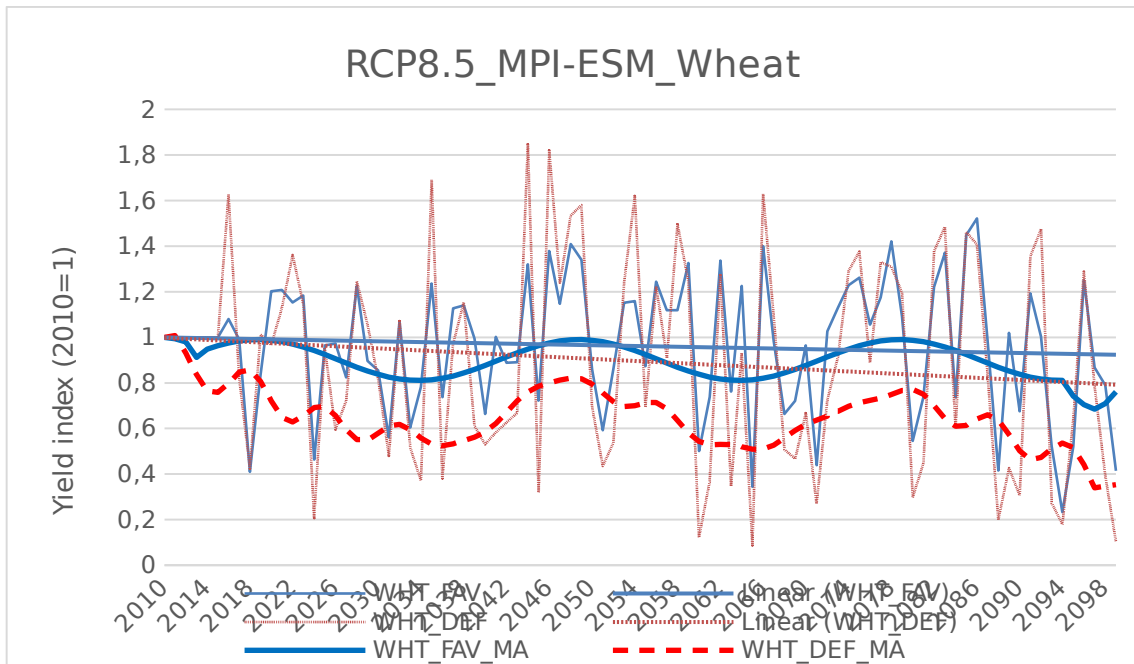
$$Q = -\ln(-\ln(1 - \frac{1}{y})) * \beta + \mu \quad (.4)$$

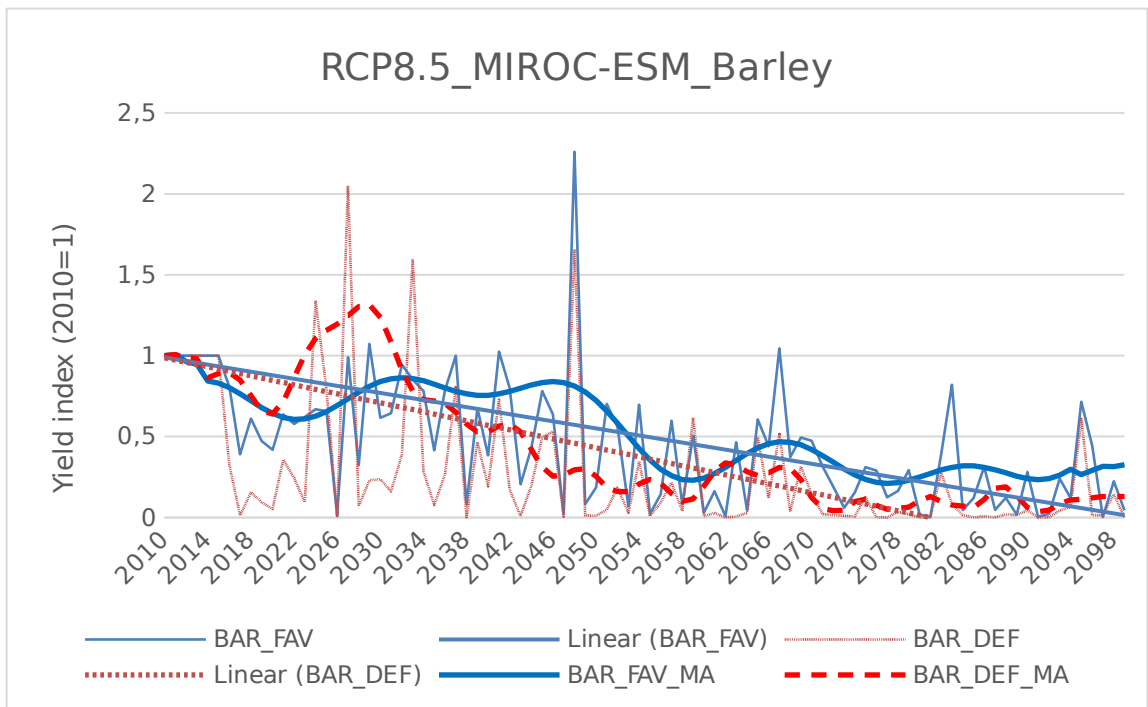


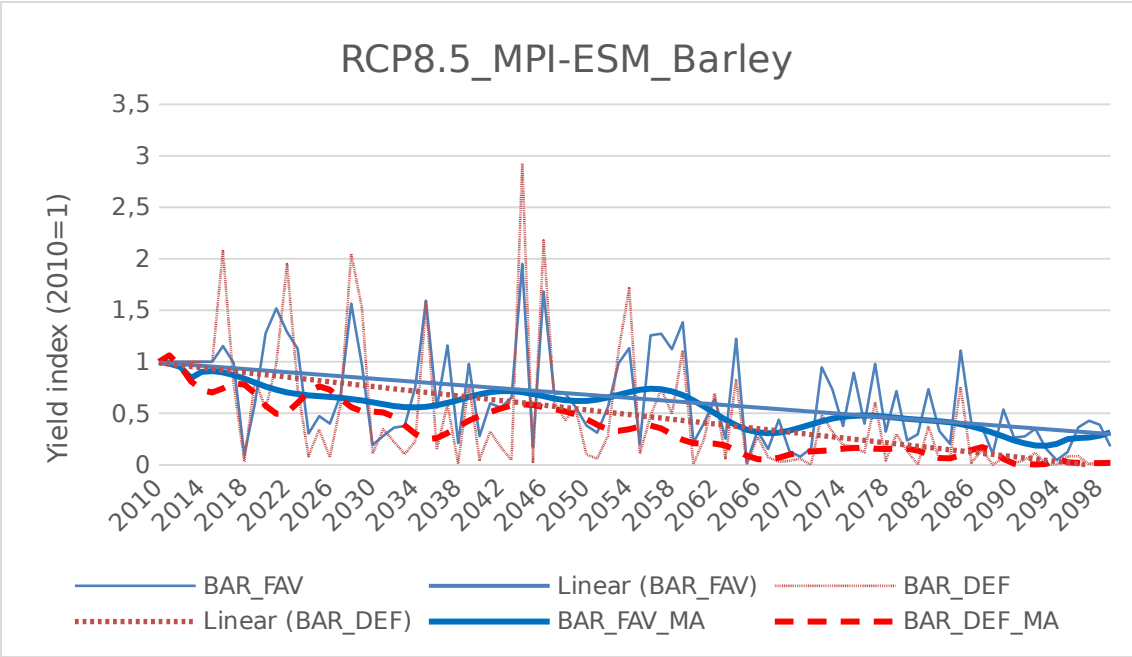
## 7. Annex 7 : Yield indices











## 8. Annex 8 : A technical description of the model

This appendix provides a technical description of the *dynamic computable general equilibrium model (DCGE)* that was developed for MOSAICC. The model is based on the theory of dynamic general equilibrium and is especially designed to simulate the evolution of the national economy over the time span of the study, driven by the change in crop yields. Special attention has been devoted to develop a generic model that can be easily adapted to account for different situations. For instance, the number of production factors, of households, of activities and of commodities is can be freely chosen by the user. This was done by using the indexing facilities provided by Dynare. This flexibility allows for using the model on different countries and adapting the specification of the model to the problem under studied and data availabilities.

The DCGE model is standard for the economic modelling literature of developing countries. It has the main features of Lofgren et al. (2002) that was designed to represent African agriculture with various applications to the economy-wide effects of climate variability in African countries (Thurlow et al., 2009; Pauw et al., 2010). The dynamic is essentially driven by exogenous factors such as the productivity of production factors (of special interest here the land), or the evolution of the population. Prices and quantities are fully flexible and adjust after a shock to insure the equilibrium. This type of equilibrium is said Walrasian because the equilibrium between supply and demand is always satisfied simultaneously on all markets (production factors, commodities, savings, current account). Moreover the specification of the model allows for a high level of detail about activities, transfers between agents and taxes. More specifically:

- Commodities can be produced by various Activities. For example, Commodity “wheat” can be produced in various regions and/or by irrigated and non-irrigated farms and/or “small” and “large” farms.
- Different households can be distinguished. For example “rural” and “urban”.
- Can account for “home” production, i.e. commodities produced and consumed at the farm.
- Full accounting for tax system (direct and indirect taxes) and transfers between governments and households.
- Demand based on linear expenditure system (LES), where demand is split between subsistence demand (income-independent) and “luxury” demand. This allows for marginal income elasticity to differ from average income elasticity (and is able to conform to “Engels Law”).
- Allows return to factors to differ between sectors (e.g. agriculture and manufacturing).



## Sets

$a \in A$	Activities
$c \in C$	Commodities
$c \in CT \subset C$	Transaction service commodities (trade margins)
$f \in F$	Factors of production
$i \in INS$	Institutions (domestic and ROW)
$i \in INSD \subset INS$	Domestic institutions (Households and government)
$i \in INSDNG \subset INSD$	Domestic non-government institutions
$h \in H \subset INSDNG$	Households
$t \in T$	Time

## Parameters

$cwts_c$	Weight of commodity $c$ in CPI
$ica_{c,a}$	Quantity of $c$ per unit of aggregate intermediate input $a$
$icd_{cc}$	Quantity of commodity $c'$ as trade input per unit of $c$ produced and sold domestically
$ice_{cc}$	Quantity of commodity $c'$ as trade input per exported unit of $c$
$icm_{cc}$	Quantity of commodity $c'$ as trade input per imported unit of $c$
$inta_a$	Quantity of aggregate intermediate input per activity unit
$iva_a$	Quantity of value-added per activity unit
$mps_i$	Base-year marginal propensity to save for domestic private institution $i$
$pwe_c$	FOB export price (FCU)
$pwm_c$	CIF import price (in Foreign currency units - FCU)
$qdst_c$	Quantity of stock change
$qg_c$	Base-year quantity of government demand
$qinv_c$	Base-year quantity of fixed investment demand
$shif_{if}$	Share of domestic institution $i$ in income from factor $f$
$shii_{ii}$	Share of net income of $i'$ to $i$ ( $i, i' \in INSDNG$ )
$ta_a$	Tax rate for activity $a$
$te_c$	Export tariff rate
$tf_f$	Direct tax rate for factor $f$
$tins_i$	Direct tax rate for institution $i$
$tm_c$	Import tariff rate
$tq_c$	Rate of sales tax (as share of composite price inclusive of sales tax)
$trnsfr_{ii'}$	Transfer from institution $i'$ to institution $i$
$tva_a$	Rate of value-added tax for activity $a$

### Greek symbols

$\alpha^{ac}_c$	Shift parameter in domestic aggregation function
$\alpha^q_c$	Armington function shift parameter
$\alpha^t_c$	CET function shift parameter
$\alpha^{va}_a$	Efficiency parameter in value added function
$\beta^a$	Capital sectoral mobility parameter
$\beta^h_{ach}$	Marginal share of consumption spending on home commodity c from activity a for household h
$\beta^m_{ch}$	Marginal share of consumption spending on marketed commodity c for household h
$\gamma^h_{ach}$	Subsistence consumption of home commodity c from activity a for household h
$\gamma^m_{ch}$	Subsistence consumption of marketed commodity c for household h
$\delta^{ac}_{ac}$	Share parameter in domestic aggregation function
$\delta^q_c$	Armington function share parameter
$\delta^t_c$	CET function share parameter
$\delta^{va}_{fa}$	Share parameter for factor f in activity a in value added function
$\epsilon^{va}_a$	Elasticity of substitution between factors of production in activity a
$\epsilon^{ac}_c$	Elasticity of transformation of activities a in commodity c
$\epsilon^t_c$	Elasticity of transformation between domestic and export sales of commodity c
$\epsilon^q_c$	Elasticity of substitution between domestic and imported commodity c
$\theta_{a,c}$	Yield of output c per unit of activity a
$\rho^{ac}_c$	CES domestic aggregation function exponent
$\rho^q_c$	Armington function exponent
$\rho^t_c$	CET function exponent
$\rho^{va}_a$	CES value added function exponent

### Exogenous variables

FSAV	Foreign savings (FCU)
QFS <sub>f</sub>	Endowment of factor f

### Endogenous variables

EG	Government expenditure
EH <sub>h</sub>	Household consumption expenditures

EXR	Exchange rate (LCU per FCU)
GSAV	Government savings (or deficit)
MPS	Marginal propensity to save adjustment variable
MPS <sub>i</sub>	Marginal propensity to save for domestic private institution i
PA <sub>a</sub>	Output price of activity a
PC	Consumer price index
PDD <sub>c</sub>	Demand price for commodity produced and sold domestically
PDS <sub>c</sub>	Supply price for commodity produced and sold domestically
PE <sub>c</sub>	Export price (Local currency unit - LCU)
PINTA <sub>a</sub>	Aggregate intermediate input price for activity a
PK <sub>ft</sub>	Unit price of capital in period t
PM <sub>c</sub>	Import price in LCU including transaction cost
PQ <sub>c</sub>	Composite commodity price
PQF <sub>f,a</sub>	Price of factor f in activity a
PVA <sub>a</sub>	Value-added price of activity a
PXAC <sub>ac</sub>	Price of commodity c from activity a
PX <sub>c</sub>	Aggregate producer price for commodity c
QA <sub>a</sub> activity a)	Level of domestic activity a (quantity of output produce by activity a)
QD <sub>c</sub>	Quantity of domestic output sold domestically
QE <sub>c</sub>	Quantity of exports
QF <sub>f,a</sub>	Quantity demanded of factor f by activity a
QG <sub>c</sub>	Government consumption demand for commodity c
QH <sub>ch</sub>	Quantity of consumption of marketed commodity c for household h
QHA <sub>ach</sub>	Quantity of home commodity c from activity a consumed by household h
QINT <sub>ca</sub>	Quantity of commodity c used as intermediate input by activity a
QINTA <sub>a</sub>	Quantity of aggregate intermediate input
QINV <sub>c</sub>	Quantity of fixed investment demand for commodity c
QM <sub>c</sub>	Quantity of imports
QQ <sub>c</sub>	Composite supply to domestic market
QVA <sub>a</sub>	Quantity of aggregate value added of activity a
QXAC <sub>ac</sub>	Marketed output quantity of commodity c from activity a
QX <sub>c</sub> commodity c	Aggregate marketed quantity of domestic output of commodity c
TRII <sub>ir'</sub>	Transfer from institution i' to i (i ∈ INSDNG)
WALRAS equilibrium)	Saving-investment imbalance (slack variable that should be zero in equilibrium)
YF <sub>f</sub>	Income of factor f
YG	Government revenue

$Y_{if}$	Income of factor f to domestic institution i
$Y_i$	Income of institution i

Variable in first difference and growth rate are respectively referred as:  
 $\Delta X_t = X_t - X_{t-1}$  and  $\dot{X}_t = \frac{X_t}{X_{t-1}} - 1$ .

## PRODUCTION

### Top level of production function is Leontief

$$QVA_a = i v a_a \cdot QA_a \quad (1)$$

$$QINTA_a = i n t a_a \cdot QA_a \quad (2)$$

*“quantities of aggregate value added and intermediate inputs are a constant fractions of activity level”*

### Factor demand

The factor demand results from the maximization of profit assuming a CES production function:

$$\text{Max} \left\{ PVA_a \cdot (1 - t v a_a) \cdot QVA_a - \sum_f P Q F_{f,a} Q F_{f,a} \right\} \text{ s.t. } QVA_a = \alpha_a^{va} \cdot \left( \sum_f \delta_{f,a}^{va} \cdot Q F_{f,a}^{\rho_a^{va}} \right)^{\frac{1}{\rho_a^{va}}}$$

The elasticity of substitution  $\varepsilon_a^{va} = \frac{1}{\rho_a^{va} - 1}$  is negative.

The F.O.C. for factor demand are:

$$\frac{Q F_{f,a}}{QVA_a} = \varphi_{f,a}^{va} \left( \frac{P Q F_{f,a}}{PVA_a \cdot (1 - t v a_a)} \right)^{\varepsilon_a^{va}} \quad (3)$$

with  $\varphi_{f,a}^{va} = (\alpha_a^{va})^{-\rho_a^{va}} \cdot (\delta_{f,a}^{va})^{-1}$

*“marginal cost of factor f in activity a is equal to marginal revenue”*

### Intermediate input demand

$$QINT_{c,a} = i c a_{c,a} \cdot QINTA_a \quad (4)$$

### Commodity production and allocation

$$QXAC_{a,c} + \sum_h QHA_{a,c,h} = \theta_{a,c} \cdot QA_a \quad (5)$$

This specification allows that one activity produces multiple commodities (cattle -> milk, beef). In most cases however, each activities will produce only one commodity.

### Output aggregation

The representative firm maximize the profit from selling its aggregate output of commodity c from its various activities subject to an aggregate activity to commodity function with imperfect possibility of transformation (CET function):

$$\text{Max} \left\{ PX_c \cdot QX_c - \sum_a PXAC_{a,c} \cdot QXAC_{a,c} \right\} \text{ s.t. } QX_c = \alpha_c^{ac} \cdot \left( \sum_a \delta_{a,c}^{ac} \cdot QXAC_{a,c}^{\rho_c^{ac}} \right)^{\frac{1}{\rho_c^{ac}}}$$

The elasticity of transformation  $\varepsilon_c^{ac} = \frac{1}{\rho_c^{ac} - 1}$  is negative.

Alternatively, we could consider that (domestic and foreign) consumers minimize the cost of consumption of commodity c subject to the constraint of a CET function that represents the possibilities of transformation of the products from activities a into commodity c:

$$\text{Min} \left\{ \sum_a PXAC_{a,c} \cdot QXAC_{a,c} \right\} \text{ s.t. } QX_c = \alpha_c^{ac} \cdot \left( \sum_a \delta_{a,c}^{ac} \cdot QXAC_{a,c}^{\rho_c^{ac}} \right)^{\frac{1}{\rho_c^{ac}}}$$

In both cases, the F.O.C. giving the demand of commodity c addressed to activity a:

$$\frac{QXAC_{a,c}}{QX_c} = \varphi_{a,c}^{ac} \left( \frac{PXAC_{a,c}}{PX_c} \right)^{\varepsilon_c^{ac}} \quad (6)$$

With  $\varphi_{a,c}^{ac} = (\alpha_c^{ac})^{-\rho_c^{ac}} \cdot (\delta_{a,c}^{ac})^{-1}$

### Market output

$$PX_c \cdot QX_c = PDS_c \cdot QD_c + PE_c \cdot QE_c \quad (7)$$

Market output value is equal to domestic sales and export sales

### INTERNATIONAL TRADE

## Export and domestic supply

The representative firm maximizes its revenue from selling its aggregate output of commodity  $c$  on the domestic and external market subject to CET function between domestic and export sales:

$$\text{Max} \{ PDS_c \cdot QD_c + PE_c \cdot QE_c \} \text{ s.t. } QX_c = \alpha_c^t \cdot \left( \delta_c^t \cdot QE_c^{\rho_c^t} + (1 - \delta_c^t) \cdot QD_c^{\rho_c^t} \right)^{\frac{1}{\rho_c^t}}$$

This gives the allocation of marketed domestic output between domestic and export sales. Here the elasticity of transformation (  $\varepsilon_a^t = 1/(\rho_c^t - 1)$  ) between domestic and export sales is positive: the isoquant corresponding to the output transformation function is concave to the origin.

This formulation implicitly assumes that the external market is perfectly competitive: producer can sell all the quantity she wishes on the external market at the foreign price ( $p_{we_c}$ ). This is only realistic in the case of a small exporting country. An alternative would be to export are constrained by the foreign demand.

Combining the FOC  $\frac{QE_c}{QD_c} = \left( \frac{PE_c}{PDS_c} \cdot \frac{1 - \delta_c^t}{\delta_c^t} \right)^{\frac{1}{\rho_c^t - 1}}$  with the CES function gives the domestic and export supply:

$$\frac{QD_c}{QX_c} = \varphi_c^{ds} \left( \frac{PDS_c}{PX_c} \right)^{\varepsilon_c^t} \quad (8)$$

$$\text{With } \varphi_c^{ds} = (\alpha_c^t)^{-\rho_c^t} \cdot (1 - \delta_c^t)^{-1}$$

$$\frac{QE_c}{QX_c} = \varphi_c^e \left( \frac{PE_c}{PX_c} \right)^{\varepsilon_c^t} \quad (9)$$

$$\text{With } \varphi_c^e = (\alpha_c^t)^{-\rho_c^t} \cdot (\delta_c^t)^{-1}$$

Equivalently, we could have replace equation (8) and (9) by the FOC  $\frac{QE_c}{QD_c} = \left( \frac{PE_c}{PDS_c} \cdot \frac{1 - \delta_c^t}{\delta_c^t} \right)^{\frac{1}{\rho_c^t - 1}}$  and the production function

$QX_c = \alpha_c^t \cdot \left( \delta_c^t \cdot QE_c^{\rho_c^t} + (1 - \delta_c^t) \cdot QD_c^{\rho_c^t} \right)^{\frac{1}{\rho_c^t}}$ . The result would be exactly the same. The advantage of our specification is that we can impose a Leontief or Cobb-Douglas function with having the problem of division by zero.

## Import and domestic demand



We assume that domestic consumers minimize the cost of consumption of commodity  $c$  subject to the constraint of a CES function between domestic and imported goods:

$$\text{Min} [PDD_c \cdot QD_c + PM_c \cdot QM_c] \text{ s.t. } QQ_c = \alpha_c^q \cdot (\delta_c^q \cdot QM_c^{\rho_c^q} + (1 - \delta_c^q) \cdot QD_c^{\rho_c^q})^{\frac{1}{\rho_c^q}}$$

The elasticity of substitution,  $\varepsilon_c^q = 1/(\rho_c^q - 1)$  is negative.

Combining the FOC  $\frac{QM_c}{QD_c} = \left( \frac{PM_c}{PDD_c} \cdot \frac{1 - \delta_c^q}{\delta_c^q} \right)^{\frac{1}{\rho_c^q - 1}}$  with the CES function gives the domestic and import demand:

$$\frac{QD_c}{QQ_c} = \varphi_c^{dd} \left( \frac{PDD_c}{PQ_c \cdot (1 - tq_c)} \right)^{\varepsilon_c^q} \quad (10)$$

$$\text{With } \varphi_c^{dd} = (\alpha_c^q)^{-\rho_c^q} \cdot (1 - \delta_c^q)^{-1}$$

$$\frac{QM_c}{QQ_c} = \varphi_c^m \left( \frac{PM_c}{PQ_c \cdot (1 - tq_c)} \right)^{\varepsilon_c^q} \quad (11)$$

$$\text{With } \varphi_c^m = (\alpha_c^q)^{-\rho_c^q} \cdot (\delta_c^q)^{-1}$$

## INSTITUTIONS

### Factor income

$$YF_f = \sum_a PQF_{f,a} QF_{f,a} \quad (12)$$

$$YF_f = \sum_a [PQF_{f,a} QF_{f,a} (1 - v_{f,a})] \text{ for } f = \text{capital}$$

### Factor income distribution among institutions (private, government, ROW)

$$YIF_{i,f} = \text{shif}_{i,f} \cdot [(1 - tf_f) \cdot YF_f] \quad (13)$$

### Income of institutions (private, government, ROW)

$$YI_i = \sum_f YIF_{i,f} + \sum_{i'} TRII_{i,i'} \quad (14)$$

$i$  and  $i'$  refers to all institutions. If  $i = \text{ROW}$ , this is the income of the rest of the world from domestic institutions (private & government) since  $TRII_{i,i} = 0$ .

### Infra-institutional transfers

$$\begin{aligned} TRII_{i,i'} &= shii_{i,i'} \cdot (1 - MPS_{i'}) \cdot (1 - tins_{i'}) \cdot YI_{i'} \\ TRII_{i,gov} &= transfr_{i,gov} \cdot PC \\ TRII_{i,row} &= transfr_{i,row} \cdot EXR \end{aligned} \quad (15)$$

$i'$  refers to domestic private institutions (exclude government) whereas  $i$  refers to all institutions. Also this would not change the property of the model, it is generally assumed that there is not auto-transfer ( $TRII_{i,i} = 0$ ).

### Household consumption expenditures

$$\begin{aligned} h \in H \\ i \in \text{INS} \end{aligned} \quad EH_h = \left( 1 - \sum_i shii_{i,h} \right) \cdot (1 - MPS_h) \cdot (1 - tins_h) \cdot YI_h \quad (16)$$

### Household consumption spending on marketed commodities

$$PQ_c QH_{c,h} = PQ_c \cdot \gamma_{c,h}^m + \beta_{c,h}^m \left( EH_h - \sum_{c'} PQ_{c'} \cdot \gamma_{c',h}^m - \sum_a \sum_{c'} PXAC_{ac'} \cdot \gamma_{a,c',h}^h \right) \quad (17)$$

### Household consumption spending on home commodities

$$PXAC_{a,c} QHA_{a,c,h} = PXAC_{a,c} \cdot \gamma_{a,c,h}^h + \beta_{a,c,h}^h \left( EH_h - \sum_{c'} PQ_{c'} \cdot \gamma_{c',h}^m - \sum_{a'} \sum_{c'} P_{a'} \right) \quad (18)$$

### Government revenue

$$YG = \sum_{i \in \text{INSDNG}} tins_i \cdot YI_i + \sum_f tf_f \cdot YF_f + \sum_a tv_a \cdot PVA_a \cdot QVA_a + \sum_a ta_a \cdot PA_a \cdot Q_a \quad (19)$$

### Government expenditure

$$\begin{aligned}
PQ_c \cdot QG_c + \dot{i} \sum_{i \in INS} TRII_{i,gov} \\
EG = \sum_c \dot{i}
\end{aligned}
\tag{20}$$

## SYSTEM CONSTRAINTS

**Demand = supply in factor market**

$$\sum_a QF_{f,a} = QFS_f
\tag{21}$$

**Demand = supply in commodity markets**

$$\begin{aligned}
QINT_{c,a} + \dot{i} \sum_h QH_{c,h} + QG_c + QINV_c + qdst_c \\
QQ_c = \sum_a \dot{i}
\end{aligned}
\tag{22}$$

**External balance: foreign savings (current account balance in domestic currency)**

$$\begin{aligned}
SAV_{row} = \sum_c pwm_c \cdot EXR \cdot QM_c + YI_{row} - \sum_c pwe_c \cdot EXR \cdot QE_c - \sum_{i \in INS} TRII_{i,row} \\
SAV_{row} = SAVFC_{row} \cdot EXR
\end{aligned}
\tag{23}$$

**Domestic savings: government balance and households savings**

$$\begin{aligned}
SAV_{gov} = YG - EG \\
SAV_h = MPS_h \cdot (1 - tins_h) \cdot YI_h
\end{aligned}
\tag{24}$$

**Internal balance: savings = investment**

$$\tag{25}$$

$$\sum_i SAV_i = \sum_c PQ_c \cdot QINV_c + \sum_c PQ_c \cdot qdst_c - v_{f,a} \cdot PQF_{f,a} \cdot QF_{f,a} + WALRAS$$

$i$  refers to all institutions. WALRAS is a variable that should be zero in equilibrium.

### **Marginal propensity to save (domestic private institution)**

We assume that the marginal propensity to save for domestic private institution  $i$  adjust in order to guaranty the equilibrium between saving and investment.

$$MPS_i = mps_i \cdot MPS \quad (26)$$

## **PRICES**

### **Value added price**

$$PVA_a \cdot (1 - tva_a) \cdot QVA_a = \sum_f PQF_{f,a} \cdot QF_{f,a} \quad (27)$$

### **Production factor price**

The price of the production factor  $f$  is assumed common across activity which implies the perfect mobility of production factor across activities.

$$PQF_{f,a} = PQF_f \quad (28)$$

### **Consumer price index**

$$PC = \sum_c PQ_c \cdot cwts_c \quad (29)$$

With  $cwts_c = \frac{\sum_h PQ_c QH_{c,h}}{\sum_c \sum_h PQ_c QH_{c,h}}$

The consumer price index is used as *numéraire*:  $PC=1$

### **Import price**

$$PM_c = pwm_c \cdot (1 + tm_c) \cdot EXR \quad (30)$$

### **Export price**

$$PE_c = pwe_c \cdot (1 - te_c) \cdot EXR \quad (31)$$

### **Demand price**

Assuming the absence of trade and service margin, in this basic version of the model, the demand price for commodity produced and sold domestically equals the supply price for commodity produced and sold domestically.

$$PDD_c = PDS_c \quad (32)$$

### **Commodity price**

$$PQ_c \cdot (1 - tq_c) \cdot QQ_c = PDD_c \cdot QD_c + PM_c \cdot QM_c \quad (33)$$

Absorption: “Total domestic spending on a commodity at domestic demander prices”

### **Activity price**

$$PA_a \cdot (1 - ta_a) \cdot QA_a = PVA_a \cdot QVA_a + PINTA_a \cdot QINTA_a \quad (34)$$

Revenue and costs (*Zero profit*) “Total revenue of activity a (net of tax) is exhausted by payments to factors and intermediate input”

### Activity price

$$PA_a = \sum_c PXAC_{a,c} \cdot \theta_{a,c} \quad (35)$$

### Aggregate intermediate input price

$$PINTA_a = \sum_c PQ_c \cdot ica_{c,a} \quad (36)$$

### Market output price

$$PX_c \cdot QX_c = \sum_a PXAC_{a,c} \cdot QXAC_{a,c} \quad (37)$$

Alternatively we could have write the  $QX_c = \alpha_c^{ac} \cdot \left( \sum_a \delta_{a,c}^{ac} \cdot QXAC_{a,c} \rho_c^{ac} \right)^{\frac{1}{\rho_c}}$  instead of (37).

### CLOSURE RULES

The existence of a solution imposes the adoption of the so-called closing rules. In particular satisfying of the external and internal balances imposes certain constraint on the choice of certain endogenous variables. We used the default closing rule:



External balance: Foreign savings (current account deficit) is exogenously fixed; exchange rate (EXR) is flexible (endogenous)

Internal balance: Investment are exogenously fixed; nongovernment savings rates are endogenous

In both cases, we could have assumed the contrary. Without the slack variable WALRAS and the choice of a *numéraire*, the set of equation (1)-(37) constitute a system of  $n$  equations and  $n$  unknown. Yet the model cannot be solved because the internal balance (25) is nothing else but a reformulation of the demand-supply equilibrium Equations (22). Equation (25) could be dropped or alternatively the extra slack variable WALRAS can be added. But then model is under-identified (the number of endogenous variables is higher than the one of equations). This is solved by choosing one price as the *numéraire*. Here we chose the consumer price index ( $PC$ ). A common alternative in the literature is to take the exchange rate ( $EXR$ ). The inclusion of the variable WALRAS provides a good way to check if the calibration and the specification of the model is correct. If the model is consistently calibrated and formulated, WALRAS is always equal to zero (even after a shock).

In the DCGM, the dynamic is exogenous:

- $\gamma_{ch}^m$  (income-independent demand) grows at the same rate as population growth
- $QFS_{labor}$  grows at the same rate of population growth (or growth of population between 15 and 65)
- Growth in total factor productivity (TFP) in  $\alpha^{va}_a$
- Government spending  $QG_c$  and transfers  $trnsfr_{i,gov}$  grow exogenous
- In the basic version investment  $QINV_c$  grows also exogenously

If these exogenous variables are constant, all the endogenous variables are constant too.

## IDENTITIES

Identities are endogenous variables that do not affect the other endogenous variables and can thus be calculated outside the model. When they are important economic indicator such the GDP, it is however useful to calculate them within the model for facilitating the interpretation of the result. We defined the following identities:

### Gross Domestic Product (GDP)

For accountancy reason, the GDP can be calculated in two ways: (1) as the sum of the domestic and external demand minus import and intermediary consumption; (2) as the sum of the value added of the activities and of the tax that are not included in the value added. In value (nominal terms), the outcome of this 2 formula is strictly equivalent.

$$\begin{aligned}
 GDP_{VAL} &= \sum_c \left[ PQ_c \cdot QQ_c + pwe_c \cdot EXR \cdot QE_c - pwm_c \cdot EXR \cdot QM_c + \sum_a \sum_h PX \right. \\
 GDP_{VAL} &= \sum_a \left[ PA_a \cdot QA_a - PINTA_a \cdot QINTA_a \right] + \sum_c \left[ tm_c \cdot pwm_c \cdot QM_c \cdot EXR + \right. \quad (38)
 \end{aligned}$$

The real GDP (or GDP in volume) is calculated keeping assuming constant price (here the base year prices are equal to one). The real GDP according to the 2 definitions are thus not fully equivalent:

$$\begin{aligned}
 GDP &= \sum_c \left[ QQ_c + pwe_c \cdot QE_c - pwm_c \cdot QM_c + \sum_a \sum_h QHA_{a,c,h} \right] - \sum_a QINTA_a \\
 &= \left[ QA_a - QINTA_a \right] + \sum_c \left[ tm_c \cdot pwm_c \cdot QM_c + te_c \cdot pwe_c \cdot QE_c + tq_c \cdot QQ_c \right] \quad (39) \\
 GDP &= \sum_a \dot{i}
 \end{aligned}$$

We can deduce the price of the GDP from the nominal and real GDP:

$$PGDP = GDP_{VAL} / GDP \quad (40)$$

### Self-sufficiency indicator

indicator of food security is the ratio of domestic self-sufficiency in food, as the ratio between (apparent) domestic consumption (X+M-E) and domestic production (X).

$$SS_c = QX_c / (QX_c - QE_c + QM_c) \quad (41)$$

## 9. Annex 9 : Installation and configuration of CC Impact tool

This annex reports the installation and the configuration of the Impact CC component of the Dissemination portal of the MOSAICC project.

### 9.1. User requirements

#### Types of users

- decision makers => Overview
- students => Analysis

#### Types of information:

- Maps, Charts and Tables
- Time aggregations: Year, Climate Seasons, Crop Season
- Models and Scenarios

### 9.2. Technology overview

The technology used to implement the TCP Web Portal is **open-source**, that guarantees high availability of support and update.

#### LAMP environment

LAMP is an archetypal model of web service solution stacks, named as an acronym of the names of its original four components:

- the Linux operating system,
- the Apache HTTP Server,
- the MySQL relational database management system (RDBMS), and
- the PHP programming language.

The LAMP components are largely interchangeable and not limited to the original selection. As a solution stack, LAMP is suitable for building dynamic web sites and web applications

#### DBMS

## **CMS**

A **CMS**, i.e. a **Content Management System**, is a computer application that allows publishing, editing and modifying content, organizing, deleting as well as maintenance from a central interface.

There are many open-source CMS, but the most widely used are the following:

- WordPress
- Joomla!
- Drupal

They are all written in PHP, that is a server-side scripting language designed for web development but also used as a general-purpose programming language: its development began in 1994 and the last stable version is 5.6.9 released on May 14, 2015.

FAO adopted the open-source CMS called **TYPO3**, that is, along with Drupal, Joomla! and WordPress, among the most popular content management systems worldwide. However it is more widespread in Europe than in other regions: the biggest market share can be found in German-speaking countries. TYPO3 is an enterprise CMS which is used for corporate and company websites with different access levels, users, membership access etc.

Considering the features of the CMS, their popularity and the type of web site to be developed, Drupal appears to be the most suitable. Also the local communication consultant, Ms. Laila Triki, considered this solution adequate for this application.

## **WordPress**

WordPress began as an innovative, easy-to-use blogging platform. With an ever-increasing repertoire of themes, plugins and widgets, this CMS is widely used for other website formats also.

Best use cases:

Ideal for fairly simple web sites, such as everyday blogging and news sites; and anyone looking for an easy-to-manage site. Add-ons make it easy to expand the functionality of the site.

#### Features:

Ease of use is a key benefit for experts and novices alike. It's powerful enough for web developers or designers to efficiently build sites for clients; then, with minimal instruction, clients can take over the site management. Known for an extensive selection of themes. Very user-friendly with great support and tutorials, making it great for non-technical users to quickly deploy fairly simple sites.

#### Ease of use:

Technical experience is not necessary; it's intuitive and easy to get a simple site set up quickly. It's easy to paste text from a Microsoft Word document into a Wordpress site, but not into Joomla and Drupal sites.

### **Joomla!**

Joomla offers middle ground between the developer-oriented, extensive capabilities of Drupal and user-friendly but more complex site development options than Wordpress offers.

#### Best use cases:

Joomla allows you to build a site with more content and structure flexibility than Wordpress offers, but still with fairly easy, intuitive usage. Supports E-commerce, social networking and more.

#### Features:

Designed to perform as a community platform, with strong social networking features.

#### Ease of use:

Less complex than Drupal, more complex than Wordpress. Relatively uncomplicated installation and setup. With a relatively small investment of effort into understanding Joomla's structure and terminology, you have the ability to create fairly complex sites.

### **Drupal**

Drupal is a powerful, developer-friendly tool for building complex sites. Like most powerful tools, it requires some expertise and experience to operate.

Best use cases:

For complex, advanced and versatile sites; for sites that require complex data organization; for community platform sites with multiple users; for online stores

Features:

Known for its powerful taxonomy and ability to tag, categorize and organize complex content.

Ease of use:

Drupal requires the most technical expertise of the three CMSs. However, it also is capable of producing the most advanced sites. With each release, it is becoming easier to use. If you're unable to commit to learning the software or can't hire someone who knows it, it may not be the best choice.

### **Mapserver**

MapServer is an open source development environment for building spatially enabled internet applications.

### **Tools and Libraries**

GDAL...

#### **9.3. Server installation**

- Operating system
- Web server
- DBMS
- Tools



## 9.4. CMS installation

The installation of any CMS requires to go through the following steps:

- CMS download
- DBMS configuration:
  - creation of the DB user for the CMS
  - creation of the DB for the CMS
- CMS unpack
- CMS initialization

### **CMS download**

The last stable release of Drupal is the version 7.37, available since May 7, 2015 (16 days ago).

The Drupal core is a compressed tar ball of 3.09 MB.

URL: <http://ftp.drupal.org/files/projects/drupal-7.37.tar.gz>

### **DBMS configuration**

A good practice for CMS installation is to create a specific DB user for the web site and then a dedicated DB, owned by the just create user.

#### **DBMS user:**

- name = 'cci\_tcp\_morocco'
- password = 'Rabat.2015'
- permissions: NOCREATEDB NOCREATEROLE NOREPLICATION

```
create user cci_tcp_morocco login encrypted password 'Rabat.2015' NOCREATEDB  
NOCREATEROLE NOREPLICATION;
```

#### **New DB:**

- name = 'cci\_tcp\_morocco'
- owner = 'cci\_tcp\_morocco'
- extension:
  - postgis
  - postgis\_topology

### **CMS unpack**

A good practice for CMS installation is to unpack the tar ball in the web area, usually “/var/www”, and then rename the folder with the web site name:

- tar -xzf drupal-7.37.tar.gz
- mv drupal-7.37 cci\_tcp\_morocco

Then we can perform a proper configuration of the web server. If the web server is Apache 2.4.x, we can configure it as follows:

```
alias /cci_tcp_morocco "/var/www/cci_tcp_morocco"  
<Directory "/var/www/cci_tcp_morocco">  
    Options Indexes FollowSymLinks MultiViews  
    AllowOverride None  
    Require all granted  
</Directory>
```

Then the web server needs to restart to enable the new configuration.

### **CMS initialization**

Once the DBMS is configured and the CMS unpacked the installation of Drupal can start: it is sufficient to open the browser and point to the new virtual directory “[http://localhost/cci\\_tcp\\_morocco](http://localhost/cci_tcp_morocco)”.

## Select an installation profile



### ► Choose profile

Choose language

Verify requirements

Set up database

Install profile

Configure site

Finished

Standard

Install with commonly used features pre-configured.

Minimal

Start with only a few modules enabled.

Save and continue

## Choose language



✓ Choose profile

### ► Choose language

Verify requirements

Set up database

Install profile

Configure site


Finished

English (built-in)

[Learn how to install Drupal in other languages](#)

Save and continue

## Requirements problem



- ✓ Choose profile
- ✓ Choose language
- ▶ **Verify requirements**
- Set up database
- Install profile
- Configure site
- Finished

Web server	Apache/2.4.12 (Linux/SUSE)
PHP	5.6.6
PHP register globals	Disabled
PHP extensions	Enabled
Database support	Enabled
PHP memory limit	256M
<b>✘ File system</b>	
The directory <code>sites/default/files</code> does not exist. An automated attempt to create this directory failed, possibly due to a permissions problem. To proceed with the installation, either create the directory and modify its permissions manually or ensure that the installer has the permissions to create it automatically. For more information, see <a href="#">INSTALL.txt</a> or the <a href="#">online handbook</a> .	
Unicode library	PHP Mbstring Extension
<b>✘ Settings file</b>	
The settings file does not exist. The Drupal installer requires that you create a settings file as part of the installation process. Copy the <code>/sites/default/default.settings.php</code> file to <code>/sites/default/settings.php</code> . More details about installing Drupal are available in <a href="#">INSTALL.txt</a> .	

Check the error messages and [proceed with the installation](#).


It is necessary to perform a little configuration by command line:

```
cd /var/www/cci_tcp_morocco
cd sites/all
chown -R wwwrun:root default
```

Further reading: <https://www.drupal.org/documentation/install/settings-file>.

Then, reloading the page, the set-up proceeds properly.

## Database configuration



- ✓ Choose profile
- ✓ Choose language
- ✓ Verify requirements
- ▶ **Set up database**
  - Install profile
  - Configure site
  - Finished

**Database type \***

MySQL, MariaDB, or equivalent  
 SQLite  
 PostgreSQL

The type of database your Drupal data will be stored in.

**Database name \***

cci\_tcp\_morocco

The name of the database your Drupal data will be stored in. It must exist on your server before Drupal can be installed.

**Database username \***

cci\_tcp\_morocco

**Database password**

●●●●●●●●

▶ **ADVANCED OPTIONS**

Save and continue

It is a good practice to configure the advanced options as well:

▶ **ADVANCED OPTIONS**

These options are only necessary for some sites. If you're not sure what you should enter here, leave the default settings or check with your hosting provider.

**Database host \***

127.0.0.1

If your database is located on a different server, change this.

**Database port**

If your database server is listening to a non-standard port, enter its number.

**Table prefix**

drupal\_

If more than one application will be sharing this database, enter a table prefix such as *drupal\_* for your Drupal site here.

Clicking on “Save and continue” the installation starts:



Once the installation is completed, it is necessary to provide some information about the new web site:



## Configure site



- ✓ Choose profile
- ✓ Choose language
- ✓ Verify requirements
- ✓ Set up database
- ✓ Install profile
- ▶ **Configure site**

Finished

### SITE INFORMATION

#### Site name \*

TCP Morocco - Climate Change Impact Portal

#### Site e-mail address \*

mauro.evangelisti@fao.org

Automated e-mails, such as registration information, will be sent from this address. Use an address ending in your site's domain to help prevent these e-mails from being flagged as spam.

### SITE MAINTENANCE ACCOUNT

#### Username \*

admin

Spaces are allowed; punctuation is not allowed except for periods, hyphens, and underscores.

#### E-mail address \*

mauro.evangelisti@fao.org

#### Password \*

••••••••

Password strength:

**Strong**

### SERVER SETTINGS

#### Default country

Morocco

Select the default country for the site.

#### Default time zone

Africa/Casablanca: Saturday, May 23, 2015 - 09:51 +0100

By default, dates in this site will be displayed in the chosen time zone.

### UPDATE NOTIFICATIONS

Check for updates automatically


Receive e-mail notifications

The system will notify you when updates and important security releases are available for installed components. Anonymous information about your site is sent to [Drupal.org](http://Drupal.org).

Save and continue

An finally the installation is done!

### Drupal installation complete

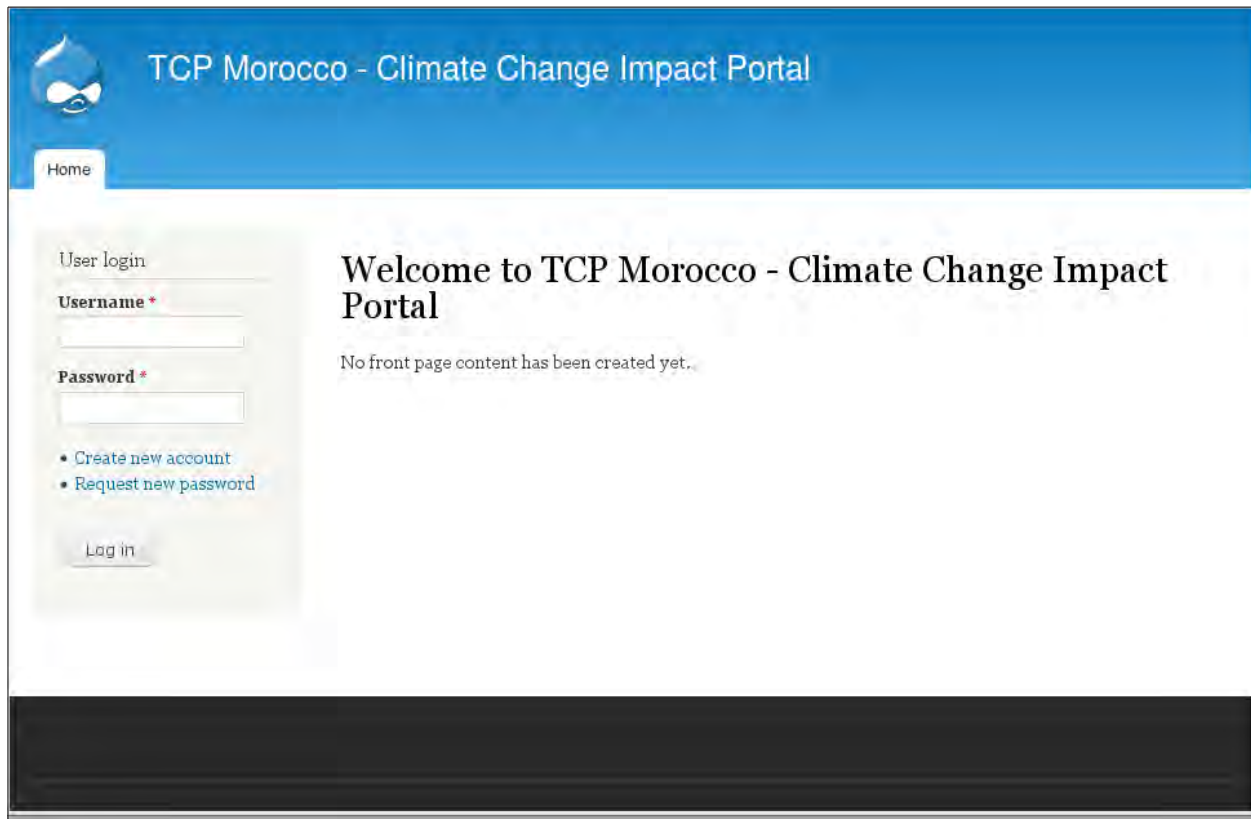


Congratulations, you installed Drupal!

[Visit your new site.](#)

- ✓ Choose profile
- ✓ Choose language
- ✓ Verify requirements
- ✓ Set up database
- ✓ Install profile
- ✓ Configure site
- ✓ Finished

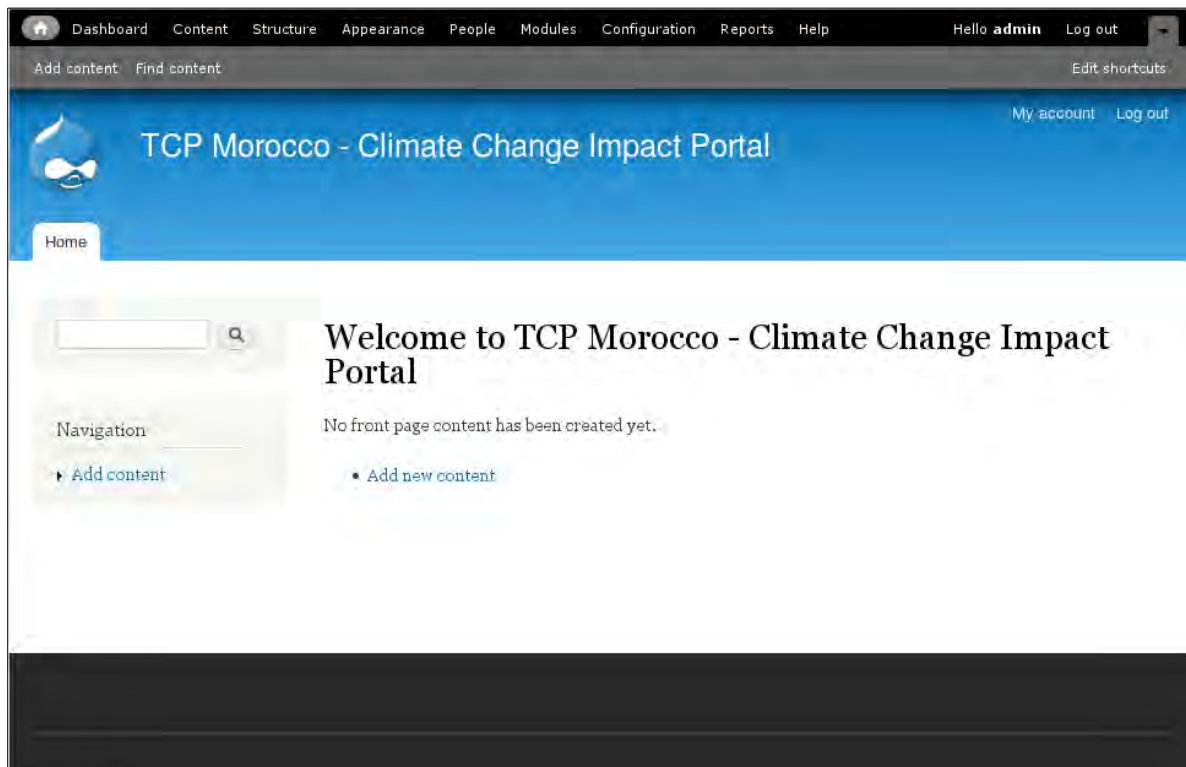
The new web site has the default aspect of any Drupal site:



At this point Drupal 7 is installed and ready to be configured.

## 9.5. CMS configuration

The configuration of the CMS requires the administrative user (admin) logs in. A black top bar appears and gives access to the Drupal configuration functions.



## Language support

The TCP Web Portal must be available in some languages, i.e. English, French and Arabic.

In order to enable multiple languages in Drupal some operations are required:

- Open the “*translation server*”: <https://localize.drupal.org/download>
- Download the required languages, i.e. French and Arabic
- Copy the downloaded files (`drupal-7.37.fr.po` and `drupal-7.37.ar.po`) in “`profiles/standard/translations`”
- Go to Modules, and then ensure that the **Locale** module is enabled; it requires the other module called “**Content translation**”
- Go to Configuration, and then click Languages
- Click **Add languages**, select French, and then click Save configuration.
- Click **Add languages**, select Arabic, and then click Save configuration.

ENABLED	NAME	VERSION	DESCRIPTION	OPERATIONS
<input checked="" type="checkbox"/>	<b>Image</b>	7.37	Provides image manipulation tools. Requires: File (enabled), Field (enabled), Field SQL storage (enabled) Required by: Drupal (Field type(s) in use - see Field list)	<a href="#">Help</a> <a href="#">Permissions</a> <a href="#">Configure</a>
<input checked="" type="checkbox"/>	<b>List</b>	7.37	Defines list field types. Use with Options to create selection lists. Requires: Field (enabled), Field SQL storage (enabled), Options (enabled)	<a href="#">Help</a>
<input checked="" type="checkbox"/>	<b>Locale</b>	7.37	Adds language handling functionality and enables the translation of the user interface to languages other than English. Required by: Content translation (disabled)	
<input checked="" type="checkbox"/>	<b>Menu</b>	7.37	Allows administrators to customize the site navigation menu.	<a href="#">Help</a> <a href="#">Permissions</a> <a href="#">Configure</a>
<input checked="" type="checkbox"/>	<b>Node</b>	7.37	Allows content to be submitted to the site and displayed on pages. Required by: Drupal	<a href="#">Help</a> <a href="#">Permissions</a> <a href="#">Configure</a>
<input checked="" type="checkbox"/>	<b>Number</b>	7.37	Defines numeric field types. Requires: Field (enabled), Field SQL storage (enabled)	<a href="#">Help</a>

Home » Administration » Configuration » Regional and language » Languages

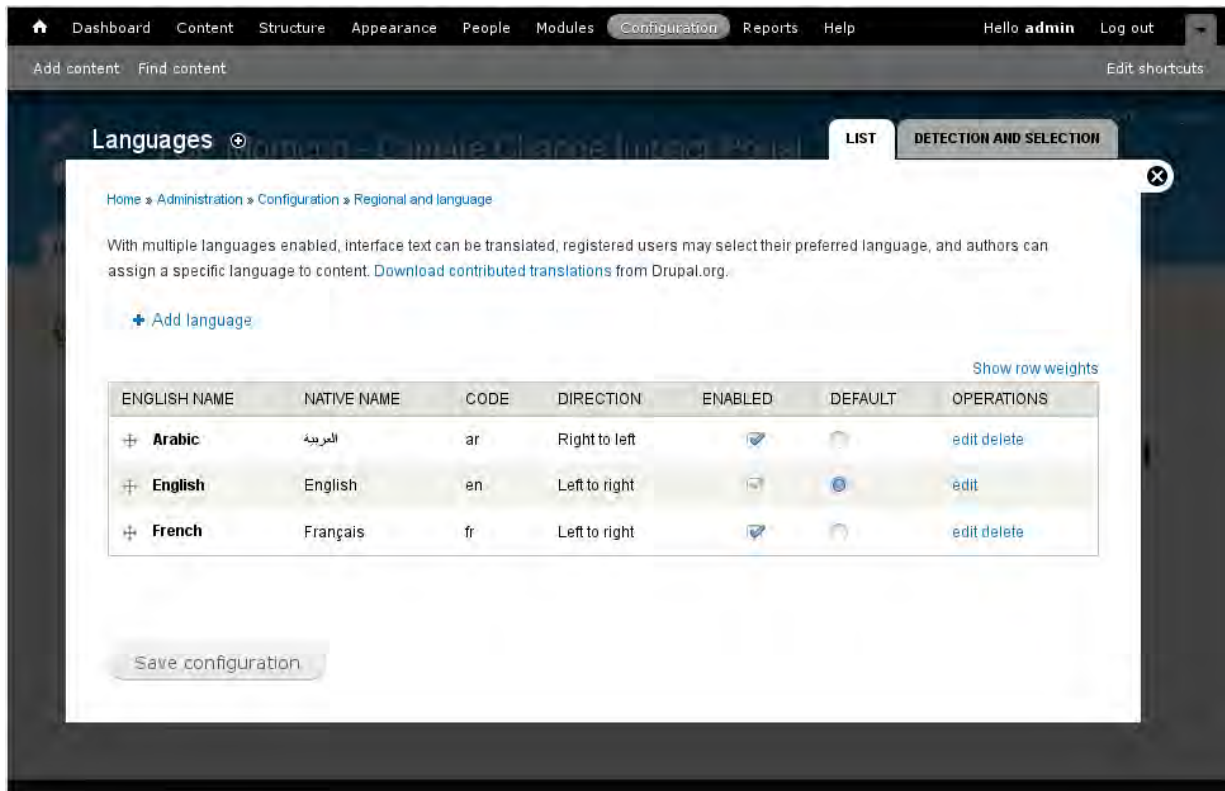
Add a language to be supported by your site. If your desired language is not available in the *Language name* drop-down, click *Custom language* and provide a language code and other details manually. When providing a language code manually, be sure to enter a standardized language code, since this code may be used by browsers to determine an appropriate display language.

**PREDEFINED LANGUAGE**

**Language name**

Use the *Custom language* section below if your desired language does not appear in this list.

**CUSTOM LANGUAGE**



Several modules exist that extend the multilingual capabilities of Drupal, but at least the following must be installed:

- Internationalization (i18n) module, which provides several important features not currently built into Drupal core
- Localization update, which automatically fetches updated translations of strings hardcoded in all the core and contributed modules installed on the web site

### Variable

Variable module provides a registry for meta-data about Drupal variables and some extended Variable API and administration interface. This module is required from the Internationalization (i18n) module.



Download the module from “<https://www.drupal.org/project/variable>” and then run the following commands:

```
cd /var/www/cci_tcp_morocco
cd sites/all/modules
tar -xzf /download/variable-7.x-2.5.tar.gz
```

Once it is installed, the sub-modules must be enable from the Drupal configuration bar, *Modules* section.

### **Internationalization (i18n) module**

Drupal 7.x has some built-in multilingual support to provide a localized user interface and translatable content. However, not everything is yet localizable/translatable. This package tries to fill the gaps that still exist. A few of the important features which the Internationalization package provides are:

- A proper multilingual menu system
- Multilingual blocks
- Multilingual taxonomy

Download the module from “<https://www.drupal.org/project/i18n>” and then run the following commands:

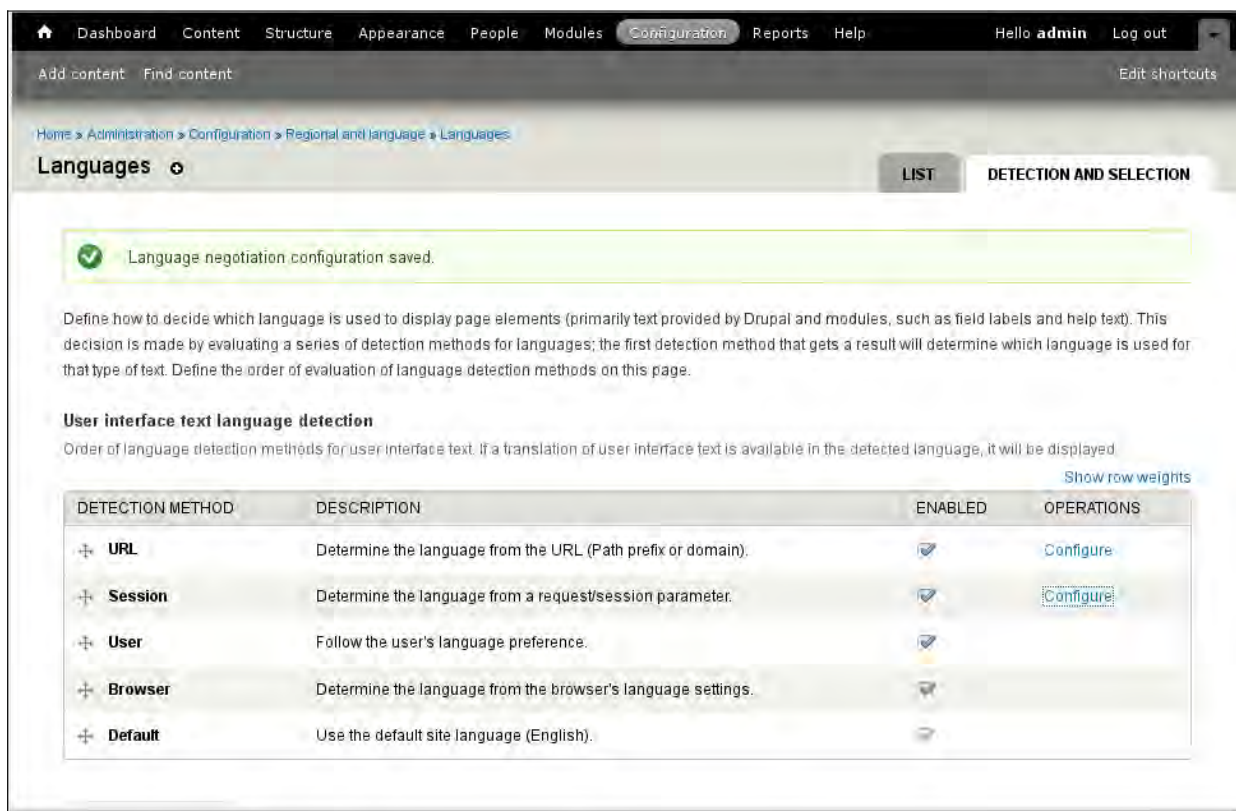
```
cd /var/www/cci_tcp_morocco
cd sites/all/modules
tar -xzf /download/i18n-7.x-1.13.tar.gz
```

Once the module i18n is installed, the Drupal modules must be be enabled from the Drupal configuration bar, *Modules* section, “*Multilingual – Internationalization*” package:

- Block languages
- Internationalization
- Menu translation

- Multilingual content
- Multilingual select
- String translation
- Synchronize translations
- Taxonomy translation
- Translation redirect (SEO)
- Translation sets

Once the Internationalization module is installed, Drupal needs to know what languages has to use when the user accesses the site. This kind of configuration can be done from the Drupal configuration bar, *Regional* section, *Language* item, *Detect and selection* tab, as shown in the next picture:



### Localization update (l10n\_update) module

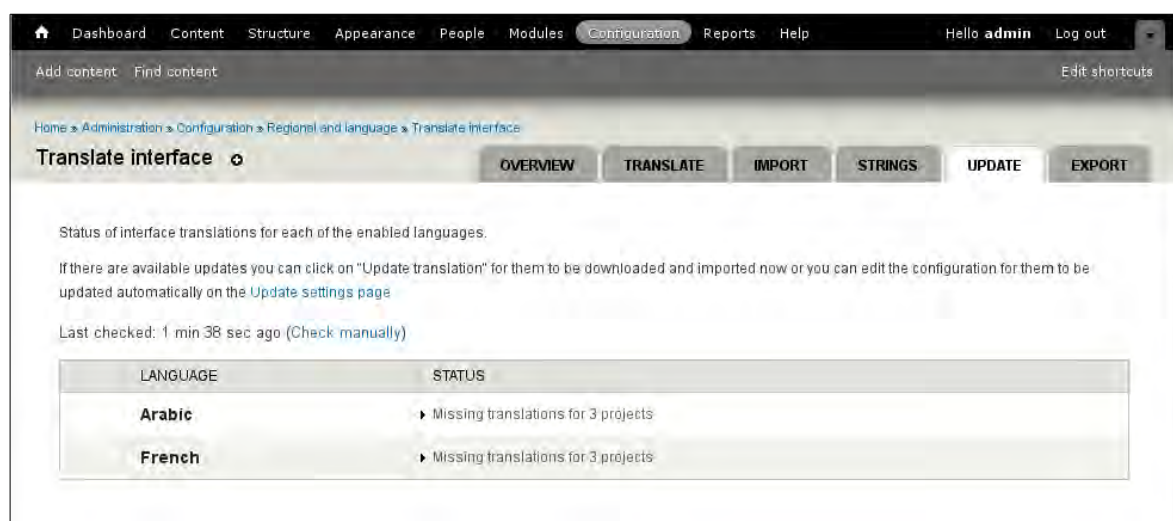
This module is based on concepts very similar to Drupal core's update module. Modules and themes with their corresponding drupal.org projects are identified and translations are downloaded for the appropriate versions.

Download the module from “[https://www.drupal.org/project/l10n\\_update](https://www.drupal.org/project/l10n_update)” and then run the following commands:

```
cd /var/www/cci_tcp_morocco
cd sites/all/modules
tar -xzf /download/l10n_update-7.x-2.0.tar.gz
```

Once it is installed, the module “**Localization update**” must be enable from the Drupal configuration bar, *Modules* section. Then the following operations are required in the configuration bar:

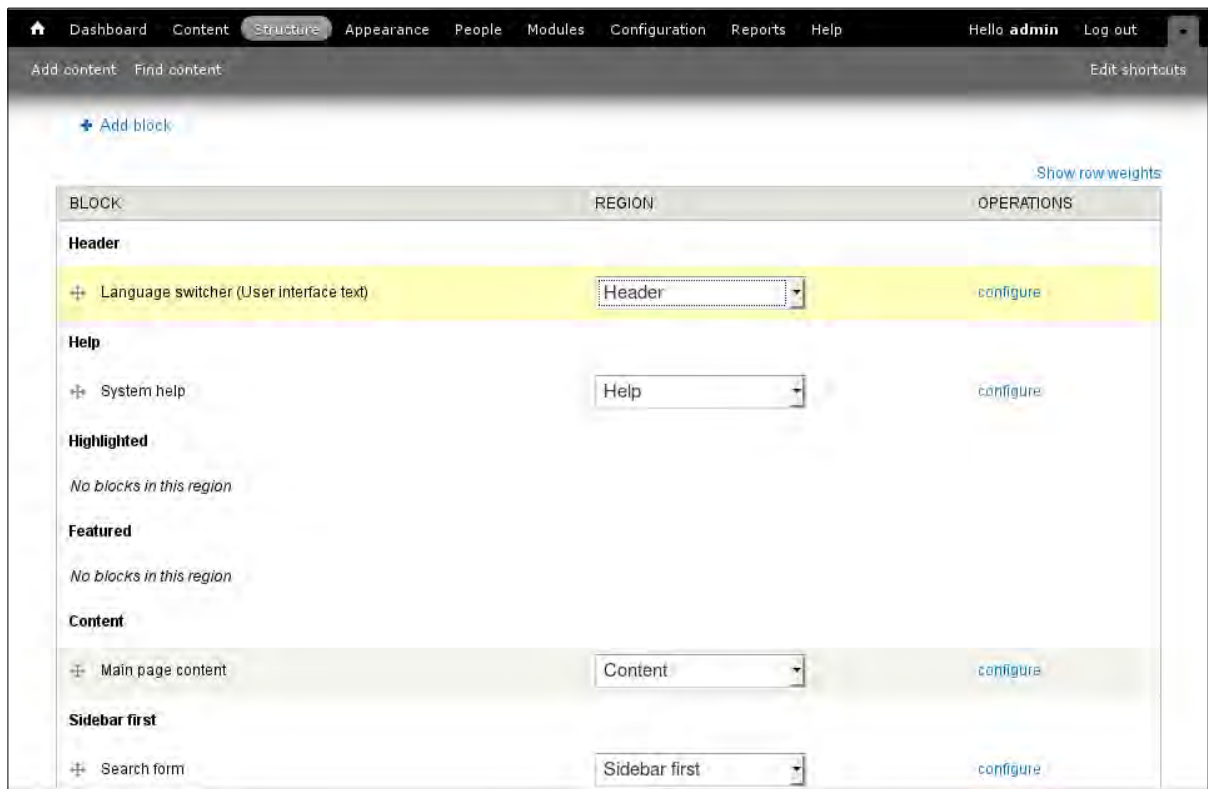
- Regional
  - Translate interface
    - Update tab



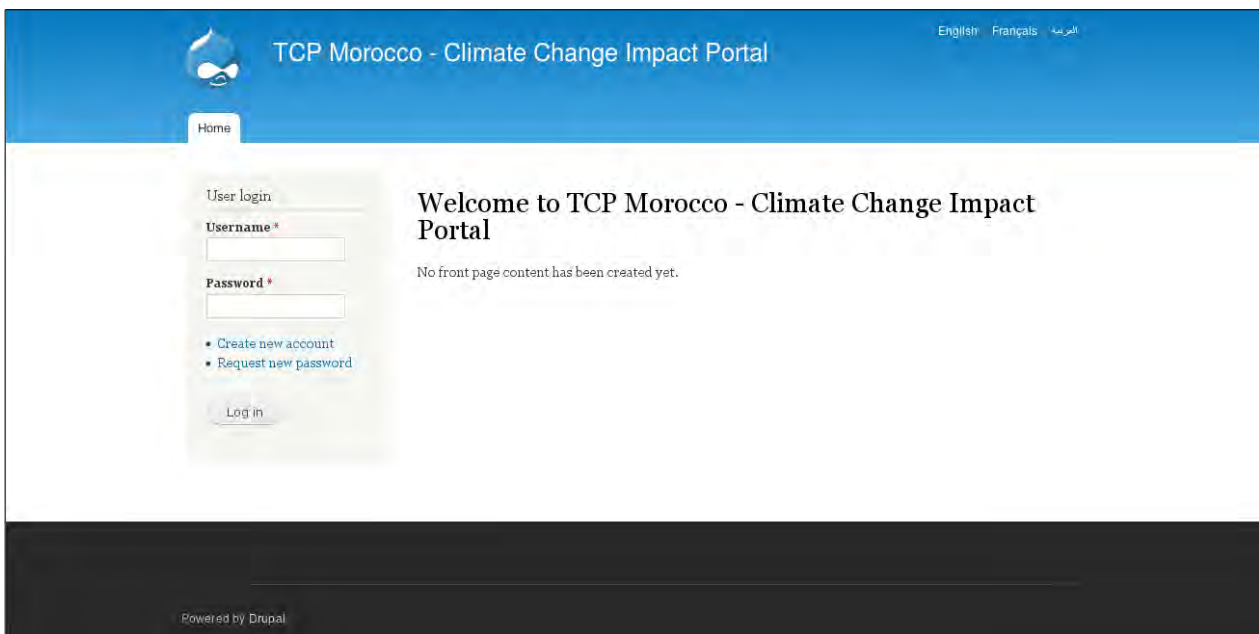
Further reading: <https://www.drupal.org/node/1412862>.

## Enable language switcher

In order to enable the Language switcher it is necessary to enable the related block from the Drupal configuration bar, *Structure* section, *Blocks* item.

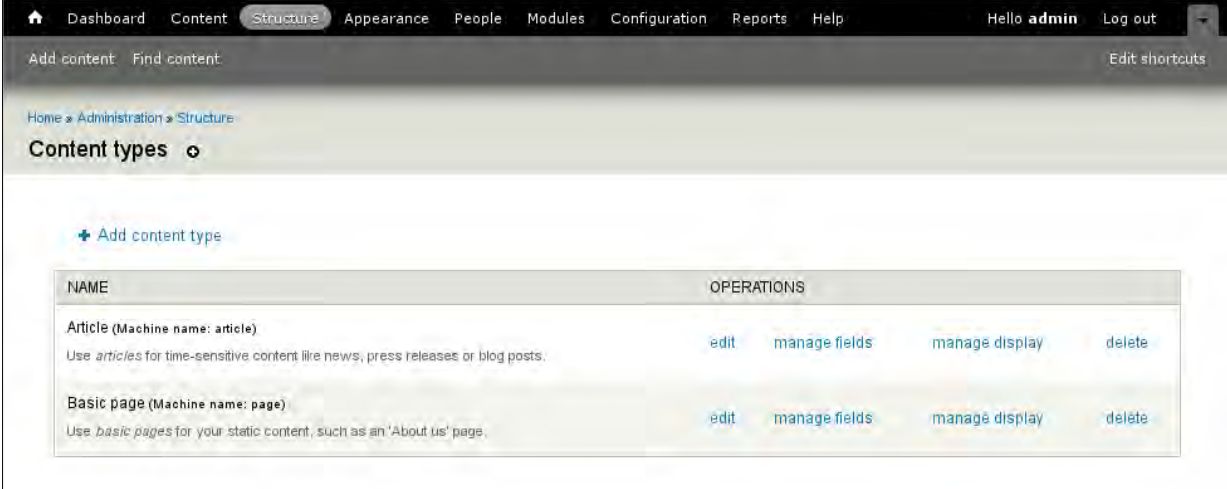


Once the language switcher is enabled, the list of enabled languages is displayed on the top right of the page. The order of the languages can be changed in Drupal configuration bar, *Configuration* section, *Regional* panel, *Language* item. The home will then displays as follows:



## Translatable content

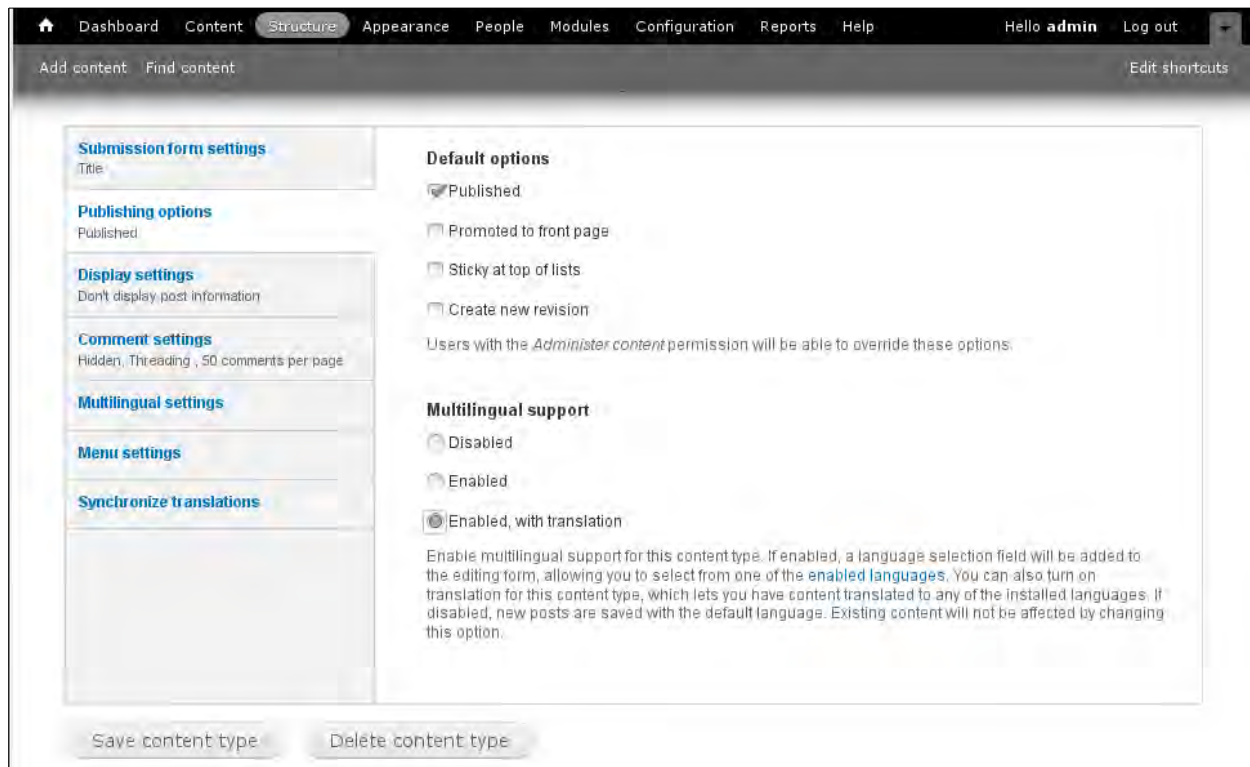
Drupal needs to know the types of content that are available in more languages. It must be configured from the Drupal configuration bar, *Structure* section, Content types item:



The screenshot shows the Drupal administration interface. The top navigation bar includes links for Dashboard, Content, Structure (selected), Appearance, People, Modules, Configuration, Reports, and Help. The user is logged in as 'admin'. The main content area is titled 'Content types' and features a '+ Add content type' link. Below this is a table with two rows of content types:

NAME	OPERATIONS
<b>Article</b> (Machine name: article) <small>Use <i>articles</i> for time-sensitive content like news, press releases or blog posts.</small>	<a href="#">edit</a> <a href="#">manage fields</a> <a href="#">manage display</a> <a href="#">delete</a>
<b>Basic page</b> (Machine name: page) <small>Use <i>basic pages</i> for your static content, such as an 'About us' page.</small>	<a href="#">edit</a> <a href="#">manage fields</a> <a href="#">manage display</a> <a href="#">delete</a>

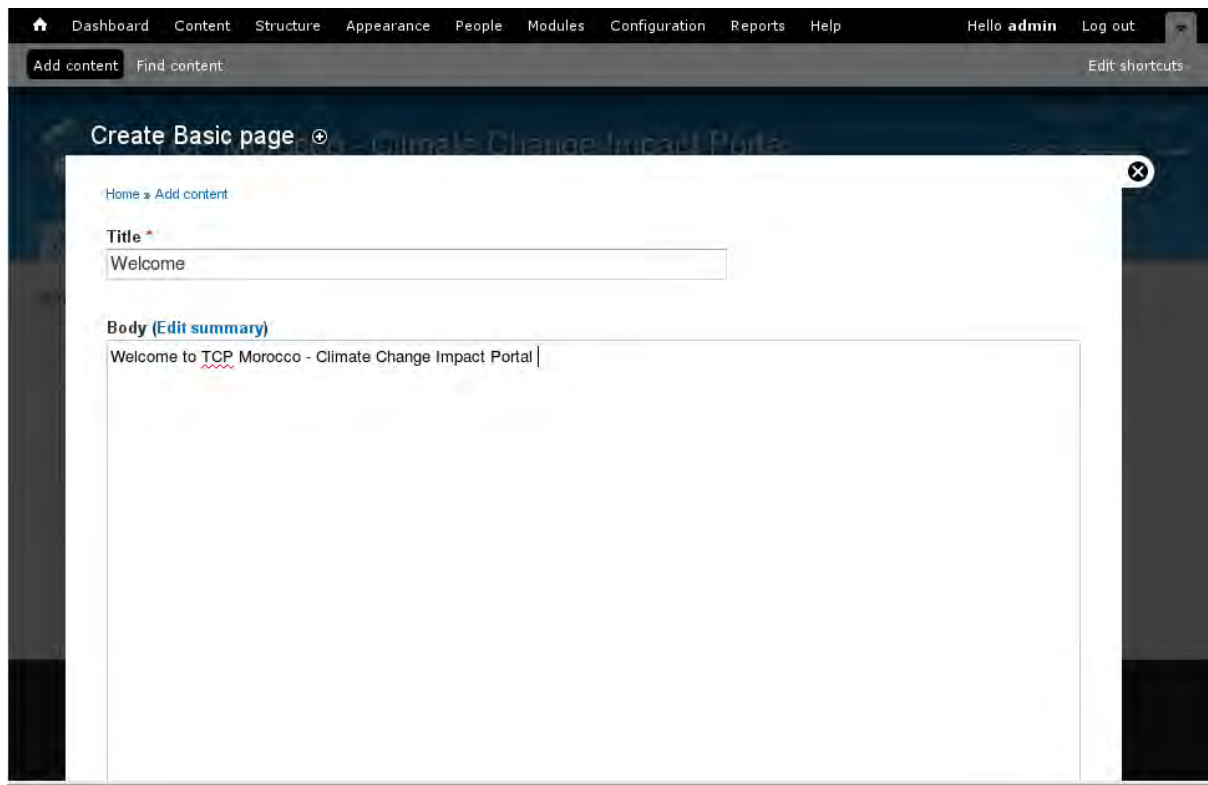
Each content type that must be available in more languages requires to be configured, by clicking on the **“edit”** link. Once the property page opens, scroll down and click on *“Publishing options”* and then select the option **“Enabled, with translation”** in the *“Multilingual support”* block as shown in the picture below:



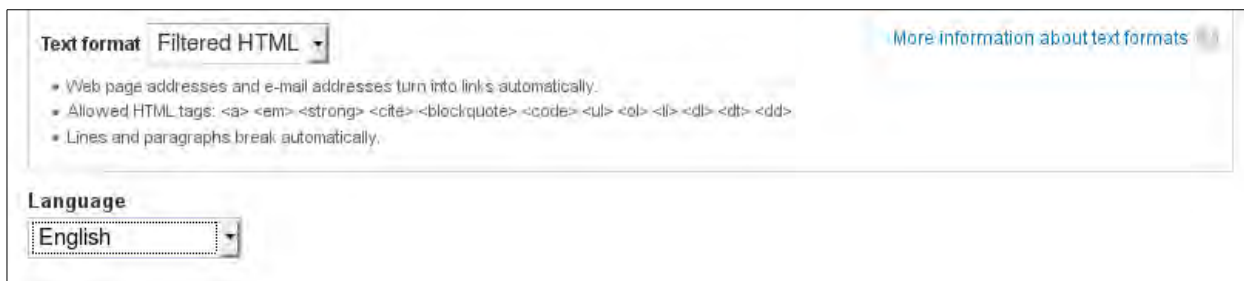
## Welcome page in more languages

The welcome page can be created by adding a new “basic page”:





Notice how there's a language selection dropdown: the English language is selected.



Once the page is saved the *“Translate”* tab appears next to the *“Edit”*, that allows to translate the page in the other languages:

Dashboard Content Structure Appearance People Modules Configuration Reports Help Hello admin Log out

Add content Find content Edit shortcuts

### Translations of *Welcome*

VIEW EDIT TRANSLATE

Home » Welcome

Translations of a piece of content are managed with translation sets. Each translation set has one source post and any number of translations in any of the [enabled languages](#). All translations are tracked to be up to date or outdated based on whether the source post was modified significantly.

LANGUAGE	TITLE	STATUS	OPERATIONS
English (source)	Welcome	Published	<a href="#">edit</a>
French	n/a	Not translated	<a href="#">add translation</a>
Arabic	n/a	Not translated	<a href="#">add translation</a>

**SELECT TRANSLATIONS FOR WELCOME**

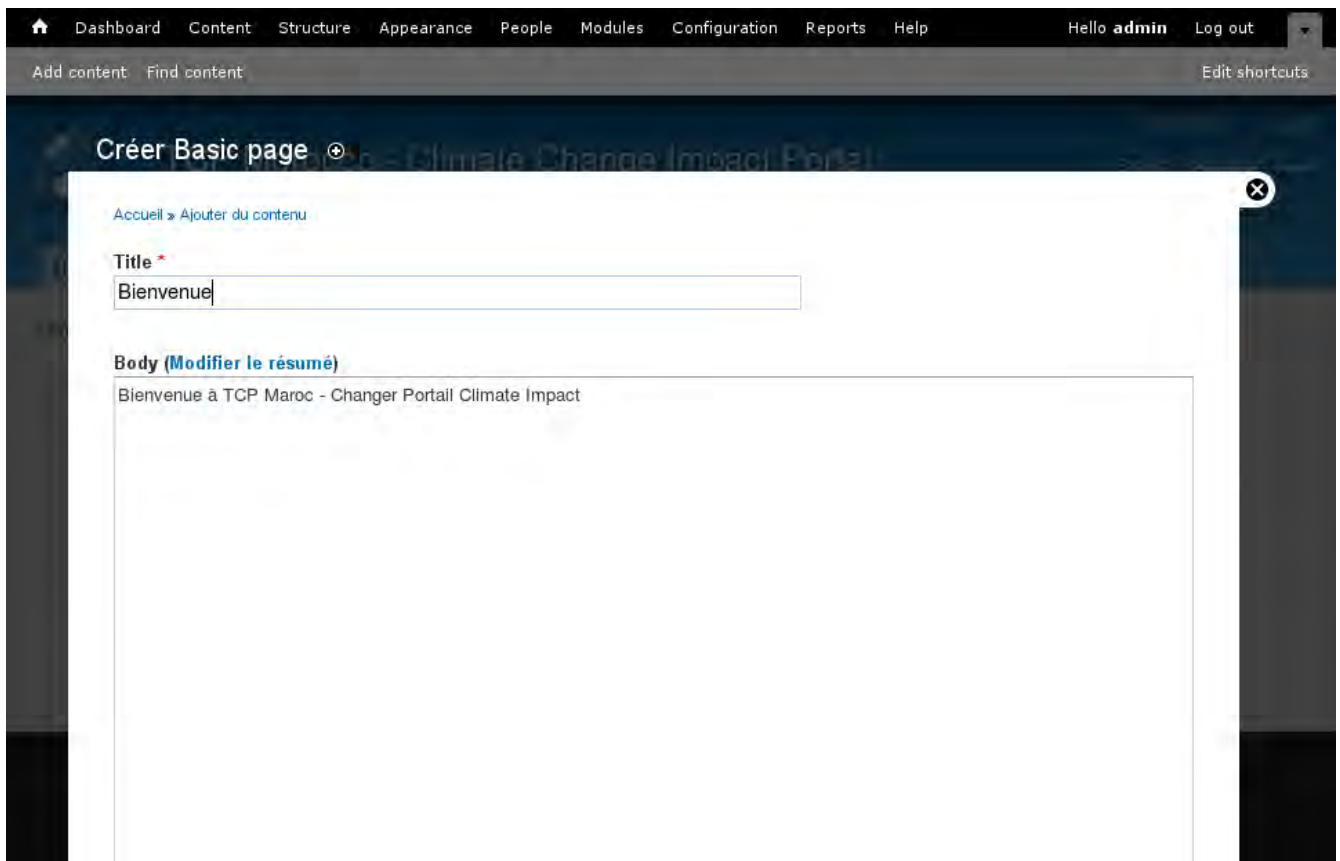
Alternatively, you can select existing nodes as translations of this one or remove nodes from this translation set. Only nodes that have the right language and don't belong to other translation set will be available here.

French

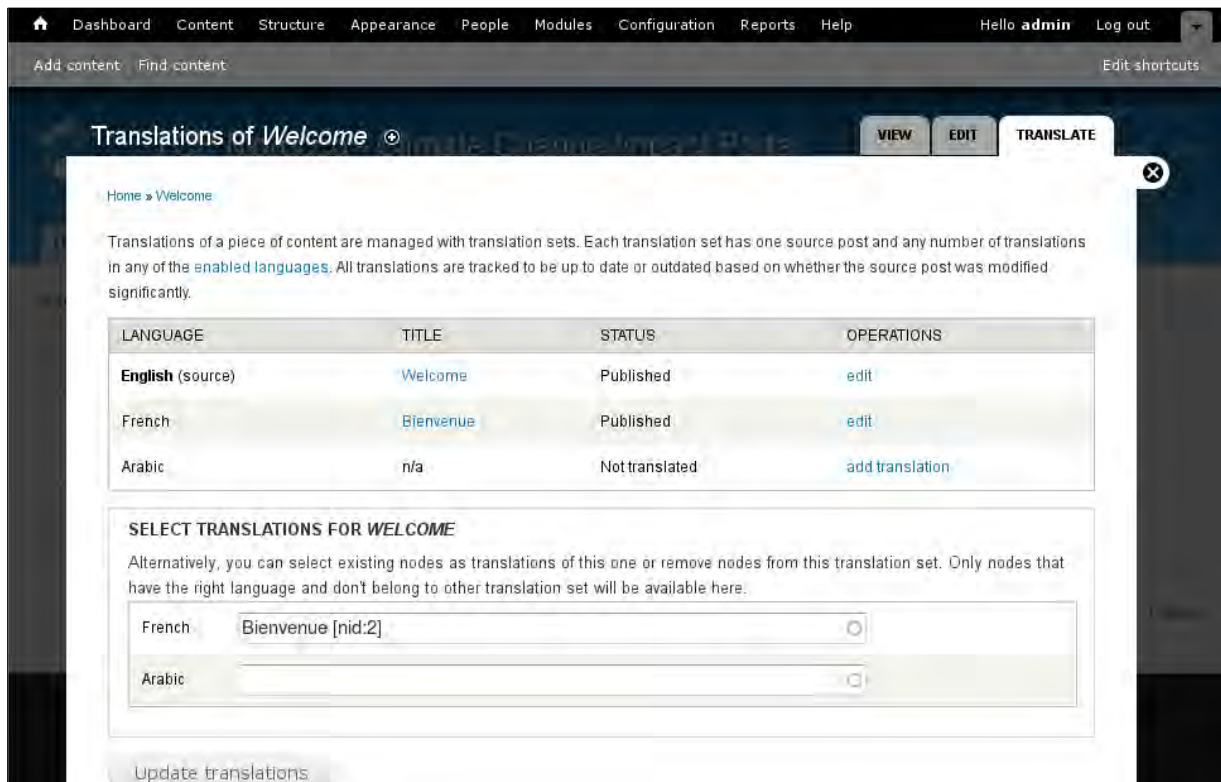
Arabic

Update translations

Choose a language to translate to and click on [add translation](#) to the right, under the *Operations* column. Translate your content and click *Save*.



Clicking again on the “*Translate*” tab shows the translation status:



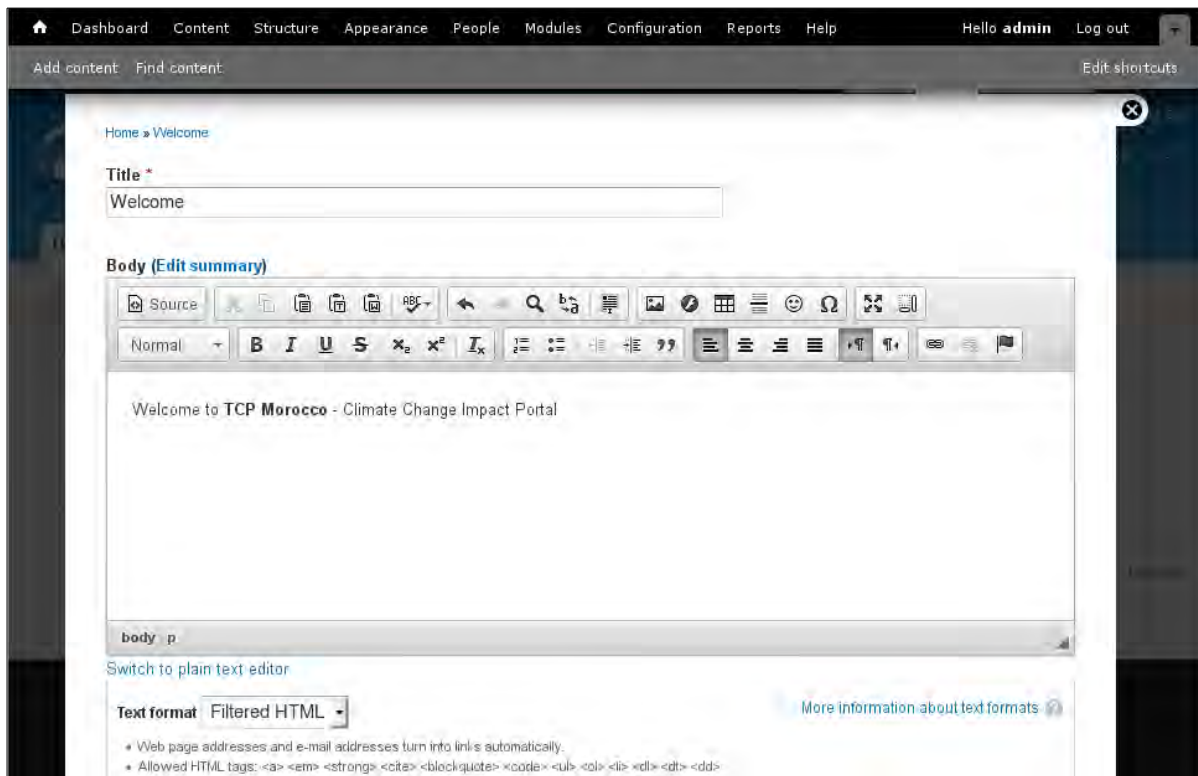
## WYSIWYG editor

Drupal doesn't provide any default WYSIWYG editor: one of the most common configuration is the modules CKEditor and IMCE.

### CKEditor

This module will allow Drupal to replace textarea fields with the CKEditor - a visual HTML editor, usually called a WYSIWYG editor. This HTML text editor brings many of the powerful WYSIWYG editing functions of known desktop editors like Word to the web. It's very fast and doesn't require any kind of installation on the client computer.

Once installed, the page editing changes as follows:



## IMCE

IMCE is an image/file uploader and browser that supports personal directories and quota.

In order to use IMCE with CKEditor it is necessary to configure it in: *“Configuration » Content Authoring » CKEditor”* for each defined profile (Filtered HTML and Full HTML). Once the profile editor opens, scroll down to “File browser settings” and select IMCE in all the “File browser type” combo-boxes. Moreover, it is better to change the root of the media like *“%b%f/media/”* that corresponds to *“/cci\_tcp\_morocco/sites/default/files/media/”*.

## 9.6. CMS customization

The customization of any CMS mainly consists of the graphic theme and the ad-hoc modules.

The Web Portal for the TCP has just three ad-hoc modules:

- Result Overview
- Result Analysis
- Documents

Drupal uses the following strings for the configured languages:

- en = English
- fr = French
- ar = Arabic

The custom modules belong to the same packages, i.e. "TCP MOROCCO - CLIMATE CHANGE IMPACT PORTAL":

ENABLED	NAME	VERSION	DESCRIPTION	OPERATIONS
<input type="checkbox"/>	<b>TCP Morocco - Climate Change Impact Portal - Result Analysis</b>		TCP Morocco - Climate Change Impact Portal - Result Analysis	
<input type="checkbox"/>	<b>TCP Morocco - Climate Change Impact Portal - Result Overview</b>		TCP Morocco - Climate Change Impact Portal - Result Overview	

External LibrariesThe TCP Web Portal uses some libraries, that require other libraries:

- GeoExt
  - OpenLayers 2.x
  - ExtJS-3
- GeoExt2
  - OpenLayers 3.x
  - ExtJS-4

All the libraries are installed in `"/var/www/cci_tcp_morocco/sites/all/libraries"`.

### GeoExt

Installation commands:

```
cd /var/www/cci_tcp_morocco/sites/all/libraries
wget https://github.com/downloads/geoext/geoext/GeoExt-1.1.zip
```



```
unzip GeoExt-1.1.zip
```

## **OpenLayers 2.x**

Installation commands:

```
cd /var/www/cci_tcp_morocco/sites/all/libraries
wget http://github.com/openlayers/openlayers/releases/download/release-2.13.1/OpenLayers-2.13.1.tar.gz
tar -xzf OpenLayers-2.13.1.tar.gz
```

## **ExtJS 3.x**

Installation commands:

```
cd /var/www/cci_tcp_morocco/sites/all/libraries
svn checkout http://extjs-public.googlecode.com/svn/extjs-3.x/include extjs-3
```

## **GeoExt2**

Installation commands:

```
cd /var/www/cci_tcp_morocco/sites/all/libraries
wget https://github.com/geoext/geoext2/archive/v2.0.3.tar.gz
tar -xzf v2.0.3.tar.gz
mv geoext2-2.0.3 GeoExt2-2.0.3
```

## **OpenLayers 3.x**

Installation commands:

```
cd /var/www/cci_tcp_morocco/sites/all/libraries
wget https://github.com/openlayers/ol3/releases/download/v3.5.0/v3.5.0.zip
unzip v3.5.0.zip
mv v3.5.0 OpenLayers-3.5.0
```

## **ExtJS 4.x**

## Installation commands:

```
cd /var/www/cci_tcp_morocco/sites/all/libraries
svn checkout http://extjs-public.googlecode.com/svn/extjs-4.x/include extjs-4
```

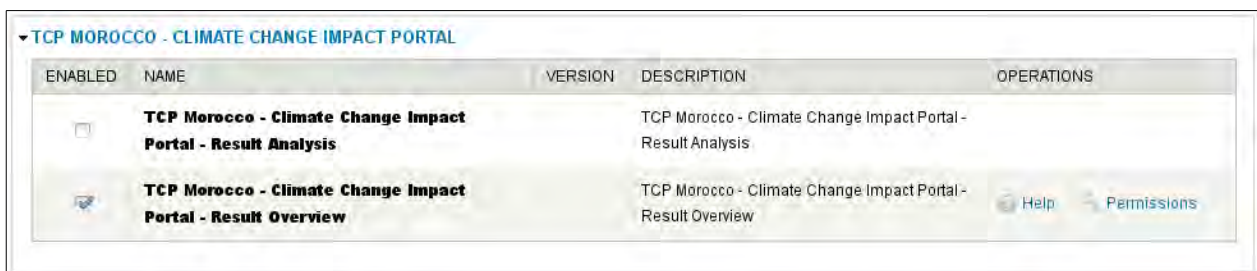
### 9.7. Result Overview Module

This modules has two components:

- a Drupal block that allows the user to perform some basic selections
- a Drupal module content that displays the page content

It is necessary to install and enable the module before attempting to enable the block.

Click on the “Modules” item in the configuration dashboard, scroll down to the package “TCP MOROCCO – CLIMATE CHANGE IMPACT PORTAL” and enable the module “**TCP Morocco - Climate Change Impact Portal - Result Overview**”:



ENABLED	NAME	VERSION	DESCRIPTION	OPERATIONS
<input type="checkbox"/>	<b>TCP Morocco - Climate Change Impact Portal - Result Analysis</b>		TCP Morocco - Climate Change Impact Portal - Result Analysis	
<input checked="" type="checkbox"/>	<b>TCP Morocco - Climate Change Impact Portal - Result Overview</b>		TCP Morocco - Climate Change Impact Portal - Result Overview	<a href="#">Help</a> <a href="#">Permissions</a>

Click on the “**Save configuration**” button to store the information. When the page reloads, scroll down to the package “TCP MOROCCO – CLIMATE CHANGE IMPACT PORTAL” and click on the “Permissions” link next to the just installed module; then scroll down the new page to the item “Access content for the ...” and check the boxes as in the picture below:

PERMISSION	ANONYMOUS USER	AUTHENTICATED USER	ADMINISTRATOR
Administer actions	<input type="checkbox"/>	<input type="checkbox"/>	<input type="checkbox"/>
Use the administration pages and help	<input type="checkbox"/>	<input type="checkbox"/>	<input type="checkbox"/>
Use the site in maintenance mode	<input type="checkbox"/>	<input type="checkbox"/>	<input type="checkbox"/>
View the administration theme	<input type="checkbox"/>	<input type="checkbox"/>	<input type="checkbox"/>
View site reports	<input type="checkbox"/>	<input type="checkbox"/>	<input type="checkbox"/>
<small>Warning: Give to trusted roles only; this permission has security implications.</small>			
Block IP addresses	<input type="checkbox"/>	<input type="checkbox"/>	<input type="checkbox"/>
<b>TCP Morocco - Climate Change Impact Portal - Result Overview</b>			
Access content for the TCP Morocco - Climate Change Impact Portal - Result Overview module	<input type="checkbox"/>	<input checked="" type="checkbox"/>	<input type="checkbox"/>
<b>Taxonomy</b>			
Administer vocabularies and terms	<input type="checkbox"/>	<input type="checkbox"/>	<input type="checkbox"/>
Edit terms in Tags	<input type="checkbox"/>	<input type="checkbox"/>	<input type="checkbox"/>
Delete terms from Tags	<input type="checkbox"/>	<input type="checkbox"/>	<input type="checkbox"/>
<b>Toolbar</b>			
Use the administration toolbar	<input type="checkbox"/>	<input type="checkbox"/>	<input type="checkbox"/>

Then click on the **“Save permissions”** button at the end of the page.

In order to enable the module it is necessary to enable the related block from the Drupal configuration bar, *Structure* section, *Blocks* item.

The module is listed in the **“Disabled”** group as *“TCP Morocco - Climate Change Impact Portal - Result Overview”*: it must be activated by selecting the group where it must work, i.e. **“Content”**, and that configuration must be saved using the *“Save blocks”* button at the end of the page. When the page reloads the block will be listed in the *“Content”* block: it must be dragged on the top of that list, before *“Main page content”* as displayed below:

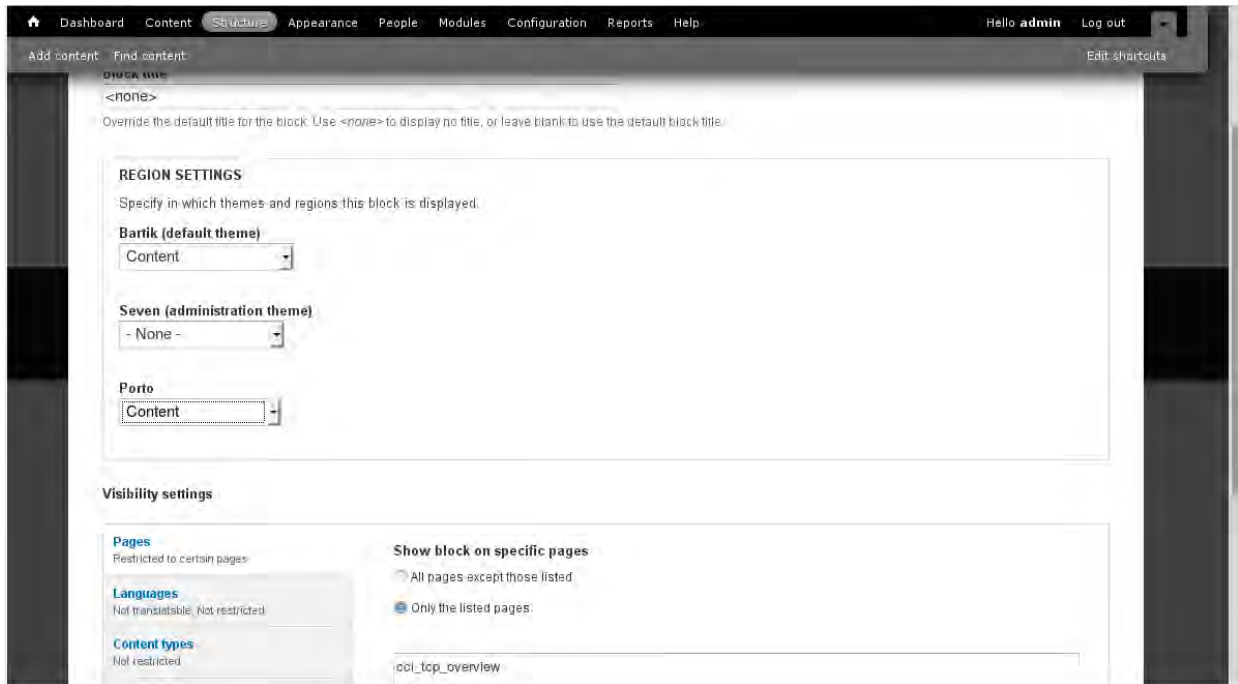
Content		
<input type="checkbox"/> TCP Morocco - Climate Change Impact Portal - Result Overview	Content	<a href="#">configure</a>
<input type="checkbox"/> Main page content	Content	<a href="#">configure</a>

Then it must be configured as follows:

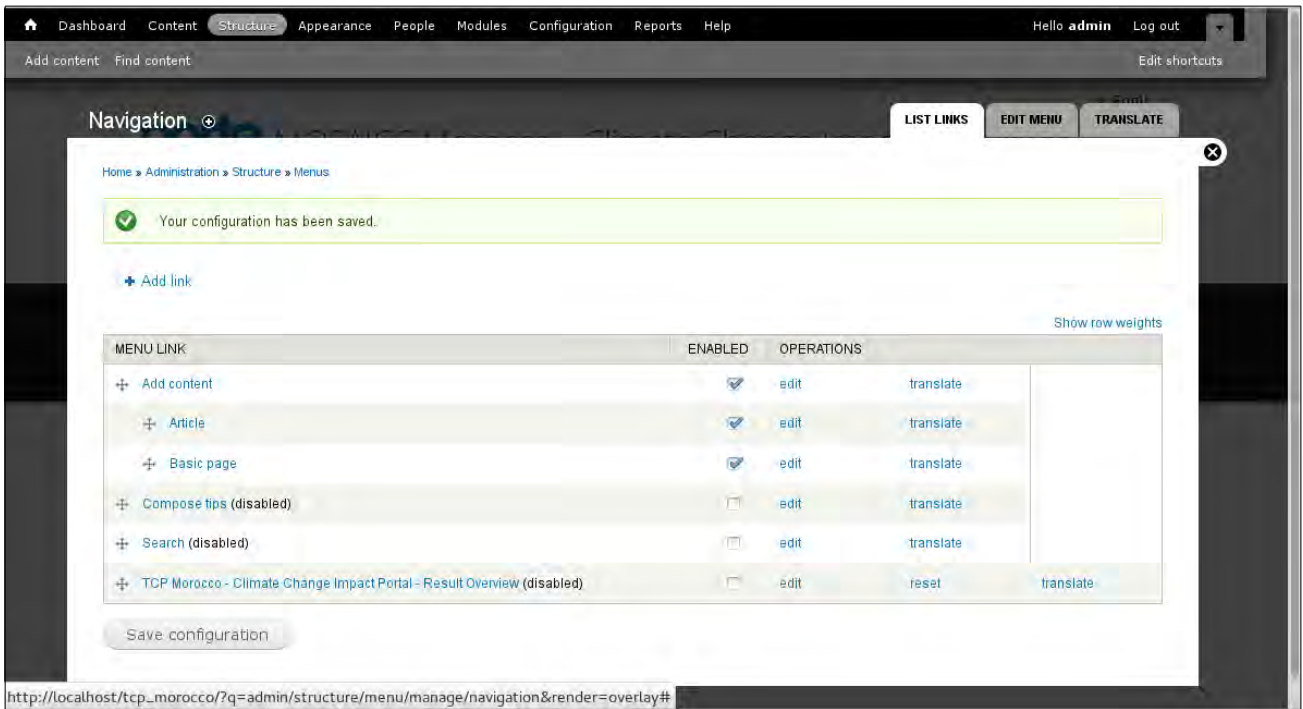
- Block Title = *“<none>”*
- Visibility settings:
  - Pages:
    - Show block on specific pages:

- Only the listed pages: “cci\_tcp\_overview”

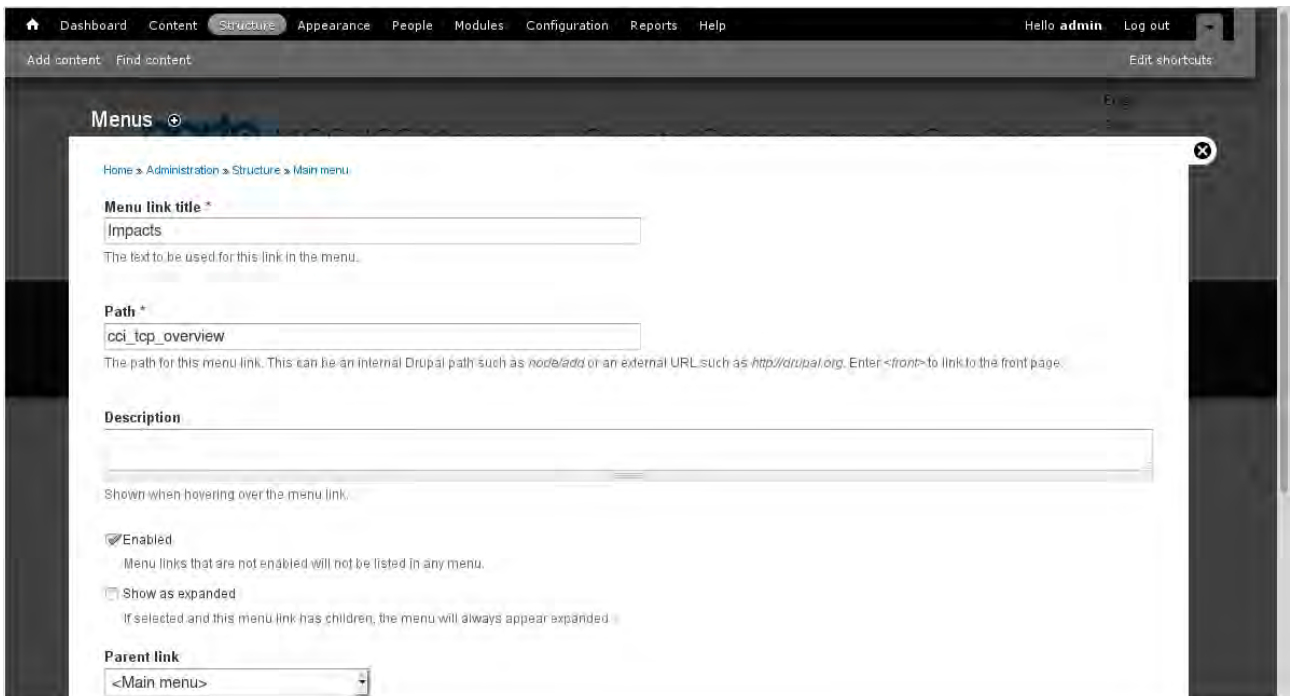
The picture below shows the configuration interface:



The last part of the configuration is linked to the menu: by default a link to a new module appears in the “Navigation menu”. If we prefer to link the module from the “Main menu” we need to change the default set-up. First of all, we have to disable the link in the “Navigation menu” by clicking on the “*Structure*” item on the dashboard; then we have to select the “*Menus*” item and finally click the link “*list links*” next to “Navigation”. Click on the check box to disable the menu item linked to the module as in the picture below:

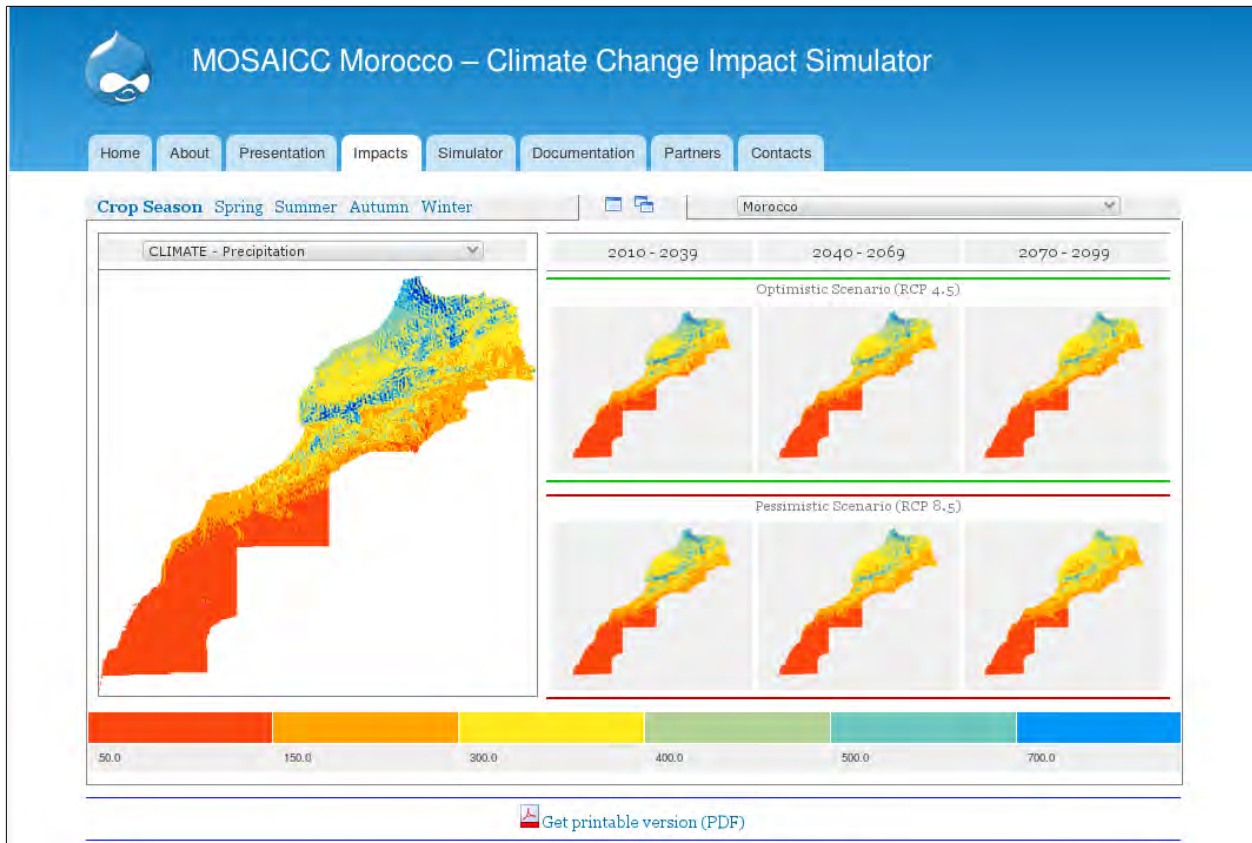


The second part of the menu configuration requires to “*Add link*” next to “Main menu” in “*Menus*”, that appears in “*Structure*” from the dashboard. Fill the form as follows:



Click on the “**Save**” button.

If the module is properly installed when the user clicks on the item “Impacts” of the main menu the following situation appears:



The module has several requirements:

- DB configuration is stored in “sites/all/modules/cci\_tcp\_overview/db.cfg”
- OpenLayers must be installed on the root of the Drupal installation
- JPGraph must be installed in “sites/all/JPGraph”

The DB configuration file has the following content:

```
database=cci_tcp_morocco
username=cci_tcp_morocco
password=Rabat.2015
host=127.0.0.1
```



The module uses the data stored in the PostgreSQL DB and some files archived in the folders “\_LAYERS” and “\_MAPS” on the root of the Drupal installation.

The structure of the “\_MAPS” folder follows this rule :

- \_MAPS
  - <COMPONENT>
    - <PERIOD>
      - <MODEL>
        - <SCENARIO>

The folder “<COMPONENT>” can be “CLIMATE” or “HYDROLOGY”.

The folder “<PERIOD>” can be “1970-2000” or “2010-2099”.

The folder “<MODEL>” can be “AVERAGE” or ...

The folder “<SCENARIO>” can be “RCP45” or “RCP85”.

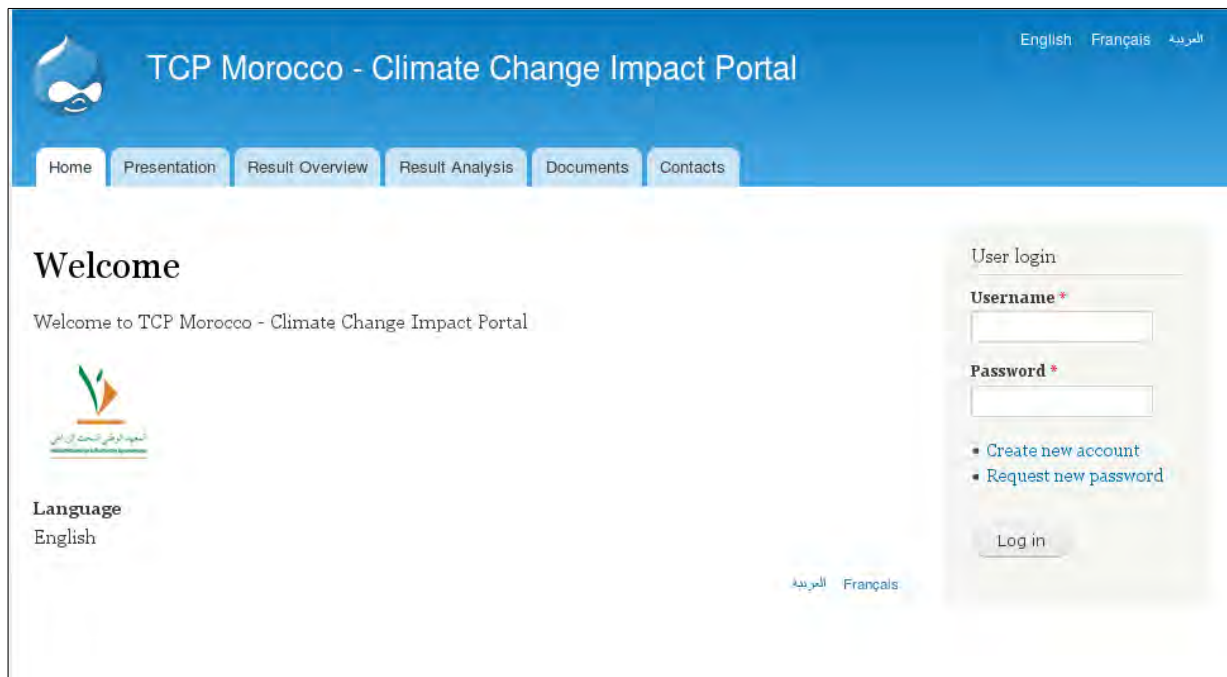
The “\_LAYERS” folder stores the geographic files:

- AdmLev\_1.shp
- AdmLev\_2.shp
- AdmLev\_3\_A.shp
- AdmLev\_3\_B.shp
- AdmLev\_3.shp
- Agroecological\_Zones.shp
- OfficialBasins.shp
- roi\_dem.tiff

The files are actually listed in a table in the DB.

### **Graphic Theme**

The draft version of the page layout just focuses on the menu organization, translated in the three languages.



English version of the draft home page



French version of the draft home page



Arabic version of the draft home page...

## 10. Annex 10 : Architecture of the Simulation Tool

### 10.1. Architecture

#### 10.1.1. Description of the tools

The general architecture has been designed using open source softwares (Figure 66):

- Operating System: *Linux* ;
- Database management system : *PostgreSQL*, and its geographical component ;
- Cartographic Server : *Mapserver*;
- Web Server : *Apache* ;
- Mapping client : *OpenLayers*.

The architecture secures the access to the system, improve the speed of Web access and enables access to Google maps, OpenStreet maps and ad-hoc generated basemaps.

#### 10.1.2. Linux server

The Linux operating system is a free implementation of UNIX system, with POSIX specifications. Linux-based systems predominate for supercomputers. For computer servers, the market is shared with other Unix and Windows.

#### 10.1.3. Web Apache

The Apache web server allows the dissemination of information on the Web. Apache is the most popular web server on Internet (almost 65% market share worldwide). It allows to define a specific configuration for each shared file or directory, and can also sets access restrictions.

#### 10.1.4. PostgreSQL / PostGIS

PostgreSQL is an open source (Berkeley Software Distribution) database management system. PostgreSQL can be freely used, modified and

distributed, whatever the intended purpose, whether private, commercial or academic. It supports a large part of the SQL standard, while offering many modern features:

- Complex queries;
- Foreign keys;
- Triggers;
- Views;
- Transactional integrity;
- MVCC or multi-version concurrency control.

Many business applications are built on PostgreSQL, which remains the relational database management system the most accomplished in the field of open source. The PostgreSQL-PostGIS extension can store objects or geographic data. It allows the management of spatial index type, and calculation, analysis and questioning of geographic objects.

#### **10.1.5. MapServer**

MapServer is an open source spatial data rendering engine, written in C. It allows the upload of spatial data and interactive mapping applications on the web. MapServer is installed on a Web server and can connect to spatial data sources to produce maps to client applications via the Web. It supports standard WMS, WFS and WCS OGC. MapServer is renowned for its performance, robustness and quality of cartographic rendering. It is supported by OSGeo and widely tested by a large community of users. MapServer rivals many proprietary solutions of the biggest software companies in the field of geomatics.

#### **10.1.6. OpenLayers**

OpenLayers is an open source JavaScript library, which allows the integration and interaction with various sources of free maps and data layers. OpenLayers can connect to services, such as Google Maps, OpenStreet Maps, Bing Maps and also to local data provided by web mapping software, supporting OGC standards. To this end, it is independent from any map server. The library is based on AJAX technology and allows the construction of tile images, sending several requests to different servers. OpenLayers separates the tools of the map (the map interface) from map databases.

### 10.1.7. Languages

To combine information from various tools as presented above, a number of programming languages were used:

- HTML / CSS languages, JavaScript / Ext / GeoExt and PHP, for the realization of the interface of the Simulation Tool;
- SQL language and Spatial SQL from Postgis for querying the database;

#### ✓ **HTML/CSS**

HTML (HyperText Markup Language) is the basic language to design pages for publication on the Web. It allows content shaping of a web page. CSS (Cascading Style Sheets) is used for the presentation of HTML documents. It separates the structure of a web page from its various presentation styles. Both languages were chosen to perform particular data entry forms.

#### ✓ **JavaScript/ExtJs/GeoExt**

JavaScript is a scripting language that is used in interactive web pages. Javascript improve HTML, allowing to execute commands on the client side, that is to say at the Web browser. ExtJs is a JavaScript library for building interactive web applications. This library includes many components, such as advanced forms, rich and dynamic graphics tables, trees, menus and toolbars, panels and advanced dialogs. GeoExt is a Javascript library that allows to create rich cartographic interfaces. It is the combination of the OpenLayers library for its geospatial features and ExtJS for its interface tools.

#### ✓ **PHP**

PHP (Hypertext Preprocessor) is an interpreted language (a scripting language) and executed on the server side. PHP is one of the most used languages in web development and was improved since version 5. It has almost 3,000 available functions, in a variety of applications and covers virtually all areas related to web applications. Almost all DBMS market can interface with PHP (commercial or from the open domaine). It was selected to extract data from the database and return them to the customer by the AJAX protocol.

#### ✓ **Spatial SQL/SQL**

SQL (Structured Query Language) is a standard computer language for use with relational databases. The SQL data manipulation language



section allows to search, add, modify or delete data in relational databases. While the spatial SQL allows to manipulate geo-referenced data stored in relational databases.

## 10.2. Installation and configuration of the map server

The following tutorial shows the installation and configuration of the map server, on the recent distribution of Ubuntu Server, with Apache and PHP5 installed.

### 10.2.1. Installation and configuration of PostGreSQL

Version 9.3 of PostgreSQL is installed by default with Ubuntu. However, if this is not the case the following statement can do it :

```
$ sudo apt-get install postgresql
```

The PHP library should be also installed :

```
$ sudo apt-get install php5-pgsql
```

During PostgreSQL installation, a user is added directly in the distribution. The user allows the control of the DBMS. However, it is necessary to create a new user, the first being the root user.

#### Connexion avec l'utilisateur postgres :

```
$ sudo -s -u postgres
```

Launch of PostgreSQL and creating a user (adding a password and user right to create database) :

```
postgres: $ psql
postgres: > CREATE USER user_name ;
postgres: > ALTER ROLE user_name WITH CREATEDB;
postgres: > ALTER USER user_name WITH ENCRYPTED PASSWORD 'mot-de-passe';
postgres: > \q
postgres: $ exit
```

#### Adding the PostgreSQL extension in PHP :

```
$ sudo nano /etc/php5/apache2/php.ini
```

### 10.2.2. Installation and configuration of PostGIS

#### Installation:

```
$ sudo apt-get install postgis
```

#### Configuration:

```
sudo su - postgres
createdb template_postgis
psql -q -d template_postgis -f /usr/share/postgresql/9.3/contrib/postgis-2.0/postgis.sql
psql -q -d template_postgis -f /usr/share/postgresql/9.3/contrib/postgis-2.0/spatial_ref_sys.sql
psql -q -d template_postgis -f /usr/share/postgresql/9.3/contrib/postgis_comments.sql
cat <<EOS | psql -d template_postgis
UPDATE pg_database SET datistemplate = TRUE WHERE datname =
'template_postgis';
REVOKE ALL ON SCHEMA public FROM public;
GRANT USAGE ON SCHEMA public TO public;
GRANT ALL ON SCHEMA public TO postgres;
GRANT SELECT, UPDATE, INSERT, DELETE ON TABLE public.geometry_columns TO
PUBLIC;
GRANT SELECT, UPDATE, INSERT, DELETE ON TABLE public.spatial_ref_sys TO PUBLIC;
EOS
```

### 10.2.3. Installation of phpPgAdmin

phpPgAdmin is a tool for the system administrator, to manage the PostgreSQL database via the Web.

```
$ sudo apt-get install phppgadmin
```

It is necessary to add a symbolic link:

```
$ sudo ln -s /usr/share/phppgadmin /var/www/
```

Then simply connect with favorite browser to the URL: `http // domain-name / phppgadmin`

#### 10.2.4. Installation of MapServer

```
apt-get install mapserver-bin  
apt-get install cgi-mapserver  
apt-get install php5-mapscript
```

Add the PHPMapScript extension (which is a set of PHP functions to steer MapServer with the scripting language) in php.ini:

```
$ sudo nano /etc/php5/apache2/php.ini
```

-> add the following line :

```
extension=php_mapscript.so
```

Since now that the system is an operational map server, it only remains to edit the map file that meet the needs.

#### 10.2.5. Edition of MapFile

The map file is the MapServer configuration file. It is a text file that contains all the parameters necessary for MapServer, for the generation of cartographic material, whether static or dynamic. It is composed of a hierarchy of objects wherein each object may contain other objects and / or properties.

The map file is written on the basis of the documentation within the site of the <http://www.mapserver.org/mapfile/> editor:

- Creates a WMS;
- Defines the connection parameters to PostgreSQL data;
- Specifies the projections of layers;
- Creates symbols in the various classes.

### 10.3. Setting up the database with PostgreSQL / PostGIS

From the logic diagram of the data presented above is performed to create the database tables and relationships between tables.

### 10.4. Development of the map interface

The map interface is the window that will hold the maps. Its development has been achieved through the use of cartographic client OpenLayers with Javascript, ExtJs and GeoExt. This map interface contains



the maps and manipulation tools. The map is composed of basemaps (Google Maps and Open Streets Maps) and secondary layers.

## 10.5. API OpenLayers API, Ext and GeoExt

The OpenLayers API does not require installation. There are two modes of use of the OpenLayers library :

- It is possible to directly access online to the library by the following line of code:

```
<script src="http://www.openlayers.org/api/2.12/OpenLayers.js"></script>
```

This option makes the platform dependent from OpenLayers site, and . could slow down the implementation of the platform.

Instead, it can be download and use locally by calling the script "OpenLayers.js" :

```
<script src="./OpenLayers/OpenLayers.js"></script>
```

This second option was chosen. The OpenLayers archive was downloaded, unpacked and placed in a folder on the web server. To use the library GeoExt, it is necessary to download the package and unzip it to a location on the web server. Then the library can be used using the scripts below:

```
<script type="text/javascript" src="GeoExt/script/GeoExt.js"></script>
```

```
<link rel="stylesheet" href="GeoExt/resources/css/geoext-all.css" type="text/css">
```

## 10.6. Using basemaps

### 10.6.1. Google Maps

Google Maps is a web mapping service that provides default usable maps. These maps are generated by Google from data sources, such as Tele Atlas, Navteq, IGN, Spot Image, etc. Regions of the globe do not have the same accuracy in terms of data coverage, due to lack of interest, lack of access and the legislation in force in each country. Google offers several views including the classic map, terrain, satellite. These default maps can be changed by changing the visibility and background color. To integrate the Google Maps, Google Maps API is called into an HTML file and then the maps is initialized in a JavaScript file.

## Calling the Google Maps API

```
<script type="text/javascript" src="http://maps.googleapis.com/maps/api/js?v=3.9&sensor=false">
</script>
```

### 10.6.2. Open Street Maps

OpenStreetMap is a project founded in 2004, that aims to freely provide available reference mapping. Unlike sources from proprietary data, the OpenStreetMap license is much less restrictive. It therefore offers greater flexibility. The call for OpenStreetMap is done in HTML file like this:

```
<script src=" >
```

## **INRA**

Ennasr Avenue - Rabat, Morocco -  
PO BOX 415 RP Rabat Morocco  
+212 537 770955

## **FAO-Representation in Morocco**

4, Prince Sidi Mohamed Street,  
Rabat-Souissi 10170 PO BOX 1363,  
Rabat +212 537 654308 +212 537  
654552



**MOSAICC  
MAROC**

Modelling System for Agricultural  
Impacts of Climate Change  
[www.changementclimatique.ma](http://www.changementclimatique.ma)

2015 Edition

[contact@changementclimatique.ma](mailto:contact@changementclimatique.ma)